Chromatin and epigenetic regulation of Herpes Simplex Virus 1 lytic genomes

by

MiYao Hu

A thesis submitted in partial fulfillment of the requirements for the degree of

Doctor of Philosophy

Department of Biochemistry
University of Alberta

Abstract:

Primary herpes simplex virus 1 (HSV-1) infections are common in childhood, affecting mainly the oropharyngeal mucosa. The virus is then transported to the neuronal bodies in the trigeminal ganglia, where it establishes lifelong latency. Although latent infections are asymptomatic, HSV-1 reactivates upon a variety of stresses, producing recrudescence of disease and spreading infection. Lytic infections are treated with several drugs, but latency and reactivation cannot be cured or prevented. HSV-1 chromatin and epigenetic regulation during lytic and latent infections have been studied for decades. HSV-1 genomes are regularly chromatinized into inaccessible chromatin during latency but become more accessible during reactivation. Epigenetics thus likely play a major role in the regulation of HSV-1 transcription, replication, and reactivation from latency. Although HSV-1 DNA is non-regularly chromatinized in lytic infections, most current models assume a similar epigenetic regulation for HSV-1 as for cells.

To evaluate the chromatinization of HSV-1 genomes during lytic infections, I performed nuclease protection assay coupled with bio-physical fractionation, to separate viral DNA-nucleoprotein complexes by hydrodynamic ratios, followed by deep sequencing (in collaboration with Dr. Depledge) of each fraction. Gene sampling and cluster analyses indicated that chromatin dynamics relate to the transcriptional competency of HSV-1 genomes, not the transcriptional levels of any individual genes or groups of genes. The transcriptionally competent genomes are in highly dynamic, and

accessible, chromatin and the incompetent ones in far less dynamic, or accessible, chromatin. Moreover, chromatin insulator elements such as the CCCTC binding factor (CTCF) flank highly transcribed genome regions from mostly non-transcribed ones. My findings indicate that chromatin is a key regulator of HSV-1 transcription during lytic infections in that chromatin provide a first level of regulation, dictating transcriptional competency. I thus uncovered a new level of viral transcription regulation. During reactivation, the HSV-1 chromatin also changes from regular, mostly inaccessible, chromatin to a far more dynamic, and accessible, state. My findings during the lytic infections thus also provide a framework to better understand HSV-1 latency and reactivation.

Preface:

Figure 1 of my thesis was from a paper published by Rochat, R. H., C. W. Hecksel and W. Chiu (2014). "Cryo-EM techniques to resolve the structure of HSV-1 capsid-associated components." Methods Mol Biol **1144**: 265-281. Figure used under CC-BY 4.0 license

Figure 2,3, and 5, figure 11, and figure 28 of my thesis were from a recently accepted manuscript by Schang, L. M., Hu, M., Flores Cortes, E., and Sun, K. (2021), “Chromatin-mediated epigenetic regulation of HSV-1 transcription as a potential target in antiviral therapy.” Anti-viral Research, AVR-D-21-00150R1. I’m responsible of creating these figures. Figure used under CC-BY 4.0 license.

Figure 6 of my thesis was from a paper published by Bracken, A. P., G. L. Brien and C. P. Verrijzer (2019). "Dangerous liaisons: interplay between SWI/SNF, NuRD, and Polycomb in chromatin regulation and cancer." Genes Dev **33**(15-16): 936-959. Figure used under under CC-BY 4.0 license

Figure 7 to 9 of my thesis was from a paper published by Hasan, N. and N. Ahuja (2019). "The Emerging Roles of ATP-Dependent Chromatin Remodeling Complexes in Pancreatic Cancer." Cancers (Basel) **11**(12). Figure used under CC-BY 4.0 license.

Figure 10 of my thesis was from a paper published by Kingston, R. E. and G. J. Narlikar (1999). "ATP-dependent remodeling and acetylation as regulators of chromatin fluidity." Genes Dev **13**(18): 2339-2352. Figure used under CC-BY 4.0 license

Figure 31 of my thesis was from a paper published by Chen, Q., L. Lin, S. Smith, J. Huang, S. L. Berger and J. Zhou (2007). "CTCF-dependent chromatin boundary element between the latency-associated transcript and ICP0 promoters in the herpes simplex virus type 1 genome." J Virol **81**(10): 5192-5201. Figure used under CC-BY 4.0 license

Chapter 3 of my thesis has been modified from a paper published as Hu, M., D. P.

Depledge, E. Flores Cortes, J. Breuer and L. M. Schang (2019). "Chromatin dynamics and the transcriptional competence of HSV-1 genomes during lytic infections." PLoS Pathog **15**(11): e1008076. The original sequencing data from Dr. Depledge is open accessible at https://www.ncbi.nlm.nih.gov/bioproject/PRJNA550980. I'm responsible of all the analyses of the data and assembling all figures except for Figure 15, which was performed by co-auther Esteban Flores Cortes.

Table of Contents

List of Tables

Chapter 2: Material and Methods

List of Figures

Chapter 1: Introduction

Chapter 3: Results

Chapter 4: Discussion

List of abbreviations used in this Thesis

AA: Anacardic acid

ACF: ATP-utilizing chromatin assembly and remodeling factor

ActD: Actinomycin D

ACV: Acyclovir

Ada2: Adenosine deaminase 2

ARID1A/B: AT-Rich interaction domain 1 A/B

ARS: Autonomously replicating sequence

Asf-1: Anti-silencing factor 1

ATM: Serine/Threonine kinase

ATP: Adenosine triphosphate

Atrx: ATP-dependent helicase

ATRX: ATP-dependent helicase

AutoN: Autoinhibitory N-terminal

BAF: ATP-dependent BRG1/BRM associated factor

bHLH: Basic helix–loop–helix protein

bp: Basepair

BPTF: Bromodomain PHD finger transcription factor

BRG: Brahma-related gene

BRM: Brahma

CAF-1: Chromatin assembly factor 1

CBP/P300: CREB-binding protein/E1A binding protein 300

CDK: Cyclin dependent kinases

CENP-A: Centromere protein

ACERF: Cat eye syndrome critical region protein-containing remodeling factor

CHD: Chromodomain helicase-DNA binding complexes

ChIP: Chromatin immunoprecipitation

CHRAC: Chromatin accessibility complex proteins

CHX: Cycloheximide

Chz1: Chaperone for Htz1/H2A-H2B dimer 1

CLOCK: Circadian locomotor output cycles kaput complex

CPE: Cytopathogenic effects

CTCF: CCCTC-binding factor

Daxx: Death-domain associated protein

Dls1: Dpb3-like subunit of ISW2/yCHRAC complex 1

DMEM: Dulbecco's modified eagle’s medium

DMOG: Dimethyloxalyglycine

DMSO: Dimethyl sulfoxide

DNAse: Deoxynuclease

Dpb4: DNA polymerase B (II) subunit 4

DPF1/2/3: Double PHD fingers 1/2/3

DSB: Double strand break

dUTPase: Deoxyuridine nucleotidohydrolase

E: Early

EBF1: Early B-cell factor 1

EBNA1: EBV nuclear antigen

EBV: Epstein-Barr virus

EC_{50}: Half maximal effective concentration

EdC: 5-Ethynyl-2'-deoxycytidine

EdU: 5-Ethynyl-2'-deoxyuridine

EMSA: Electrophoretic mobility shift assay

Esa1: Essential SAS2-related acetyltransferase

EtBr: Ethidium bromide

EYFP: Enhanced yellow fluorescent protein

EZH1/2: Enhancer of zeste 1/2 polycomb repressive complex

FAD: Flavin adenine dinucleotide

FAIRE: Formaldehyde-assisted isolation of regulatory elements

FBS: Fetal bovine serum

FISH: Fluorescence in situ hybridization

FoxA: Forkhead box protein A

GAL4: Galactose-induced gene 4

gB, gC, etc: Glycoprotein B, glycoprotein C, etc.

GCE: Genome copy equivalents

Gcn5: General control non-derepressible 5

GFP: Green fluorescent protein

GNAT: GCN5-related N-acetyltransferases family

HAT: Histone acetyltransferase

HCF-1: Host cell factor 1

HDAC: Histone deacetylase

Hel/Prim: Helicase/primase complex

HIN: Hematopoietic interferon-inducible nuclear antigens

HIRA: Histone cell cycle regulator

HMT: Histone methyltransferases

HP1: Heterochromatin protein 1

HSA: Helicase SANT-associated

Hsp70: Heat shock protein 70

HSV-1: Herpes simplex virus 1

HVEM: Herpesvirus entry mediator

IBP: Insulator-binding protein

ICP0/ICP4/ICP8: Infected cell polypeptide 0/4/8

IE: Immediate early

IFI16: Interferon-inducible protein 16

INO80: Inositol-responsive gene expression regulator

Inr: Initiator

iPOND: Isolation of proteins on nascent DNA

ISWI: Imitation switch

Itc1: Imitation switch two complex 1

JHDM: JMJC domain-containing histone demethylation protein 1

JMJD: Jumonji domain proteins

KDM: Histone lysine demethylases

Klf4: Kruppel-like factor 4

KMT: Lysine methyltransferases

KSHV: Kaposi’s sarcoma associated herpesvirus

L: Late

LacZ: Beta-galactosidase

LANA: Latency associated nuclear antigen

LAT: Latency associated transcripts

LMP: Latent membrane protein

LNCaP: Androgen-sensitive human prostate adenocarcinoma

Loc1/2/3: Localization of mRNA protein 1/2/3

LSD1: Lysine-specific demethylase 1A

MAO: Monoamine oxidase

MBD: Methyl CpG binding protein

MCN: Micrococcal nuclease

MNNG: N-methyl-N'-nitro-N-nitrosoguanidine

mouse TG: Mouse trigeminal ganglia

MTA: 5’-deoxy-5’-methylthioadenosine

MYST: MOZ, Ybf2/Sas3, Sas2 and Tip 60 containing complex

NaBu: Sodium butyrate

NAP1: Nucleosome assembly protein 1

N-cor: Nuclear receptor co-repressor

ND10: Nuclear domain 10

NegC: Negative regulator of coupling

NER: Nucleotide excision repair

NF1: Neurofibromatosis type 1

NFR: Nucleosome free region

NGF: Nerve growth factor

NoRC: Nucleolar remodelling complex

NuA4: Nucleosomal acetyltransferase of histone H4

NURF: Nucleosome remodeling factor

OBP: Origin binding protein

Oct-1: Octamer-binding transcription factor 1

Oct3: Octamer-binding protein 3

OriL: DNA replication origin at unique long

OriS: DNA replication origin at repeat short

PAA: Phosphonoacetic acid

PAF: RNA polymerase II associated factor 1

Pax7: Paired box 7

PBAF: Polybromo-associated BAF complex

PBRM1: Polybromo domain 1

PBS: Phosphate buffered saline

PCNA: Proliferating cell nuclear antigen

PHD: Plant homeodomain

PHO5: Phosphate metabolism protein 5

PIC: Pre-initiation complex

PML: Promyelocytic leukemia

PRV: Pseudorabies virus

PU.1: PU-binding protein 1

PWWP: Pro-Trp-Trp-Pro domain protein

Rap1: Ras-proximate-1 or Ras-related protein 1

RbAP: Retinoblastoma-binding protein

RCC: Regulator of chromosome condensation

Reb1: RNA polymerase I enhancer binding protein 1

RecA: Recombinase A

REST/CoREST: RE1-silencing transcription factor/REST corepressor

RL: Repeat long

Rosco: Roscovitine

RRase: Ribonucleotide reductase

RS: Repeat short

RSC: Remodeling the structure of chromatin

SAGA: Spt-Ada-Gcn5 acetyltransferase

SANT: Swi3, Ada2, N-cor, TFIIB

SBX: Suberohydroxamic

SEAP: Secreted embryonic alkaline phosphatase

Set1: Su(var)3-9, enhancer-of-zeste and trithorax 1

SFM: Serum free medium

SnAC: Snf2 ATP coupling

Sox2: Sex determining region Y-box 2

SP1: Specificity protein 1

SRCAP: Snf2 related CREB-binding protein activator protein

SWI/SNF: Mating type switching/ sucrose fermentation

TAD: Topologically associated domain

TAF3: Transcription associated factors 3

TBP: TATA binding protein

TCP: Tranylcypromine

TFIID, TFIIB, etc,: Transcription factor II D/B

Tip5: Transcription termination factor I-interacting protein 5

TK: Thymidine kinase

TSA: Trichostatin A

UL: Unique long

US: Unique short

VP16/VP5: Virion protein 16/5

VPA: Valproic acid

WAC: WW domain-containing adapter protein with coiled-coil

WICH: WSTF-SNF2h complex

WSTF: Williams syndrome transcription factor

wt: Wild type

XPB/XPD: Xeroderma pigmentosum type B/D

Chapter 1: Introduction

The HSV-1 genome has been proposed to be nucleosome-free in lytically infected cells, but accumulating recent evidence challenges that model. Newer models propose that the HSV-1 genome is assembled in “irregular” chromatin (discussed in section 1.4). However, the encapsidated HSV-1 genomes enter the nucleus as protein-free DNA. I will first introduce the Herpesviridae in general, and then how their genomes enter the infected cell nuclei.

HSV-1 genome does not encode any histone-like proteins or chromatin remodeling enzymes. The “irregular” HSV-1 chromatin thus likely results from complex host-virus interactions and uses cellular proteins and complexes. The regulation of the cellular chromatin has been used as the model to understand the HSV-1 chromatin during lytic and latent infections. To understand the literature regarding HSV-1 chromatin and HSV-1 epigenetics, I will first introduce the structure and the regulation of cellular chromatin dynamics by epigenetic regulation (histone variants, histone tail modifications, and ATP-dependent chromatin remodeling), as well as the roles of chromatin on regulating transcription.

I will then introduce the different models proposed for the HSV-1 chromatin during latent, quiescent, or lytic infections, including their possible protein composition. Next, I will review the previous studies regarding epigenetic regulation of HSV-1 transcription, which were mostly performed using small molecule epigenetic regulators or knockouts.

1.1 Herpesviridae

The *Herpesviridae* family includes viruses infecting a broad range of hosts, among them eight that infects humans. The herpesviruses are classified according to their biological properties into alpha Herpesviridae, beta Herpesviridae and gamma Herpesviridae. The alphaherpesviruses, including HSV-1, typically infect a broad range of hosts and have a short life cycle (about 24 h). In tissue culture, HSV-1 can infect many cell lines from different species including rabbit, mouse, and human. However, natural infection of HSV-1 in vivo is only reported in humans. Nonetheless, mouse and rabbits can be infected for experimental purpose producing both lytic and latent.

The herpes virion is generally 150 to 200nm in diameter, and is constituted by a lipid bilayer membrane envelope, a proteinaceous layer called the tegument, and a protein capsid containing a single copy of the double stranded linear DNA genome.

The envelope is derived from host cell membranes, and contains embedded viral glycoproteins, named mostly alphabetically such as, gB, gC, etc. These membrane glycoproteins are required for attachment, and viral membrane fusion, as well as for egress.

After membrane fusion, the proteinaceous tegument and the capsid enter the cell. The tegument includes viral proteins that activate transcription of the viral genes. For HSV-1 and HSV-2, these are VP16, ICP0, and ICP4.

Once inside the cell, the icosahedron capsid migrates to the nuclear pores along the

tubulin network fibers. The linear double stranded DNA is then ejected out of the capsid and into the nucleus through the portal complex. The herpes genomes range from approximately 124k bp to 240k bp (Honess 1984) and encode about 70 to 160 genes.

The herpesviruses are also classified according to their genomes. The type A herpes genomes contain one unique sequence flanked by two copies of a repeat region at both ends. The type B genomes contain one unique sequence flanked by multiple repeats at the ends. The type C genomes contain repeat regions at the ends of the unique region, and the unique long (UL) region itself contains multiple internal repeats. The type D genomes contain unique long and unique short (US) regions with repeat regions at both ends of the unique short. The type E genomes contained a UL region, a US region, two unique long repeat (Rl) regions at both ends of the UL, and two unique short repeats (Rs) at both end of the US. The type F genomes contain only a unique region. The HSV-1 genome is type E.

1.2 Herpes simplex virus 1 (HSV-1) or human herpes virus 1 (HHV1)

1.2.1 HSV-1 virion and entry

As all Herpesviridae, the HSV-1 virion is composed of a lipid bilayer envelope derived from the host cell membrane (Fig 1A), a tegument (Fig 1A), and a capsid (Fig 1B).

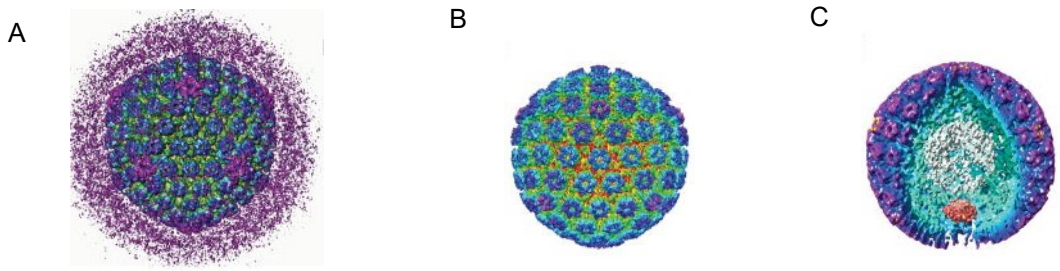

Figure 1: Cryo-EM of HSV-1 virion. (A): 3D reconstructions of the complete infectious HSV-1 virion showing the proteins of the tegument. (B): 3D reconstructions of the HSV-1 capsid. (C): 3D reconstructions of the portal complexes and HSV-1 DNA inside the capsid. Ref:(Rochat, Hecksel et al. 2014). Figure used under CC-BY 4.0 license.

The glycoproteins gB, gD, and gH/gL are essential for attachment and entry. First, gC or gD bind to cell surface heparan sulfate. The next step requires gD binding to the host receptors herpesvirus entry mediator (HVEM), or nectins 1 or 2 (Lazear, Carfi et al. 2008). Binding triggers a conformational change in gD, which then activates gH/gL by yet unknown mechanisms (Atanasiu, Saw et al. 2010, Atanasiu, Saw et al. 2016). The activated gH/gL then activates gB, which contacts with the host cell membranes to allow fusion (Zeev-Ben-Mordehai, Vasishtan et al. 2016). The membrane-proximal, transmembrane, and cytoplasmic domains of gB form unique trimeric pedestal which is stabilized by the ectodomain of gB (soluble extracellular domain) at the postfusion conformation (Cooper, Georgieva et al. 2018).

The HSV-1 tegument contains more than 24 viral proteins (Spear and Roizman 1972, Heine, Honess et al. 1974). Some of the proteins in the tegument play important roles in capsid and virion assembly [VP22, (Benboudjema, Mulvey et al. 2003)], nuclear

egress [UL31, US3, ICP34.5, UL36, UL37, and UL51, (Xu, Che et al. 2016)], capsid transportation to the nucleus [UL36, (Cardone, Newcomb et al. 2012)], and viral transcription [VP16, (Campbell, Palfreyman et al. 1984)].

After the capsids enter the cytoplasm, a subset of tegument proteins are transported to the nucleus independently from the capsids, along the cytoskeleton microtubules (Liashkovich, Hafezi et al. 2011). The capsids dock at the nuclear pore and the HSV-1 DNA is then released through the nuclear portal into the nucleus by the internal pressure of the tightly packed HSV-1 genome (Bauer, Li et al. 2015).

The linear double stranded HSV-1 genome, approximately 152k bp long, is associated with the polyamine spermine inside the capsid (Gibson and Roizman 1971). The entire genome encodes more than 82 proteins and is 68% GC.

1.2.2 HSV-1 lytic and latent life cycle

The linear HSV-1 genome is circularized in the nucleus (Garber, Beverley et al. 1993). Two mechanisms of circularization have been proposed, end to end ligation of the termini (Mocarski and Roizman 1982, Strang and Stow 2005), or homologous recombination (Yao, Matecic et al. 1997) mediated by the cellular DNA ligase co-factors Regulator of chromosome condensation 1 (RCC1) (Umene and Nishimoto 1996) or Regulator of chromosome condensation 4 (RCC4) (Muylaert and Elias 2007).

Transcription of the circularized HSV-1 genome starts by binding of the VP16/HCF-1 (Host cell factor 1)/Oct-1 (Octamer transcription factor 1) complexes to the TAATGARAT

(R for purine) sequences in the immediate early (IE) gene promoters. VP16 is a tegument protein, and HCF and Oct-1 are constitutively expressed cellular proteins. Consequently, activation of IE gene transcription does not require previous protein synthesis. VP16 associates with HCF-1 in the cytoplasm. The complex then re-localizes to the nucleus via the nuclear localization signal at the C-terminus of HCF-1. Meanwhile, Oct-1 binds to the TAATGARAT sequences in the HSV-1 IE gene promoters and then it recruits the VP16/HCF-1 complex to them. The VP16/Oct-1/HCF-1 complexes in turn recruit a variety of transcription factors and chromatin remodelers to activate transcription of the IE genes (Fig 2).

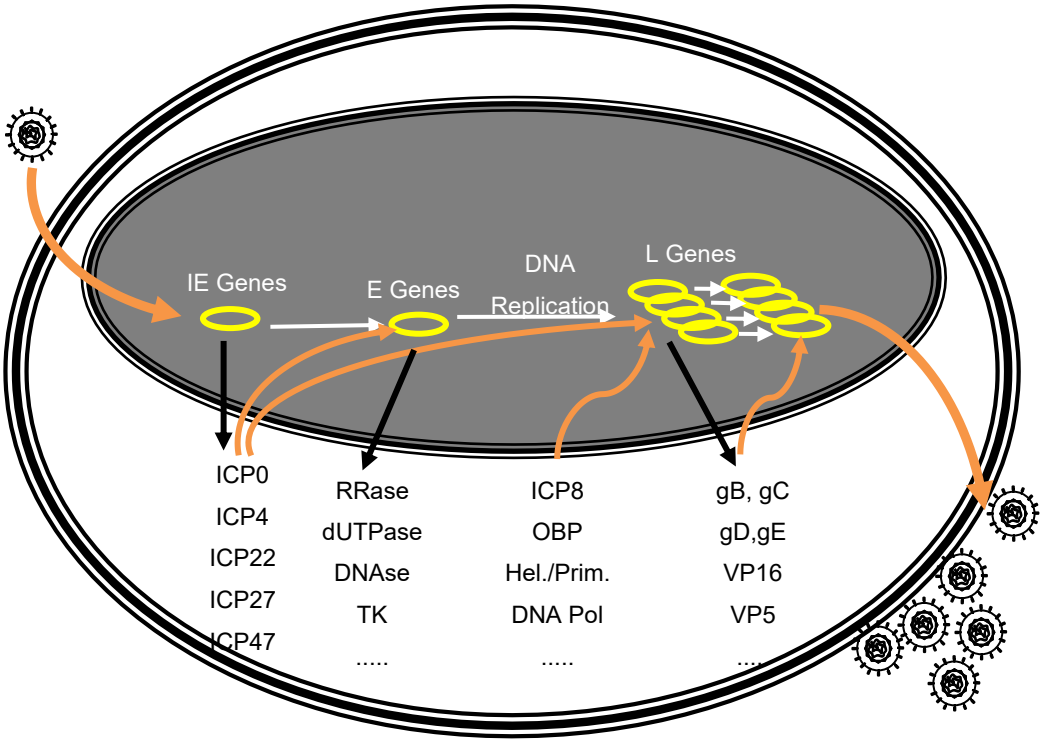

Figure 2: cartoon representation of the HSV-1 lytic cycle. The cell is represented by the circle with two thin black lines and one thick black line in between. The Nuclei is represented by the gray circle within two thin black lines and one thick black line in between. The HSV-1 virions are represented by the spiked small circles with black

drawings inside. The HSV-1 intracellular genomes are represented by the yellow circle. (Schang, Hu et al. 2021) Figure used under CC-BY 4.0 license.

Two of the five IE proteins are essential to active E gene transcription, ICP4 and ICP0. ICP4 is an indirect viral activator of transcription that interacts with TBP, TFIIB, and TFIID (Kristie and Roizman 1986, Sampath and Deluca 2008). ICP0 is an E3 ubiquitin ligase that somewhat activates HSV-1 transcription. Although the exact mechanism of activation of transcription E or L genes is not yet fully understood, the promoters of the E genes contain fewer transcription factor binding sites than those of the IE genes, and those of L genes contain basically none. The promoter of the E gene (TK) contains two copies of SP1 binding sites, one NF1 binding site and one TATA binding box in comparison to that of IE gene (ICP4) that contains two TAAGARAT sequences, four SP1 binding sites, one TATA binding box and one ICP4 binding site (Fig 3).

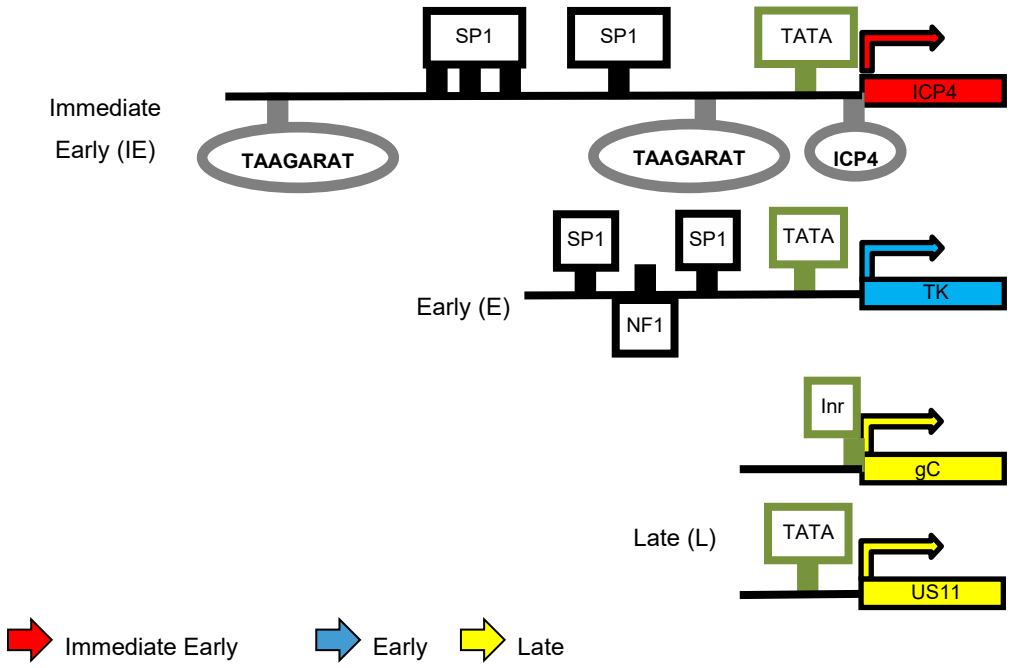

Figure 3: Examples of promoter composition of HSV-1 IE, E, and L genes. Binding sites of each transcription factors are represented by colored square (Imbalzano, Coen et al. 1991, Gu and DeLuca 1994, Kuddus, Gu et al. 1995, Lieu and Wagner 2000, Schang, Hu et al. 2021). Figure used under CC-BY 4.0 license.

Seven of the E genes are essential for HSV-1 DNA replication (the two subunits of the DNA polymerase, the single stranded DNA binding protein ICP8, the three subunits of the DNA helicase-primase complex, and the origin binding protein) (Challberg 1986). The circularized HSV-1 genome serves as the template for replication (Strang and Stow 2005). In one of the models for circular HSV-1 DNA replication, bidirectional replication first starts at one of the three origins of replication, to amplify circular theta DNA. Later, replication would switch to a rolling circle mechanism to form linear concatemer structures (Muylaert, Tang et al. 2011). Alternatively, the concatemer structures could

also be formed through strand invasion during HSV-1 replication. The evidence supporting this model includes ICP8 inducing strand exchange and invasion in a ATP-dependent manner (Nimonkar and Boehmer 2003, Nimonkar and Boehmer 2003), and the HSV-1 alkaline nuclease inducing single strand annealing (Weller and Coen 2012).

Transcription of L genes is activated after the onset of HSV-1 DNA replication. The promoters of the L genes are even less complex than those of the E genes, containing only a TATA box or an Inr (initiator sequence) at the transcription starting site (Fig 3). L genes encode proteins involved in encapsidation and structural proteins, such as the major capsid protein VP5, the envelope glycoproteins, and the tegument protein VP16 (Fig 2).

There are four types of capsids at the late stages of HSV-1 lytic infection: procapsids, and A, B, or C capsids. Procapsids are the precursors of the A, B, and C capsids. A, B, and C capsids have the same overall structure, although they differ in the minor proteins (Heming, Conway et al. 2017). Seven HSV-1 proteins are required for packaging of the HSV-1 genome into the capsids, UL6, UL15, UL17, UL25, UL28, UL32 and UL33 (Heming, Conway et al. 2017). Twelve UL6 molecules form a portal allowing the HVS-1 DNA to enter into the capsid (Cardone, Winkler et al. 2007). UL15, UL28 and UL33 form the terminase complex, which is essential for cleavage and packaging of the virion HSV-1 DNA. UL17, UL25 and UL36 form the capsid vertex, a specific structural component important for HSV-1 DNA cleavage, packaging and encapsidation (Fan,

Roberts et al. 2015).

After the primary infection on the skin, the HSV-1 virions are transported to the neuronal bodies in the trigeminal ganglia where they establish latency. HSV-1 replicates less, or not at all in the neurons (Fig 4). Most of the HSV-1 genomes instead form silenced chromatin from which only the latency associated transcripts (LAT) are transcribed. LATs are a family of RNAs transcribed from the LAT locus, which is located in the repeat regions adjacent to ICP0 gene. The long LAT transcript is 8.3k bp long, but it is then spliced into a 2k bp stable intronic RNA, which is then further spliced into a 1.5k bp RNA (Zabolotny, Krummenacher et al. 1997). The chromatin and the transcription regulation of latent HSV-1 genomes are discussed later (Page 45).

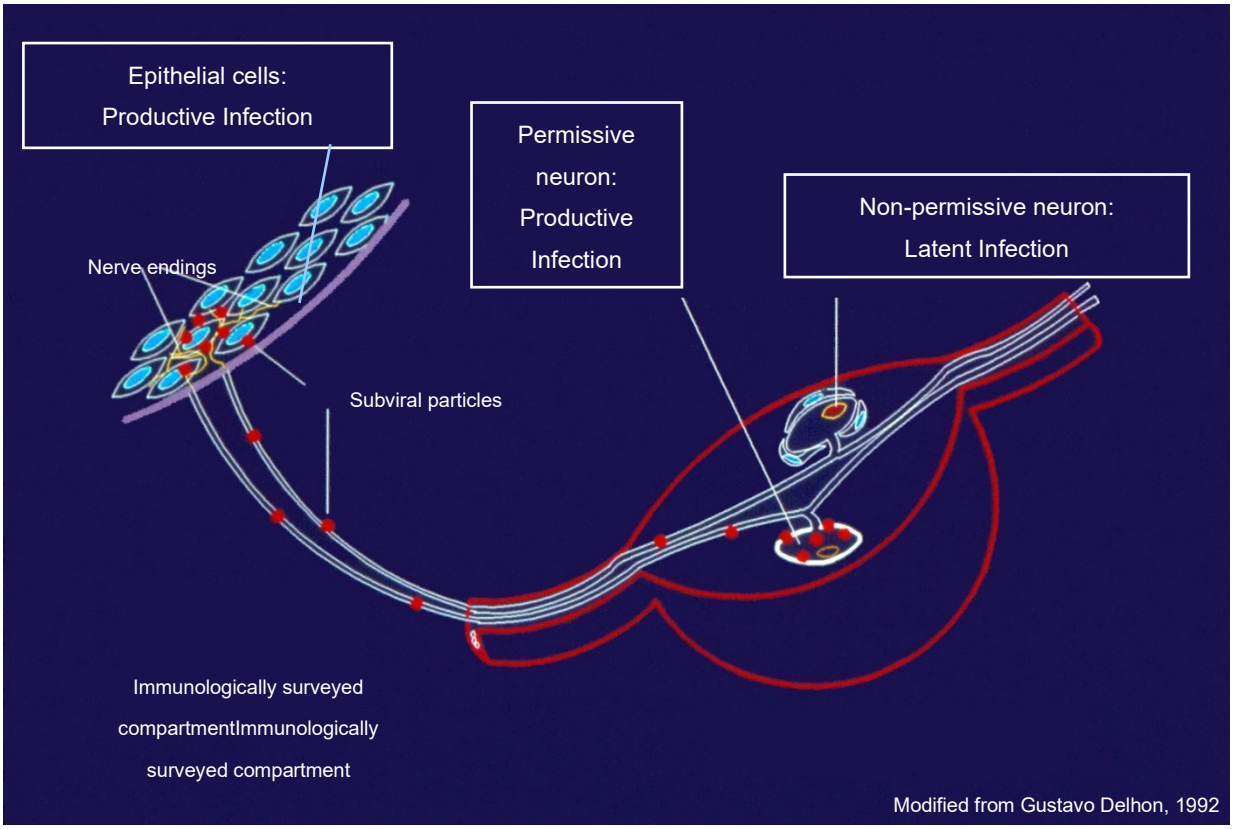

Figure 4: cartoon representing HSV-1 lytic and latent infections. (Schang, Hu et al.

2021) Figure used under CC-BY 4.0 license.

1.2.3 HSV-1 pathology

The primary HSV-1 infection occurs at the mucosal surfaces. These infections generally cause cell death and inflammatory responses. Infection and replication of HSV-1 sometimes causes multinucleated structures (many nuclear within the same cell plasma membrane), called syncytia (Whitley, Kimberlin et al. 2007). Cold sores are formed by the fluid trapped between the epidermis and dermal layer, which contains virions, cell debris, inflammatory cells, and the multinucleated cells (Whitley, Kimberlin et al. 2007). Recurrent ocular infection causes herpes stromal keratitis, the leading causes of infectious blindness besides corneal transplant, and second only to trauma (Farooq and Shukla 2012).

After the HSV-1 virions enter the neuron, latency is established. Although uncommon, HSV-1 can also cause encephalitis. HSV-1 latency usually is asymptomatic, without production of viral proteins. However, latently infected HSV-1 genomes can be reactivated upon a variety of factors including stress. Reactivated HSV-1 virions travel back to the epithelial cells and produce infectious virions (Fig 4).

1.3 Chromatin and transcription

1.3.1 Chromatin

The diploid DNA of a single human cell is composed of more than 10^{12} of DNA base pairs and would be about 2 to 3 meters in length if all 46 DNA segments were

connected head to tail. To store such long molecules into the nucleus, DNA is packaged into chromatin, a chain of repeated units called nucleosomes. The nucleosome core particles are composed of 146 bp of DNA wrapped 1.75 turns around a histone octamer, which consists of two copies of each histone H2A, H2B, H3 and H4 (Kornberg 1974, Luger, Mader et al. 1997). Linker histone H1 binds to the exit and entry point of the core particle to form a full nucleosome. The stability of the different histones in the core particle differs. One H2A/H2B dimer is released from the nucleosome at 0.35 M NaCl, while the remaining hexamer is stable below 1.2 M (Kawashima and Imahori 1982). Assembly of the octamer *in vitro* starts with the assembly of one H2A/H2B and one H3/H4 heterodimers, and then a second H3/H4 dimer interacts with the H3/H4 dimer of the tetramer through the helix in histone H3, forming a hexamer (Luger, Mader et al. 1997). Histone H2B of the second H2A/H2B dimer then interacts with H4 of the hexamer to form the octamer (Luger, Mader et al. 1997).

The repeated nucleosome chain is further compacted to form higher order chromatin structures. One of the commonly studied structures is the 30 nm fiber. Crystal structures of 30 nm fiber has only been acquired in the relaxed form. The structure of the compacted, or *in vivo*, 30 nm fiber remains to be resolved (Adhireksan, Sharma et al. 2020). Two major models of the 30nm fiber structure have been proposed, solenoid and zigzag. The solenoid model is based on the X-ray structure of an eight-nucleosome chain. It proposes that the nucleosomes coil around a central vanity with six

nucleosomes per turn, resulting in first nucleosome interacting with the fifth or sixth nucleosome, forming an one-start helix (Finch and Klug 1976). Evidence for the zigzag model was observed under electron microscopy. It proposes that two chains of nucleosomes crisscross between each stack, producing a two-start helix (Bednar, Horowitz et al. 1995, Dorigo, Schalch et al. 2004). The solenoid model was once thought to be more thermodynamically stable, as a zigzag type fiber can only be observed if the chromatin is frozen before collapsing into the solenoid state (Razin and Gavrilov 2014). However, in vitro studies indicate that the status of the chromatin fiber is determined by length of the linker DNA, binding of histone H1 or high mobility group proteins (HMGP), chromatin modellers, and the post-translation modification of the histone tails (Razin and Gavrilov 2014). For example, an X-ray crystal structure of a tetranucleosome fiber with 167 bp nucleosomal repeat length (Schalch, Duda et al. 2005), and an electron microscopy of a eleven nucleosome array with 200 nucleosomal repeat length (Grigoryev, Arya et al. 2009) both showed a zigzag type fiber. However, neither of these two in vitro zigzag fibers contained linker histone H1 or HMGPs. Nucleosome interaction analyses of the chromatin fiber with long nucleosomal repeat length (>200 bp) revealed that one nucleosome preferred to interact with the next fifth or sixth one downstream, suggesting that long nucleosomal repeat lengths prefer solenoid type fibers (Grigoryev, Arya et al. 2009). Interestingly, electron microscopy of a 48 nucleosome fiber showed heterogeneous fiber conformations, in which the compacted

zigzag fiber fragments were interspersed by solenoid fiber fragments (Grigoryev, Arya et al. 2009).

Binding of linker histones also alters the compaction of the chromatin fibers. Using computational tools and data from chicken histone H5 (homolog to mammalian histone 1) interaction sites, some models have been proposed that histone H5 binding alters the chromatin fibers (Wong, Victor et al. 2007). In the 177 nucleosome repeat length fiber, the entry and exit linker DNA is fully wrapped onto the histone octamer and histone H5 was bound in between. Such nucleosome conformation resulted in the entire fiber being tightly compacted in zigzag like fibers (Wong, Victor et al. 2007). As the nucleosome repeat length increases, the linker DNA at entry and exit points was more available and able to form a pocket for histone H5 binding. At 237 bp nucleosome repeat length, binding of histone H5 resulted in a more relaxed, solenoid like structures (Wong, Victor et al. 2007).

The in vitro tetranucleosome fiber experiments also showed that the acidic surface created by histone H2A and H2B interacts with the tail of histone H4 of the neighborhood nucleosome (Schalch, Duda et al. 2005). Histone H2A.Z, a variant of canonical histone H2A, contains two more histidine residues in the acidic patch and resulted in preferential binding of heterochromatin protein 1 (HP1) (Fan, Rangasamy et al. 2004). Binding of HP1 generally silences genes and compacts chromatin. In contrast, histone H2A.B, another variant of canonical H2A that lacks the acidic patch, destabilized

the 30nm fiber formation (Zhou, Fan et al. 2007).

Acetylation, or mutation to a non-charged residue, of the neighborhood histone H4K16, but not K5, K8, or K12, decreased the stability of fiber folding (Allahverdi, Yang et al. 2011, Yang and Arya 2011). In vitro assembly of chromatin fibers containing single acetylated histone H4K16 was sufficient to prevent formation of 30nm fiber or any higher order chromatin structures (Shogren-Knaak, Ishii et al. 2006). Interestingly, Kaposi's sarcoma-associated herpesvirus (KSHV) genome encodes a latency-associated nuclear antigen (LANA) that interacts with the acidic patch of histone H2A/H2B, although it has no sequence homology with histone H4 tail. This property of LANA is thought to be important for latent KSHV genomes to be segregated to daughter cells during mitosis, but not through nucleosome interaction (Barbera, Chodaparambil et al. 2006).

Although the 30nm fiber is studied extensively in vitro, its presence in vivo has not been documented. Several studies indicated that 30nm fiber was not compact enough to fit eukaryotic DNA into nuclei (reviewed in (Tremethick 2007, Razin and Gavrilov 2014)), this structures has not been observed in the nuclei by imaging techniques (Horowitz-Scherer and Woodcock 2006). Instead, chromatin fibers throughout cell cycle are about 60-80nm at interphase or 500 to 750 nm at metaphase (Kireeva, Lakonishok et al. 2004). The structure of these fibers remains unknown.

1.3.2 Chromatin regulation of DNA-dependent processes

In vivo chromatin assembly and disassembly is far more complex than in vitro, involving multiple proteins. Newly synthesized H3/H4 dimers are acetylated in their N-terminal tails in the cytoplasm by B-type histone acetyltransferases (HATs) (Jackson, Shires et al. 1976, Verreault, Kaufman et al. 1998). Although such acetylation is critical for incorporation of H3/H4 into chromatin, knockout of the only known B-type HAT in *S. cerevisiae*, Hat1, does not have any significant impact (Kleff, Andrulis et al. 1995). ASF1 (anti-silencing factor 1) binds to the H3/H4 dimer and transports it into the nucleus via importin-4 (Agez, Chen et al. 2007, Jasencakova, Scharf et al. 2010). Inside the nucleus, histones are assembled in chromatin under different conditions by different histone chaperones. CAF-1 (Chromatin assembly factor 1) deposits H3/H4 onto newly synthesized DNA. Although the exact mechanism is not fully understood, CAF-1 is recruited to the newly synthesized DNA by PCNA (proliferating cell nuclear antigen), the DNA polymerase processivity factor at the DNA replication foci (Shibahara and Stillman 1999). NAP1 (nucleosome assembly protein 1) associates with H2A/H2B dimers (Ito, Tyler et al. 1997) and the complexes enter the nucleus during the G1-S phase transition, to then assemble H2A/H2B dimer in nucleosomes. The disassembly of nucleosomes reverses the assembly process.

Nucleosome disassembly and reassembly during DNA repair are similar as during DNA replication (Linger and Tyler 2007). During nucleotide excision repair, CAF-1 and PCNA couple at the nucleotide excision repair site, where CAF-1 and Asf1 mediate

chromatin assembly bidirectionally (Gaillard, Martini et al. 1996, Gaillard, Moggs et al. 1997). Chromatin assembly at double strand breaks (DSB) during DNA repair is less understood. Nonetheless, CAF-1 is known to be also recruited to the double strand break sites created by N-methyl-N'-nitro-N-nitrosoguanidine (Jiao, Bachrati et al. 2004) or bleomycin (Nabatiyan, Szuts et al. 2006), and Asf1 mutant yeast strains are more sensitive to DSB inducing agents (Linger and Tyler 2007).

Transcription is another process that uses DNA as a template. When the DNA is regularly chromatinized both in the promoter and gene body, transcription initiation is inhibited (Knezetic and Luse 1986, Lorch, LaPointe et al. 1987). The promoters of highly transcribed genes are usually DNAse hypersensitive (McGhee, Wood et al. 1981). However, these promoters are still chromatinized (Steger and Workman 1997), and the DNAse hypersensitive sites also include non-transcribed genes (Ercan and Simpson 2004). Therefore, the chromatin status of the promoter of a gene does not directly correlate with its transcription activity.

Different levels of chromatin compaction and nuclear distribution have been noted for long time. Heterochromatin and euchromatin were defined originally as compacted DNA (more intense DNA dye signal) or less condensed DNA, respectively. Later, heterochromatin was classified into constitutive and facultative (Brown 1966). Heterochromatin or euchromatin domains were proposed to provide local environments suitable for regulation of gene transcription (Xin, Liu et al. 2003). Other studies have

revealed that hetero or euchromatin do not correlate well with the locations of genes at the chromosome level. For example, human satellite DNA alpha and satellite 2 were exclusively found in heterochromatin, whereas some of the satellite 3 was in euchromatin, even though none of these three satellite DNAs encode genes or are transcribed under normal conditions (Gilbert, Boyle et al. 2004). Gene transcription also has limited correlation with heterochromatin or euchromatin. Differential fractionation of eukaryotic genomes indicated that many transcriptional inactive genes are in euchromatin, and active ones in heterochromatin (Gilbert, Boyle et al. 2004). Therefore, it was proposed that open or compact chromatin domains rather provide landscapes that facilitate transcriptional activities but do not directly regulate transcription (Gilbert, Boyle et al. 2004).

1.3.3 Insulator elements and chromatin

There are no membrane-associated boundaries inside nuclei. The open or compact chromatin landscape is thus maintained by other mechanisms. Interestingly, the borders between heterochromatin and euchromatin are sharp rather than gradual (Gilbert, Boyle et al. 2004).

Insulator elements are DNA sequences characterized by their abilities of acting as enhancer-blocking or function as barrier shielding genes from position-effect variegation (Dorman, Bushey et al. 2007). Insulators were discovered in Drosophila variegation and block interactions between enhancers and promoters. Inserting a pair of the Drosophila

insulator Su(Hw) diminished its enhancer-blocking activity (Muravyova, Golovnin et al. 2001). Furthermore, fluorescence in situ hybridization (FISH) showed that two Su(Hw) formed DNA loops attaching to the nuclear matrix (Byrd and Corces 2003). Insertion of the insulator upstream of the promoter successfully blocked the enhancer-promoter interaction, as tested by the expression level of downstream reporter genes (Kellum and Schedl 1991). Insertion of a reporter gene near transcriptionally active genes should increase the transcription level of the reporter, and insertion near transcription inactive genes should decrease it as consequence of regulation by long-distance regulatory elements. However, the transcription level of the inserted reporter gene was not affected by its location when the gene was flanked by two insulator elements (Chung, Whiteley et al. 1993).

Insulators recruit insulator-binding proteins (IBPs). Although there are many IBPs in yeast, CTCF (CCCTC-binding factor) is the only IBP found in mammalian. IBP binding to the insulator blocks the interaction of regulatory elements such as, for example enhancers and silencer, with distant promoters. Interestingly, loss of enhancer-blocking activities by binding of dCTCF in two tandem copies of adjacent Su(Hw) insulators (Muravyova, Golovnin et al. 2001) was only observed when the two insulators were in opposite orientations (Kyrchanova, Toshchakov et al. 2008). Insulators also block spreading of histone marks. Chip-seq of the bithorax complex of Drosophila melanogaster PS7 cells revealed CTCF at many boundaries where levels of H3K27m

changes, although not at all of them (Bowman, Deaton et al. 2014). The proposed model was that CTCF is not sufficient to limit the spread of histone modifications in the entire genome. There are more than a dozen of IBPs in Drosophila, and others might likely participate in the regulation of the spread of histone modifications too. In mammalian cells CTCF is the only IBPs identified. Perhaps the role of CTCF in regulating spread of histone modifications genome-wide in mammalian cells is more important than in Drosophila. CTCF also forms chromatin loops when acting with cohesin. CTCF can establish long-distance enhancer-promoter interactions (even for enhancers that are > 1Mb away) and establish chromatin topologically associated domains (TADs) by chromatin looping.

TADs are captured by Hi-C, which evaluates the crosslinking frequencies between distant genomic loci as a proxy of their positions in 3D space (Ozdemir and Gambetta 2019). CTCF bound to pairs of convergently oriented CTCF-binding sites was enriched at the boundaries of TADs (Rao, Huntley et al. 2014, Sanborn, Rao et al. 2015, Fudenberg, Imakaev et al. 2016). Deletion of one convergently oriented binding site in the mouse alpha globin gene resulted in extension of the loop until the next available convergently oriented binding site (Hanssen, Kassouf et al. 2017). Reinsertion of the CTCF binding site convergently, but not the oppositely oriented binding site, re-established the chromatin loop (de Wit, Vos et al. 2015).

1.3.4 ATP-dependent chromatin remodeling

ATP-dependent chromatin complexes can slide an octamer across the DNA, alter the composition of the octamer with histone variants, partially disassembly the octamer, make the nucleosomal DNA more accessible while still associated with the octamer, or evict the octamer from the DNA (Fig 5). The different families of remodeling complexes are named by their ATPase subunits. These families include SWI/SNF, INO80, ISWI, and CHD (Becker and Workman 2013).

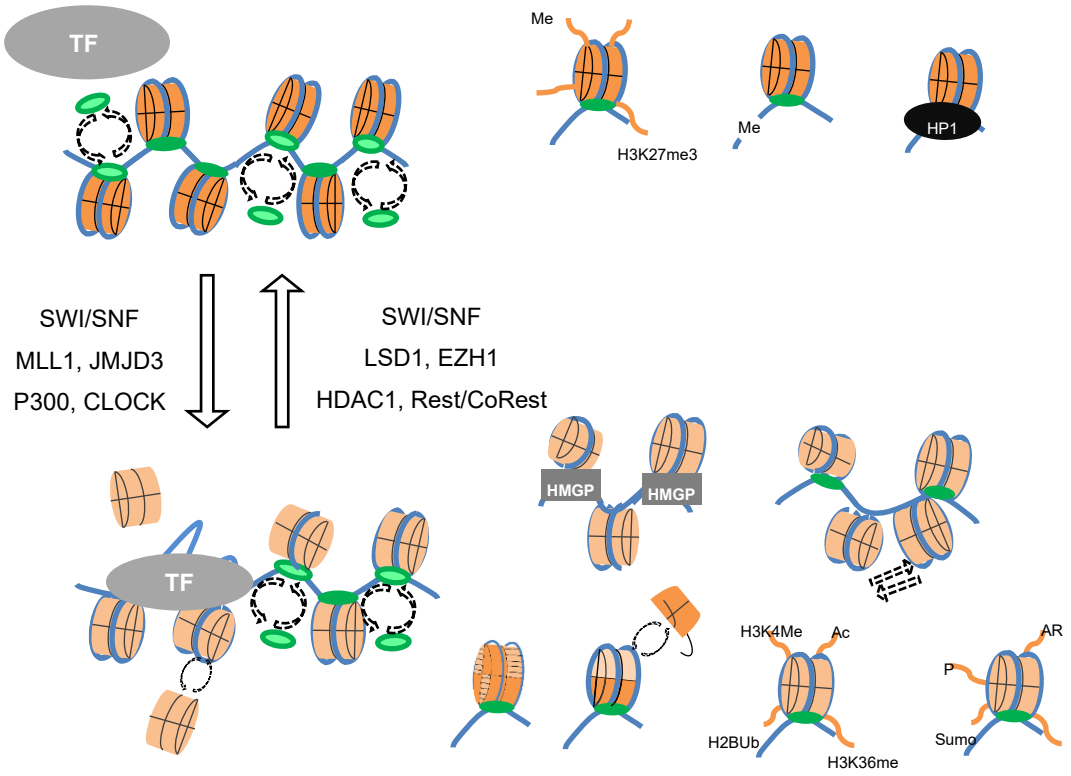

Figure 5: Cartoon representation of common epigenetics regulation between compact, less dynamic chromatin and open, dynamic chromatin. (Schang, Hu et al. 2021). Figure used under CC-BY 4.0 license.

The ATPase subunits of the SWI/SNF complexes include a post HSA (helicase

SANT (Swi3, Ada2, N-cor, and TFIIB)-associated) and HSA domain, two RecA-like lobes with an insertion in between, an Snf2 ATP coupling domain (Snf2 ATP coupling), an AT hook, and a bromo domain. The ATPase subunit of the ISWI complexes include an autoinhibitory N-terminal domain, two RecA-like lobes with insertion, negative regulator of coupling domain, and a four helicase SANT slide domain. The ATPase of the CHD complexes contain a chromo domain, a PHD (plant homeodomain) finger, RecA-like lobes, and a SANT slide domain. Finally, the ATPase subunit of INO80 complexes contain a HSA/post HSA domain, and two RecA-like lobes with a long insertion (Fig 6) (Bracken, Brien et al. 2019).

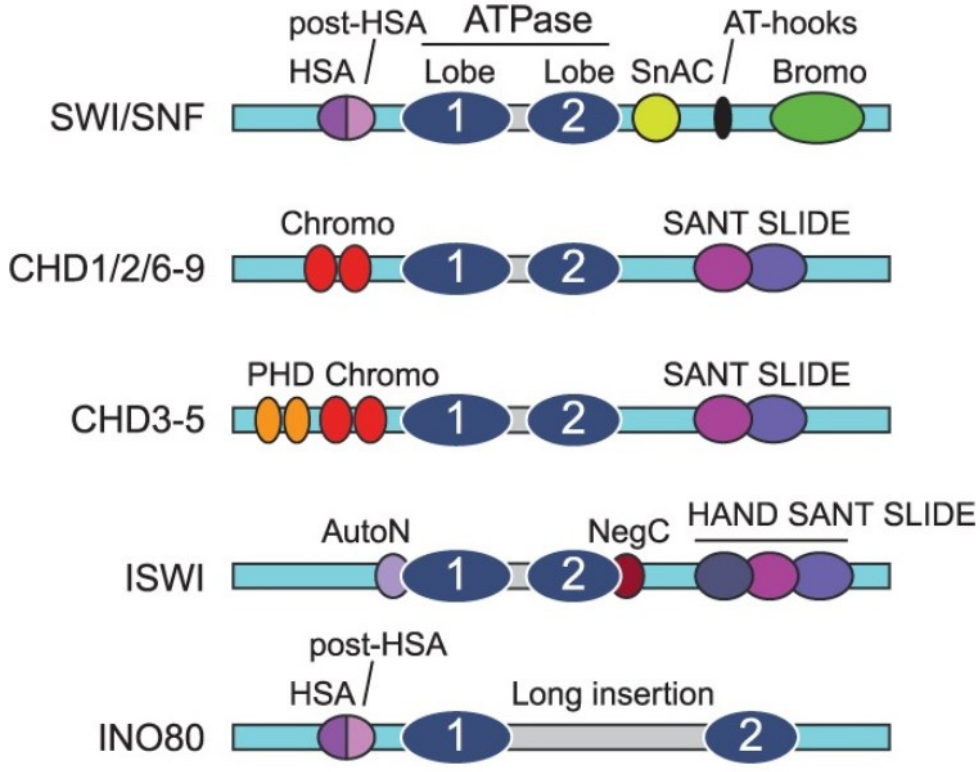

Figure 6: Domains of the ATPase subunits of SWI/SNF, CHD, ISWI, and INO80. From (Bracken, Brien et al. 2019). Doi: 10.1101/gad.326066.119. Figure used

Although the catalytic subunits of these families are different, the ATP-driven DNA translocation mechanism is similar (Bracken, Brien et al. 2019). The ATPase subunit binds to the position 2 of the nucleosome. Before ATP binding, the two Walker motifs of the lobe 1 are placed distantly from lobe 2 (open state). ATP binding causes conformational changes that pushes the two Walker motif towards lobe 2 (close state), and hydrolysis of the ATP relaxes the Walker motifs letting them return to the open state. Each ATP hydrolysis causes translocation of one DNA basepair (Clapier, Iwasa et al. 2017, Li, Xia et al. 2019). The non-catalytic subunits of the remodeling complexes interact with histone H2A/H2B dimers with the linker histone H1 of the same nucleosome, to prevent movement of the remodeler during the DNA translocation (Clapier, Iwasa et al. 2017, Li, Xia et al. 2019).

The diversity of the subunits of each chromatin remodeler complexes results in their different specific roles in regulating chromatin. Many of the ISWI subfamily and some of the CHD subfamily complexes are responsible for evenly spacing nucleosome in the typical arrays. SWI/SNF often increases DNA accessibility, whereas CHD often decreases it (Bracken, Brien et al. 2019).

1.3.4.1 SWI/SNF

The name SWI/SNF comes from screening genes involved in mating type switching (SWI), or sucrose fermentation (SNF) in *Saccharomyces cerevisiae* (Neigeborn and

Carlson 1984, Stern, Jensen et al. 1984, Abrams, Neigeborn et al. 1986). It describes a family of remodelers. Two of the most abundant SWI/SNF subfamilies in mammalians are BAF (SWI/SNF in yeast) and PBAF (RSC in yeast). Their main ATPase subunits are BRG1 or hBRM for BAF and BRG1 for PBAF. The subunits ARID1A/B and DPF1/2/3 are only found in BAF whereas the subunits polybromo (PBRM1), BRD7, ARID2, and PHF10 are found in PBAF(Fig 7) (Bracken, Brien et al. 2019).

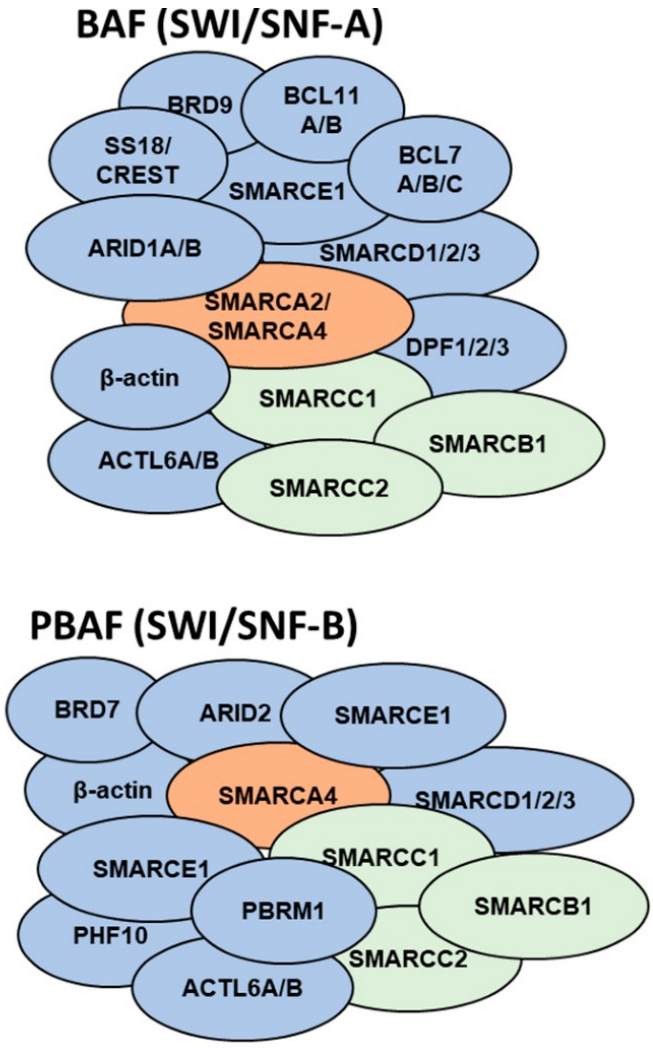

Figure 7: Complexes of human SWI/SNF (BAF and pBAF). From (Hasan and Ahuja 2019) doi.org/10.3390/cancers11121859. Figure used under CC-BY 4.0 license.

Transcription of the HO gene is restricted in yeast with functionally null SWI/SNF. However, mutations in the histones H3 and H4 at the DNA binding residues, or mutations of the interface of H2A-H2B dimer that disrupts chromatin, partially restore transcription (Kruger, Peterson et al. 1995). SWI/SNF also increased the binding of GAL4 to nucleosome DNA in the presence of ATP (Cote, Quinn et al. 1994, Kwon, Imbalzano et al. 1994). Purified BRG1/hBRM disrupts *in vitro* mono- and poly-nucleosome arrays in the presence of ATP, but less so than complete SWI/SNF complexes (Phelan, Sif et al. 1999). Although BRG1/hBRM are the main ATPases, the other subunits are also critical. Through global mapping of binding sites using ChIP-Seq, SWI/SNF was mapped mostly to genomic regions excluding histone H3K27me3 (a marker of repression of transcription), with few exceptions (Euskirchen, Auerbach et al. 2011). Sixty percent SWI/SNF complexes contained at least one of the three subunits, INI1, BAF155 or BAF170. Sixty seven percent of the SWI/SNF complexes containing these three subunits were bound close to RNA Pol II, whereas 43% of those contain only one or two of them bound close to predicted enhancers. These results suggest that SWI/SNF containing these three subunits are coupled with activation of transcription whereas SWI/SNF with one or two of these subunits are more likely involved in enhancer related transcription regulation (Euskirchen, Auerbach et al. 2011). Nonetheless, more than 90% of the SWI/SNF binding sites were coupled with at least a

CTCF (17%), a predicted enhancer (43%), or RNA Pol II (40%) binding sites (Euskirchen, Auerbach et al. 2011). The non-catalytic SWI/SNF subunits are important in determining the functions of the complex. Both SWI/SNF and RSC (PBAF in human) generate “nucleosome free” regions (NFRs). However, SWI/SNF generated NFRs were on average 50 bp shorter than those in transcriptionally active genes, whereas RSC generated NFRs equal of size in transcriptionally active genes on *in vitro* assembled chromatin (Krietenstein, Wal et al. 2016).

As SWI/SNF remodels chromatin, it is involved in many DNA-dependent processes. SWI/SNF is required for the proper function of the yeast replication origin ARS121 (autonomously replicating sequence), but not of other ARS tested (Flanagan and Peterson 1999). It is hypothesized that the binding site for yeast transcription factor ABF1 keep other ARS nucleosome free, whereas ARS121 does not contain ABF1 binding sites (Flanagan and Peterson 1999). Mutation of the ABF1 site in ARS1 increased the requirement for SWI/SNF (Flanagan and Peterson 1999). SWI/SNF complexes also co-localized near replication origins in HeLa cells. Through ChIP-Seq, 32% of the replication origins were within 100 bp of a SWI/SNF binding sites (Euskirchen, Auerbach et al. 2011).

SWI/SNF also plays a role in DNA repair. SWI/SNF deficient yeast was more sensitive to DNA damage induced by doxorubicin, cisplatin, or UV or IR light (Chai, Huang et al. 2005, Park, Park et al. 2006, Xia, Jaafar et al. 2007, Lans, Marteijn et al.

2010, Kothandapani, Gopalakrishnan et al. 2012, Watanabe, Ui et al. 2014). BRM and BRG1 co-localized to IR-induced DSB sites with histone H2A.x through ATM (Park, Park et al. 2006). BRG1 also binds to H2A.x containing nucleosomes by interacting with acetylated histone H3 (Lee, Park et al. 2010). Histone H2B phosphorylated by AMP-activated protein kinase and H3 and H4 histone acetylation by CBP/P300 recruit BRM to the DSB sites (Ogiwara, Ui et al. 2011, Ui, Ogiwara et al. 2014). SWI/SNF also increased DNA accessibility, and thus increased nucleotide excision repair in mononucleosomes with DNA damaged through UV or cisplatin in vitro (Hara and Sancar 2002, Gaillard, Fitzgerald et al. 2003).

1.3.4.2 ISWI

ISWI (imitation switch) was first identified in *Drosophila melanogaster*. It is a helicase with homology to the yeast Swi2/Snf2 gene. Mammalian ISWI contains two ATP-dependent helicases, SNF2H and SNF2L, in complexes with two to seven subunits per complex. ISWI complexes are thus classified as cat eye syndrome critical region protein-containing remodeling factors (CERF) (SNF2L, HSS, bromodomain, CECR2), NURF (SNF2L, retinoblastoma-binding protein 46 and 48 - RbAP48, RbAP46, HSS, DTT, BPTF, bromodomain, and PHD), CHRAC (SNF2H, HSS, WAC, DTT, Acf1, bromodomain, PHD, CHRAC15, and CHRAC17), ACF (SNF2H, HSS, WAC, DTT, bromodomain, Acf1, and PHD), WICH (SNF2H, HSS, WAC, DTT, WSTF, bromodomain, and PHD), NoRC (SNF2H, HSS, DTT, MBD, Tip5, bromodomain, and PHD), and

remodeling and spacing factor (RSF) (SNF2H, HSS, RSF1, PHD) (Bartholomew 2014). Yeast ISWI complexes, which contain Isw1 or Isw2 as their helicases, are classified into ISW1a (Isw1, HSS, and Ioc3), ISW1b (Isw1, HSS, Ioc2, Ioc4, and Pro-Trp-Trp-Pro domain protein - PWWP), and ISW2 (Isw2, HSS, Imitation switch two complex 1 (Itc1), WAC, DTT, DNA polymerase B subunit 4 (Dpb4), and Dpb3-like subunit of ISW2/yCHRAC complex 1 (Dls1) (Fig 8) (Bartholomew 2014).

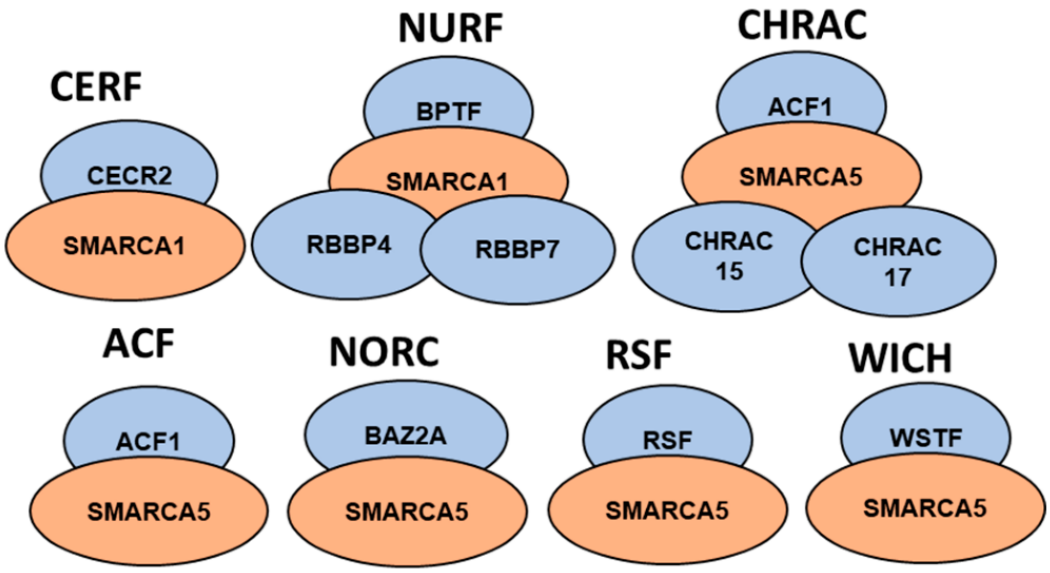

Figure 8: Complexes of ISWI. From (Hasan and Ahuja 2019). doi.org/10.3390/cancers11121859. Figure used under CC-BY 4.0 license.

Yeast ISW2 repositions nucleosomes towards the nucleosome free regions in the promoters to prevent RNA Pol II dependent transcription (Whitehouse, Rando et al. 2007, Zentner, Tsukiyama et al. 2013). It also attenuates S phase checkpoint activity (Au, Rodriguez et al. 2011). ISW1b interacts with histone H3K36me3 in the gene bodies

to promote reassembling of chromatin after transcription (Tirosh, Sigal et al. 2010, Maltby, Martin et al. 2012, Smolle, Venkatesh et al. 2012). ISW1a and b also regulate RNA Pol II elongation and proper termination, respectively (Morillon, Karabetsou et al. 2003). The *Drosophila* ACF complex assembles regularly spaced nucleosomes via the histone chaperone Nap1 (Fyodorov and Kadonaga 2002, Torigoe, Urwin et al. 2011). RSF assembles centromeric chromatin with histone H3 variant CENP-A (Perpelescu, Nozaki et al. 2009). The non-catalytic subunit Acf1 (found in ACF and CHRAC complexes), and CHRAC14 and 16 increase nucleosome sliding (Eberharter, Ferrari et al. 2001, Bonaldi, Langst et al. 2002, Eberharter, Vetter et al. 2004, Hartlepp, Fernandez-Tornero et al. 2005). The non-catalytic subunit NURF301 (BPTF in mammalians) was proposed to modulate the nucleosome mobilization properties of the NURF complex, changing it from pushing nucleosomes toward the end of DNA fragments to moving them towards the center (Langst, Bonte et al. 1999, Brehm, Langst et al. 2000).

Binding of ISWI complexes to chromatin is also epigenetically regulated. Histone H3K4me3 recruits ISWI complexes via their PHD domain, and it is also required for Isw1 to correctly position RNA Pol II (Santos-Rosa, Schneider et al. 2003, Wysocka, Swigut et al. 2006). The Histone H2A variant H2A.Z increases the chromatin remodeling ability of all human ISWI complexes (Goldman, Garlick et al. 2010). Macro H2A was proposed instead to decrease ACF complex binding to chromatin (Angelov, Molla et al.

2003). Moreover, histone H4K12 and K16 acetylation reduces ISWI chromatin remodeling by decreasing the rate of ATP hydrolysis (Clapier, Langst et al. 2001, Clapier and Cairns 2012).

1.3.4.3 INO80

INO80 was identified in yeast as a regulator of inositol-responsive gene expression (Ebbert, Birkmann et al. 1999). INO80 is further classified into Swr1 in yeast or, Snf2 related CREB-binding protein activator protein (SRCAP), in mammals and Ino80 (p400). INO80 complexes are proposed to regulate nucleosome spacing (Yen, Vinayachandran et al. 2012, Gerhold and Gasser 2014), and modulate transcription (Morrison and Shen 2009, Hogan, Aligianni et al. 2010). Knockout of INO80 in yeast or its RNAi knockdown in HeLa cells caused dysregulation of approximately 15% of the genes, half of which was upregulated and the other half, downregulated (Cao, Ding et al. 2015, Yao, King et al. 2016). INO80 was preferentially recruited to chromatin templates with a 20 bp longer linker DNA compared to regularly spaced nucleosomes (Mavrich, Ioshikhes et al. 2008), and it was found in about 90% of the nucleosome free regions at the TSSs and TTSs in yeast (Yen, Vinayachandran et al. 2013). *In vitro*, INO80 recognizes and establishes NFRs differing from RSC, ISW2, and ISW1a (Fig 9) (Krietenstein, Wal et al. 2016).

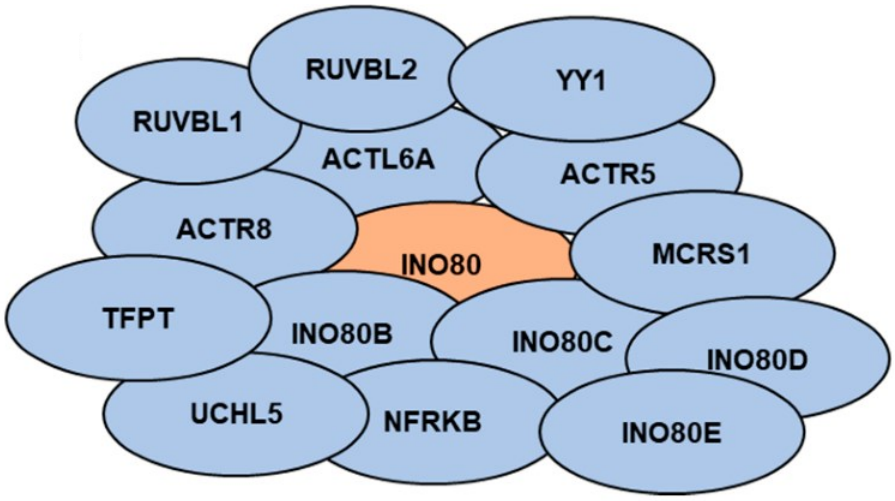

Figure 9: Complexes of INO80. From (Hasan and Ahuja 2019). doi.org/10.3390/cancers11121859. Figure used under CC-BY 4.0 license.

Swr1 is an ATPase of the SWR1 remodeling complex. SWR1 exchanges histone H2A.Z/H2B dimers with canonical H2A/H2B ones (Mizuguchi, Shen et al. 2004). Either free H2A.Z or canonical H2A containing nucleosomes increase Swr1 ATPase activity (Luk, Ranjan et al. 2010). INO80 related repression of transcription may be accounted to by inhibition of H3K79 methylation, which negatively affects RNA polymerase elongation (Xue, Van et al. 2015).

1.3.4.4 CHD

The chromodomain helicase-DNA binding (CHD) complexes contain an chromodomain, Snf2-like helicase, a DNA-binding domain, and other subunits (Jones, Cowell et al. 2000). CHD1 and 2 are classified into the CHD subfamily I, containing a DNA binding domain with preference for AT-rich sequences (Delmas, Stokes et al.

1993). DNA binding occurs through minor groove interactions (Stokes and Perry 1995). CHD1, with chaperone Nap1, is proposed to assemble nucleosomes onto DNA, and also to promote regular spacing between them (McKnight, Jenkins et al. 2011). It is also proposed to disassemble nucleosomes at promoter regions (Walfridsson, Khorosjutina et al. 2007). Drosophila CHD1 assembles histone H3.3 onto chromatin, too (Konev, Tribus et al. 2007). Human CHD1, but not yeast CHD1, binds to histone H3K4me2/3 through its chromodomains (Sims, Chen et al. 2005). Interestingly, depletion of yeast CHD1 chromodomain does not affect binding of histone H3, and recruitment of yeast CHD1 is independent of the methylation status of histone H3K4 (Morettini, Tribus et al. 2011).

CHD3 and 4 are classified as subfamily II. They are ATPases of the deacetylase NuRD (nucleosome remodeling and histone deacetylation) complex, which is recruited to promoters (Murawska and Brehm 2011). Histone H3K4 methylation reduces NuRD recruitment (Zegerman, Canas et al. 2002). NuRD is also recruited to chromatin containing methylated DNA through its MBD2 (methyl-CpG-binding proteins) subunit (Zhang, Ng et al. 1999). When bound at DNA methylated sites, it represses transcription (Feng and Zhang 2001). The NuRD complexes was not recruited to the nucleus of MBD2 knockout *Drosophila* embryo, in which the overall DNA methylation level is low (Fig 10) (Marhold, Kramer et al. 2004).

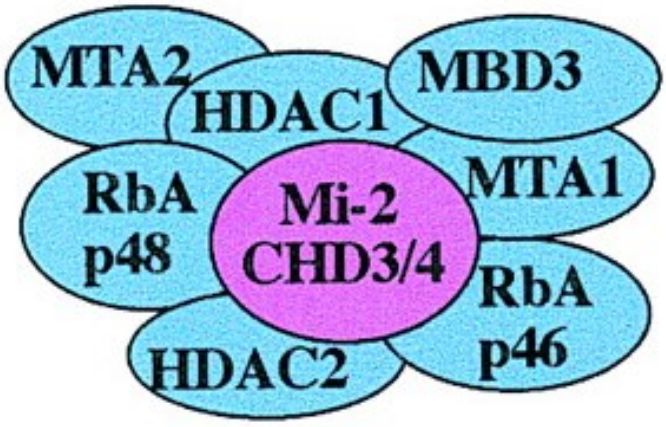

Figure 10: Complexes of the NuRD complex of CHD3/4. From (Kingston and Narlikar 1999). DOI: 10.1101/gad.13.18.2339. *Figure used under CC-BY 4.0 license.*

NuRD complexes perform ATP-dependent chromatin remodeling and histone deacetylation. Their ability to remodel chromatin is independent of their deacetylase activities, and thus histone deacetylase inhibitors have no impact on NuRD-dependent nucleosome sliding. In contrast, their ATPase activities stimulate their histone deacetylase activity (Tong, Hassig et al. 1998). The underlining model is that the deacetylase activity requires first the chromatin to be remodeled to become accessible (Tong, Hassig et al. 1998). Histone deacetylases generally associate with repressive chromatin. Consistently, NuRD is recruited to silencing chromatin containing histone H3K9me3 and heterochromatin protein HP1 (Schultz, Friedman et al. 2001).

CHD5 to 9 are classified in subfamily III, characterized by having additional non conserved functional motifs. Some members contain PHD domains or chromodomains

similar to those in the CHD classified in subfamily II (Murawska and Brehm 2011). CHD7 ChIP-Seq indicated its enrichment at DNAse I hypersensitive sites, together with histone H3K4me, as a marker for enhancers (Schnetz, Bartels et al. 2009). CHD7 binds via its chromodomain to H3K4me1, 2, and 3 *in vitro* (Schnetz, Bartels et al. 2009). CHD7 is enriched at enhancers. One possible function of CHD7 is to indirectly loop enhancers to the TSSs, as it also co-localizes near the promoters of active genes (Schnetz, Bartels et al. 2009). Although the exact mechanism of regulation of transcription by CHD7 is not fully understood, it interacts with many remodeling complexes such as BAF and PBAF (Schnetz, Bartels et al. 2009).

CHD8 also binds to the enhancers of genes induced by the androgen receptor (AR) in prostate cancer cells. Depletion of CHD8 reduces AR binding and, consequently, inhibits transcription of the AR-responsive genes (Menon, Yates et al. 2010).

1.3.5 Chromatin regulation of transcription before pre- initiation

Chromatin immunoprecipitation and high-resolution microarrays and sequencing studies showed that most RNA polymerase II promoters in yeast contain an apparently “nucleosome-free” region, which is DNAse hypersensitive and provides sites for transcription factor binding (Yuan, Liu et al. 2005). The apparent nucleosome-free region is flanked by two deacetylated nucleosomes with the histone H2A variant, H2A.Z (Liu, Kaplan et al. 2005, Raisner, Hartley et al. 2005). The transcriptional competent genes (those with the apparent nucleosome-free region flanked by H2A.Z containing

nucleosomes in the promoters) are proposed to then recruit chromatin remodelers. The remodelers remove two H2A/H2B dimers to NAP1 and two H3/H4 dimers to Asf1. After this remodeling, the preinitiation complexes are recruited (Workman 2006). Ras-proximate-1 or Ras-related protein 1 (Rap1) (Yu and Morse 1999) and RNA polymerase I enhancer Binding Protein 1 (Reb1) (Raisner, Hartley et al. 2005) are the two chromatin remodelers that generate the apparent nucleosome-free region flanked by the nucleosomes containing H2A.Z. Although the mechanisms are not fully understood, “pioneer factors” may recognize, and bind to, their consensus DNA sequences in fully chromatinized DNA. Pioneer factors are studied mostly during development, which involves the activation of previously fully silenced genes.

The pluripotency pioneer factors Oct3, Sex Determining region Y-box 2 (Sox2) and Kruppel-Like Factor 4 (Klf4) are recruited to fully chromatinized DNA, where they initiate chromatin remodeling by introducing chromatin remodelers that increase levels of H3K4me1/2 at the enhancers and H3K4me2/3 at the transcription starting sites (Koche, Smith et al. 2011). Oct3, SOX2 or Klf4 do not bind to H3K9me3 enriched chromatin (Koche, Smith et al. 2011, Soufi, Donahue et al. 2012). Other potential pioneer factor, Forkhead box protein A (FoxA), binds nucleosome DNA and opens compacted chromatin (Cirillo, McPherson et al. 1998, Cirillo, Lin et al. 2002). PU-binding protein 1 promotes nucleosome depletion in heterochromatin (Heinz, Benner et al. 2010). Early B-cell factor 1 (EBF1) increases H3K4me2 at heterochromatin of the

enhancers (Gyory, Boller et al. 2012). Basic helix-loop-helix protein 1 (bHLH) increases H3K4me1 and H3K27ac during artificial fibroblast reprogramming into neurons (Wapinski, Vierbuchen et al. 2013). All these pioneer factors bind to fully chromatinized DNA and increase its accessibility (Mayran and Drouin 2018).

The ability of the pioneer factors to destabilize chromatin results from their recruitment of chromatin remodelers. Paired box 7 (Pax7) increases H3K27ac at enhancers by recruiting p300 (Mayran and Drouin 2018). Oct4 co-localizes with the SWI/SNF complexes to the enhancers (de Dieuleveult, Yen et al. 2016). The open enhancers then recruit, for example, more histone remodelers, including the ATP dependent chromatin remodelers SWI/SNF, NuRD, ISWI, and INO80, to further remove nucleosomes from the promoters. Chromatin remodelers play important roles in regulating transcription, remodeling chromatin by incorporating histone variants, modifying histone tails, or by ATP dependent nucleosome repositioning.

1.3.6 Chromatin regulation of transcription initiation

After the promoter chromatin is opened, the transcription pre-initiation complexes (PIC) are recruited. TATA box binding protein (TBP), TFIIB, TFIIF, TFIIE and TFIIH are the essential components of the RNA polymerase II pre-initiation complexes. TBP is key in PIC formation. It recognizes the TATA box, which is normally 30 bp upstream of the transcription starting site (TSS) (Ponjavic, Lenhard et al. 2006), and slightly bends the DNA upon binding (Kim, Nikolov et al. 1993). TFIIB binds DNA elements adjacent to the

TATA box (B recognition element, BRE), and interacts via different domains with both TBP and RNA polymerase II (Sainsbury, Niesser et al. 2013). TFIIF is a RNA Pol II binding factor that recruits RNA Pol II into the PIC (Sopta, Carthew et al. 1985); it also stabilizes TFIIB (Chen, Jawhari et al. 2010, Eichner, Chen et al. 2010). The role of TFIIE is not entirely clear. It enhances transcription of supercoiled DNA *in vitro* in the absence of TFIIH, suggesting that TFIIE plays a role in unwinding DNA (Timmers 1994, Holstege, Tantin et al. 1995). TFIIH is a DNA helicase complex containing two helicases, Xeroderma Pigmentosum Type B/D (XPB and XPD), and a two subunit kinase that phosphorylates the CTD of RNA pol II, Cdk7 and cyclin H. Partial PIC RNA Pol II is also observed in yeast (Zanton and Pugh 2006). The partial PICs contain no TFIIH or RNA Pol II and, interestingly, the nucleosomes are not displaced (Zanton and Pugh 2006). In contrast, complete PICs formation is coupled with increased histone acetylation and decreased histone occupancy in the promoter of the yeast phosphatase PHO5 gene (Deckert and Struhl 2001, Boeger, Griesenbeck et al. 2004, Adkins and Tyler 2006). The histone acetyltransferases Gcn5 and Esa1 are recruited to the PHO5 promoter to activate transcription (Robert, Pokholok et al. 2004).

1.3.7 Chromatin regulation of transcription elongation

Transcription elongation can start after the complete assembly of the initiation complexes. After the recruitment of the transcription elongation factors through the C-terminal domain of RNA Pol II, Ser5 and Ser2 are phosphorylated by the CDK7/cyclin H

kinase in TFIIH (Li, Carey et al. 2007). One of the elongation factors, PAF, is responsible for recruitment of chromatin remodelers to remodel chromatin during ongoing transcription. PAF recruits the H3K4 methyltransferase Set1 and stabilizes the association of Rad6, which ubiquitinates histone H2B nearby (Sun and Allis 2002, Krogan, Dover et al. 2003, Ng, Robert et al. 2003).

1.3.8 Histone variants

Histone variants are non-canonical histones that sometimes substitute the core canonical histones in chromatin. Some histone variants are expressed outside of S phase and, consequently, are incorporated into chromatin also via DNA replication-independent mechanisms (Li, Carey et al. 2007). The histone H3 variant H3.3 differs from canonical H3.1 only in five amino-acids. These five differences include a substitution of Ala to phosphorylatable Ser or Thr, and three other substitution in the major histone binding domain (Bano, Piazzesi et al. 2017). H3.3 is incorporated into chromatin by the HIRA (Tagami, Ray-Gallet et al. 2004) or Daxx/Atrx complexes (Banaszynski, Wen et al. 2013). Although H3.3 is in both active transcribed and silenced genes, the H3.3/H4 complex is more dynamic than the canonical H3/H4. Knockdown of histone H3.3 consequently decreases histone turnover and HIRA chromatin binding (Pchelintsev, McBryan et al. 2013), suggesting that the overall role of H3.3 is to increase chromatin dynamics (Weber and Henikoff 2014).

CENP-A is another histone H3 variant, which associates with the centromeric DNA.

CENP-A is larger than canonical H3 (17k Da and 14k Da, respectively), and it is incorporated into CENP-A nucleosomes in the centromeres. The crystal structure of a CENP-A histone octamer reveals a structure similar to those assembled with canonical H3 octamers (Tachiwana, Kagawa et al. 2011). CENP-A containing chromatin is generally thought to be mostly heterochromatin. Centromeric chromatin contains silencing marker H3K9me3 (Peters, Kubicek et al. 2003), and CENP-A is stably associated within the chromatin, even though some centromeric genes are transcribed (Topp, Zhong et al. 2004).

Histone H2A has seven major variants. H2A.Z is about 60% similar at the amino acid level to canonical H2A (Zlatanova and Thakar 2008). The overall structure of H2A.Z containing histone octamer is similar to that of the ones containing canonical H2A, except for an extra acidic patch provided by H2A.Z (Suto, Clarkson et al. 2000). H2A.Z nucleosomes are more dynamic than those assembled with canonical H2A, particularly if they also include H3.3. H2A.Z is incorporated into chromatin by NAP1 or by Chz1 (a specific H2A.Z chaperone), which incorporates H2A.Z preferentially over H2A (Luk, Vu et al. 2007). H2A.Z associates with both actively transcribed and silenced chromatin. However, it becomes specifically deposited at the sites flanking the “nucleosome-free” regions of the promoters, discussed above. The so called “nucleosome-free” region was actually assembled into H2A.Z/H3.3 containing nucleosomes (Henikoff 2009). H2A.Z enriched chromatin negatively correlates with DNA methylation (Conerly, Teves et al.

2010).

The Histone H2A variant H2A.B is about 50% similar to canonical H2A. High order chromatin structures are inhibited in H2A.B containing chromatin (Zhu, Zhou et al. 2007), and H2A.B exchange faster than canonical H2A (Bao, Konesky et al. 2004). Incorporation of H2A.B thus increases chromatin dynamics. H2A.B is deposited by NAP1. H2A.B is preferentially enriched on the gene bodies of actively transcribed genes (Tolstorukov, Goldman et al. 2012) whereas it is specifically excluded from the inactivated copy of the X chromosome in females (the barr body) (Chadwick and Willard 2001). H2A.B is enriched in the promoters and depleted in the gene bodies of actively transcribed genes in mouse testis (Nekrasov, Amrichova et al. 2012). However, mouse contain three histone H2A.B variants (H2A.B1 to 3), some of which are expressed specifically in the testis (Ishibashi, Li et al. 2010).

Macro H2A is about 42k Da and contains a nonhistone globular domain. Nucleosomes containing macroH2A elute at higher salt concentrations than those containing canonical H2A (Weber and Henikoff 2014). MacroH2A is generally enriched in the transcriptionally inactive female X chromosome, and in large transcriptionally silent domains (Weber and Henikoff 2014). Although macroH2A is generally associated coupled with gene silencing and genes assembled in chromatin with macroH2A are often silenced, depletion of macroH2A does not usually upregulate their transcription (Weber and Henikoff 2014). MacroH2A inhibits IL8 transcription *in vitro*.

1.3.9 Histone modifications

Core histones contain a non-structured N-terminal tail that is exposed and heavily post-translationally modified (Fig 5). Histone acetyl transferases (HATs) catalyze the transfer of acetyl groups to histone lysine residues. Type A HATs acetylate histones in the nucleus and type B acetylate newly synthesized histones in the cytoplasm. The type A HATs include the GNAT and MOZ, Ybf2/Sas3, Sas2 and Tip 60 (MYST) containing complex families, as well as p300/CBP (Brosch, Loidl et al. 2008). GCN5, a member of the GNAT family, is often found as a subunit of large HAT complexes recruited to the promoters of actively transcribed genes.

The HDACs (histone deacetylases) catalyze the removal of acetyl groups from lysine residues. The HDACs are the sirtuins, the classical HDACs, and HD2-like enzymes (Brosch, Loidl et al. 2008).

The impacts of histone acetylation on chromatin are complex. High overall acetylation levels of histones H3 and H4 decrease the tendency of nucleosomal fibers to fold into compact structures (Garcia-Ramirez, Rocchini et al. 1995), and hyperacetylated chromatin is thus more sensitive to DNAse I (Hebbes, Clayton et al. 1994). Acetylation is also proposed to have local effects on transcriptionally competent (but not necessarily transcriptionally active) genes. The chromatin of the transcriptionally competent genes within a given domains, such as at the beta-globin locus, is often hyperacetylated. The genes inside these hyperacetylated domains are

either transcriptionally active or just competent, whereas the genes outside the domain are transcriptionally inactive and hypoacetylated (Vogelauer, Wu et al. 2000, Eberharter and Becker 2002).

Acetylation at specific histone residues might also have some limited impact on chromatin stability. Acetylated H3/H4 on promoters or enhancers is often recognized by chromatin remodelers and, consequently, triggers chromatin remodeling (Litt, Simpson et al. 2001). HATs are often recruited to the promoters. Many HATs are subunits in different complexes, and their impact on transcription often depends on the specific complexes (Brown, Lechner et al. 2000). VP16 recruits Spt-Ada-Gcn5 acetyltransferase (SAGA) to the IE promoters to acetylate histone H3 at those promoters, while it also recruits NuA4 to increase acetylation of histone H4 more globally, in a domain larger than 3k bp (Vignali, Hassan et al. 2000).

Whereas histone acetylation generally associates with increased chromatin dynamics, histone methylation can increase or decrease dynamics, functioning as markers of silencing or active transcription. Lysine residues could be mono-, di- or tri-methylated, while arginine residues can only be mono- or di-methylated. The histone methyltransferases (HMTs) are responsible for transferring methyl groups to histones, and the histone lysine demethylases (KDMs), for removing them.

Multiple methylations occur on one residue, unlike acetylation. Some HMTs (or KDMs) are thus specific for adding (or removing) one of the three possible methyl

groups. For example, KMT1A/B methylates H3K9me to H3K9me3 (Peters, Mermoud et al. 2002), whereas G9a methylates H3K9me to H3K9me2 (Tachibana, Sugimoto et al. 2002), and MLL1 demethylates unmethylated H3K4 (Carmen, Milne et al. 2002). Likewise, the KDM LSD1 (Lysine-specific demethylase 1A) demethylates H3K4me1/2 (Shi, Lan et al. 2004), JHDM1A/B demethylates H3K9me2 (Tsukada, Fang et al. 2006), and JMJD2 demethylates tri-methylated histones (Cloos, Christensen et al. 2006, Klose, Kallin et al. 2006, Kubicek, Schotta et al. 2006).

The roles of histone methylation in chromatin dynamics are complex. H3K4me3 and H3K9me3 are among the best characterized methylations, as markers of active or inactive transcription, respectively. H3K4me3 is enriched approximately 2000 bp back and forward from the transcription start sites of transcriptionally active or competent genes (such as those genes not transcribed during G0 but transcribed during G1) (Smith, Chronis et al. 2009, Smith and Denu 2009). H3K4me3 interacts with transcription associated factors 3 (TAF3) to facilitate RNA Pol II recruitment (Vermeulen, Mulder et al. 2007). H3K4me spread to approximately three thousand basepairs around the promoters, and often colocalizes with p300 and another marker of transcription activity, H3K27ac (Hon, Hawkins et al. 2009).

The roles of the enrichment of H3K4me2 on promoters are not fully understood. In contrast, promoters and gene bodies enriched in H3K9me2/3 are most often silenced. H3K27me2/3 is generally associated with silenced gene promoters and non-transcribed

gene bodies. In contrast, H3K27me is often enriched in the bodies of transcriptionally active genes, but such enrichment is depleted further away from the transcription start sites (TSS) (Bernstein, Duncan et al. 2006).

H3K36me is generally enriched at the gene bodies of transcriptionally active genes, specifically close to the TSS. H3K36me3 is enriched at the TSS of actively transcribed genes, and then depleted gradually through the gene bodies to approximately 2000 bp away (Hon, Wang et al. 2009). H3K79me2/3 (spreads approximately 500 bp backward and 1000 bp forward at the TSS) and H4K20me (spreads approximately 1000 bp towards 3') are both enriched in the gene bodies of transcriptionally active genes (Barski, Cuddapah et al. 2007), whereas H4K20me3 is enriched at the promoters of transcriptionally inactive genes (Hon, Wang et al. 2009).

The histones are also ubiquitylated. Ubiquitination involves three steps that finally conjugate ubiquitin to lysine residues. Poly-ubiquitylated proteins are often targeted for degradation, but mono-ubiquitylated histones are recognized by, or recruit, chromatin remodelers. About 5 to 15% of H2A, and 1 to 10% of H2B are ubiquitylated (Wright, Wang et al. 2012).

Mono-ubiquitylated H2B can induce H3K4 and H3K79 tri-methylation through Set1 and Dot1 (Briggs, Xiao et al. 2002, Dover, Schneider et al. 2002, Ng, Xu et al. 2002). H3K4 and K79 tri-methylation often associate with transcriptionally active genes, as discussed above and, therefore, H2B-Ubiquitin is generally considered to increase

chromatin dynamics. Indeed, H2B-Ubiquitin is enriched in the gene bodies of transcriptionally active genes (Dover, Schneider et al. 2002).

1.4 HSV-1 chromatin

1.4.1 Virion DNA

The HSV-1 DNA is not associated with histones inside the virion (Pignatti and Cassai 1980), where about 40% of the DNA negative charge is neutralized by the polyamine spermine (Gibson and Roizman 1971). This association with spermine aids to compact the HSV-1 DNA to fit into the capsid. In vitro, it also stimulates the enzymatic activities of the HSV-1 DNA polymerase purified from infected hamster kidney cells up to 2.5mM, although it is not clear if this activity is biologically relevant to HSV-1 (Wallace, Baybutt et al. 1980).

The encapsidated double strand DNA genomes have nicks and gaps (Kieff, Bachenheimer et al. 1971, Sheldrick, Laithier et al. 1973, Jacob and Roizman 1977), about 15 gaps of 30 bases long on average per genome (Smith, Reuven et al. 2014). The gaps are randomly distributed and their role, if any, remains unknown. Fixing the gaps with DNA T4 ligase did not impact the infectivity of transfected HSV-1 DNA (Smith, Reuven et al. 2014).

1.4.2 HSV-1 DNA-nuclear protein complexes during latency

Most studies of HSV-1 latency rely heavily on three models, of which the mouse is perhaps the most commonly used. Injection of HSV in the footpad would lead the

establishment of latency in spinal sensory ganglia, which is somewhat analogous to genital HSV infection in humans. Infection can also be performed at the eye, which results in establishment of latency in the trigeminal ganglia (Wagner and Bloom 1997). Latently infected spinal or trigeminal ganglia can later be excised, and used as a model of ex vivo latency and reactivation (Wagner and Bloom 1997). Other models that establish a latency-similar state in culture (quiescent infections) will be discussed in the next section.

Only the latency-associated transcript (LAT) accumulates to high levels in a subset of neurons during latency (Stevens, Wagner et al. 1987). The LAT primary RNA is about 8.3k bp long, and it is spliced producing two stable nuclear introns, about 1.5 and 2k bp (Wagner, Devi-Rao et al. 1988, Farrell, Dobson et al. 1991). The LAT RNAs are not translated (Drolet, Perng et al. 1998). It has been proposed that the LAT RNA may repress HSV-1 replication and IE genes transcription during latency or reactivation, as LAT null mutants of HSV-1 showed higher ICP4 mRNA levels than wt HSV-1 in latently infected or reactivated trigeminal ganglia (Chen, Kramer et al. 1997, Garber, Schaffer et al. 1997). LAT null mutant HSV-1 establishes about two- to three-fold fewer latent genomes compared to wt HSV, as indicated by the levels of expression of a green fluorescent protein reporter inserted downstream of the LAT promoter (Thompson and Sawtell 1997, Perng, Slanina et al. 2000). Consequently, LAT null mutations also resulted in lower levels of reactivation (Perng, Slanina et al. 2000). Transfection of LAT

into cells infected with LAT null HSV mutants did not alter reactivation, suggesting that LAT increases establishment of latency, but not reactivation, or neither (Thompson and Sawtell 1997). Knockout of LAT also decreased neuron survival. Infection with an HSV-1 strain 17 LAT null mutant resulted in more than 50% decrease in neuron survival, and four-fold decrease in the number of latently infected neurons (Thompson and Sawtell 2001).

During latency, the HSV-1 genomes are endless (Mellerick and Fraser 1987) and fully chromatinized with regularly spaced nucleosomes (Deshmane and Fraser 1989). The promoter of the LAT region is assembled into chromatin with higher levels of histones bearing markers of transcriptional active (H3K9ac, H3K4me2 and H3K14ac) than the promoter of the adjacent ICP0 gene (Kubat, Amelio et al. 2004, Kubat, Tran et al. 2004, Giordani, Neumann et al. 2008). The LAT transcript promotes enrichment in the repressive histone H3K9me3 in the chromatin of a subset of HSV-1 promoters (Wang, Zhou et al. 2005). CTCF and chromatin insulator-like elements close to the LAT promoter prevent the spread of the chromatin with repressive markers into the LAT region (Amelio, McAnany et al. 2006).

A particular insulator-like element has been studied the most, the CTRL2 (chromatin insulator elements between transcriptional active LAT and inactive ICP0 gene). CTRL2 blocks enhancer-promoter interactions when transfected into *Drosophila melanogaster* embryos, via CTCF binding to the CTCCC motif (Chen, Lin et al. 2007). Deletion of

CTRL2 did not impact HSV-1 DNA replication in neurons but it did inhibit reactivation from latency (Lee, Raja et al. 2018). CTRL2 deletion also increased H3K27me3 levels in the LAT promoter and intron during latency (Lee, Raja et al. 2018). CTCF binding to CTRL2 is dependent on LAT transcription, and is disrupted early during reactivation (Washington, Musarrat et al. 2018). Depletion of CTCF resulted in increased expression of ICP0 (which is adjacent to LAT) in latently infected rabbits (Washington, Edenfield et al. 2018). Furthermore, CTCF occupancy decreased during reactivation (Ertel, Cammarata et al. 2012). The levels of CTCF binding to different sites differ during latency and reactivation, and such differences are cell-type dependent and perhaps differentially regulated (Washington, Musarrat et al. 2018). The roles of CTCF during lytic infections will be discussed in the next section.

The levels of LAT RNA decrease upon reactivation, and so do the levels of the transcriptionally active markers H3K9ac and H3K14ac on the LAT promoter (Amelio, Giordani et al. 2006). Meanwhile, the total levels of acetylated histones in the chromatin of the ICP0 gene promoter increase (Amelio, Giordani et al. 2006). Inhibition of HDAC increases histone acetylation in the lytic genes and induces reactivation of HSV-1 from latency (Neumann, Bhattacharjee et al. 2007).

VP16, which recruits chromatin remodelers and activates transcription of IE genes during lytic infections, failed to induce reactivation (Sears, Hukkanen et al. 1991). It cannot prevent establishment of latency in sensory neurons either (Sears, Hukkanen et

al. 1991). Oct-1 levels are low (Hagmann, Georgiev et al. 1995) and HCF-1 is mostly at the Golgi in sensory neurons, which may play a role in the inhibition of transcription. Disruption of the Golgi results in accumulation of HCF-1 in nucleus (Kolb and Kristie 2008).

Some drugs that affect chromatin remodelers such as the HDAC inhibitors trichostatin A (TSA) or sodium butyrate (NaBu) reactivate latent virus (Neumann, Bhattacharjee et al. 2007). During HSV-1 17syn+ reactivation in mouse TG, sodium butyrate increases the levels of H3K9ac in as short time as 30min. It also increases the levels of H3K14ac at the promoter and exon coding region of LAT gene and on the promoters of ICP4 and ICP0 (Neumann, Bhattacharjee et al. 2007). Sodium butyrate also activates several HSV-1 promoters (LAT, ICP4, ICP0, ICP8, UL9, UL30 and UL10) by more than eight-fold in PC12 cells transiently transfected with HSV-1 promoter – CAT reporter constructs (Frazier, Cox et al. 1996).

TSA, a histone deacetylase inhibitor, activates the ICP0 promoter in infections of neurons with an ICP0 promoter – GFP reporter HSV-1 virus (Arthur, Scarpini et al. 2001). It also induces reactivation from latency in a LAT- independent (Ishihara and Sakagami 2005) manner (Danaher, Jacob et al. 2005). TSA and two more specific HDAC inhibitors, MS275 (which inhibits HDAC1) and MC1568 (which inhibits HDAC4) all induced reactivation in the presence of NGF (nerve growth factor), increasing the levels of ICP27, TK, VP16 and UL41 (Du, Zhou et al. 2013).

Activation of P300/CBP by CTB (N-(4-chloro-3-trifluoromethyl-phenyl)-2- ethoxy-benzamide) also increases ICP27, TK, and VP16 mRNA levels, and induces reactivation (Du, Zhou et al. 2013). Curcumin is a pleiotropic polyphenol that interacts non-specifically with proteins (Zhou, Beevers et al. 2011), binds to certain divalent metal ions (Fe, Cu, Mn, and Zn) (Baum and Ng 2004), and interacts with bilayer phospholipid membranes (Chen, Chen et al. 2012). As the consequences of its wide variety of molecular targets, curcumin causes many downstream cellular effects, one of them is the proteasome degradation of p300 and CBP but not PCAF and GCN5. Degradation of p300 reduces the mRNA of ICP27, TK, and VP16 at the absence of NGF (Du, Zhou et al. 2013).

siRNA knockout, as well as DMOG- (dimethyloxalyglycine) or ML324- mediated inhibition, of JMJD2 family members (JMJD2A, JMJD2B, JMJD2C and JMJD2D) reduces ICP4, ICP22 and ICP27 mRNA levels during reactivation (Liang, Vogel et al. 2013).

GSK-J4 is a JMJD3 inhibitor that inhibits demethylation of H3K27me3 (Messer, Jacobs et al. 2015). GSK-J4 increases the level of H3K27me3, and reduces the mRNA levels of ICP4, TK, and UL20, as well as production of infectious virions, during HSV-1 reactivation (Messer, Jacobs et al. 2015).

LSD1 is a flavin-dependent monoamine oxidase that also demethylase histone H3K9me3 (Liang, Vogel et al. 2009). Consequently, LSD1 is sensitive to monoamine

oxidase (MAO) inhibitors. Two MAO inhibitors, tranylcypromine (TCP) and pargyline, decreased viral yield during reactivation by more than 10,000- fold (Liang, Vogel et al. 2009). TCP also increased the levels of the heterochromatin marker H3K9me3, and decreased those of H3K9me2 and H3K27me3, on the ICP0 and ICP4 genes (Hill, Quenelle et al. 2014).

1.4.3 HSV-1 chromatin during quiescent infections.

The establishment of quiescent infection in cultured cells requires blocking the lytic cycle, either by HSV-1 replication inhibitors or by infecting with replication-defective viruses (Nicoll, Proenca et al. 2012). The HSV-1 DNA in quiescent infections is thought to be partly inaccessible, in that it remained silenced even after superinfection with an ICP0-mutant virus at MOI of 0.3 (which itself replicates in the same cell line) (Harris, Everett et al. 1989, Hobbs, Brough et al. 2001). However, superinfection of ICP0 null HSV-1 at higher MOI (MOI of 10 and 30) causes reactivation of the quiescent HSV-1 genomes (Preston 2007), although the number of the quiescent genomes decreased, in part due to competitive recombination (Preston 2007).

Several models for the inaccessibility of HSV-1 genomes during quiescent infections have been proposed. The first one proposes that the entire HSV-1 genome (including the LAT region) is fully chromatinized, enriched in histones bearing silencing markers. Consistent with this model, micrococcal nuclease (MCN) digestion releases nucleosome-sized fragments (Ferenczy and DeLuca 2009). H3K9me3, a repressive

marker, was enriched in the chromatin of the promoters of the ICP0, LAT, and gC genes, whereas the marker of transcriptional activity H4ac was depleted (Coleman, Connor et al. 2008). Upon reactivation by superinfection with wt HSV-1, the levels of H3K9me3 decreased and those of H3ac and H4ac, increased (Coleman, Connor et al. 2008). After reactivation by superinfection with HSV-2 (which produces ICP0 that reactivates HSV-1 from quiescent state), the total levels of acetylated histone H4 and H3K9ac increased on the promoters of ICP0, ICP27, gC and LAT in 1 h (Coleman, Connor et al. 2008), while those of H3K9me3 decreased. Consequently, the levels of heterochromatin protein 1 (HP1) also decreased. Acetylated histone H3 increased by only 8-fold on the ICP0 promoter, in comparison to 25-fold for other promoters (Coleman, Connor et al. 2008).

Several inhibitors of HDACs have been used to activate transcription from quiescent HSV-1 genomes. Sodium butyrate increased the level of ICP8 by 8-fold in cells infected with an ICP0 deleted HSV-1 (Poon, Gu et al. 2006).

Promyelocytic leukemia (PML) bodies have been proposed to “shield” the HSV-1 genome during quiescent infections. PML bodies, [also known as nuclear domain 10 (ND10)], are nuclear puncta consisting of about 150 proteins (Van Damme, Laukens et al. 2010). PML bodies play a role in apoptosis, regulation of gene expression, oncogenesis, and, germaine to the focus of this thesis, antiviral responses (Geoffroy, Cote et al. 2010). PML, sp100 and Daxx are three PML components that may inhibit

replication of herpesviruses, including that of HSV-1 (Zerboni, Che et al. 2013, Schilling, Scherer et al. 2017). They also inhibit replication of other unrelated viruses such as HIV (Kahle, Volkmann et al. 2015). PML is recruited to HSV-1 genomes during quiescent infections with ICP0 null-mutant viruses (Everett 2016), and is proposed to be able to ”shield” the HSV-1 genome as visualized by fluorescent microscope (Everett, Rechter et al. 2006). The highest resolution of fluorescent microscope only reaches approximately 300 nm (Huang and He 2011). It thus cannot resolve molecular interactions, which requires resolution of about 1 to 10 A°. Consequently, direct evidence for the proposed model that PML interacts with HSV-1 genome remains to be presented.

Overexpression of PML does not affect HSV-1 transcription or replication (Chelbi-Alix and de The 1999, Jensen, Shiels et al. 2001), neither does PML knockout affect replication of wt HSV-1 or ICP0-null HSV-1 (Chee, Lopez et al. 2003). HSV-1 replication decreased by about 100-fold in PML double negative 1D2 cells at moi of 0.1, but not so at moi of 5 (Xu, Mallon et al. 2016). Knockout of PML delayed degradation of sp100 by ICP0, likely due to inefficient association of ICP0 to ND10 (Xu, Mallon et al. 2016). This study suggested that PML may also have pro-HSV-1 effects rather than only anti-HSV-1 ones.

IFI16 (interferon-inducible protein 16) is a cellular innate immune sensor that contains hematopoietic interferon-inducible nuclear antigens. IFI16 has been proposed

to function as a restriction factor for HSV-1 infection (Merkl and Knipe 2019) by binding to, and accumulating on, HSV-1 genome (Johnson, Bottero et al. 2014). IFI16 might thus interact with HSV-1 DNA and if so it would be a unique component of the HSV-1 chromatin. IFI16 binds to dsDNA in a sequence-independent manner (Jin, Perry et al. 2012). Through its DNA binding ability, IFI16 is proposed to recognize foreign naked dsDNA and oligomerize onto it (Stratmann, Morrone et al. 2015), forming oligomers proportional to the length of the DNA. For DNA longer than 150 bp, IFI16 forms repeatable clusters, each containing more than ten IFI16. For DNA shorter than 150 but longer than 60 bp, IFI16 forms a cluster of about 4 molecules. DNA between 30 bp to 60 bp form complexes with only one IFI16 molecule. IFI16 cannot oligomerize on DNA that is less than 30 bp (Stratmann, Morrone et al. 2015).

1.4.4 HSV-1 chromatin during lytic infections

The earlier studies of lytic HSV-1 chromatin had reached the conclusion that the HSV-1 DNA was non-chromatinized in lytic infections. The evidence leading to this conclusion included mainly that micrococcal and other endonucleases digested HSV-1 chromatin to heterogeneously sized fragments (Fig 11) (Leinbach and Summers 1980, Lentine and Bachenheimer 1990), and that histones were apparently excluded from the HSV-1 replication compartments (Monier, Armas et al. 2000). However, many later ChIP assays indicated at least some association of HSV-1 DNA with histones, as it will be discussed below.

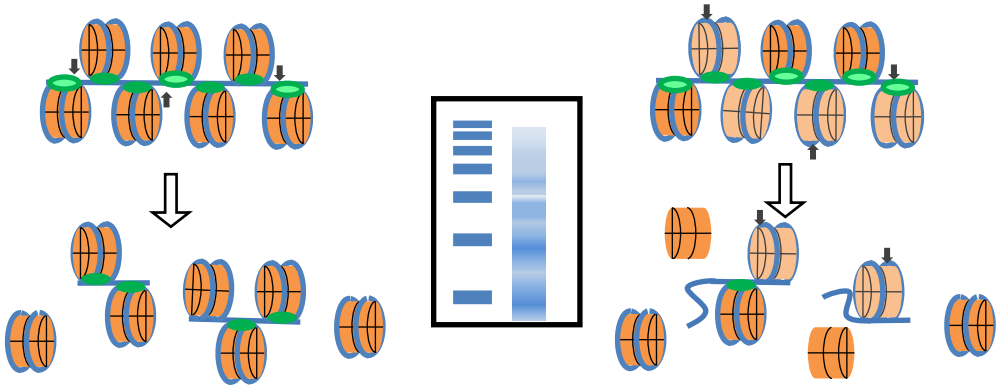

Figure 11: Nuclease protection assay of stable (left) and dynamic (right) chromatin, resulting in a nucleosome ladder or in heterogeneous sized fragments (smear with band), correspondingly. (Schang, Hu et al. 2021). Figure used under CC-BY 4.0 license.

HSV-1 infection of Sy5y cells reduced the total level of H3K9ac and H3K9me2 in infected cells, increased the total levels of H3K14ac 6 h or 10 h after infection, and did not affect those of H3K4me3 (Kent, Zeng et al. 2004). The DNA in the promoters of the ICP0, TK, and VP16 genes was associated with histones bearing the marker of transcriptional activation H3K9ac from 1 h postinfection, peaking at 3 h, and decreasing from 6 h pi. Low levels of H3K9me3 were detected at the promoters of ICP0, TK, and VP16 throughout the infection (Kent, Zeng et al. 2004). The changes in the levels of H3K14ac on the promoters of the ICP0, TK, and VP16 genes were similar to those of H3K4ac, whereas H3K14ac was less affected (Kent, Zeng et al. 2004). The repressive marker H3K4me3 was enriched on the bodies of the ICP0, TK and VP16 genes, but not on their promoters (Kent, Zeng et al. 2004). Notably, only about 0.01 to 0.05% of the input ICP0 gene DNA co-immunoprecipitated with histone H3, whereas about 3 to 10% of the VP16 gene did. The ChIP efficiencies for specific histone H3 modifications were

not as different.

About 0.6 to 1.5% of the ICP0 gene, 0.5 to 3% of the TK gene, and 4 to 5% of the VP16 gene DNA co-immunoprecipitated with H3K4me3 (Kent, Zeng et al. 2004). Histone H3 or acetylated H3 were not detected in association with the promoters of ICP0, ICP4, or ICP27, but both were detected on the gene of ICP27 and on the promoters of the TK, VP16, and gC genes (Herrera and Triezenberg 2004). Based on this evidence, a model was proposed in which the promoters of the transcribed genes (ICP0 and other IE genes) were associated with histones bearing markers of transcriptional activation, at low histone occupancy, whereas the transcriptionally inactive genes (E and especially L genes) were associated with histones bearing markers of repression, at high histone occupancy (although not at the same level as the cellular chromatin).

The histone H3 variant H3.3 was incorporated into HSV-1 chromatin at all times from infection for up to 10 h pi, whereas the variant H3.1 was only incorporated into the viral chromatin after 6 h pi (Placek, Huang et al. 2009). Treatment with the HSV-1 DNA polymerase inhibitor phosphonoacetic acid (PAA) decreased H3.1 levels by at least four-fold on the promoters of the ICP0, TK, and VP16 genes, suggesting that incorporation of H3.1 was DNA-replication-dependent (Placek, Huang et al. 2009).

ChIP thus detected histone interactions with HSV-1 DNA, but the co-immunoprecipitation efficiency was low throughout the lytic infections. A new model of

HSV-1 chromatin was then proposed, in which HSV-1 nucleosomes were separated by long linker naked HSV-1 DNA. This model could well explain the apparently low histone occupancy.

1.4.5 Epigenetics of HSV-1

Inhibition of protein methylation by 5'-deoxy-5'-methylthioadenosine (MTA, nucleoside inhibitor of methyltrasferases) decreased the total levels of H3K4me3, and hence limited the incorporation of H3K4me3 into HSV-1 chromatin (Huang, Kent et al. 2006). H3K4me3 depletion decreased the transcription levels of ICP0, TK and VP16 (Huang, Kent et al. 2006). Set1/MLL1 was identified as the KMT introducing the H3K4me3 modification in HSV-1 chromatin (Huang, Kent et al. 2006). Inhibition of another histone modifier, LSD1 (lysine-specific demethylase 1), also decreased HSV-1 replication and reactivation (Liang, Vogel et al. 2009). siRNA knockdown of LSD1, or its inhibition with MAO inhibitors, decreased H3K4me3 and increased H3K9me3 on the promoter and gene of ICP0. These treatments also reduced the mRNA and protein levels of all IE genes (Liang, Vogel et al. 2009).

Many other chromatin remodelers are also important in HSV-1 transcription regulation. Knockdown of the H3K9me1/2 demethylase JHDM2 reduced the levels of HSV-1 IE mRNA (Oh, Bryant et al. 2014). The chromatin remodeler SNF2H is recruited to the promoters of IE genes and promotes transcription of these genes (Bryant, Colgrove et al. 2011).

The histone H3/H4 acetyltransferases CLOCK complex is recruited to the viral replication compartments after the disruption of the ND10 domains. CLOCK overexpression increased the transcription of all IE, E and L genes, and compensated for ICP0 mutations (Kalamvoki and Roizman 2010). Interestingly, LSD1 also forms complexes with RESR/CoREST containing HDACs. Knockdown of LSD1 increased the transcription levels of HSV-1 IE genes, although did not affect the level of methylated H3 (Foster, Dovey et al. 2010). However, the levels of total acetylated H3 increased, suggesting that the regulation of HSV-1 transcription by LSD1 is mediated at least in part by the HDACs in the REST/CoREST complex.

Interestingly, knockout or siRNA knockdown of the HATs p300, CPB, PCAF or GCN5 did not impact viral transcription of ICP0, ICP4, or ICP27, or viral replication (Kutluay, DeVos et al. 2009). The levels of acetylated histones were not evaluated in this study. Modulation of HDACs or HATs also affects the acetylation levels of the histones in the cellular chromatin. As HSV-1 DNA enters the nuclei as protein-free DNA and the vast majority of histones are assembled in cellular chromatin, histones must be first mobilized from the cellular chromatin into the free pool to then make them available to assemble new chromatin with HSV-1 DNA (Conn and Schang 2013). Inhibition of HATs may decrease the dynamic of cellular histones. It would thus be predicted to makes histones less available to chromatinize on HSV-1 DNA and, consequently, to compromise any cellular silencing effects (Conn and Schang 2013).

Many inhibitors of histone modification have been used to study the epigenetic modification on the chromatin of HSV-1 mutant. HSV-1 ICP0 gene encodes three exons. It was not clear why several HSV-1 genes have introns and exons for splicing and it was proposed that HSV-1 mutant that the ICP0 introns were depleted (ICP0 gene was replaced by a cNDA copy of only the three exons) would have no result in HSV-1 transcription and replication (Poon, Silverstein et al. 2002). However, delay expression of E and L genes was observed in HSV-1 vCPc0 infected rabbit skin cells (Poon, Silverstein et al. 2002). Sodium butyrate, trichostain A (TSA), and *H. carbonum* toxin HDAC1/2 inhibitors, increased the expression of ICP4, ICP22 and US11 in rabbit skin cells (RSC) infected with HSV-1 strain vCPc0 as well (Poon, Liang et al. 2003). Under conditions in which HSV-1 transcription is restricted (low MOI infections with ICP0 null HSV-1 mutant), sodium butyrate increased the expression of ICP4, ICP8 and UL34 (Poon, Gu et al. 2006).

TSA also activated the ICP4 promoter in a REST/CoREST dependent pathway in 293HEK cells transiently transfected with an ICP4 expression plasmid, as evaluated by a secreted embryonic alkaline phosphatase (SEAP) reporter system. TSA had less of an effect on the activation of the same reporter by ICP22, which acts after transcription has initiated (Pinnoji, Bedadala et al. 2007). siRNA knockdown of REST or CoREST delayed the accumulation of the viral proteins ICP4, ICP0, ICP27, ICP22 and ICP8 in infections of U251 cells with HSV-1 strain F (Zhou, Te et al. 2010). TSA,

suberohydroxamic (SBX), and valproic acid (VPA) are three histone deacetylase inhibitors that decreased the transcriptional competence of HSV-1 genomes, at MOI of 50 and 100, and delayed HSV-1 replication kinetics (Shapira, Ralph et al. 2016).

Curcumin, which causes non-specific proteasome degradation of HATs among many other effects, decreased the occupancy of RNA Pol II on HSV-1 IE genes (Kutluay, Doroghazi et al. 2008), although the levels of acetylated histone H3 were not affected (Kutluay, Doroghazi et al. 2008).

Knockdown of CLOCK, or inhibition of its HAT activity, decreased the protein levels of ICP4, ICP0, ICP8 and US11 during infections with HSV-1 strain F (Kalamvoki and Roizman 2010). The histone methyltransferase inhibitor 5'-deoxy- 5'-methylthioadenosine (MTA) decreased the levels of HSV-1 gene expression by reducing H3K4me3 on HSV-1 chromatin through Set1-dependent mechanisms (Huang, Kent et al. 2006). As discussed before, the MAO inhibitors pargyline and TCP increased the levels of H3K9me3 on HSV-1 IE promoters through inhibition of LSD1 (Liang, Vogel et al. 2009). A more specific LSD1 inhibitor, OG-L002, also increased the levels of H3K9me2 (Liang, Quenelle et al. 2013).

The Jumanji-2 (JMJD2A, JMJD2B, JMJD2C and JMJD2D) family of demethylases remove H3K9me3. Depletion or inhibition of JMJD2 family of proteins (JMJD2A, JMJD2B and JMJD2D) by dimethyloxalyglycine (DMOG) decreased the levels of ICP4 and ICP27 mRNA and protein, and increased by 1.5 fold the levels of H3K9me3 on the

IE gene promoters (Liang, Vogel et al. 2013). N-(3- (dimethylamino)propyl)-4- (8-hydroxyquinolin-6-yl)benzamide (ML324), a more potent JMJD2 inhibitor ($IC_{50,}$ 10μM), is about 75-fold more efficient than DMOG at inhibiting HSV-1 ICP4 and IUCP27 mRNA level and viral yields (Liang, Vogel et al. 2013). However, the effects of ML324 on the levels of methylated histones were not evaluated (Liang, Vogel et al. 2013).

EZH2/1 are two H3K27 methyltransferases that suppress gene expression by increasing level of H3K27me3 (Arbuckle, Gardina et al. 2017). Inhibition of EZH2/1 by GSK126, GSK343 or UNC1999, interestingly decreased HSV-1 IE gene mRNA levels (Arbuckle, Gardina et al. 2017). The effects of these inhibitors were further characterized. They were proposed to act indirectly, by inducing cellular antiviral responses via upregulation of expression of genes in the proinflammatory and immune cell recruitment pathways (Arbuckle, Gardina et al. 2017).

Knockdown of the chromodomain helicase DNA binding protein CHD3 increased the mRNA levels of IE (ICP0, ICP4, ICP22 and ICP27) and E (UL29, UL 30, and UL32) genes (Arbuckle and Kristie 2014). Knockdown of CHD3 also increased the water insolubility of HSV-1 DNA in formaldehyde-assisted isolation of regulatory elements (FAIRE) assay. In these assays, protein-free DNA is in the aqueous phase after formaldehyde crosslinking whereas large nucleosome chains are in the organic phase (Arbuckle and Kristie 2014). Knockdown of the chromatin remodeler SNF2H decreased the protein levels of ICP0, ICP4 and ICP27, and increased histone H3 apparent

occupancy at the promoters of these genes (Bryant, Colgrove et al. 2011). Interestingly, the apparent increase of histone H3 occupancy was only observed at the earlier times of infection (1 to 7 h pi). At 8 h pi, similar levels of histone H3 were detected in control and siRNA-treated infections (Bryant, Colgrove et al. 2011).

Asf1a/b is a histone H3/H4 chaperone recruited to HSV-1 replication compartments by HCF-1. Knockdown of Asf1a/b decreased the protein levels of ICP4, ICP27, UL29, and gC (Peng, Nogueira et al. 2010), and increased the accessibility of the HSV-1 DNA to MCN digestion (Oh, Ruskoski et al. 2012). The promoters of ICP0, ICP4, and TK genes showed decreased apparent histone H3 occupancy, and knockout of Asf1a/b increased the expression level of IE genes, but not that of E or L genes (Oh, Ruskoski et al. 2012).

PCNA plays a critical role in HSV-1 replication. siRNA knockdown of PCNA decreased the yield of HSV-1 strain 17 by 1,000-fold (Sanders, Boyer et al. 2015). Inhibition of HATs recruitment through PCNA knockdown decreased the protection of the DNA of HSV-strain 17 against MCN digestion (Sanders, Boyer et al. 2015).

As discussed, HSV-1 DNA enters the nuclei free of proteins and it encodes no histone-like proteins. Thus, assembly of HSV-1 chromatin requires cellular histones (Conn and Schang 2013). The HSV-1 genome is only 152k bp, approximately one thousand nucleosomes in size, but it replicates more than 1,000 times in an infected nucleus. Histones are not synthesized during HSV-1 infection (Sorenson, Hart et al.

1991), and only a small amount of cellular histones are not assembled in cellular nucleosomes at any given time. Therefore, cellular histones have to be made available to assemble HSV-1 chromatin. Cellular histones are either in the free pool (temporarily not associated with DNA) or assembled in chromatin. Only about 4% of histone H2B or H2A are freely diffusing at any given time, or 15% of histone H3 and H4 (Kimura and Cook 2001). When the free histones are used by incorporation into HSV-1 chromatin, new histones must be mobilized away from cellular chromatin to maintain the balance between free pool and bound histones (Conn and Schang 2013). HSV-1 infection is thus expected to alter cellular histone dynamics. Indeed, all linker histone H1 variants H1.1, H1.2, H1.3, H1.4 and H1.5 were more dynamic in infected cells (Conn, Hendzel et al. 2008), with histone H1.2 being mobilized the most (Conn, Hendzel et al. 2008). The degree of histone H1 dynamic increased with MOI, but it was independent of HSV-1 DNA replication in that PAA had no effect on the changes of histone H1 dynamics (Conn, Hendzel et al. 2008). The increase in histone H1 dynamics also required no VP16 or ICP0, but it did require IE gene expression (Conn, Hendzel et al. 2008).

Similar analyses were performed to evaluate dynamics of H2B and H4, the two core nucleosome histones with no variant (Conn, Hendzel et al. 2011). H2B and H4, as all core histones, are more stably incorporated into chromatin than linker H1. H2B and H4 thus undergo slower exchange than histone H1, in a time scale likely irrelevant for HSV-1 infections (Conn, Hendzel et al. 2011). Nonetheless, the free pools of H2B and H4

were increased at 4 h or 7 h after infection (Conn, Hendzel et al. 2011). Notably, the slow exchange rate of H2B, but not that of H4, increased during infection, increase which did not require HSV-1 DNA replication (Conn, Hendzel et al. 2011). HSV-1 infection also increases the fast histone exchange rate and the free pool of histones H3.1 and H3.3 (Conn, Hendzel et al. 2016). Infections treated with PAA increases in the fast histone exchange rate and free pool of histone H3.1, but not those of histone H3.3. HSV-1 DNA replication thus affects H3.1 and H3.3 differently.

Transient expression of ICP4 increased the dynamics of H1.2, H2A, H2B, H3.1, H3.3, and H4 more than the expression of ICP0 or VP16 (Conn, Hendzel et al. 2011, Conn, Hendzel et al. 2016, Gibeault, Conn et al. 2016). In contrast, the dynamics of canonical H2A were not altered by ICP4 (Gibeault, Conn et al. 2016). Histone H2A has many variants, which are differentially incorporated into active or silenced gene promoters or bodies (as discussed above). H2B and H2A exists as dimers in the free pool, and dynamics of H2B were increased. Therefore, at least one H2A variants was expected to be mobilized together with H2B (Gibeault, Conn et al. 2016).

1.4.6 HSV-1 DNA replication

HSV-1 genome contains three origins of replication. *OriS* is in the repeat region between ICP4 and ICP22, and is thus present as two copies per genome. *OriL* is located in the UL region between UL29, the gene encoding for single strand binding protein ICP8, and UL30, that encoding for the DNA polymerase subunit. HSV-1 DNA

replication initiates at either one of the three origins. One of the seven essential replication proteins, the origin binding protein encoded in the UL9 gene, colocalizes with negatively supercoiled plasmids containing *OriS*, and is thought to unwind the origin (Makhov, Boehmer et al. 1996). ICP8 then forms an *OriS* hairpin, which together with the origin binding protein stimulates ATP hydrolysis (Macao, Olsson et al. 2004). The ssDNA hairpin then recruits the helicase/primase complex to fully unwind the DNA at the origin and synthesize the RNA primer. The RNA primer and helicase/primase activities are all required to recruit the HSV-1 DNA polymerase to the origin of replication (Carrington-Lawrence and Weller 2003). Replication results in long branched DNA concatemers.

In one model, HSV-1 DNA replicates in a bidirectional theta type replication early on, producing entangled circular genomes. The circular genomes then switch to rolling circle replication and form the concatemers (Muylaert, Tang et al. 2011). However, restriction cleavage of HSV-1 replication intermediates releases only few HSV-1 genome monomers, suggesting the replication intermediate is instead a non-linear branched structure (Martinez, Sarisky et al. 1996, Muylaert, Tang et al. 2011).

Cellular DNA replication requires disassembly and reassembly of chromatin. The roles of chromatin in HSV-1 replication remain to be studied in any detail.

1.5 Chromatin of other herpesvirus

Epstein - Barr virus (EBV) is a gamma 1 herpesvirus that infects about 90% of the

world population. Most EBV infections are asymptomatic. However, the viral genome remains in the nucleus as a latent episome, which can be reactivated (Hammerschmidt 2015). The primary target of latent infection is the B lymphocyte. Transcription of the EBV nuclear antigen (EBNA1), latent membrane protein (LMP) genes, and the non-translated EBV encoded RNAs depends on the type of latency (Niller, Szenthe et al. 2014). Depending on the transcription activity, EBV latency is classified into type 0 (no detectable gene expression), I (only EBNA1 is expressed), II (EBNA1 and LMPs are expressed), or III (all three classes of genes are transcribed) (Day, Chau et al. 2007). Upon reactivation, EBV establishes lytic infection in the nasopharyngeal area and gastric area epithelial cells for about 30 to 50 days (Hammerschmidt 2015).

Kaposi's sarcoma associated herpesvirus (KSHV) is a relatively widely studied gamma-2 herpesvirus. It causes Kaposi's sarcoma, primary effusion lymphoma, and multicentric Castleman's disease. Like EBV, KSHV establishes latent and lytic infections. During latency, a few viral genes, including the latency associated nuclear antigen (LANA), v-FLIP and v-Cyclin, are expressed (Juillard, Tan et al. 2016). LANA is essential to retain KSHV latent genomes. It associates with KSHV DNA and functions as attachment sites to cellular chromosomes (Juillard, Tan et al. 2016). Reactivation from latency to lytic infection is triggered by the expression of RTA, in which is regulated by LANA-mediated RBP-Jk binding sites (Gunther and Grundhoff 2010).

Like that of HSV-1, The EBV genome inside the virion is histone free and

unmethylated. During latency, the EBV genome is regularly chromatinized and hypermethylated, except for the DNA origin of replication (*OriP*) and the EBER1 non-coding RNA gene (Arvey, Tempera et al. 2013, Lieberman 2015). These two genomic regions are nuclease-hypersensitive, and their chromatin is enriched in histone H3K4 methylation and H3K9 acetylation (Arvey, Tempera et al. 2013). The chromatin boundary element CTCF is also enriched on the EBER1 gene, where it may prevent the spreading of silencing chromatin into this locus (Arvey, Tempera et al. 2013). Other histone post-translation modifications are less homogenously distributed. For example, histone H3K9 methylation is generally associated with heterochromatin (Arvey, Tempera et al. 2013). However, the distribution of H3K9 methylation on EBV chromatin depends on cell type (Murata and Tsurumi 2013). H3K9 methylation is excluded from *OriP* in Raji cells, for example, but not in LCL cells (Murata and Tsurumi 2013).

EBV chromatin is less well understood during lytic infections. One major limitation to the study of lytic EBV chromatin is that the establishment of a lytic EBV infection requires reactivation from latency, which is induced by small molecules which themselves affect chromatin remodeling (Li, Liu et al. 2016). Before reactivation, EBV DNA is mostly methylated (Flower, Thomas et al. 2011). BZLF1, a transcription activator, preferentially binds to the methylated DNA in the promoters of IE gene, and consequently actives transcription of these EBV genes (Ramasubramanyan, Osborn et al. 2012). As the reactivation proceeds, the total histone acetylation levels also increase

(Ramasubramanyan, Osborn et al. 2012). However, there is little evidence that the enrichment of acetylated histones actually modulates transcriptional activity.

Also like those of HSV-1, the encapsidated KSHV genomes are histone-free (Uppal, Jha et al. 2015). Latent KSHV genomes are also regularly chromatinized and methylated like those of EBV (Gunther and Grundhoff 2010, Toth, Maglinte et al. 2010, Toth, Brulois et al. 2013, Uppal, Jha et al. 2015). Gene ORF73 (LANA), however, is unmethylated, which is consistent with its high transcriptional activity (Gunther and Grundhoff 2010). The levels of DNA methylation on other genome positions appears to depend on cell line (Gunther and Grundhoff 2010). CTCF is also enriched at the LANA gene. It may well function, as in EBV chromatin, to prevent the silencing chromatin from spreading into the LANA gene (Uppal, Jha et al. 2015). The distribution of different histone modifications in the latent KSHV chromatin has been extensively studied (Gunther and Grundhoff 2010). Histone H3K4 tri-methylation and histone H3 acetylation are enriched in IE and E genes. The repressive marker H3K27 tri-methylation is also enriched in IE genes, resulting in poised chromatin. The L genes are instead enriched in repressive tri-methylation of H3K9 (mostly colocalized to L genes) and H3K27 (spread throughout the entire KSHV genome) (Gunther and Grundhoff 2010).

The levels of histone H3 in KSHV chromatin did not change significantly upon reactivation. In contrast, the total levels of histone H3K27 tri-methylation decreased, as expected from the high levels of transcription (Gunther and Grundhoff 2010). Histone

H3K9 tri-methylation levels remain constant (Gunther and Grundhoff 2010). As H3K9me3 is mostly colocalized to L genes, these high levels perhaps reflect the low transcriptional activity of L genes during reactivation. The chromatin of the IE genes contained bivalent histone modifications during latency (Gunther and Grundhoff 2010). Upon reactivation, acetylated histone H3 starts to be enriched in the IE genes, whereas H3K27 tri-methylation decreases (Gunther and Grundhoff 2010).

1.6 Rationale and hypothesis

Chromatin regulates cellular gene transcription in part by controlling the accessibility of DNA to transcription factors. Thus, the transcription competent genes and the transcribed ones would be in more accessible chromatin than the transcriptionally incompetent and silenced ones. If HSV-1 chromatin was regulated in the same manner as the cellular ones, then the highly transcribed or transcriptionally competent HSV-1 genes would be in more accessible chromatin than the non-transcribed or transcriptionally incompetent ones, such as the E genes in the absence of IE proteins, or the L genes before DNA replication. CHX inhibits protein translation. VP16 in the tegument can still from complexes with pre-existing HCF and Oct-1 and thus activate transcription of the IE genes in CHX treated infections (Preston, Rinaldi et al. 1998). As protein synthesis is inhibited, however. no IE protein is synthesized under these conditions and consequently, E and L genes cannot be transcribed. Rosco inhibits all HSV-1 gene transcription before initiation through inhibition of cyclin-dependent kinases

(CDK), and thus transcription of all HSV-1 genes is inhibited (Schang, Coccaro et al. 2005). Under the model that HSV-1 transcription is regulated similarly as cellular transcription is, the transcriptionally competent and transcribed IE genes would be in more accessible chromatin than the non-transcribed E or L genes in CHX treated infections. IE genes in CHX treated infections would be expected to be in similarly accessible chromatin as all HSV-1 genes in untreated infections at 7 h pi, when all HSV-1 genes are transcribed, E and L genes in CHX treated infections, in contrast, would be expected to be transcriptionally incompetent and in inaccessible chromatin, similarly to all HSV-1 genes in Rosco-treated infections.

To evaluate chromatin accessibility, chromatin of infected, treated or not, cells was subjected to serial MCN digestion. More accessible chromatin is digested into smaller complexes and least accessible into larger ones. Chromatin complexes were then fractionated according to their hydrodynamic ratios in sucrose gradients. DNA was purified from each fraction and deep sequenced to map the reads to the HSV-1 genome. The hypothesis I tested was that **all transcribed or transcriptionally competent genes, from any treated or untreated infections, are in most accessible chromatin and thus fractionate mostly together to the lighter fractions, whereas all non-transcribed or transcriptional incompetent genes, from any treated infections, are in most inaccessible chromatin and fractionate mostly together to the denser fractions.**

1.7 Significance

Intracellular HSV-1 DNA was once thought to be nucleosome-free or in sporadic nucleosomes, in which only few loci were nucleosomal, during lytic infections. More recently, more and more evidence, including previous studies from our lab, suggests instead that intracellular lytic HSV-1 DNA is in very dynamic chromatin. In contrast, the HSV-1 genome is fully chromatinized during latency.

Latent HSV-1 genomes can be reactivated upon a variety of stimuli. During reactivation, the fully, stably HSV-1 chromatin becomes dynamic. The mechanisms whereby the lytic HSV-1 dynamic chromatin converts into the stable latent chromatin to establish latency, or the stable latent chromatin converts back into the lytic dynamic chromatin during reactivation, are not fully characterized yet. My project aimed to address whether intracellular HSV-1 DNA was fully or partially chromatinized, or non-chromatinized, as well as the mechanisms determine the dynamic properties of the HSV-1 chromatin. Although the mechanisms whereby chromatin becomes dynamic are complex, one of the simplest models is that transcription correlates with the dynamic states of their own chromatin.

My goal was to characterize to what extent HSV-1 transcription related to chromatin dynamics, as the first step to reveal the roles of the dynamics of the lytic HSV-1 chromatin. This project will lead to a better understanding of the nature of lytic HSV-1 chromatin, and possibly help to unreveal the mechanisms of the “switch” between the

lytic and latent HSV-1 chromatin.

Chapter 2: Materials and Methods

2.1 Cells and virus.

VERO: African Green Monkey kidney cells were purchased from ATCC (CRL-1587). The original passage was handled by the lab technician, passage 2 were given to me as my original Vero cell source. Vero passage 2 cells were aliquoted (approximately 1 x 10^6 cells in 0.5 ml serum free media plus 0.5 ml DMSO) and stored in liquid nitrogen in 2 ml glass cryo vials. Each of these vials was thawed in a 37°C water bath as required and was then transferred into a 50 ml conical with 10 ml of 5% FBS DMEM. The cells were gently mixed inside the conical by pipetting up and down using a 5 ml pasture pipette, and then transferred into a T50 flask. Conicals were quickly span down at 500 x g for 3min and the rest of the liquid and cells if any, were transferred into the same flask. The flask was incubated in a CO_2 incubator at 37°C for 24 h, when they were checked for attachment under microscope, and the unattached cells were removed by vacuuming the supernatant. Fresh 10 ml 5% FBS DMEM was added to the flask and then they were incubated for three more days, or until confluency. Confluent cells were trypsinized and passed into two T150 flasks according to standard protocols (passage 3). These two T150 flasks were incubated in CO_2 incubator at 37°C until confluent. The frozen passage 3 cells were the Vero cell source for all experiments. Cells in the other confluent flask were passed at confluency and seeded into new containers for

experimental purposes.

2.1.1 Freezing cells

Passage 3 cells in one confluent flask were trypsinized and then frozen at 1 x 10^6 cells in 0.5 ml SFM plus 0.5 ml 10% DMSO DMEM in 2 ml glass vials in -70°C liquid nitrogen. Cells in T150 flasks were taken to the biosafety cabinet, and the supernatant was vacuumed off. Cells were washed with 10 ml warm PBS per flask, and the PBS was then vacuumed. Cells were then trypsinized with 3.0 ml 10% trypsin in 37°C CO_2 incubator until the cells were detached. The trypsin was deactivated by addition of 10 ml 5% FBS DMEM to each flask, and the cells were transferred into 50 ml conical tubes (no more than 30 ml cell suspension per conical). Cells were spun down at 200 x g for 5 min at room temp. The supernatant was carefully vacuumed off, and the cell pellet was resuspended with 2 ml 20% FBS DMEM per conical. An equal volume of 20% DMSO DMEM was then added to each conical to a final concentration of 10% FBS, 10% DMSO. The diluted cell suspensions were then aliquoted in 1.0 ml per cryovial (2 ml maximum volume) and were placed in a freezing box inside a styrofoam container. The container was placed in -80°C freezer for 24 h, and then the cryovials containing frozen cells were transferred to the liquid nitrogen tank for long term storage.

2.1.2 Thawing cells

Cryovials containing frozen cell suspensions were removed from the liquid nitrogen tank quickly to a 37°C water bath, with constant manual shaking. After the cell

suspension was thawed (no ice observed), it was transferred into a 15 ml conical (1.0 ml cell suspension for one vial into one 15 ml conical tube) containing 5 ml pre-warmed 10% FBS DMEM. The cells were mixed by pipetting up and down five time using a 10 ml glass pipette and were then transferred to a T75 flask and incubated in a 37°C CO_2 humidifier incubator.

2.1.3 Virus

The original HSV-1 KOS was originally obtained directly from Dr. P. A. Schaffer. My original viral stocks were stored at -80°C (p7 from isolation). This stock was used only once to generate my viral stock (p8). Briefly, 8 x 10^6 cells were seeded in each of four T150 flasks. After the cells were attached (in approximately 4 h), the medium was removed, and 2.5 ml inoculum was added to each flask (MOI 0.05). Cells were infected according to standard protocol (described below). The infected flasks were incubated in a humidified CO_2 incubator at 32°C for 3 to 5 days, until about half of the cells were still attached but all attached cells had clear CPE (cytopathogenic effects). Virus (p8) was harvested as per the standard protocol (described below). A small percentage (1 to 5 µl of 200 µl) of p8 virus was used to grow viral stocks passage 9 to 16 until used out or discarded. Then p8 viral stock was used again to generate a new series of viral stocks.

2.1.4 Viral stock preparation

Cells were seeded into 4 to 6 T150 flasks at 30 to 50% confluency (3 to 5 x 10^6 cells per flask). After attachment (minimum 4 h), one flask was used to count the cells per flasks.

Inocula were prepared according to the total cell number to infect with a MOI of 0.05 in a volume of inoculum calculated as the number of flasks at 2.5 ml inoculum per flask. The supernatant in each flask was vacuumed, and 2.5 ml inoculum was added. The flasks were gently rocked and then placed into a 33°C humidified CO_2 incubator for 1 h. Every 10 min, the flasks were gently rocked and rotated 90°. The inoculum was vacuumed after 1 h, and the cells were washed twice with 15 ml cold PBS in each flask. Ten ml of fresh 5% FBS DMEM was added to each flask and all flasks were incubated at 33°C in a CO_2 humidified incubator until 100% CPE (all cells rounded up with some detached). Cells were then scraped off the inner flask surface and transferred into a 50 ml conical together with the supernatant (no more than 30 ml into each 50 ml conical). The flasks were then washed with total 10 ml of serum free medium, which was then equally aliquated into the 50 ml conicals. Cells were spun down at 3,250 x g for 15min at 4°C. The supernatant containing the infectious particles were transferred into new 50 ml conicals and were pelleted at 11,000 x g for 2 h in a floor centrifuge. The pellet of the low speed centrifugation was resuspended with 1 ml SFM, and transferred to a 15 ml conical. The resuspened pellets were freeze / thawed three times in a dry ice- ethanol bath and a 37°C water bath. Prior to the finish of the high-speed centrifugation, the resuspended pellets were sonicated three times for 30 s each at power setting of 4 with Branson Ultrasonics Tapered microtip (1/4" Dia. 101-148-070). Cell debris were pelleted at 3,250 x g for 30 min at 4°C and discarded. After ultracentrifugation, the infectious

particles were pelleted, and the supernatant was discarded. The viral pellet was then resuspended with the cell lysis supernatant containing virus, and was transferred to glass vials and stored in -80°C.

Table 1: Reagents used for cell culture and virology

Reagents	Company	Cat. Number
DMEM, low glucose, pyruvate (+ L-glut, phenol red)	Gibco (ThermoFisher Scientific)	11885-084
BSA	Affymetrix	10857
Crystal Violet	Thermo Fisher Scientific	c581-100
Crystal Violet, 100 g	Amresco	0528-100G
Cycloheximide	Microbia L Source	45-C7698-1G
Dimethyl Sulfoxide Anhydrous >=99.9%	Sigma-Aldrich	276855-100 ML
DMEM	Gibco	11885-084
FBS (Lot 15A086)	Sigma Aldrich	F1051-500 ML
Methyl cellulose 500 CP	Sigma-Aldrich	M0387-250G
Sodium chloride, 99.85%, for molecular biology, DNAse, RNAse and Protease free, ACROS Organics™ - 2.5kg; Glass bottle	Acros Organics	327300025
Sodium phosphate, dibasic heptahydrate, 99+%, for analysis	Acros Organics	206515000
Tris-HCl	Promega	h5125
Triton X-100	Sigma-Aldrich	X100-100 ML
Trypsin	Thermo Fisher Scientific	15400-054
c0mplete, EDTA-free protease inhibitor tablets (x2)	Roche	1.1874E+10
Cycloheximide from microbial source	Sigma	C7698-5G
Nuclease micrococcal from Staphylococcus aureus	Sigma-Aldrich	N5386-50UN
Roscovitine, free base (x2)	LC laboratories	R-1234
Trypsin, from bovine pancreas	Sigma-Aldrich	T1426-100MG
Phosphonoacetic acid	Sigma-Aldrich	284270-10G

2.2 Reagents and compounds

Please see tables 1 to 6 for reagents used in each experiment.

2.2.1 Compounds

One hundred microliter of cycloheximide (CHX) 5 mg/ml stock solution was prepared in serum free medium (SFM). Stock solution was stored at -20°C and diluted to 50 µg/ml in DMEM-5% FBS, SFM or PBS approximately 20 minus before use. Cells were pre-treated with 1.5 ml or 2.5 ml for 150mm petri dishes or T150 flasks of 50 µg/ml CHX in DMEM-5% FBS for 1 h prior to infection. The inocula, PBS washes and DMEM-5% FBS added after infections all contained 50 µg/ml CHX.

One milliliter phosphonoacetic acid (PAA) 100 mM stock solution was prepared in SFM and adjusted to pH 7.0 with 1 N NaOH. The stock was stored at 4°C and was diluted to 400 µM in DMEM-5% FBS approximately 20 minus prior to use. PAA was added to cells after removing inocula. All PBS washes contained 400 µM PAA until harvest.

One hundred microliter of roscovitine (Rosco) 100 mM stock solution was prepared in dimethyl sulfoxide (DMSO). The stock was stored at -20°C. The stock was pre-warmed to 37 °C and diluted to 100 µM in pre-warmed DMEM-5% FBS immediate before use. Warm Rosco-containing medium was added to the cells after removing the inocula. All PBS washes contained 100 µM Rosco until harvest.

2.3 Nuclear extraction

Cells were seeded in T150 flasks (1 x 10^7 cells per flask) or 150mm dishes (5 x 10^6 cells per dish) the day before. One extra flask or dish was seeded for cell counting. Each treatment was aimed to use 2 x 10^7 cells.

Cells were infected at MOI of 10. Two and half ml per flask, or 1 ml per dish, of inoculum was prepared. Flasks or dishes were taken from the 37°C incubator and media were removed. The inocula were added to each flask or dish and the dishes were gently rocked to cover the entire surface. Flasks or dishes were transferred to the 37°C incubator for 1 h. Each flask or dish was gently rocked and rotated by 90° every 10min. After 1 h, the inoculum was vacuumed off, and the cells were washed with 15 ml per flask (5 ml per dish) of cold PBS. Then, 37°C pre-warmed 5% FBS DMEM was added to the cells and infected cells were incubated for 2 h, 4 h, 7 h or 15 h at 37°C in a humidified CO_2 incubator.

At harvesting time, flasks or dishes were transferred to the biosafety cabinet and the media was removed. Cells were washed with 10 ml 4°C PBS every 1 x 10^7 cells twice. Three milliliters of 10% trypsin were added to each flask (or 1 ml to a dish). Cells were trypsinized in the incubator until they started to come off the surface (about 1 to 2 min), while the flasks or dishes were gently rocked every 30 seconds to check the progress of the trypsinization. Trypsinization was stopped by addition of 15 ml 5% FBS media into each flask (or 5 ml per dish). Cells were then mixed inside the flasks or dishes by pipetting up and down using a 10 ml glass pipette, before transferring into one 50 ml

conical. Cells were pelleted by spinning at 3,250 x g for 10 min at 4°C. The supernatant was discarded, and the cell pellets were vortexed at power setting of 5 for 5 seconds. The lose cell pellet was then resuspended with 15 ml cold PBS for every $1x10^7$ cells, and pelleted again at 3,250 x g for 10 min at 4°C. The supernatant was removed, and the pellet was vortexed again at power setting of 5 for 5 seconds. The lose pellet was resuspended in 15 ml 4°C reticulocyte standard buffer (RSB, 10 mM Tris [pH 7.5], 10 mM NaCl, 5 mM $MgCl_2$) per 1 x 10^7 cells. Cells were pelleted once more at 3,250 x g for 10 min at 4°C. The supernatant was removed, and the pellet was resuspended in 10 ml 4°C RSB for each 1 x 10^7 cells. Cells were mixed by gently pipetting up and down with a 10 ml glass pipette, and then incubated on ice for 10 min, flipping the tubes upside down three times (to prevent pelleting). Cell membranes were lysed by adding 0.5 ml 10% (vol/vol) triton X-100 to every 10 ml of cells in RSB. Cells were mixed again by flipping the tube upside down three times, and then incubated on ice for 10 min. Nuclei were then pelleted by centrifugation at 3,250 x g for 25 min at 4°C, and the supernatant was removed by vacuuming with a small glass Pasteur pipette. The inner wall of the conical was vacuumed to remove remaining supernatant. The vacuumed tubes were stored upside down without the lid to prevent any liquid flowing back to the pellet.

2.4 Protein isolation and precipitation.

Eight hundred microliters of high salt solution (2.5 M NaCl, 50 mM Tris, 0.5% triton X-100, pH 8) with protease inhibitor (1 Complete EDTA-free protease inhibitor tablet in 2

ml water, and 320 µl was used per 1 x 10^7 nuclei) was added per 1 x 10^7 nuclei to resuspend the nuclei pellet. The nuclei pellet was vortexed for 1 min until mostly resuspended, and then lysed in a rotator for 30 min at 4°C. Nuclear debris were spun down at 16,000 x g for 10 min at 4°C. The supernatant was transferred to a new tube and 100% TCA solution (w/v) was added to a final concentration of 25% TCA. Samples were then incubated on ice for 30 min and proteins were pelleted by centrifugating at 23,000 x g for 15 min at 4°C. The supernatant was then carefully pipetted out using a P200, and the tube was left up-side-down for 10 min. Protein pellets were washed thrice with 1 ml -20°C pre-chilled acetone, and then spun down at 23,000 x g for 15 min. Protein pellets were air dried overnight at 4°C.

Table 2: Reagents used for protein extraction, purification, and analyses

Reagents	Company	Cat. Number
Acetic Acid, >99.7%, ACS	BDH	BDH3092-500 ml
Acetic Acid, Glacial (Certified ACS), Fisher Chemical - Glass/Safe-Cote; 500 mL	VWR	A38S-500
Acetone, ACS, 99.5+% 1L	Alfa Aesar	30698-K2
Applied Biosystems Fast SYBR Green Master Mix	Thermo Fisher Scientific	43-856-12
Bis Solution, 40% Acrylamide	Avantor performance materials	4969-00
Bromophenol Blue	Millipore Sigma	BX1410-7
Bromophenol Blue	VWR	B392-5
Calcium Chloride Dihydrate, ACS, >99%	Amresco	0556-500G
Caseine	VWR	21-868-0100 gm

Citric acid 99.5% A.C.S. REAGENT	Sigma-Aldrich	251275-500G
Complete EDTA-free (20 TABLETS)	Roche	11873580001
Coomassie Brilliant Blue G-250	Amresco	0615-10G
DL-dithiothreitol>=98% (TLC) >=99.0%	Sigma-Aldrich	D0632-10G
EGTA (Ethylene Glycol-bis(2-Aminoethylether-N)	Sigma-Aldrich	03777-10G
EMD Millipore Immobilon™-P PVDF Transfer Membranes	Millipore Sigma	IPVH00010
Glycerol, Laboratory Reagent	BDH	BDH1172-1Lp
Glycine, 99% 500 g	Alfa Aesar	A13816-36
LICOR IRDye 680RD Streptavidin, 0.1 mg	LI-COR Biosciences	925-68079
PVDF membrane	Millipore Sigma	IPVH00010
Sodium Bicarbonate, ACS	BDH	BDH9280-500G
Sodium chloride, 99.85%, for molecular biology, DNAse, RNAse and Protease free, ACROS Organics™ - 2.5kg; Glass bottle	Acros Organics	327300025
Sodium hydroxide, 500 g UN1823	Amresco	0583-500G
Sodium phosphate, dibasic heptahydrate, 99+%, for analysis	Acros Organics	206515000
Tri sodium citrate Dihydrate	Fisher Scientific	BP327-1
Trichloroacetic acid solution, 6.1 N, 100 mL	Sigma-Aldrich	T0699-100 ML
Tris-HCl	Promega	h5125
Triton X-100	Sigma-Aldrich	X100-100 ML
40% Acrylamide/Bis solution 29:1 (x2)	BioRad	161-0146
c0mplete, EDTA-free protease inhibitor tablets (x2)	Roche	1.1874E+10
Dithiotreitol (DTT)	Fisher	BP172-5
N',N',N',N'-Tetramethylethylendiamine	Sigma	T9281-25 ML
Odyssey Blocking Buffer (PBS)	Li-Cor (Mandel)	927-40000
Precision Plus Protein Dual Colour Standards	BioRad	161-0374
Trichloroacetic acid solution, 6.1 N, 100 mL	Sigma-Aldrich	T0699-100 ML

2.5 Continuous MCN digestion.

Each 1 x 10^7 nuclei were resuspended in 80 µl MCN digestion buffer (10 mM Tris [pH 8], 1 mM $CaCl_2$). The pellet was gently mixed by pipetting up and down using a

P200 at a volume setting of 50 µl. Twenty microliter MCN working solution was prepared by adding 1 µl of MCN stock solution (0.05 U/µl) into 19 µl MCN digestion buffer for every 1 x 10^7 nuclei. Nuclei suspension and the MCN solution were pre-warmed to 39°C for 2 min in water bath. The MCN digestion buffer with MCN was added to the nuclei suspension (at 0.05 U MCN per 1 x 10^7 nuclei in a total volume of 100 µl) and the mixture was incubated at 39°C for 2.5min. Then, ten microliter 0.05 M EDTA was added per 100 µl to quench MCN. Nuclei were pelleted at 2,000 x g for 5 min at 4°C, and the supernatant was discarded. Nuclei were lysed by incubating with chromatin extraction buffer (CEB, 1 mM ethylene glycol-bis(beta-aminoethyl ether)-N, N, N', N',- tetra-acetic acid (EGTA), 2% Triton X-100, 3 mM $MgCl_2$, 2 mM Tris [pH 8]) with 450 mM NaCl in a rotator at 4°C for 30 min. Nuclei debris and the undigested chromatin were pelleted down at 2,000 for 5 min at 4°C, and the supernatant containing digested chromatin was transferred to a new eppendorf tube.

2.6 Chromatin extraction for serial micrococcal (MCN) nuclease digestion.

Each 1 x 10^7 nuclei were resuspended in 1.5 ml chromatin extraction buffer. The pellet was gently mixed by pipetting up and down using a P1000 set at 500 µl. After the pellet was evenly resuspended, it was transferred into a 1.5 ml eppendorf tube, where it was incubated on ice for 30 min. Every 5 min, nuclei were mixed by pipetting up and down 10 times using a P1000 set at 750 µl, to ensure complete lysis of the nuclear membrane. Chromatin was then spun down at 2,000 x g for 10 min at 4°C. The

supernatant was removed, and the pellet was resuspended in 200 µl MCN digestion buffer (10 mM Tris [pH 8], 1 mM $CaCl_2$) per 1 x 10^7 cells.

2.7 Serial micrococcal digestion

Five percent of the chromatin suspension was transferred into a new tube as unfractionated and undigested chromatin, and proteinase k (20µg/ml) and 10% SDS was added to a final concentration of 1µg/ml proteinase k and 0.5% SDS. The solution was mixed by flick three times and incubated in a 37°C water bath overnight. The DNA of the unfractionated and undigested sample was purified the following day together with the digested and fractionated samples (see DNA extraction below).

The remaining chromatin was pelleted at 2,000 x g for 5 min at room temp. The supernatant was carefully pipetted out with a P200 pipette, and the chromatin pellet was disrupted by racking on a rack. The pellet was resuspended in 40 µl of MCN digestion buffer containing 0.05 U MCN per 1 x 10^7 nuclei. The tube was quickly flicked three times and was immediately spun down at 800 x g for 5 min at room temp in a fixed angle rotor. The supernatant (soluble chromatin) was removed and transferred to eppendorf tubes containing 10 µl 0.05 M EGTA to immediately quench MCN. The pellet (insoluble chromatin) was disrupted by racking on a rack and was resuspended with fresh 40 µl of MCN digestion buffer containing 0.05 U MCN per 1 x 10^7 nuclei. The digestion procedure was repeated six times. The supernatants from the six rounds of digestion were pooled together and resolved in sucrose gradients.

Table 3: Reagents used for continuous and serial MCN digestion and sucrose fractionation.

Reagents	Company	Cat. Number
DMEM, low glucose, pyruvate (+ L-glut, phenol red)	Gibco (ThermoFisher Scientific)	11885-084
Complete EDTA-free (20 TABLETS)	Roche	11873580001
DMEM	Gibco	11885-084
EGTA (Ethylene Glycol-bis(2-Aminoethylether-N)	Sigma-Aldrich	03777-10G
FBS (Lot 15A086)	Sigma Aldrich	F1051-500 ML
Nuclease micrococcal from Staphylococcus aureus	Sigma-Aldrich	N5386-50UN
Proteinase K, Molecular Biology Grade	New England Biolabs (NEB)	P8107S
Sucrose	Sigma-Aldrich	S5016-500G
Tris-HCl	Promega	h5125
Triton X-100	Sigma-Aldrich	X100-100 ML
Trypsin	Thermo Fisher Scientific	15400-054
Tube, Thinwall, Polypropylene, 13.2 mL, 14 x 89 mm (qty. 50)	Beckman Coulter	331372
c0mplete, EDTA-free protease inhibitor tablets (x2)	Roche	1.1874E+10
Nuclease micrococcal from Staphylococcus aureus	Sigma-Aldrich	N5386-50UN
Proteinase K from Tritrachium album	Sigma-Aldrich	P6556-100MG
Trypsin, from bovine pancreas	Sigma-Aldrich	T1426-100MG

2.8 Sucrose gradient ultracentrifugation

Continuous 0 to 10% sucrose gradients were prepared using a Gradient Master instrument with sucrose gradient buffer (SGB) (10 mM Tris [pH 8.0], 1.5 mM $MgCl_2$, and 0.5 M EGTA) containing 200 mM NaCl. One 12.5 ml clear ultracentrifugation tube per treatment (Beckham) was labeled at 6.25 ml mark with a specific 6.25 ml measuring instrument for these tubes. Zero percent sucrose SGB buffer was filled to the mark on a leveled surface. Eight milliliter of the 10% sucrose SGB buffer was next loaded at the

bottom using a filling syringe. The tip of the syringe was carefully inserted to the bottom of the tube, and 10% sucrose SGB buffer was gently ejected until the 10% sucrose SGB buffer reached the mark. The tube was then placed in a gradient maker to generate a continuous 0-10% sucrose gradient. Then, 600 µl of the very top gradient was removed using a P1000 pipette on a leveled surface.

Soluble chromatin was gently loaded on the top of the gradients with a P1000 pipette. The soluble chromatin was ejected gently and slowly with the tip pointing against the inner wall. The loaded sucrose gradients were transferred into previously balanced SW-40 Ti metal tube holders and rebalanced. SGB buffer (0% sucrose) was added dropwise to any lighter tubes as necessary until balanced. The gradients were then centrifuged at 400,000 x g in a SW-40 Ti rotor for 180 min at 4°C with slow deceleration.

After centrifugation, the tubes were sealed with parafilm and hold with a metal clamp. Thirteen eppendorf tubes were prepared per gradient, each marked at 1 ml with a black marker. The bottom of the gradient tube was pierced with a needle. The tip of the needle was slowly rotated while piercing through, generating a hole with smooth edge. One eppendorf tube was placed underneath the hole, and then the parafilm seal was broken with a needle to start collecting the fractions. The collecting eppendorf tube was replaced by a new one when reaching the 1 ml mark. The collecting procedure was repeated until no liquid dropped from the gradient. Only 0.5 ml of liquid was expected at

the last fraction. The pellet at the bottom of the gradient was recovered with 1 ml of STE (10 mM Tris [pH 7.5], 100 mM NaCl, 1 mM EDTA) after the removal of the final fraction.

One quarter of each collected fraction was transferred to a new eppendorf tube for DNA analysis. Twenty microgram per milliliter protease K and 10% SDS were added to each fraction to a final concentration of 1mg/ml protease K and 0.5% SDS. The samples were incubated in a 37°C water bath overnight. Next day, 1 : 1 (vol/ vol) phenol/chloroform was added to each fraction. The tubes were then placed in an eppendorf rack and held firmly by placing another rack on top. The two racks were firmly held together and flipped upside down 20 times to mix the phenol/chloroform and aqueous phases. The tubes were spun down at 23,700 x g for 5 min at room temp for phase separation. The liquid phase was transferred into a new eppendorf tube with a P1000 pipette, and the DNA was precipitated with 1 ml of -20°C pre-chilled isopropanol at -20°C for 1 h. The precipitated DNA was pelleted at 23,700 x g for 30 min at 4°C. The supernatant was removed with a P1000 pipette, and the pellet was washed twice with 1.5 ml 70% ethanol. The DNA pellets were air dried overnight in vacuum, and then resuspended in TE (10mM Tris, 1mM EDTA, pH8.0) buffer. The tubes containing DNA in TE were then incubated in a 37°C water bath for 30min to solubilize the DNA.

Two percent agarose gels were prepared by mixing 2.6 g of agarose and 130 ml TAE buffer in a 250 ml flask. The mixture was microwaved for 3 min until the agarose was totally dissolved, shaking every minute. The agarose solution was air cooled for 10

to 20 min at room temperatures and 10 mg/ml EtBr was added to a final concentration of 0.1 mg/ml. The flask was shaken gently, and the solution was then poured onto the gel casting chambers with a 20-well comb. Agarose gels were polymerized for 1 h at room temperature. The DNA of non-MCN digested and non-fractionated chromatin was sonicated into smaller fragments prior to resolution in agarose gels (or sequencing). To load the gels, 10% of the resuspended DNA in each fraction was transferred onto parafilm as a drop, at the same spots were the 2 µl droplet of the 6X DNA loading dye solution had been spotted. The 12 µl DNA plus loading dye was loaded into each well and the DNA was resolve at 70V for 1 h.

The remaining DNA was sealed with parafilm and shipped on ice packs for sequencing.

2.9 Protein analyses

The remaining three quarters in each chromatin fraction was subjected to trichloroacetic acid (TCA) precipitation as described before. After the pellets were air dried for 30min, they were resuspended in 20 µl loading buffer (2% SDS, 10% glycerol, 60 mM Tris (pH 7.4), 0.01% bromophenol blue, 10 mM DTT). The resuspended proteins were denatured by boiling for 10 min. The boiled tubes were immediately buried in ice to cool them fast. Proteins were resolved in 14% SDS gel for resolution of histones, or 10% SDS gel for resolution of ICP4, ICP8 or VP5, at 15 V for 1 h and then 30 V until the front dye ran out of the gel (approximately 8 to 12 h).

2.10 Protein transfer

The gels were carefully transferred into small plastic boxes. Stacking gels were removed, and the resolving gels were soaked in western transfer buffer for 30 min. Nylon membranes were cut to size and activated by soaking in methanol for 3 min before soaking them in western transfer buffer until transfer. The transfer cassette was assembled following the standard protocol for protein transfer with a Bio-Rad protein transfer apparatus. The transfer chamber was filled with western blot transfer buffer and the proteins were transferred for about 15 h (overnight) at 400 mA. The next day, the membranes were carefully removed from the cassette and air dried unless proceeded directly to western blot.

Table 4: Antibodies used for Western blots

Antibodies	Company	Cat. Number
PML (PG-M3): sc-966	Santa Cruz Biotechnology	sc-966
HSV-1 ICP8 monoclonal	Santa Cruz Biotechnology	sc-53329 (10A3)
HSV-1 ICP4 monoclonal	Virusys Corporation	H1A021-100
HSV VP5 monoclonal	Virusys Corporation	HA018-100
Anti-CTCF Antibody, Anti-CTCF	EMD Millipore	07-729
Normal Rabbit IgG, Normal Rabbit IgG	EMD Millipore	12-370
Rabbit IgG, polyclonal - Isotype Control (ChIP Grade)	Abcam	ab171870
Anti-histone H2A	Abcam	88770
Anti-histone H2A	Abcam	13932
Anti-histone H2B	Abcam	52484
Anti-histone H2B	Abcam	1790
Anti-histone H3	Abcam	1791

Anti-histone H4	Abcam	7311
Anti-histone H4	Abcam	31830
Anti-protamine P1	Abcam	66978
Anti-protamine P2	Abcam	190791
Anti-phosphoserine	Millipore	1603
Anti-ubiquitin	Millipore	9408
Anti-ICP4	Abcam	P1101
Anti-ICP4	Abcam	H1A021-100
HSV ICP5 monoclonal	Tantec Biosystems	MABV18010

2.11 Hybridization

Agarose gels were soaked in 1 M HCl for 30 min on a shaker at room temperature. Excess liquid was discarded, and the gels were rinsed with distilled water, and then soaked in alkaline transfer buffer (0.4 N NaOH, 1 M NaCl) for 15min at room temperature, always on a shaker. The alkaline transfer buffer was replaced for another 15min incubation at room temperature. The gels were next rinsed with distilled water and soaked in neutralizing buffer (1 M Tris (pH7.4), 1.5 M NaCl) for 15min at room temperature, always on a shaker. Meanwhile, BioDyn B0.45 nylon membranes and two layers of the thick filter paper were cut to size and soaked in 10x SSC buffer (1.5 M NaCl, 150 mM trisodium citrate, pH 7.0). DNA in the agarose gels was capillary transferred according to standard protocols.

Prior to hybridization, the membrane was completely moistened by soaking in water. Hybridizations were at 75°C for viral, or 68°C for cellular, probes in pre warmed hybridization tubes (one for each membrane, or empty tube for balancing). Rapid hybrid buffer (Amersham Biosciences, Piscataway, NJ) (5 ml per membrane) was also pre-

warmed. Pre-wet membranes were rolled onto a long tweezer and carefully delivered into the middle of the hybridization tube. The membranes were carefully attached to the inner surface, and air bubbles were removed using the long tweezer. Membranes were prehybridized with 10 ml rapid hybrid buffer for one hour at designated temp in a rotating oven.

The probe (HSV-1 EcoRI restriction fragment JK) was denatured by boiling and labeled by random priming according to the manufacturer's instructions (Amersham Biosciences). Labeled probe was added to the pre-warmed 5 ml rapid hybrid buffer in a conical tube, and the mixture was pulled into membrane-containing hybridization tube for hybridization at 75°C for 4 h. Membranes were carefully removed from the tube by a long tweezer, and immediately washed twice with hybridization wash buffer 1 (75 mM NaCl, 7.5 mM sodium citrate, 0.5% SDS) for 15 min at room temperature. The membrane was then rinsed with distilled water, and carefully sealed using plastic wrap. The sealed membrane was exposed to Kodak PhosphorImager screens for 72 h for viral probe or 24 h for cellular probe. The signal was analyzed in a Bio-Rad FX molecular imager.

Table 5: Reagents used for DNA Southern blot hybridization

Reagents	Company	Cat. Number
Agarose, Molecular Biology Grade, Low Melting Point, 25 g	IBI Scientific	IB70051
BioTrace™ NT Nitrocellulose Transfer Membranes, Pall Laboratory	Pall Corporation	66485
Calcium Chloride Dihydrate, ACS, >99%	Amresco	0556-500G
Hydrochloric acid 37% A.C.S.	Sigma-Aldrich	320331-500 ML

Magnesium Chloride Hexahydrate, ACS	BDH	BDH9244-500 g
Na2HPO4 heptahydrate	Thermo Fisher Scientific	AC206515000
Rapid-Hyb Buffer,GE Healthcare, RPN1635, pack of 125 mL	GE Healthcare	RPN1635
Sodium Bicarbonate, ACS	BDH	BDH9280-500G
Sodium chloride, 99.85%, for molecular biology, DNAse, RNAse and Protease free, ACROS Organics™ - 2.5kg; Glass bottle	Acros Organics	327300025
Sodium hydroxide, 500 g UN1823	Amresco	0583-500G
Sodium phosphate, dibasic heptahydrate, 99+%, for analysis	Acros Organics	206515000
Tris-HCl	Promega	h5125
Rediprime II Random Prime Labelling system	Amersham (GE)	RPN1633

2.12 RNA extraction.

Vero cells (1 x 10^7 per treatment) were seeded in a petri dish and infected for 7 h the next day according to the standard protocol. The cells were rinsed with cold PBS, and 1.0 ml TRIZOL reagent was added to each dish to directly lyse the cells. The dish was held 45° and the reagent was pipetted up from the bottom and discharged at the top using a P1000 several times. The dishes were then placed on an ice-water bath for 5 min. The lysates were transferred to 2 ml eppendorf tubes with P1000. Chloroform was added to the mixture (0.2 ml per 1 ml of TRIZOL), and vortexed. The samples were centrifuged at 12,000 x g for 15 min at 4°C. After phase separation, the RNA was in the top clear aqueous phase. About three quarters of the aqueous phase was transferred to a new tube, and isopropanol was added to fill the tube immediately. Samples were chilled at -20°C for 30 min, and RNA was spun down at 12,000 x g for 10 min at 4°C.

The supernatant was carefully pipetted out with P1000. The RNA pellet was washed with 1 ml isopropanol and pelleted again at 12,000 x g for 10 min at 4°C. RNA was then stored in isopropanol at -80°C.

Table 6: Reagents used for RNA extraction and purification

Reagents	Company	Cat. Number
DMEM, low glucose, pyruvate (+ L-glut, phenol red)	Gibco (ThermoFisher Scientific)	11885-084
Cycloheximide	Microbia L Source	45-C7698-1G
DMEM	Gibco	11885-084
EGTA (ETHYLENE GLYCOL-BIS(2-AMINOETHYLETHER)-N)	Sigma-Aldrich	03777-10G
FBS (Lot 15A086)	Sigma Aldrich	F1051-500 ML
Phosphonoacetic acid	Sigma-Aldrich	284270-10G
TRIzol™ Reagent	Thermo Fisher Scientific	15596026
Cycloheximide from microbial source	Sigma	C7698-5G
Roscovitine, free base (x2)	LC laboratories	R-1234
TRIzol Reagent	Ambion (Thermofisher)	15596-026

2.13 RNA visualization.

RNA samples taken from the -80°C freezer were spun down at 12,000 x g for 10 min at 4°C. Then, the supernatant was pipetted out using P1000, and the RNA pellet was resuspended in 50 µl DEPC-treated water. A 1% agarose-bleach gel was casted following Aranda et. al., 2012. Briefly, 1 g agarose was weighed, and 100 ml TAE buffer was added to the agarose in a 250 ml flask. One milliliter Clorox bleach was added to the agarose-TAE mixture (1% V/V) and incubated for 5 min on the bench. The agarose was then melted in a microwave for 2 min, and then 5 µl of 10 mg/ml EtBr was added to

the agarose solution. Agarose was then casted into a chamber following the standard protocol. Twenty microliters of the RNA solution were loaded to each lane and resolved at 70 V for 1 h.

2.14 Library preparation and Illumina sequencing (Performed by collaborator Dr. Depledge)

Total DNA was quantitated using a Qubit HS DNA assay (Thermo Fisher). Sequencing libraries were constructed using 200 ng of input DNA. End repair, A-tailing and adapter ligation were performed using reagents from the SureSelect XT Reagent Kit (Agilent), each step followed by a cleanup procedure using AMPure XP beads (Beckman Coulter) at 1.8 x concentration. Following adapter ligation, four rounds of PCR (Herculase II, Agilent) were performed to enrich for correctly adapter-ligated fragments. Initial denaturation was at 98°C for 2 min, followed by 4 cycles of denaturation (98°C, 30 s), annealing (65°C, 30 s) and extension (72°C, 1 min), and finally a 10 min extension step at 72°C. Libraries were purified as described above and diluted 1:6 with nuclease free water. A second round of PCR (6 cycles) using 15 µl of input was performed using indexing primers available in the SureSelect XT Reagent Kit and PCR conditions as outlined above except for an adjustment to the annealing temperature (to 57°C). Final libraries were analysed using a Qubit Fluorimeter and Tapestation prior to sequencing across 8 runs on an Illumina MiSeq (2x150 bp PE reads, 300 cycle kit).

RNASeq libraries were prepared using the SureSelect Strand-Specific RNA Library Prep for Illumina Multiplexed Sequencing (Protocol version D0, 2015), multiplexed, and sequenced on a single Illumina NextSeq run (2x34 bp PE reads, 75 cycle v2 high output).

Sequence run data were de-multiplexed using bcl2fastq2 v2.17 under stringent conditions (—barcode mismatches 0). Demultiplexed datasets were trimmed using TrimGalore software (http://www.bioinformatics.babraham.ac.uk/projects/trim_galore/) to remove low quality 3' ends and aligned against the HSV-1 strain 17 genome (NC_001806) using BWA [57]. Genome-wide coverage and read depth data were calculated using custom scripts following the generation of pileup files using SAMTools [58]. RNASeq data were processed as above, except that alignment of reads against the HSV-1 strain 17 genome was performed using the splice-aware BBMap (http://sourceforge.net/projects/bbmap/) with default parameters.

2.15 Sequence data analyses

2.15.1 DNA per fraction

Percentage of HSV-1 DNA to total DNA was calculated by the ratio of HSV-1 DNA reads to total DNA reads in each fraction. HSV-1 DNA genome copy equivalents in each fraction were then calculated by multiplying the genome copy equivalents in the total DNA by the percentage of HSV-1 DNA in each fraction. The number of HSV-1 genome copy equivalents in each fraction was divided by the number of genome copy

equivalents in the total undigested and unfractionated HSV-1 DNA to give the percentage of HSV-1 genome copy equivalents recovered in each fraction, or to the addition of the number of HSV-1 genome copy equivalents in all fractions and pellet to give the percentage of HSV-1 genome copy equivalents in each fraction.

2.15.2 Normalized DNA reads

DNA reads (250 bp window) were generated for the entire HSV-1 genome for each fraction. Total DNA reads of soluble and insoluble chromatin at any given genomic position were divided to the DNA reads in the unfractionated chromatin at the same position, to give the normalized DNA reads for that position in each chromatin fraction.

2.15.3 HSV-1 DNA locus in each fraction.

HSV-1 DNA reads in each fraction for each position were corrected by the number of HSV-1 genome copy equivalents in that fraction. The corrected HSV-1 DNA reads in each position were then normalized to the total HSV-1 DNA reads in that position in the same fraction, to give the number of HSV-1 genome copy equivalents in each genome position in every fraction. The sum of the number of HSV-1 genome copy equivalents in each position in all fractions was then normalized to the number of HSV-1 genome copy equivalents in the same position of the undigested and unfractionated chromatin, to give the recovery of each HSV-1 locus after digestion.

2.15.4 Gene sampling.

The number of DNA reads equal or larger to one mapping to every 250 bp window was manually counted as 1. Then, the manually corrected reads were assigned to each gene according to their positions. Gene sampling was calculated as the sum of the manually corrected DNA reads of that gene, normalized to the sampling of the same gene in the undigested and unfractionated chromatin. Sampling of all genes in each kinetic class was averaged to give the average sampling of that kinetic class. Gene sampling of all genes in each fraction was averaged to give the mean sampling. Mean sampling in each fraction was divided by the overall mean sampling to analyze sampling enrichment in each fraction.

Chapter 3: Results

Most of this section has been published with article:
https://doi.org/10.1371/journal.ppat.1008076

3.1 Micrococcal nuclease digested HSV-1 DNA fragments fractionated as nucleosome-size complexes in sucrose gradient

To validate my technique, chromatin of cells infected with HSV-1 for 7 h were harvested and subjected to continuous or serial digestions. The digested chromatin fragments were loaded into 0 - 10% sucrose gradients, to be resolved by their hydrodynamic ratios (Fig 12A). The DNA was extracted from each fraction, loaded into 2% agarose gels, electrophoresed, and visualized by ethidium bromide (EtBr) staining. Both the continuous and serial protocols resulted in the total chromatin being digested into mono- to poly-nucleosome sized fragments. The smallest nucleosome-size complexes (mono- or di-) fractionated to the lowest density sucrose fractions (fraction 12 and 13, close to 0% sucrose), and the largest ones, to the densest (fraction 0 and 1, close to 10% sucrose), as expected (Fig 12A). The intermediate sized complexes were distributed into fractions 2 to 11.

During the serial digestion protocol, each round of digestion is performed while the samples are being fractionated by centrifugation. The newly digested chromatin fragments remain in the soluble fraction while the undigested chromatin pellets down. After centrifugation, the soluble fraction was transferred to a new tube where MCN was

immediately quenched. The undigested pelleted chromatin was resuspended with fresh MCN and digested again during centrifugation for a second round, for a total of six rounds of digestion; six rounds have been shown to release most of the soluble chromatin fragments (Lacasse and Schang 2012). Serial digestion thus protects the most accessible chromatin fragments, which are released early during digestion, from further digestion. During continuous digestion, in contrast, the most accessible chromatin fragments are released early during the digestion and then continuously exposed to MCN.

Knowing that the DNA in each fraction had the appropriate nucleosome sizes. I tested the fractionation of the histones. If the gradients resolved indeed poly-nucleosome complexes, then all core histones would fractionate to all fractions. I extracted proteins from each fraction and resolved them in 14% polyacrylamide SDS gel electrophoreses. All four histones were tested in all fractions by western blots (Fig 12B). As expected, all core histones were detected in all fractions, although their amounts varied. These blots are not directly quantitative. As different fractions had widely different amounts of protein (and DNA), different percentages of each fraction needed to be loaded to have all fractions in the dynamic range (Fig 12B). Moreover, as some fractions had to be loaded entirely in one gel and we could not strip and re-blot the same gels so many times, histones H2A and H2B were evaluated in individual experiments, different from the one used to evaluate H3 and H4.

3.2 Intracellular HSV-1 DNA was differentially protected between continuous MCN digestion and serial MCN digestion

Cellular chromatin was equally protected during both digestion protocols, I then evaluated the HSV-1 DNA in each fraction. The DNA in each fraction was electrophoresed, transferred to a PVDF membrane, and then visualized by hybridization (Fig 12C). Intracellular HSV-1 DNA was digested into mostly small sized complexes (Fraction 10 to 12) during continuous digestions, which migrated similarly as the DNA in cellular mono-, di-, and tri- nucleosomes (Fig 12C). In contrast, the intracellular HSV-1 DNA was protected similarly to the cellular DNA during this serial digestion. The HSV-1 DNA fractionated as the smallest complexes to fractions 11 and 12, as intermediate sized complexes to fractions 5 to 11, and as the largest complexes to fractions 2 to 4 (Fig 12C). These results were most consistent with previous studies by Dr. Lacasse (Lacasse and Schang 2012), indicating that I could use these techniques to evaluate the chromatinization of the intracellular HSV-1 DNA.

A

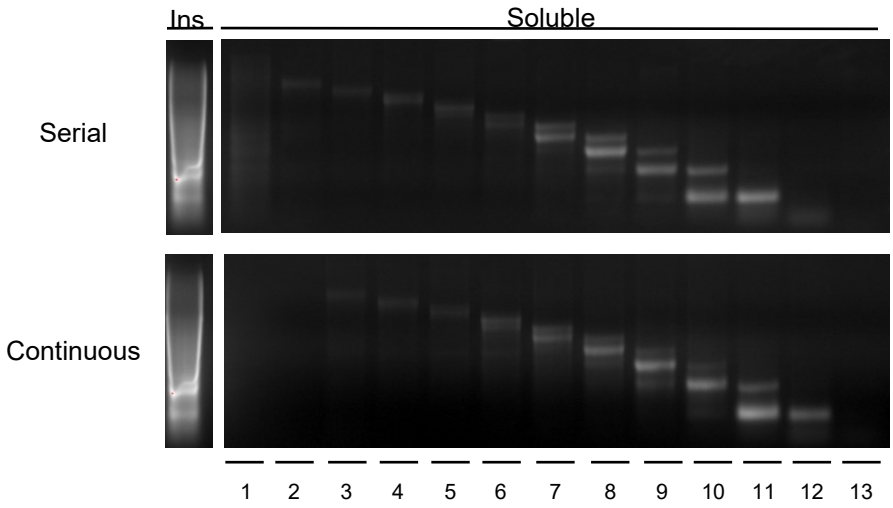
Ins
Soluble
Serial
Continuous
1 2 3 4 5 6 7 8 9 10 11 12 13

B

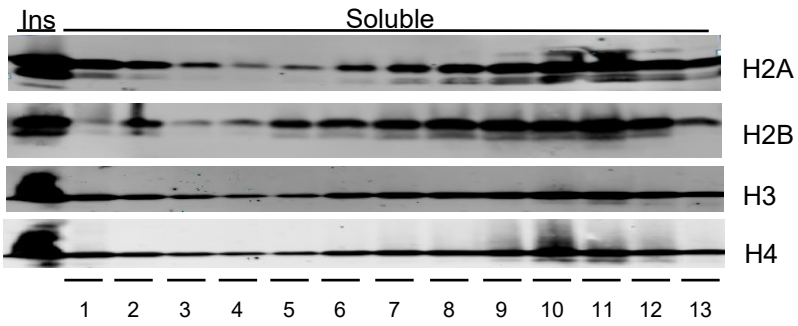
Ins
Soluble
H2A
H2B
H3
H4
1 2 3 4 5 6 7 8 9 10 11 12 13

C

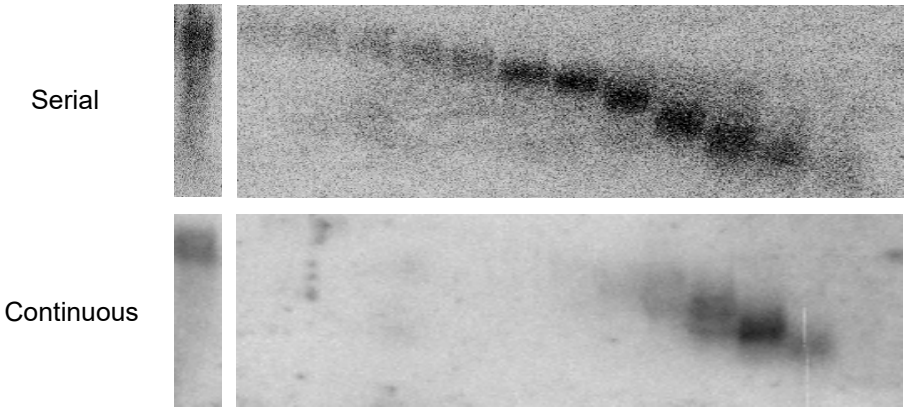
Serial
Continuous

Figure 12: At 7 h after infection, HSV-1 DNA was differentially protected from continuous or serial MCN digestion to sizes of mono to poly-nucleosomes that fractionated in complexes with the hydrodynamic ratios of mono to poly-nucleosomes. Nuclei of infected cells were subjected to continuous or serial MCN digestion. (A) Chromatin fragments separated by hydrodynamic ratios in a 0–10% sucrose gradient, and resolved in 2% agarose gel electrophoresis, stained with EtBr. (B) HSV-1 DNA in each fraction visualized by hybridization with a radiolabelled HSV-1 probe. (C) All core histones were detected in each fraction by western blots. Different percentages had to be loaded in different fractions because the total protein amount in each fraction varies through a wide range. Due to the limitation of loading volume and sample availability, the observed amounts of histones in each fraction are not proportional to their total amounts in each fraction (Hu, Depledge et al. 2019). Figure used under CC-BY 4.0 license.

3.3 Most Intracellular HSV-1 DNA was neither encapsidated nor protein-free, but rather in histone-DNA complexes

Intracellular HSV-1 DNA has been proposed to be mostly nucleosome-free (introduction, section 1.4). It was possible that nucleosome-free HSV-1 DNA non-specifically interacted with cellular chromatin, and consequently, fractionated together with it. HSV-1 DNA could also be protected in intracellular capsids. Encapsidated HSV-1 DNA is fully inaccessible to nuclease and it would thus be protected as full-length genomes in complexes fractionating to the bottom of the sucrose gradient.

To test if the intracellular HSV-1 DNA fractionated as protein-free HSV-1 DNA or encapsidated DNA, encapsidated HSV-1 DNA was extracted from infectious virions, and then protein-free HSV-1 DNA was extracted from the purified capsids. Encapsidated or protein-free HSV-1 DNA were then spiked into the extracted cellular chromatin from mock infected cells before performing the nuclease protection assays in parallel with

chromatin extracted from cells infected with HSV-1 for 7 h.

At 7 h, there were approximately 845 genome copy equivalents (GCE) per nucleus. Therefore, approximately 800 GCE per nuclei of the protein-free or encapsidated HSV-1 DNA was spiked into the cellular chromatin. If the intracellular HSV-1 DNA was mostly protein-free and fractionated with with cellular chromatin through non-specific interactions, one would expect the spiked protein-free HSV-1 DNA would fractionate similarly as the intracellular HSV-1 DNA.

The DNA-protein complexes of each treatment were fractionated in sucrose gradients after the nuclease protection assay, and the DNA in each fraction was extracted and deep sequenced (by Dr. Depledge). The number of genome copy equivalents of HSV-1 DNA in each fraction was calculated and plotted in the X-axis against the fraction number in the Y-axis (Fig 13). Most of the spiked protein-free HSV-1 DNA was totally degraded and not detected. Most of the detected HSV-1 DNA fractionated as the smallest complexes (fractions 10 to 12), none fractionated to the intermediate fractions and little fractionated to the largest complexes (perhaps trapped by large cellular chromatin). All protected encapsidated HSV-1 DNA fractionated as the largest complexes to the insoluble fractions, as expected. Intracellular HSV-1 DNA, in contrast, was enriched as the smallest complexes in fractions 10 to 12, and as the largest complexes in insoluble fraction and fraction 1, but also fractionated to the intermediate fractions (fraction 2 to 9) (Fig 13). The fractionation pattern of the

intracellular HSV-1 DNA was not a simple addition of the spiked protein-free and encapsidated HSV-1 DNA, and the intracellular DNA was protected to a much larger extent than protein-free HSV-1 DNA. It is of course possible that a fraction of the intracellular DNA is encapsidated and part protein-free.

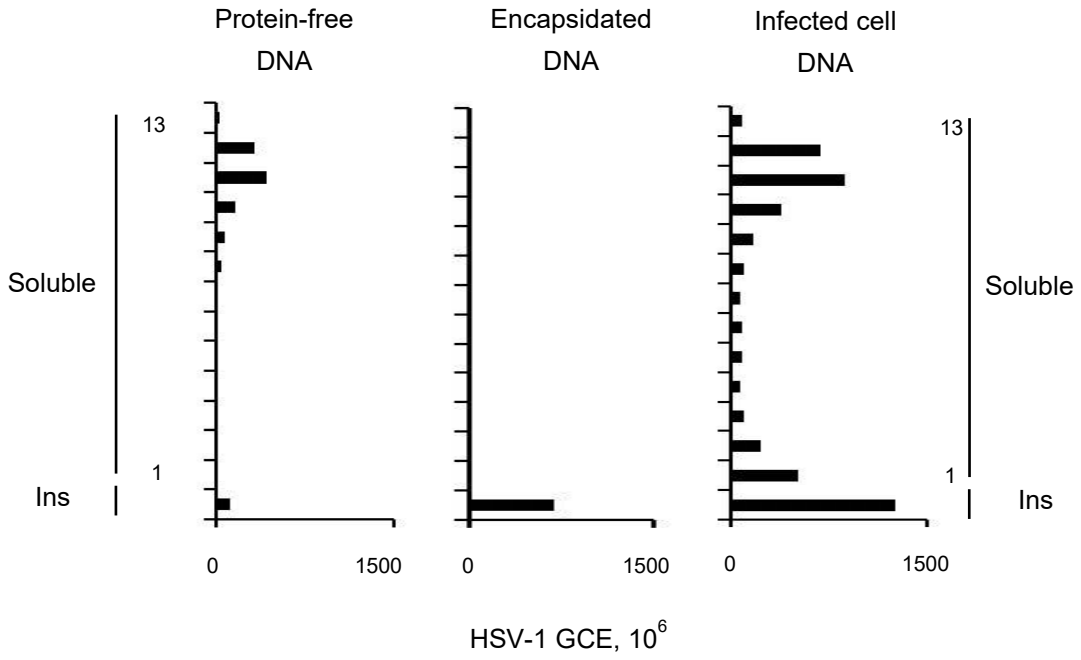

Figure 13: Intracellular HSV-1 DNA is differentially protected from MCN digestion than deproteinized or encapsidated DNA. Bar graph showing the number of HSV-1 genome copy equivalents in each fraction. Chromatin of HSV-1 infected cells was digested and fractionated. DNA in each fraction was subjected to deep sequencing. Ins, insoluble chromatin; GCE, genome copy equivalents. (Hu, Depledge et al. 2019). Figure used under CC-BY 4.0 licens.

Intracellular HSV-1 DNA could also be protected by other nucleoprotein complexes containing no histones. To test for this possibility, proteins were extracted from the insoluble and all soluble fractions and blotted against VP5 (the major capside protein),

ICP4, and ICP8 (two major HSV-1 DNA binding proteins).

There was little (10%) detectable VP5 in the soluble fraction, and most (90%) fractionated into insoluble fractions, as expected (Fig 14A). It was unlikely thus that VP5 would have protected most HSV-1 DNA in the soluble fractions. Thirty percent of ICP4 and 20% of ICP8 was detected in the soluble fractions. ICP4 and ICP8 were then blotted in each soluble fraction (Fig 14B). Most ICP8 fractionated to fractions 10 to 12, whereas ICP4 was more evenly fractionated to fractions 5 to 13 (Fig 14B).

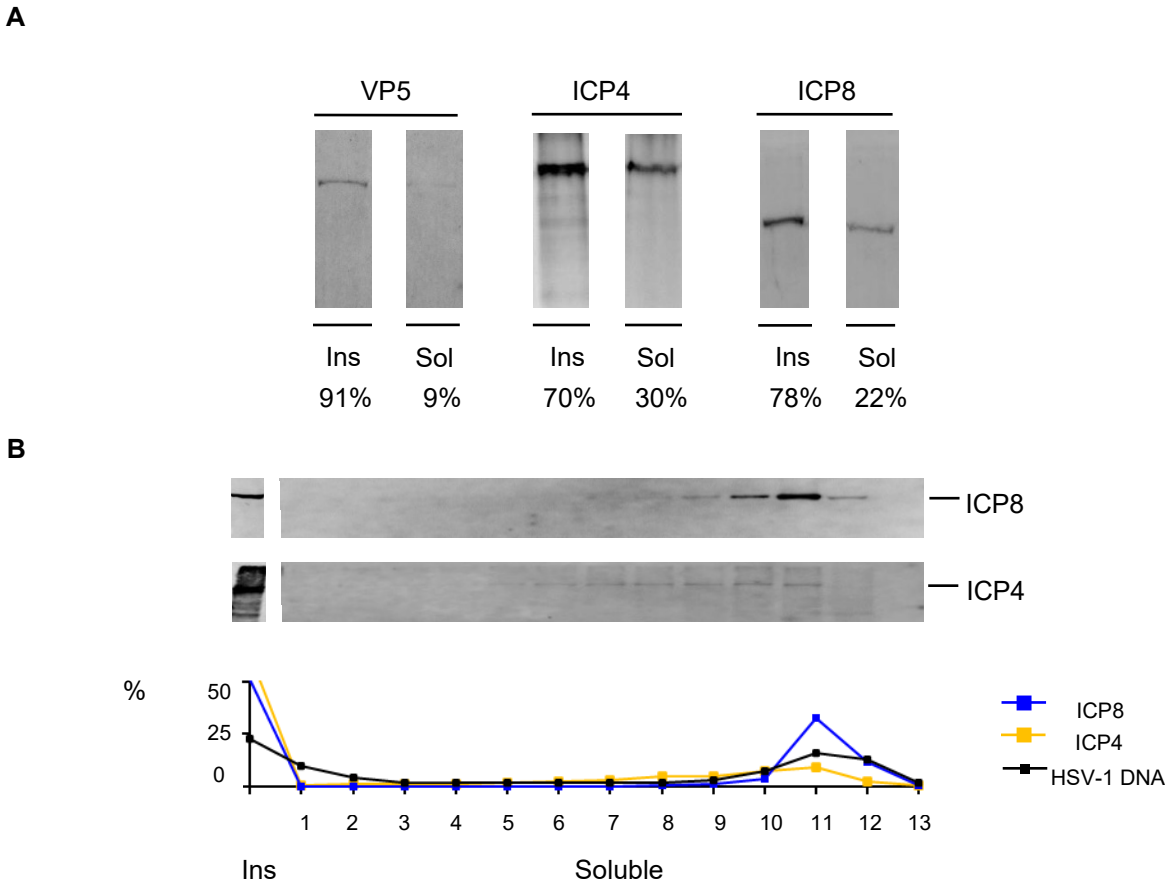

Figure 14. Fractionation of the major HSV-1 DNA binding proteins.

(A) Western blots of VP5, ICP4 and ICP8 in the insoluble and soluble chromatin fractions. Results representative of two independent repeats. (B) Fractionation of ICP4, ICP8, and HSV-1 DNA after serial MCN digestion and sucrose gradient centrifugation. Western blots of ICP4 and ICP8, and line graph presenting the percentage of ICP4, ICP8 and HSV-1 DNA in each fraction. VP5 was below sensitivity levels in all fractions. Ins, insoluble chromatin fraction; sol, soluble chromatin fraction. Average of three (ICP8) or two (ICP4) independent experiments. (Hu, Depledge et al. 2019). Figure used under CC-BY 4.0 license.

If intracellular HSV-1 DNA fractionated as nucleosome complexes, histones would be expected to interact with the HSV-1 DNA. Another PhD student, Esteban Flores, performed chromatin immunoprecipitation analyses of all fractions of serially digested chromatin of cells infected with HSV-1 for 7 h (Fig 15). HSV-1 DNA was coimmunoprecipitated with histone H3 in all fractions, including those containing little HSV-1 DNA (i.e., fraction 13). Therefore, most intracellular HSV-1 DNA fractionated as nucleosome complexes.

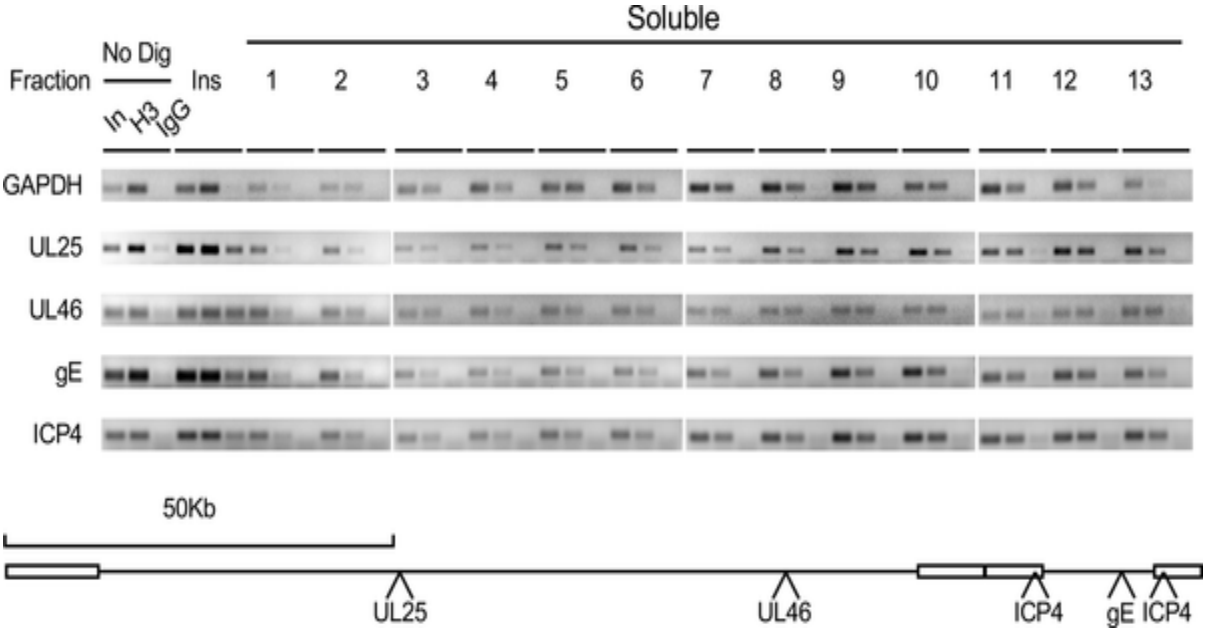

Figure 15: HSV-1 DNA was protected from serial MCN digestion at 7 h after infection to sizes of mono to poly-nucleosomes that fractionated in complexes with the hydrodynamic ratios of mono to poly-nucleosomes and contain histone H3.

Nuclei of infected cells were subjected to serial MCN digestion and then cross-linked. Chromatin immunoprecipitation of HSV-1 DNA with histone H3. EtBr-stained agarose gels of saturating PCR for cellular (GAPDH) or HSV-1 (UL25, UL46, ICP4, or gE) DNA co-immunoprecipitated with histone H3. Cartoon presenting the positions of the PCR amplicons in the HSV-1 genome at bottom. In, input (2%); H3, anti-histone H3 antibody; IgG, isotype antibody control (labeled only in the No Dig sample for simplicity); No Dig, undigested unfractionated chromatin; Ins, insoluble chromatin. This figure and the related experiments were prepared and performed by Mr. Esteban Flores. (Hu, Depledge et al. 2019). Figure used under CC-BY 4.0 license.

3.4 All HSV-1 genes were in similarly accessible chromatin even if they were differentially transcribed

Chromatin regulates DNA accessibility, and thus DNA-dependent processes such as transcription. Knowing that intracellular HSV-1 DNA was mostly in nucleosomes, the transcribed HSV-1 genes could well be in more accessible chromatin than the non-transcribed ones. To test this model, I modulated HSV-1 transcription with cycloheximide (CHX) or roscovitine (Rosco). CHX inhibits translation of all proteins, resulting no expression of the IE proteins while IE genes are highly transcribed as a result of the lack of inhibition by ICP4. Rosco indirectly inhibits transcription of all HSV-1 genes through not yet characterized mechanisms. According to the simplest model, the highly transcribed IE genes in CHX treated infections would be in most accessible chromatin, and thus would fractionate as the smallest complexes. All HSV-1 genes under Rosco treatment would be in least accessible chromatin and thus fractionate as large

complexes.

To test this model, intracellular HSV-1 DNA was serially digested, and the chromatin fragments were separated by sucrose gradients. DNA was then extracted from each fraction and deep sequenced (by Dr. Depledge, the raw sequencing data is open accessible at https://www.ncbi.nlm.nih.gov/bioproject/PRJNA550980). The number of DNA reads of each HSV-1 gene in each fraction was calculated and subjected to cluster analyses. Transcribed genes would be in accessible chromatin and thus cluster together, whereas non-transcribed genes would be in least accessible chromatin and also cluster together, and away from the transcribed ones. Most HSV-1 genes clustered together in non-treated cells infected for 7 h. Surprisingly, most HSV-1 genes from CHX treated infections also clustered together, as did all genes from Rosco treated infections (Fig 16A). Contrary to the expectation, the transcribed IE genes from the CHX treated infections did not cluster together with the transcribed genes in untreated infections. Neither did the non-transcribed E and L genes from CHX treated infections cluster together with the genes from Rosco treated infections.

All HSV-1 genes were enriched in the insoluble fraction and fraction 1, and in fractions 12 and 13, whereas depleted in the intermediate fractions in 7 h untreated infections. Most HSV-1 genes were enriched in the insoluble fraction and fraction 1, and in fraction 12 in CHX treated infections. A few HSV-1 genes of CHX treated infections clustered with HSV-1 genes from Rosco treated infections, but with no obvious specific

pattern (i.e., not correlated with transcription levels or kinetic classes). Most HSV-1 genes of Rosco treated infections were enriched in fraction 1, and fraction 12, and thus clustered further away from the genes of untreated infections. The few exceptions still did not correlate with transcription levels nor kinetic classes.

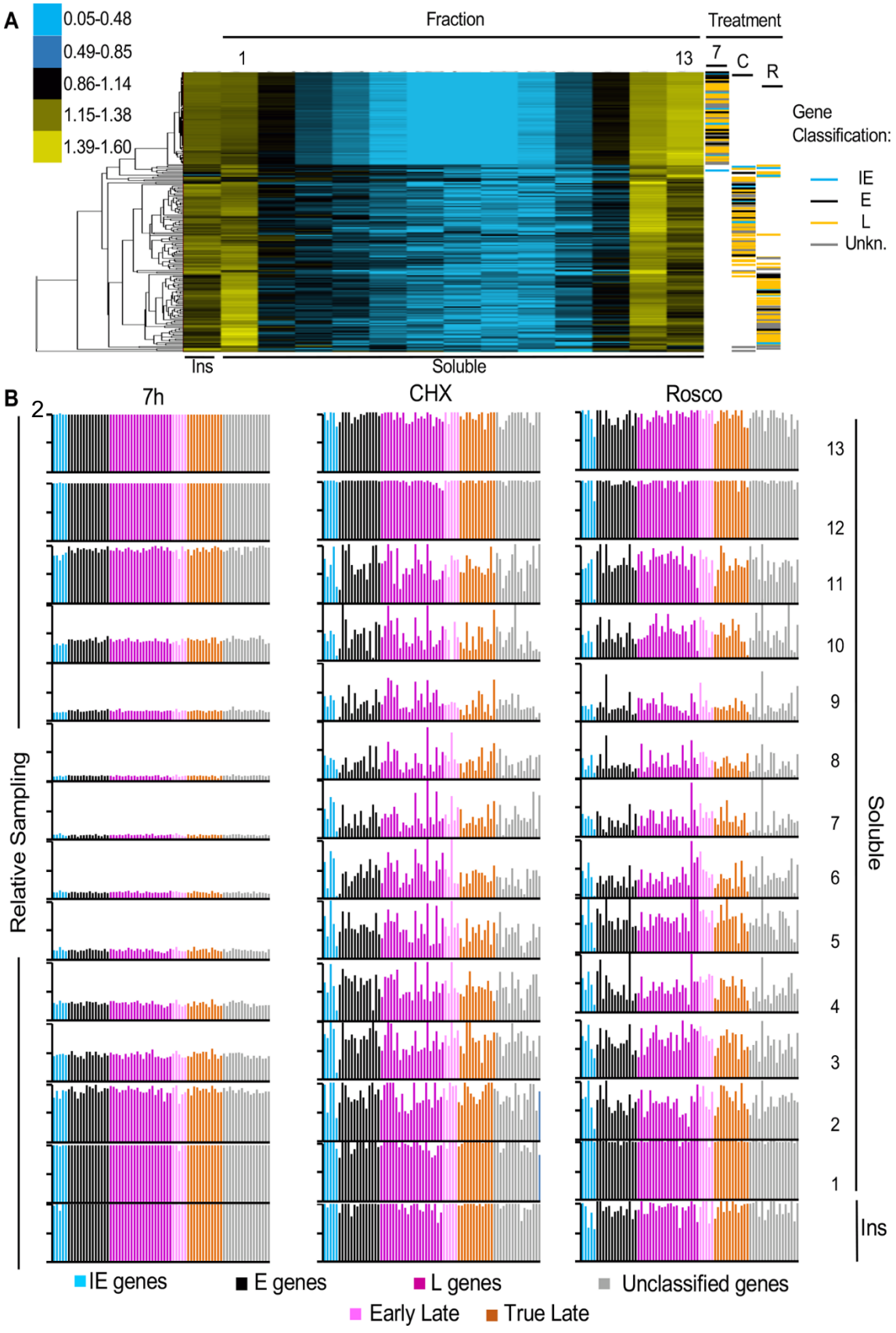
A
0.05-0.48
0.49-0.85
0.86-1.14
1.15-1.38
1.39-1.60
Fraction
1
13
Treatment
7
C
R
Gene Classification:
IE
E
L
Unkn.
Ins
Soluble
B
7h
CHX
Rosco
2
13
12
11
10
9
8
7
6
5
4
3
2
1
Ins
Soluble
Relative Sampling
IE genes
E genes
L genes
Unclassified genes
Early Late
True Late

Figure 16: All HSV-1 genes resolved together to the least and most accessible chromatin fractions. (A) Cluster analyses of the number of DNA reads for IE, E or L genes in each fraction. Cluster analysis was performed with Cluster 3.0 from Stanford University, visualized with Java Treeview. Color key on the left indicates ratio of reads in fraction over reads in the total DNA (ranges are in log_2). 7, 7 h pi, untreated infections; C, CHX- treated infections; R, roscovitine-treated infections. (B) Gene sampling of each HSV-1 gene in each fraction. Sampling of each HSV-1 gene was calculated and normalized to the sampling of the same gene in the undigested and unfractionated chromatin. Each gene is color coded according to kinetic class. Blue, IE genes; black, E genes; dark purple, unclassified L genes; light purple, early L genes; brown, true L genes; grey, unclassified genes. Ins, insoluble chromatin fraction. (Hu, Depledge et al. 2019). Figure used under CC-BY 4.0 license.

Notably, HSV-1 genes were less depleted in the intermediate fractions in CHX or Rosco treated infections than in untreated infections (Fig 16A). As a avert, my approach evaluates HSV-1 chromatin accessibility at the population level, not at the individual genome level. Therefore, the accessibility of a given gene at the population level did not directly correlate with its transcription level.

To further test whether the accessibility of any individual gene was related to its transcription level, I individually evaluated the fractionation of each known HSV-1 gene. For the accessibility of a gene to be related to its transcription level, the entire gene (but not necessarily its promoter) would be expected to be similarly accessible. Consequently, the entire gene would fractionate as a unit in the relevant fractions and deep sequencing would sample DNA sequences covering most of the gene in those fractions. As HSV-1 genes range from 170bp to 9,490bp, I analyzed the relative sampling of each gene in each chromatin fraction or in the unfractionated chromatin.

The fraction of a given gene sampled in each fraction was then normalized to the fraction of the same gene sampled in the unfractionated chromatin and expressed as percentage (gene sampling).

The sampling of each gene was calculated in each fraction and plotted according to kinetic groups (Fig 16B). At 7 h after infection, the least (insoluble chromatin and fractions 1 and 2) and most (fractions 11 to 13) accessible chromatin were enriched in fully sampled HSV-1 genes, whereas the intermediately accessible chromatin contained only random samplings of each gene. Fractions 3 and 10 sampled approximately half of each HSV-1 gene, whereas the rest of the intermediate fractions had sampled only less than 20% of each at our sequencing depth. No individual HSV-1 gene was differentially sampled across all fractions. Although the sampling of several genes deferred in a single fraction, these experiments were not designed, or had the power to, analyze individual genes.

When transcription of E and L genes was inhibited (in infections treated with CHX), the transcriptionally active IE genes still fractionated as the transcriptionally inactive E and L genes (Fig 16B). The least (insoluble chromatin and fraction 1) and most (fractions 12 to 13) accessible chromatin were enriched in completely sampled HSV-1 genes. In the intermediately accessible chromatin, each gene was sampled less frequently at our sequencing depth—albeit not nearly to the same extent as in the untreated infections. Fractions 2 to 5 and fraction 11 sampled 40–60% of each HSV-1

gene, and fractions 6 to 10, 25% - 40%.

No HSV-1 genes fractionated differently when HSV-1 transcription was inhibited with Rosco either, and the least (insoluble chromatin and fraction 1) and most (fractions 12 to 13) accessible chromatins were again enriched in mostly fully sampled HSV-1 genes (Fig 16B). As in the infections treated with CHX, the depletion in fully sampled genes in the intermediately accessible chromatin in comparison to untreated infections was only partial. Fractions 2 to 4 and fraction 11 sampled 40–60% of each HSV1 gene, and factions 5 to 10, 25–40%.

The depletion in fully sampled genes in the intermediate accessible chromatin could have been an artifact resulting from too little HSV-1 DNA in them. However, fully sampled HSV-1 genes resolved to the insoluble chromatin, and to fractions 1, 12, 13 and the insoluble chromatin in infections treated with CHX or Rosco. These fractions contained as little HSV-1 DNA as the intermediate fractions in the untreated infections, which contained only partially sampled genes.

From the analyses of the untreated, CHX-, or Rosco-treated infections together, the accessibility of all genes at the genome population level related to the overall levels of transcription of the genomes, whereas the accessibility of any single gene did not relate to its own transcription levels.

To evaluate the global accessibility, the average gene sampling for IE, E and L genes in each kinetic class was calculated in each fraction (Fig 17A). At 7 h after

infection, the least and most accessible chromatins were enriched in fully sampled HSV-1 genes of all three kinetic classes. The other fractions were in contrast partially depleted of fully sampled genes (Fig 17A). The enrichment in fully sampled IE, E, or L genes in only the least and most accessible chromatins was not altered when only IE genes were transcribed to high levels (CHX), no gene was transcribed to high levels (Rosco), or all IE, E and L genes were transcribed to high levels (Fig 17A). In contrast, the depletion in fully sampled genes in the intermediately accessible chromatin was less marked in CHX or Rosco-treated infections. I concluded that transcription and accessibility of genes in any kinetic class are not directly related (Figs 16 and 17). As these experiments were repeated only once, no statistical analyses were performed.

The sampling of all genes in all fractions was averaged. Sampling of all genes in each fraction was then expressed as enrichment over the average sampling and plotted together with the percentage of HSV-1 DNA in each fraction (Fig 17B). At 7 h after infection, the least (insoluble chromatin to fraction 2) and most (fractions 11 to 13) accessible chromatins that were enriched in fully sampled HSV-1 genes had most of the HSV-1 DNA. The most accessible chromatin that was enriched in fully sampled genes had 31% of the HSV-1 DNA, and the least accessible chromatin that was equally enriched in fully sampled genes, 35%. Although the fractions containing the most accessible chromatin could also contain some naked DNA, the presence of fully sampled genes indicates that the DNA in these fractions had not been digested

extensively, contrary to what would have been expected from naked DNA.

The intermediately accessible chromatin (fractions 3 to 10), which contained 34% HSV-1 DNA, contained only partially sampled genes (Fig 17B). This depletion in fully sampled genes was not a result of a mix of chromatinized and protein-free HSV-1 DNA. Protein-free HSV-1 DNA did not resolve to these intermediate fractions (Fig 13) and DNA from an E and a L gene in these fractions co-immunoprecipitated with histone H3 (Fig 15).

The distribution of HSV-1 DNA was markedly distinct from that of the cellular DNA (dashed black line) in untreated infections, indicating obvious biophysical differences between the viral and cellular chromatin under these conditions.

When most HSV-1 transcription was inhibited with CHX, the least accessible chromatin that was enriched in fully sampled HSV-1 genes (insoluble chromatin and fraction 1) had 22% of the HSV-1 DNA. In contrast, the most accessible chromatin that was enriched in fully sampled genes (fractions 12 and 13) had only 2% of the HSV-1 DNA (Fig 17B). Similarly, when HSV-1 transcription was inhibited with Rosco, the least accessible chromatin that was enriched in fully sampled HSV-1 genes (insoluble chromatin and fraction 1) had 15% of the HSV-1 DNA whereas the most accessible chromatin that was also enriched in fully sampled genes (fractions 12 and 13), had only 4% of the HSV-1 DNA (Fig 17B). The intermediately accessible chromatin, containing only partially sampled genes, contained 75–80% of the HSV1 DNA. In both conditions,

the depletion in fully sampled genes in the intermediately accessible chromatin was only partial and progressive, with less depletion in the least accessible intermediate chromatin (fractions 1–6) and more in the most accessible ones (fractions 7–9).

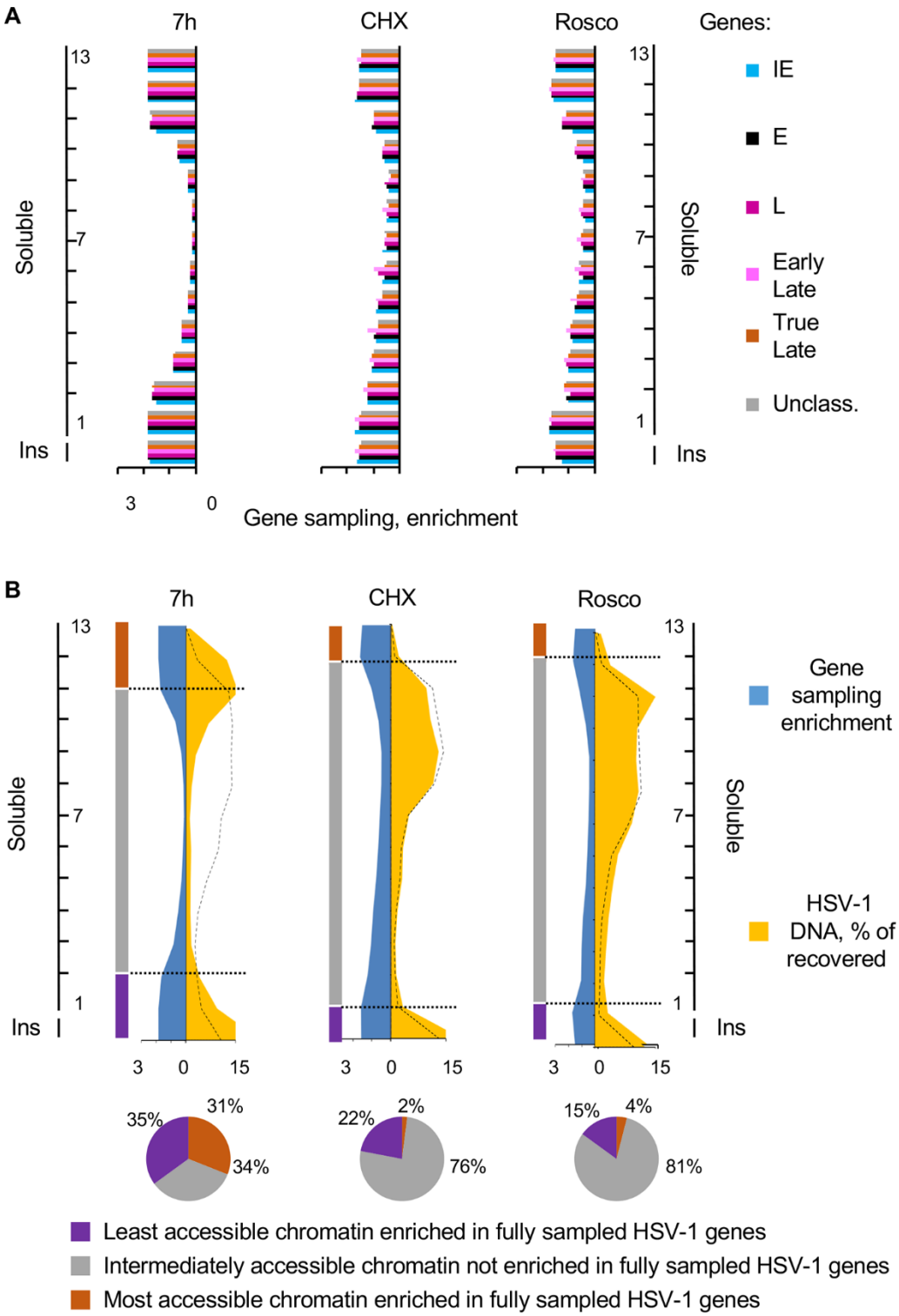
A
7h
CHX
Rosco
Genes:
IE
E
L
Early Late
True Late
Unclass.
Soluble
Ins
13
7
1
3
0
Gene sampling, enrichment
B
7h
CHX
Rosco
Gene sampling enrichment
HSV-1 DNA, % of recovered
15
35%
31%
34%
22%
2%
76%
15%
4%
81%
Least accessible chromatin enriched in fully sampled HSV-1 genes
Intermediately accessible chromatin not enriched in fully sampled HSV-1 genes
Most accessible chromatin enriched in fully sampled HSV-1 genes

Figure 17: The most and least accessible chromatin enriched in fully sampled HSV-1 genes contained more HSV-1 DNA when transcription was active.

(A) Bar graphs showing average sampling of all genes in each HSV-1 gene kinetic groups in each fraction. Sampling of each HSV-1 gene was calculated and normalized to the sampling of the same gene in the undigested and unfractionated chromatin. The normalized sampling of all genes in each group was then averaged. Blue, IE genes; black, E genes; dark purple, unclassified L genes; light purple, early L genes; brown, true L genes; grey, unclassified genes. (B) Area graphs and pie charts presenting relative enrichment in gene sampling and percentage of HSV-1 DNA in each fraction. Gene sampling in each fraction is expressed as ratio to the average sampling to present the relative enrichment in fully sampled genes in each fraction. The distribution of the cellular chromatin is indicated by the dotted black line. Pie charts indicating the percentages of the HSV-1 DNA in the most accessible chromatin fractions containing completely sampled HSV-1 genes (brown), in the intermediate accessible chromatin fractions containing random samplings of each gene (grey), or in the least accessible chromatin fractions containing completely sampled HSV-1 genes (purple). Ins, insoluble chromatin fraction. (Hu, Depledge et al. 2019).

When viral transcription was globally inhibited with either CHX or Rosco, the distribution of the viral DNA very much replicated that of the cellular DNA, indicating similar biophysical properties between the viral and cellular chromatin when most of the viral genome is not transcribed.

In summary, the HSV-1 chromatin had similar biophysical properties to the cellular chromatin when there was limited HSV-1 transcription, but it was far more accessible when the genomes were highly transcribed. Moreover, the total levels of HSV-1 DNA in the most accessible chromatin that was enriched in fully sampled genes related to the overall transcription level of the genomes.

3.5 Changes in the accessibility of HSV-1 chromatin as infection progresses

I next evaluated the HSV-1 chromatin as the infection progressed. At 2 h after infection with 10 pfu/cell, there were approximately 20 HSV-1 genome copy equivalents per cell, constituting 0.2% of the DNA in the cell. The HSV-1 DNA was enriched in the least accessible chromatin (insoluble chromatin and fractions 1–2), with a very minor relative enrichment in the most accessible chromatin (fractions 9–11) and depleted in the intermediately accessible chromatin (fractions 3–8) (Fig 18).

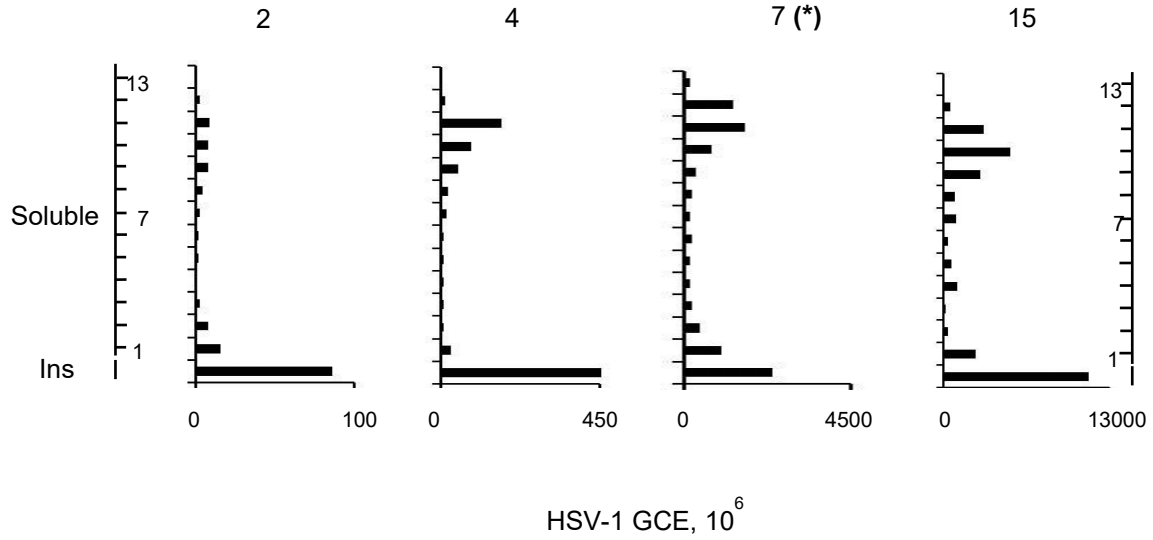

Figure 18: Differential fractionation of HSV-1 DNA throughout infection.
Bar graphs showing HSV-1 genome copy equivalents in each fraction. ***(*)*** *Data from Figure 13 presented again for comparison. Ins, insoluble chromatin fraction; GCE, genome copy equivalent. (Hu, Depledge et al. 2019).* Figure used under CC-BY 4.0 license.

The distribution of the HSV-1 DNA changed at 4 h, when there were approximately 90 HSV-1 genome copy equivalents per cell, constituting 0.8% of the nuclear DNA. HSV-1 genomes were then enriched in the least (mostly in the insoluble chromatin) and in the most accessible chromatin (fractions 9–11), while they were depleted in the

intermediately accessible chromatin (fractions 2–8).

As already discussed, there were approximately 850 HSV-1 genome copy equivalents per cell, constituting 6% of the nuclear DNA, at 7 h after infection. The HSV-1 genomes were also enriched in the most and, less so, in the least accessible chromatin and depleted in the intermediately accessible chromatin (Fig 13–presented again in Fig 18 for comparison). At 15 h after infection, there were approximately 2,650 HSV-1 genome copy equivalents per cell, constituting 20% of the nuclear DNA. At this time, the HSV-1 DNA was also enriched in the least (insoluble chromatin and fraction 1) and most (fractions 9–11) accessible chromatin (Fig 18), but also less depleted in the intermediate fractions.

3.6 The accessibility of all HSV-1 genes increases in synchrony as the infection progresses

No particular HSV-1 gene was differentially accessible at 7 h pi, regardless of whether transcription was inhibited or not (Fig 16), and the most accessible chromatin was enriched in fully sampled genes only when there was abundant transcription (Fig 17). Both the most and least accessible chromatins contained fully sampled HSV-1 genes (Fig 16). One possibility was that the most accessible chromatin contained transcriptionally competent genomes and the least accessible one, transcriptionally silenced ones (and potentially encapsidated DNA although VP5 was barely detectable at this time), whereas the intermediately accessible chromatin contained genomes

transitioning between states. Then, the fractionation of the HSV-1 genomes would be expected to change from the least accessible chromatin toward the most accessible one as infection progresses.

To test this model, I analyzed the accessibility of the viral chromatin as the infection progressed. When evaluated by their fractionation, IE, E and L genes clustered together according to time after infection, not to kinetic class (Fig 19A). All IE, E, and L genes were relatively underrepresented in the most accessible chromatin and thus clustered the furthest away at 2 h, when there is limited HSV-1 transcription, from genes of 4 and 15 h infections. IE, E and L genes were all enriched in the most and least accessible chromatin at 4 h, when there is already widespread HSV-1 transcription. At 15 h, the depletion in the intermediately accessible chromatin was uniform across genes but less uniform across fractions.

Genes of all kinetic classes resolved similarly and were similarly sampled in each fraction at all infection times (Fig 19B).

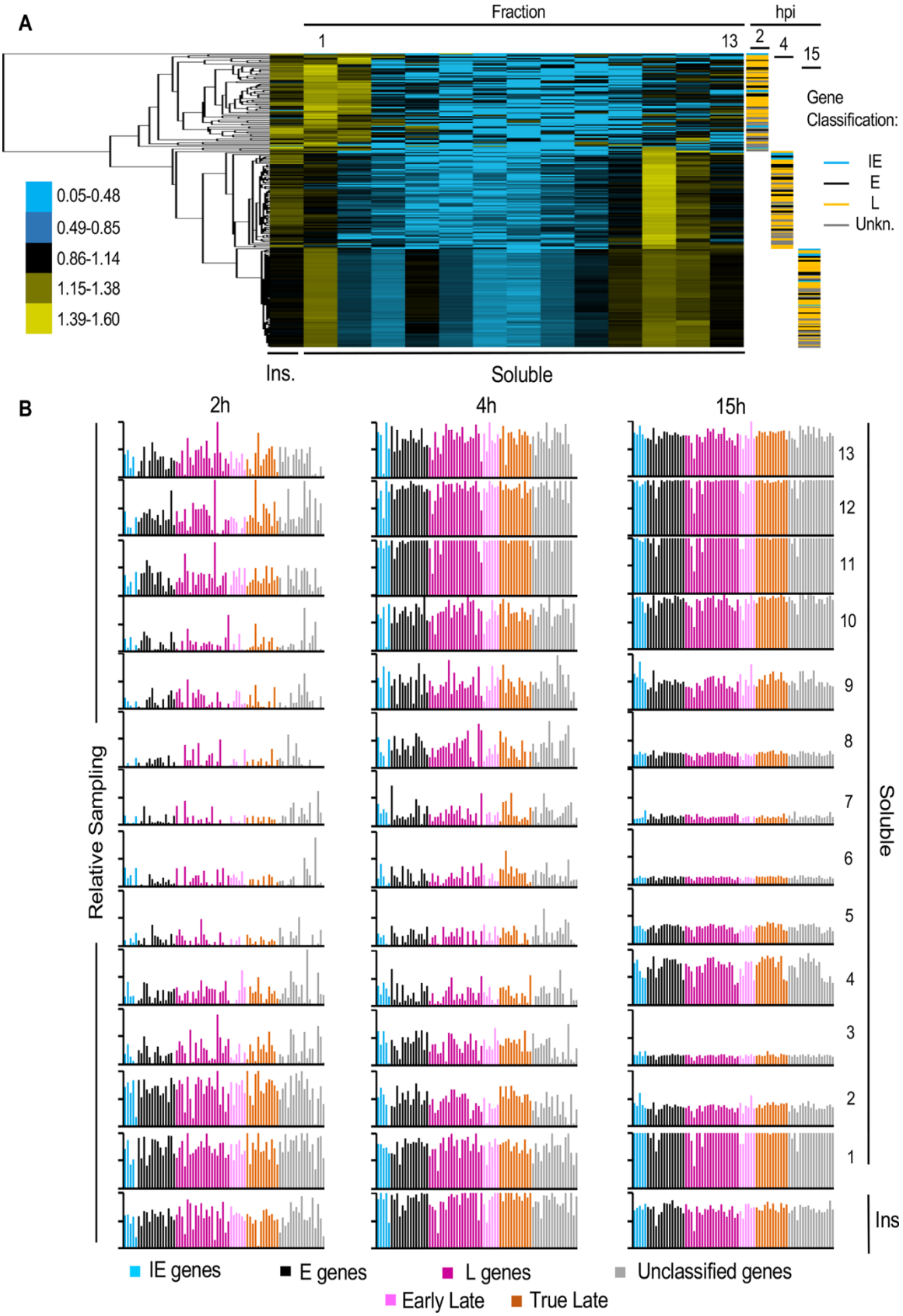
A
Fraction
1
13
hpi
2
4
15
Gene Classification:
IE
E
L
Unkn.
0.05-0.48
0.49-0.85
0.86-1.14
1.15-1.38
1.39-1.60
Ins.
Soluble
B
2h
4h
15h
Relative Sampling
13
12
11
10
9
8
7
6
5
4
3
2
1
Soluble
Ins
IE genes
E genes
L genes
Unclassified genes
Early Late
True Late

Figure19: All HSV-1 genes resolved together to the least and most accessible chromatin fractions as infection progressed. (A) Cluster analyses of the number of DNA reads from IE, E and L genes in each fraction. Cluster analysis was performed using Cluster 3.0 from Stanford University, visualized with Java Treeview. (B) Bar graphs showing sampling of each HSV-1 genes at 2 h, 4 h, and 15 h after infections. Sampling of each HSV-1 gene was calculated and normalized to the sampling of the gene in the undigested and unfractionated chromatin. The sampling of each gene was plotted according to kinetic class. Blue, IE genes; black, E genes; dark purple, unclassified L genes; light purple, early L genes; brown, true L genes; grey, unclassified genes. Ins, insoluble chromatin fraction. (Hu, Depledge et al. 2019).

To analyze potential differences among IE, E or L genes, I averaged the sampling of all genes in each kinetic class. At 2 h, the least accessible chromatin fractions (insoluble, fractions1 and 2) were enriched in fully sampled HSV-1 genes of all kinetic classes (Fig 20A). The fully sampled genes were depleted in the intermediately accessible fractions, although not to the extent as in 7 h infections. The most accessible chromatin fractions (fractions 11 to 13) were only partially enriched in fully sampled genes (Fig 20A). As infection progressed, the least accessible chromatin fractions (insoluble and fractions 1 and 2 at 2 h, or insoluble and fractions 1 at 4 or 15 h) were enriched in fully sampled HSV-1 genes of all kinetic classes, as were the most accessible fractions (fractions 11 to 13 at 2 h, or fractions 10 to 13 at 4 or 15 h) (Fig 20A).

Sampling of all genes in all fractions was again averaged and the sampling in each fraction was expressed as enrichment over the average sampling and plotted together with the percentage of HSV-1 DNA in each fraction as in Fig 17B.

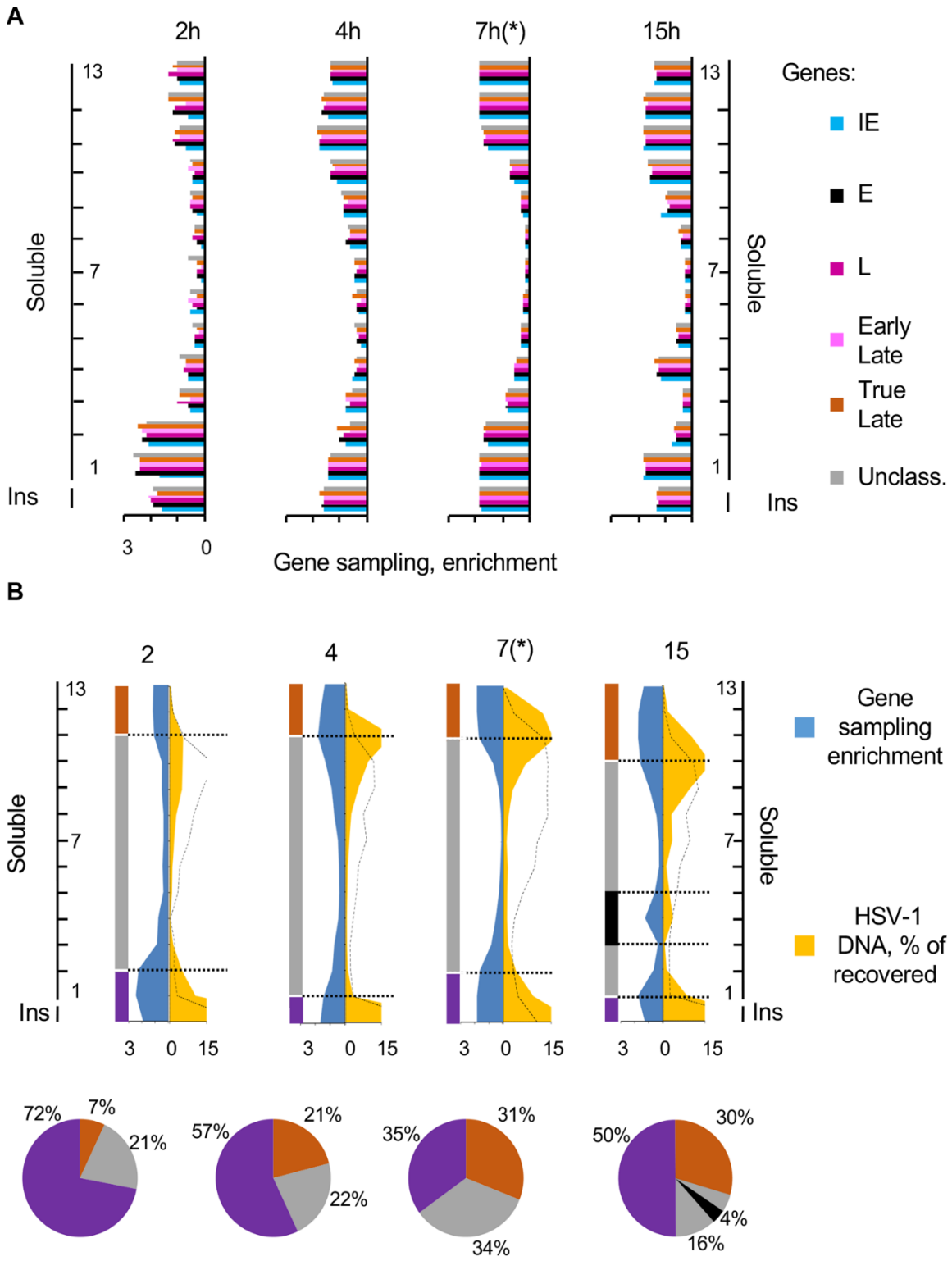
A
2h
4h
7h(*)
15h
13
7
1
Ins
Soluble
3
0
Gene sampling, enrichment
Genes:
IE
E
L
Early Late
True Late
Unclass.
B
2
4
7(*)
15
Gene sampling enrichment
HSV-1 DNA, % of recovered
72%
7%
21%
57%
21%
22%
35%
31%
34%
50%
30%
4%
16%
Least accessible chromatin enriched in fully sampled HSV-1 genes
Intermediately accessible chromatin not enriched in fully sampled HSV-1 genes
Most accessible chromatin enriched in fully sampled HSV-1 genes

Figure 20. The most and least accessible chromatin enriched in completely sampled HSV-1 genes contained more HSV-1 DNA as the infection progressed. (A) Bar graphs showing average sampling of the genes in each HSV-1 gene kinetic class in each fraction at 2, 4 and 15 hours after infection. (*) The graph and data from 7 h are presented again for comparison. Sampling of each HSV-1 gene was calculated and normalized to the sampling of the gene in the undigested and unfractionated chromatin. The normalized sampling of all genes in each group was then averaged. Blue, IE genes; black, E genes; dark purple, unclassified L genes; light purple, early L genes; brown, true L genes; grey, unclassified genes. (B) Area graphs showing relative enrichment in completely sampled genes and percentage of HSV-1 DNA in each fraction. Gene sampling in each fraction is expressed as ratio to the average sampling (relative enrichment). The distribution of the cellular chromatin is indicated by the dotted black line. ***(*)*** *Data from Fig 5 presented again for comparison. Pie charts showing percentage of HSV-1 DNA in the most accessible chromatin fractions containing completely sampled HSV-1 genes (brown), in the intermediate accessible chromatin fractions containing random sampling of each gene (grey), in the least accessible chromatin fractions containing completely sampled HSV-1 genes (purple), or in the intermediate accessible chromatin fractions but containing fully sampled HSV-1 genes (black). Ins, insoluble chromatin fraction. (Hu, Depledge et al. 2019).* Figure used under CC-BY 4.0 license.

At 2 h after infection, the least accessible (insoluble chromatin to fraction 2) chromatin that was enriched in fully sampled HSV-1 genes had 72% of the HSV-1 DNA (Fig 20B). The intermediately accessible chromatin that was only partially depleted of fully sampled genes contained 21% HSV-1 DNA (fractions 2 to 10). The most accessible (fractions 11 to 13) chromatin that was only partially enriched in fully sampled HSV-1 genes (20–40% of each gene) had only 7% of the HSV-1 DNA (Fig 20B). The distribution of the viral DNA was somewhat similar to that of the cellular DNA, albeit more enriched in the least accessible chromatin.

At 4 h, the least (insoluble chromatin to fraction 1) and most (fractions 11 to 13)

accessible chromatin that enriched in fully sampled HSV-1 genes had 57% or 21% of the recovered HSV-1 DNA, respectively. At this time, there was a more marked depletion in gene sampling in the intermediately accessible chromatin, and the distribution of the viral DNA started to differ from that of the cellular DNA more markedly, with a clear enrichment of viral DNA in the most accessible chromatin.

At 7 h, as already discussed (Fig 17B–presented again in Fig 20B for comparison), the least (insoluble chromatin to fraction 2) and most (fractions 11 to 13) accessible chromatin that was enriched in fully sampled HSV-1 genes had 35% or 31% HSV-1 DNA, respectively. There was a marked depletion of HSV-1 DNA in the intermediately accessible chromatin and the distribution of cellular and viral DNA differed the most.

At 15 h, the least (insoluble chromatin to fraction 1) and most (fractions 10–13) accessible chromatin enriched in fully sampled HSV-1 genes had 50% or 30% of HSV-1 DNA, respectively (Fig 20). At this time, HSV-1 DNA was also enriched, together with fully sampled HSV-1 genes, in the intermediately accessible chromatin in fraction 4 (4%).

3.7 Selected short HSV-1 DNA sequences are more underrepresented in the undigested and unfractionated HSV-1 chromatin than in the digested and fractionated one

To analyze if there were large scale differences in the accessibility of different HSV-1 loci, the genome copy equivalent (GCE) for each genome position in each fraction was calculated. The GCE values were plotted in logarithmic scale against genome

position using a 250 bp sliding window.

Consistently with the cluster analyses, the entire HSV-1 genomes were similarly accessible at 7 h. No genomic region was obviously enriched or depleted in any fractions and conversely depleted or enriched in others, as indicated by the lack of converse GCE changes of these regions in different fractions (Fig 21), and the total recovery of the HSV-1 DNA in each locus in all fractions was equally proportional to the total HSV-1 DNA in that locus before digestion and fractionation (Fig 21).

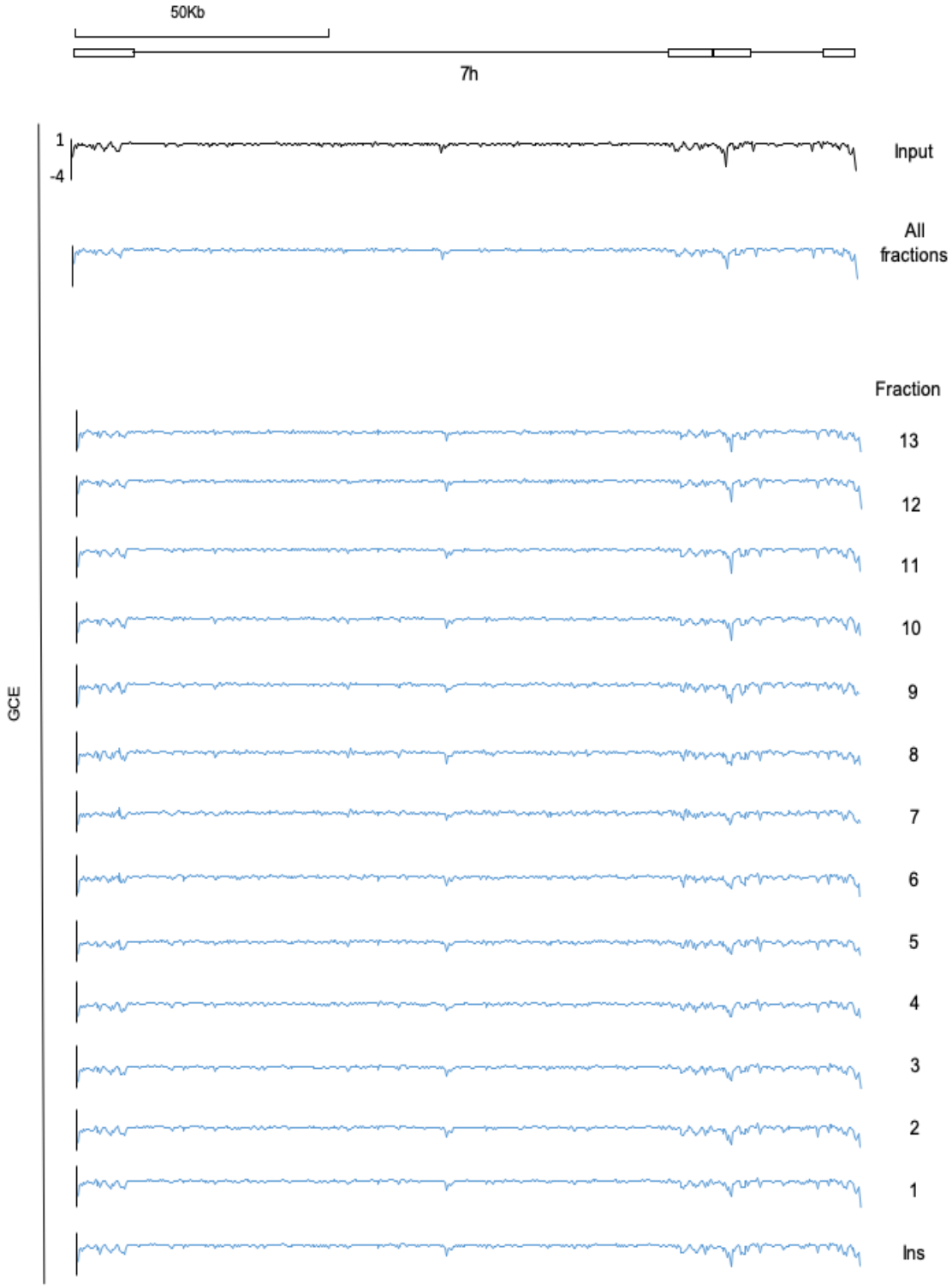
50Kb
7h
1
-4
Input
All fractions
Fraction
13
12
11
10
9
8
7
6
5
4
3
2
1
Ins
GCE

Figure 21: No HSV-1 genomic region was overrepresented in some fractions and compensatively underrepresented in others. Line graphs showing the number of HSV-1 genome copy equivalents (GCE) at each locus in each soluble fraction, the insoluble fraction, the overlap of all insoluble and soluble fractions, and undigested and unfractionated chromatin fraction at 7 hours after infection. Y-axis, GCE in logarithmic scale. X-axes, genome position (cartoon on top). Ins, insoluble chromatin fraction. (Hu, Depledge et al. 2019). Figure used under CC-BY 4.0 license.

As the HSV-1 genome is widely transcribed at 7 h after infection, I analyzed the genomes in infections treated with CHX or Rosco to test transcribed and non-transcribed loci. When E and L gene transcription was inhibited with CHX, only the IE genes were transcribed to a high level. However, the transcribed IE loci did not fractionate differently from the non-transcribed E or L loci. No obvious HSV-1 genome region, and particularly no IE locus, was enriched in any fraction and consequently depleted from other (Fig 22). A few sequencing artifacts map to the same positions in several fractions (fractions 8 through 10, for example) and the undigested and unfractionated chromatin fraction. All HSV loci, including the IE, were also proportionally recovered in the digested and fractionated chromatin over the undigested and unfractionated one (Fig 22).

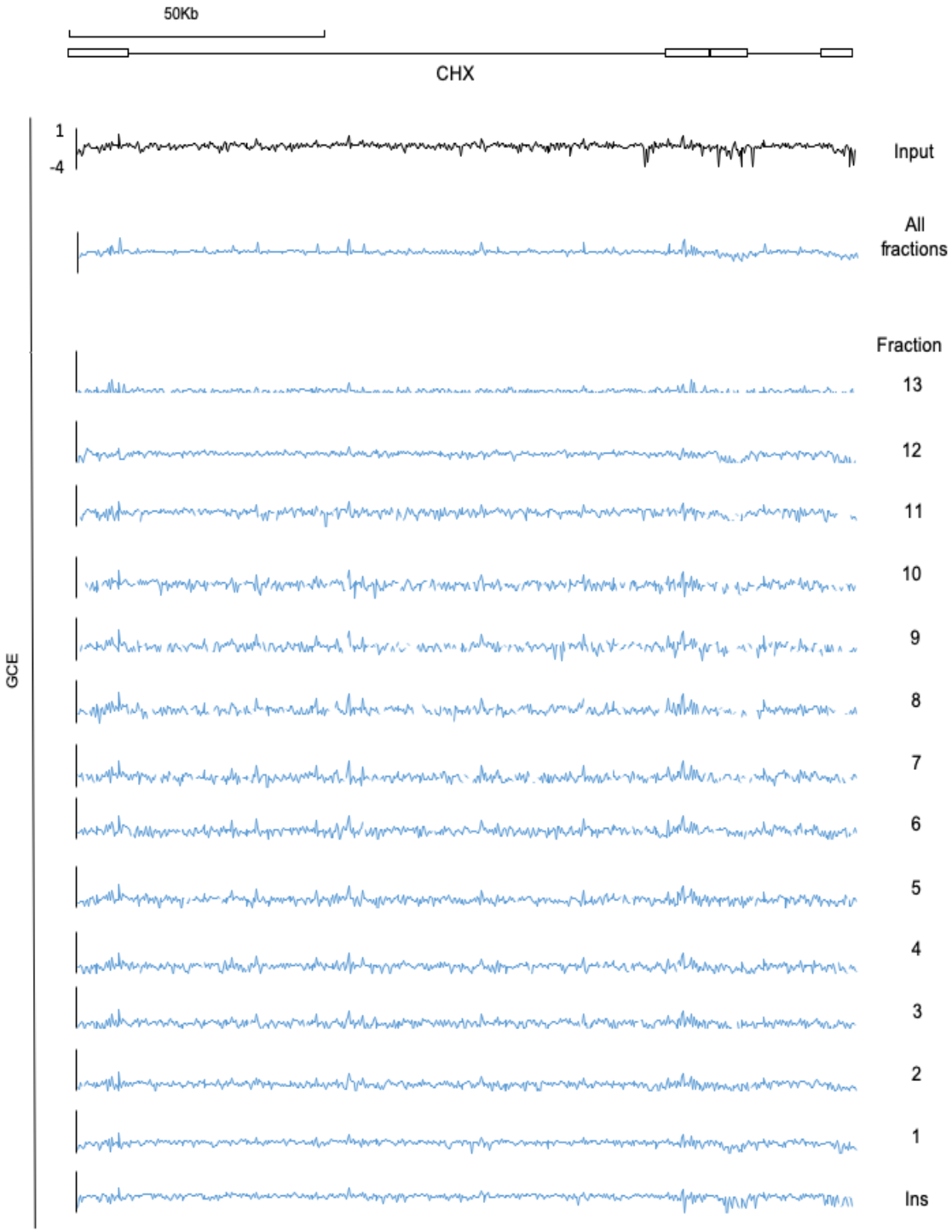
50Kb
CHX
1
-4
Input
All fractions
Fraction
13
12
11
10
9
8
7
6
5
4
3
2
1
Ins
GCE

Figure 22: No HSV-1 genomic region was overrepresented in some fractions and compensatively underrepresented in others when only the IE genes were transcribed. Line graphs showing the number of HSV-1 genome copy equivalents (GCE) at each locus lots for each soluble fraction, the insoluble fraction, the overlap of all insoluble and soluble fractions, and undigested and unfractionated chromatin fraction at 7 hours after infection treated with CHX. Y-axis in logarithmic scale. X-axes, genome position (cartoon on top). Ins, insoluble chromatin fraction. (Hu, Depledge et al. 2019).

When HSV-1 transcription was inhibited with Rosco, the levels of transcription were low through the entire genome, including the IE genes. As in all other conditions, no specific HSV-1 locus was enriched in any fraction and compensatory depleted in others (Fig 23). The same sequencing artifacts detected in the CHX samples were evident in the same positions (for example, fractions 7 through 10).

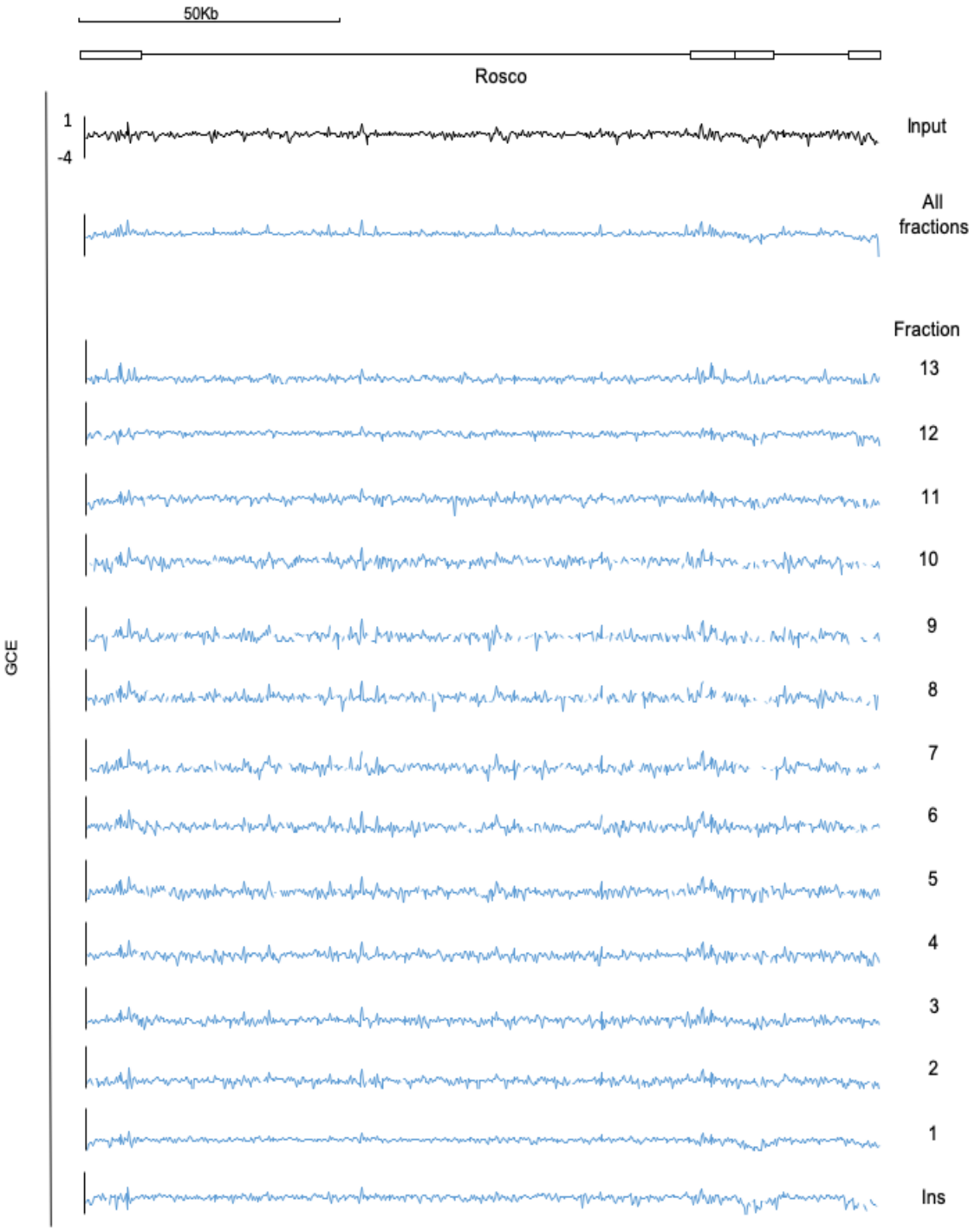
50Kb
Rosco
1
-4
Input
All fractions
Fraction
13
12
11
10
9
8
7
6
5
4
3
2
1
Ins
GCE

Figure 23: No HSV-1 genomic region was overrepresented in some fractions and compensatively underrepresented in others when HSV-1 transcription was restricted. Line graphs showing the number of HSV-1 genome copy equivalents (GCE) at each locus in each soluble fraction, the insoluble fraction, the overlap of all insoluble and soluble fractions, and undigested and unfractionated chromatin fraction at 7 hours after infection treated with Rosco. Y-axis in logarithmic scale. X-axes, genome position (cartoon on top). Ins, insoluble chromatin fraction. (Hu, Depledge et al. 2019).

To evaluate a condition in which only some loci are not highly transcribed in a context of globally active transcription, I used PAA. No gene loci fractionated differently in infections treated with PAA, in which HSV-1 IE and E genes were transcribed to high levels whereas the L genes were not, either (Fig 24).

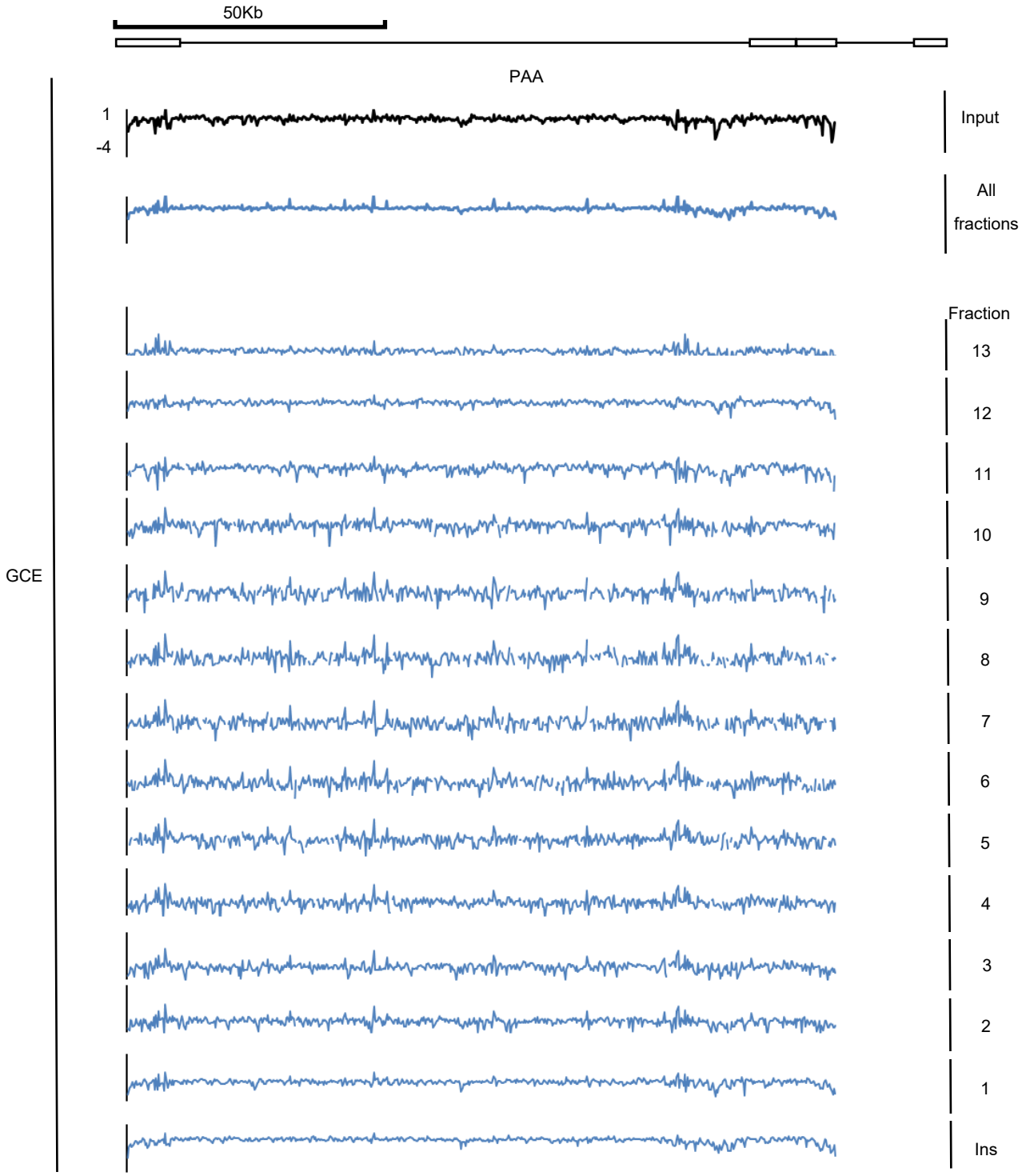

Figure 24: No HSV-1 genomic region was overrepresented in some fractions and compensatively underrepresented in others when HSV-1 replication was inhibited. Line graphs showing the number of HSV-1 genome copy equivalents (GCE) at each locus in

each soluble fraction, the insoluble fraction, the overlap of all insoluble and soluble fractions, and undigested and unfractionated chromatin fraction at 7 hours after infection treated with PAA. Y-axis in logarithmic scale. X-axes, genome position (cartoon on top). Ins, insoluble chromatin fraction.

3.8 The short sequences overrepresented in the chromatin fractions flank highly transcribed HSV-1 genes

To analyze if there were large scale differences in the accessibility of different HSV-1 loci, the number of HSV-1 DNA reads for each genome position in each fraction was corrected by the HSV-1 genome copy equivalents in the same fraction. The addition of the genome copy equivalents in each position in all fractions were normalized to the HSV-1 DNA genome copy equivalents in the same position in the unfractionated and undigested chromatin to give the relative genome copy equivalents of that position after digestion and fractionation. The normalized values were plotted against genome position using a 250 bp sliding window. The coverage of HSV-1 RNA was plotted likewise to evaluate the transcription levels at each locus (Fig 25). One sequence in the repeat region appeared to have been relatively enriched to some extent in the digested and fractionated over the undigested and unfractionated chromatin at 7 h infections; it mapped to a CTCF binding site (Amelio, McAnany et al. 2006) (empty downward arrow). However, 16 short sequences of less than 250bp were relatively overrepresented in the digested and fractionated chromatin over the undigested and unfractionated one in CHX treated infections (Fig 25). Seven of them, including five of the six most overrepresented,

map to previously mapped CTCF binding sites (empty arrows) or chromatin insulator-like elements (black solid circles) in strain 17 (Lang, Li et al. 2017). Treatment of Rosco resulted some low levels of transcription through the genome and lower levels of IE transcription than in CHX treated infections (Fig 25). As in the previous cases, however, 15 short sequences of less than 250bp were slightly and relatively overrepresented in the digested and fractionated chromatin over the undigested and unfractionated one, albeit not nearly as overrepresented as in the CHX-treated infections (Fig 25). One of these sequences map to chromatin insulator-like elements (black solid circle) (Amelio, McAnany et al. 2006). Nine short sequences were again relatively overrepresented in the digested and fractionated chromatin over the undigested and unfractionated one in the PAA-treated infections, albeit again not nearly as much as in the CHX-treated infections (Fig 25). Two map to a previously mapped chromatin insulator like elements (black solid circle) (Amelio, McAnany et al. 2006), and another to a previously mapped CTCF binding site (empty downward arrow) (Lang, Li et al. 2017).

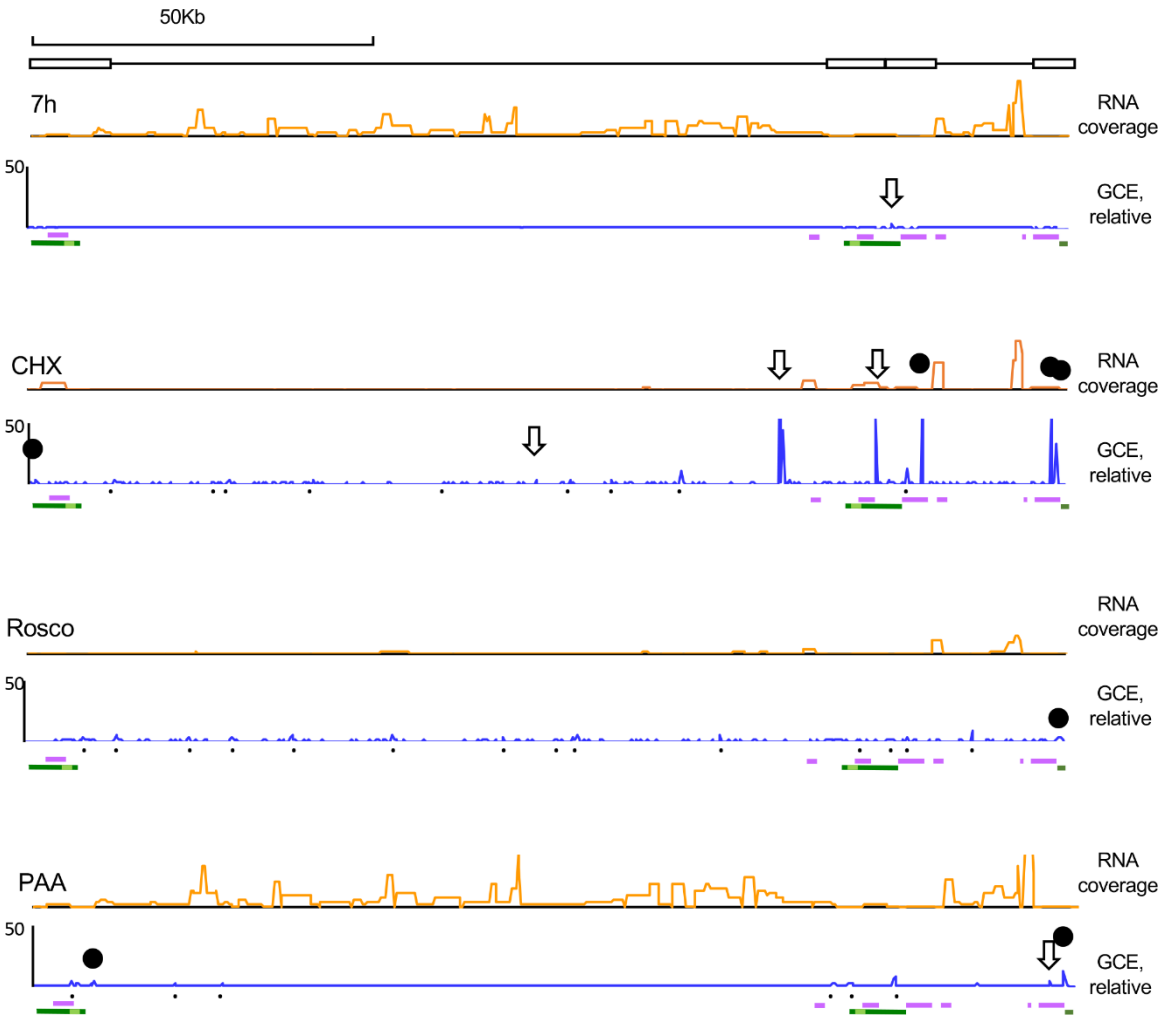

Figure 25. No HSV-1 loci fractionated differently regardless of transcription levels, but short overrepresented sequences flanked transcribed genes when transcription was restricted. Line graphs showing HSV-1 number of genome copy equivalents (GCE) in each genome position in untreated infections, or in infections treated with CHX, Rosco, or PAA at 7 h pi, normalized to the number of HSV-1 genome copy equivalents in the respective position of undigested and unfractionated chromatin (blue line). Orange line graphs, HSV-1 RNA reads. X-axes, genome position (cartoon on top). Black downward empty arrows, CTCF binding sites in strain 17; black solid circles, chromatin insulator-like elements in strain 17; black dots, other overrepresented sequences; purple bars underneath genome plots, IE genes; dark green bars underneath genome plots, LAT; light green bar, stable LAT; GCE, genome copy equivalent. (Hu, Depledge et al. 2019).

As the relatively most overrepresented short sequences in the digested and fractionated chromatin mapped to the internal and terminal repeats, which encode most of the IE genes, the LAT, and some other genes, the HSV-1 repeats were evaluated in more detail (Fig 26). In infections treated with CHX, the six dominant peaks flanked the highly transcribed IE loci, separating them from the rest of the genome (which is non-transcribed, orange line on top). No similar dominant peaks flanking the IE genes were observed in the untreated infections, in which there is abundant transcription across the entire genome, or in the infections treated with Rosco, in which there was little transcription across the genome, or with PAA, in which there is abundant transcription of IE and E but not L genes (Fig 26).

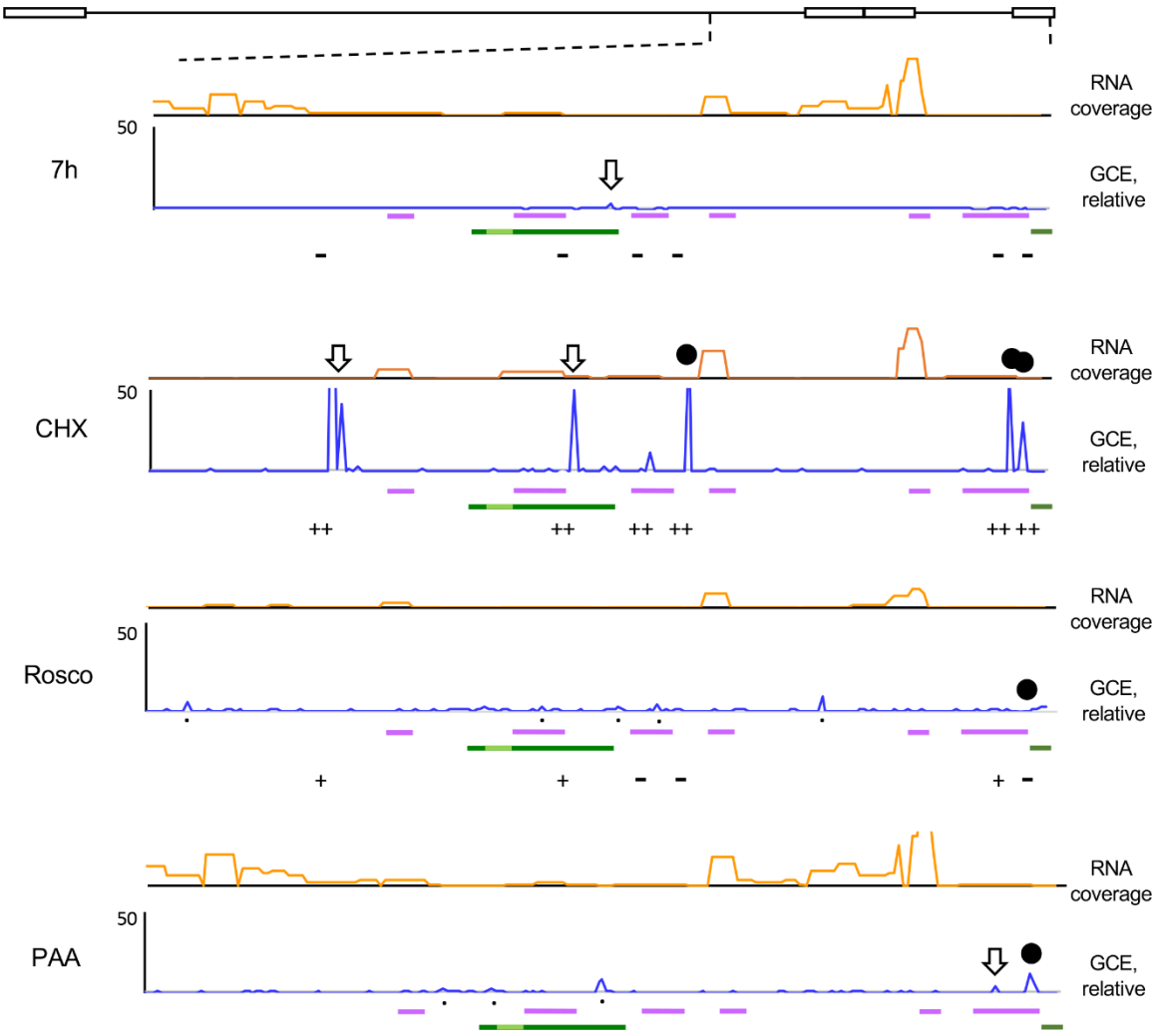

Figure 26. Enlargement of the repeats region, from position 100k bp to 152k bp. Orange lines graphs, HSV-1 RNA reads. X-axes, genome position (cartoon on top). Blue lines, HSV-1 number of genome copy equivalents (GCE) in each genome position. Black downward empty arrows, CTCF binding sites in strain 17; black solid circles, chromatin insulator-like elements; black dots, other overrepresented short sequences; purple bars underneath genome plots, IE genes; dark green bars underneath genome plots, LAT; light green bar, stable LAT; GCE, genome copy equivalent. ++ sequences co-immunoprecipitated with CTCF by ChIP in two independent experiments; + sequences co-immunoprecipitated with CTCF by ChIP in one of two independent experiments; - sequences not co-immunoprecipitated with CTCF by ChIP in either of the two independent experiments. Mr. Esteban Flores performed the CTCF ChIP experiments. (Hu, Depledge et al. 2019). Figure used under CC-BY 4.0 license.

No peaks thus separated the IE genes from the rest of the genome when the overall transcription level was high (untreated or PAA treated), or low (infections treated Rosco) across the entire genomes.

The relatively overrepresented sequences were often underrepresented in both the undigested and unfractionated and some also in the digested and fractionated chromatin, which is more obvious when the data are plotted in a logarithmic scale (Fig 27). When so, however, they were more underrepresented in the undigested and unfractionated chromatin than in the digested and fractionated chromatin.

There was only one just visible overrepresented short sequence in the digested and fractionated chromatin in the untreated infections, when the overall transcription level was high, nine in PAA treated infections, when L genes are not transcribed, sixteen, including six very predominant ones, in the chromatin of CHX treated infections, when only the IE genes were transcribed, and fifteen in the chromatin of Rosco treated infections, when the overall transcription level was low.

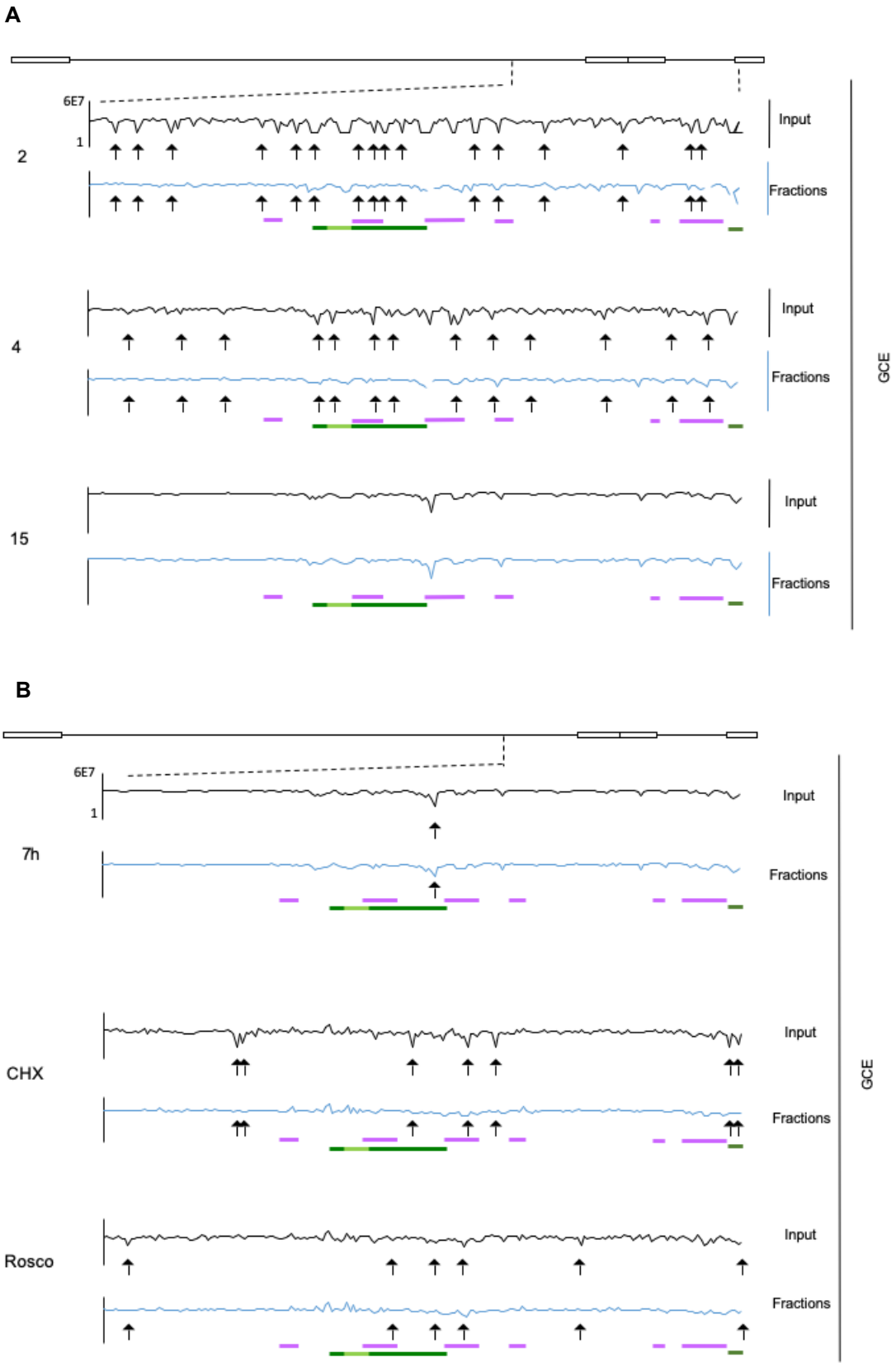
A
6E7
1
2
Input
Fractions
4
Input
Fractions
15
Input
Fractions
GCE
B
6E7
1
7h
Input
Fractions
CHX
Input
Fractions
Rosco
Input
Fractions
GCE

Figure 27: The overrepresented peaks result from fewer DNA reads in the unfractionated, undigested HSV-1 DNA in untreated infections for 2, 4, or 15 h (A) or infections treated with Rosco or CHX (B). Line graphs showing the number of HSV-1 genome copy equivalents (GCE) in each genome position in all fractions (blue) and in the undigested and unfractionated chromatin (black), in untreated infections, or infections treated with CHX or Rosco. Y-axis in logarithmic scale. X-axes, genome position (cartoon on top); upward arrows, the peaks overrepresented; purple bars underneath genome plots, IE genes; dark green bars underneath genome plots, LAT; light green bar, stable LAT. (Hu, Depledge et al. 2019). Figure used under CC-BY 4.0 license.

The sequences underrepresented in the undigested and unfractionated chromatin of CHX treated infections that had not been experimentally mapped as CTCF binding sites in HSV-1 KOS included sequences recognized by CTCF in strain 17 or predicted in silico to be potential CTCF binding sites in strain KOS (Fig 28). I thus explored whether these peaks comprised sequences recognized by CTCF. Sequences on the previously described CTRS3 (the third CTCF binding site located at the repeat short region), CTRS1/2 and CTa'm (the CTCF binding site located at the repeat "a'" sequences) (Amelio, McAnany et al. 2006), as well as the CTCF binding sites recognized by primers B1# and B9# (Lang, Li et al. 2017) in strain 17, and a proposed new CTCF binding site in the ICP4 gene, all co-immunoprecipitated with CTCF above background in two independent experiments in infections treated with cycloheximide (Fig 26, ChIP by Esteban Flores). Consistent with the much reduced magnitude of the overrepresentation of all peaks in the rosco-treated infections in the MCN-seq, only the CTRS1/2 sequences and those amplified with primers B1# and B9# co-

immunoprecipitated with CTCF above background and each in only one of two independent experiment under these conditions (Fig 26; ChIP performed by Mr. Esteban Flores). Consistent with the lack of underrepresented sequences in the undigested and unfractionated chromatin in the MCN-seq experiments, none of these sequences co-immunoprecipitated with CTCF above background in the untreated infections in either of the two independent experiments (Fig 26).

3.9 The number of short sequences, that are less depleted in the digested and fractionated chromatin than in the undigested and unfractionated chromatin, decreases as the infection progresses

I next evaluated the number and location of the short sequences relatively overrepresented in the digested and fractionated chromatin as the infection progressed.

At 2 h after infection, 41 short sequences were clearly overrepresented, including 30 predominant ones (Fig 28). Although the total HSV-1 genome copy equivalents were similar to those in the infections treated with CHX, the distribution of these relatively overrepresented sequences was markedly different. The relatively overrepresented short sequences were evenly distributed through the genome at 2 h, rather than clustered flanking the IE genes as in the infections treated with CHX. Nonetheless, most IE genes were still flanked by sequences with limited accessibility (Fig 28B).

There were 23, 1, or no short sequences relatively overrepresented at 4, 7 or 15 h, respectively. The overrepresented peaks included, again, previously mapped chromatin-

insulator like sequences (solid black circles) (Amelio, McAnany et al. 2006) and CTCF binding sites (empty downward arrows) (Lang, Li et al. 2017), or both (black downward arrows) (Fig 28).

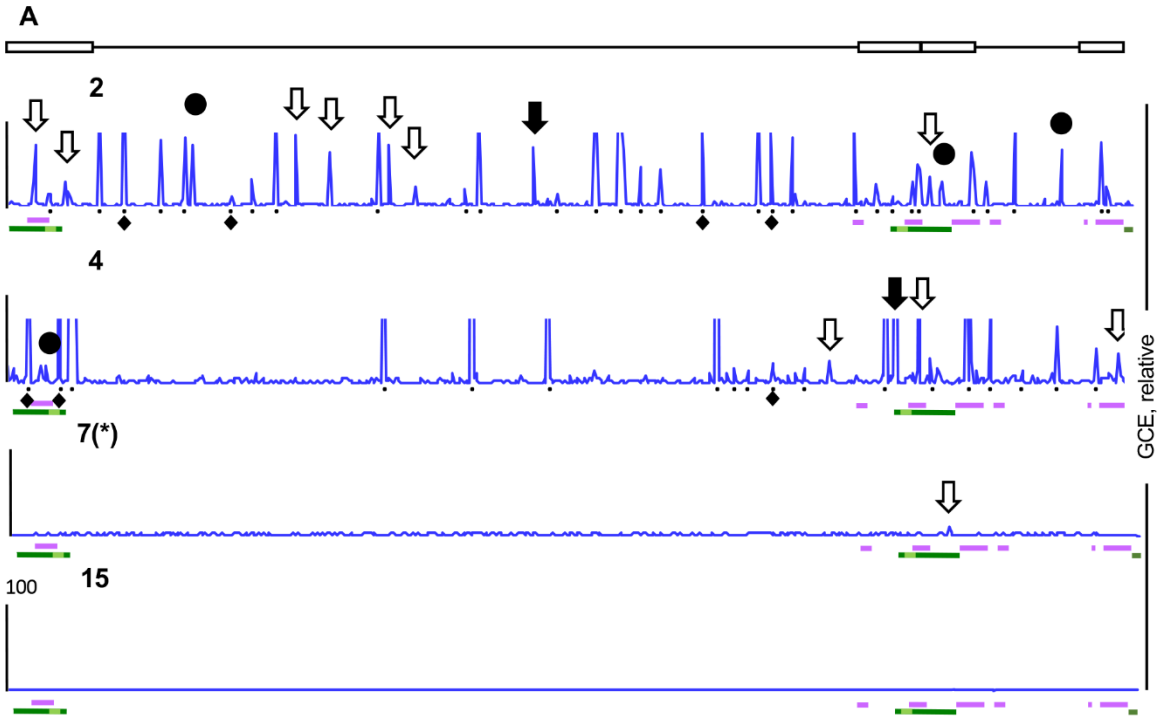
A
2
4
7(*)
100
15
GCE, relative

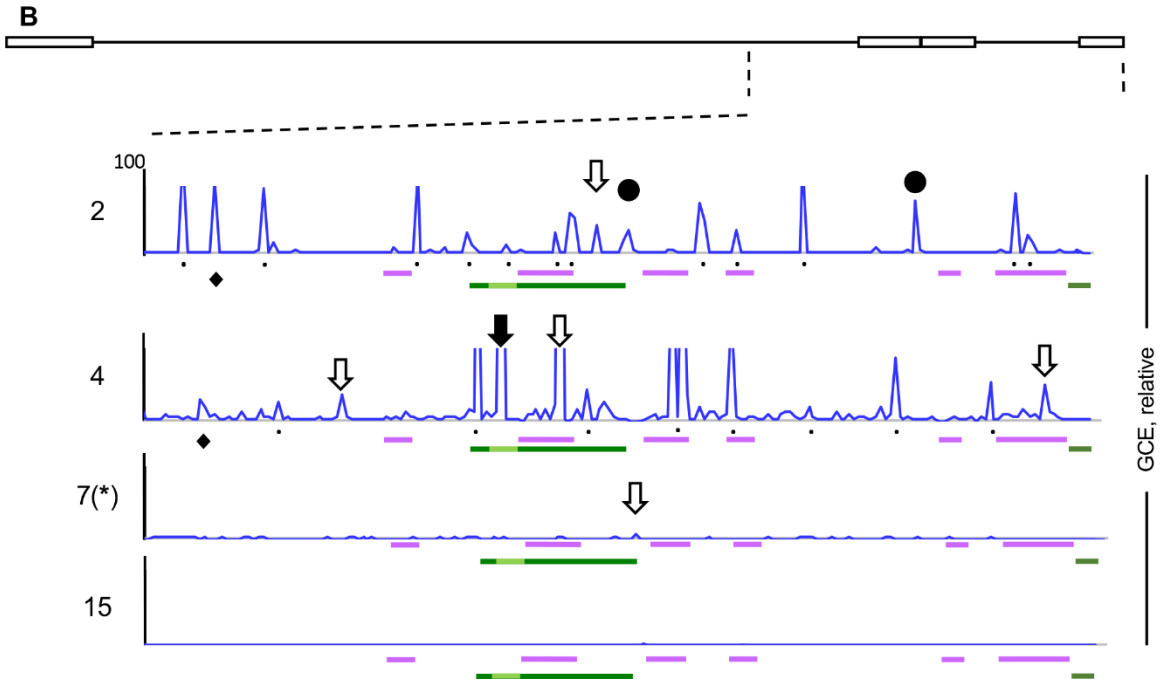
B
100
2
4
7(*)
15
GCE, relative

*Figure 28: The number of overrepresented short sequences decreases as infection progresses. Line graphs showing number of HSV-1 genome copy equivalents in each genome position at 2, 4, 7 (*), or 15 h pi, normalized to the number of HSV-1 genome copy equivalents in the same position of the respective undigested and unfractionated chromatin. X-axes, genome position (cartoon on top). *: data from Fig 9 presented again for comparison. Black downward empty arrows, CTCF binding sites; black solid circles, chromatin insulator-like elements; black downward solid arrows, CTCF binding- and chromatin insulator-like elements; black dots, peaks of the DNA plots; black diamonds underneath the plots, the seven overrepresented sequences that do not contain the AT-rich motifs; purple bars underneath genome plots, IE genes; dark green bars underneath genome plots, LAT; light green bar, stable LAT; GCE, genome copy equivalent. (A) Presentation of relative HSV-1 DNA plots through the entire genome; (B) Enlargement of the relative HSV-1 DNA plots of the repeat region, from position 100k bp to 152k bp. (Hu, Depledge et al. 2019).* Figure used under CC-BY 4.0 license.

Chapter 4: Discussion

My project aimed to address whether intracellular HSV-1 DNA was fully or partially chromatinized, or non-chromatinized, as well as whether the dynamics of HSV-1 chromatin were directly related to transcription levels. Although the mechanisms whereby chromatin dynamics are regulated are complex, one of the simplest models proposes that it relates to the local transcriptional activity (i.e., highly transcribed genes have the most dynamic chromatin whereas non-transcribed genes have the least). I characterized to what extent the chromatin dynamics related to HSV-1 transcription. My project leads to a better understanding of the mechanisms whereby epigenetics can regulate lytic HSV-1 chromatin, and has possibly identified new principles in epigenetic-mediated cellular antiviral activities.

My results showed that chromatin dynamics relate to the transcriptional competency

of HSV-1 genomes, not the transcriptional levels of any individual genes or groups of genes. The transcriptionally competent genomes are in highly dynamic chromatin and the incompetent ones in far less dynamic, or accessible, chromatin. Moreover, chromatin insulator elements such as CTCF flank highly transcribed genome regions from mostly non-transcribed ones.

My findings indicate that chromatin dynamics are a key regulator of HSV-1 transcription during lytic infections in that they provide a first level of regulation, dictating transcriptional competency. I thus uncovered a new level of viral transcription regulation. As the latent HSV-1 chromatin is far less dynamic than the lytic one, my studies also uncover a potential mechanism participating in transcription silencing during latency, inhibition of chromatin dynamics.

During cellular transcription regulation, chromatin remodelers are often recruited to chromatin containing genes that has already been previously post-translationally modified, whereas fully silenced chromatin inhibits transcription, at least in vitro (Imbalzano, Kwon et al. 1994) and in vivo (Han and Grunstein 1988). Under full silencing, crucial transcription factors such as TATA-binding protein (Imbalzano, Kwon et al. 1994), TFIIB (Knezetic and Luse 1986), or GAL4 (in yeast) (Taylor, Workman et al. 1991), cannot access the promoters. These promoters become accessible, as shown by nuclease hypersensitivity, during transcription activation (Boeger, Griesenbeck et al. 2003). Whether the hypersensitive sites are cause or a consequence of transcription

has not been resolved (Boeger, Griesenbeck et al. 2003). Hypersensitive sites have been observed at the hsp70 gene promoter while transcription is inhibited (Karpov, Preobrazhenskaya et al. 1984), for example. Likewise, 400bp hypersensitive sites have been observed by electron microscopy on the promoters of about 20% of the viral genomes in SV-40 infected cells, regardless of whether the genomes were transcribed or not (Jakobovits, Bratosin et al. 1980). Micrococcal nuclease digestion of the promoter of the PHO80 yeast gene released mono-, di-, and tri-nucleosome-sized fragments, indicating that it was accessible, when transcription was inactive (Boeger, Griesenbeck et al. 2003). Upon transcription activation, fewer tri- and di-nucleosome-sized fragments were produced, whereas the mono-nucleosome sized fragments were enriched, indicating an even increased accessibility (Boeger, Griesenbeck et al. 2003). The promoter chromatin may thus be more dynamic when the regulated gene is highly transcribed.

The infecting protein-free HSV-1 genomes localize to the nucleus. HSV-1 encodes several indirect viral activators of transcription, but not any protein known to directly activate transcription or modulate chromatin, or histone-like proteins that could assemble chromatin-like nucleoprotein structures. Moreover, the cellular transcription complexes transcribe all HSV-1 genes. The simplest model would be that the most highly transcribed HSV-1 genes are more accessible to transcription proteins than any non-transcribed ones, as is the case in cellular chromatin. To challenge this model, I

digested chromatin of infected cell nuclei with micrococcal nuclease. The digested chromatin fragments were then separated by their hydrodynamic ratio. The more accessible genes are digested into smaller fragments and the least accessible, into larger ones. DNA was extracted from the different chromatin fractions and sequenced, as was the total RNA. Under the simplest model, the transcribed HSV-1 genes would be in the most accessible chromatin and would thus fractionated to the top fractions, and non-transcribed HSV-1 genes would have been in least accessible chromatin and thus fractionate to the bottom fractions.

To analyze the fractionation of each HSV-1 gene, the normalized DNA reads of each gene in each fraction were subjected to cluster analysis. As shown by the RNA plots (Fig 25), all HSV-1 genes were transcribed to high level at 7 h pi, as expected. However, only the IE genes were transcribed to high level if the infected cells were treated with CHX, also as expected, and no HSV-1 genes were transcribed to high level when the infected cells were treated with Rosco. According to the simplest model, all highly transcribed genes (all genes at 7 h pi and the IE genes in CHX treated infections) would have similarly fractionated mostly to the most accessible fractions and therefore would have clustered together. Non-transcribed genes (E, and L genes in CHX treated infections or all genes of Rosco treated infections) would have also similarly fractionated, but mostly to the least accessible chromatin and thus also clustered together. However, all HSV-1 genes in each treatment clustered together, regardless of their individual

transcription levels (Fig 16). All genes at 7 h pi clustered together, and away from all genes in CHX- or Rosco-treated infections. All genes of CHX treated infections also clustered somewhat away from those in Rosco treated infections, although there were some overlaps between the fractionations in these last two treatments (Fig 16).

These results suggested that the accessibility of each HSV-1 gene does not directly correlate with its individual transcription level. Instead, all HSV-1 genes were enriched in the most and least accessible chromatin when the overall transcription level was high (7 h or 15 h pi). In CHX- or Rosco-treated infections, in contrast, entire genomes fractionated away from the most accessible chromatin. Importantly, the IE genes, which are highly transcribed in CHX, fractionated together with the non-transcribed E or L genes.

As an alternative model, thus, chromatin may regulate the transcription competency of entire HSV-1 genomes. Under conditions of active transcription, then, the entire HSV-1 genomes would be highly accessible. In this model, all genes in these genomes are transcriptionally competent, but not necessarily transcribed. HSV-1 transcription follows a sequential pattern. Transcription of the IE genes is activated immediately after HSV-1 genomes enters the nucleus. IE proteins then activate transcription of E genes, and transcription of L genes is activated after DNA replication. The overall transcription levels of HSV-1 also increase as infection progresses. As measured by RNA-seq, the RNA level of any gene was relatively low at 2 h, and increased at 3, 4, 6, 8, 12, and 16 h

after infection (Harkness, Kader et al. 2014). Classic RNA hybridization had revealed some time ago that only the IE genes were transcribed to high level in infections treated with CHX, a few genes (about 12) were transcribed to high level at 2 h pi, and more than half of all HSV-1 genes were transcribed to high level at 8 h pi (Stingley, Ramirez et al. 2000). Consistently, our RNA-seq results conform, as expected, that there is an overall low transcription level across entire HSV-1 genomes in infections treated with Rosco, only IE genes are transcribed to high level in infections treated with CHX, and most of the genes are transcribed to high level at 7 h pi in untreated infections (Fig 25).

Rosco acts before initiation of HSV-1 transcription, while has no affects on either initiation or ongoing HSV-1 transcription (Diwan, Lacasse et al. 2004). Furthermore, Rosco inhibits transcription of viral genes on HSV-1 genomes, but not transcription driven by viral promoters recombined into the cellular genome (Diwan, Lacasse et al. 2004). These findings suggested that inhibition of HSV-1 transcription by Rosco is HSV-1 genome, but not gene or promoter, specific. It is thus tempting to speculate that rosco-inhibits HSV-1 transcription by acting at the chromatin level. Consistently, there was little HSV-1 transcription across the HSV-1 genome in Rosco treated infections (Fig 25).

Under the model proposing that HSV-1 genomes are more accessible when highly transcribed, one would expect them to be least accessible when transcription is the most restricted early in infection and become more accessible as the infection progresses. In our results, HSV-1 chromatin was enriched in the least and

intermediately accessible fractions when the overall HSV-1 transcription level was low (such as infections treated with CHX or Rosco, Fig 17). Under these conditions, the fractionation pattern of this most inaccessible HSV-1 chromatin was similar to that of the bulk cellular chromatin (Fig 17), indicating that the accessibility of HSV-1 chromatin was similar to the bulk cellular chromatin. The fractionation of the HSV-1 chromatin was perhaps slightly different from that of the cellular chromatin at 2 h pi, with a minor shift towards the fractions containing more accessible chromatin (Fig 20). As infection progressed to 4, 7, and 15 h, the HSV-1 chromatin was enriched more and more in the fractions containing the most and least accessible chromatins (Fig 20).

Only a few HSV-1 genomes are transcribed (estimated 3.7 genomes per cell at moi of 10, (Kobiler, Lipman et al. 2010)). These transcribed genomes would be in the most dynamic chromatin and would then be difficult to silence after the viral IE proteins are expressed. Perhaps the IE protein ICP4 has preference for binding to the genomes in transcriptional competent chromatin because of their higher accessibility. ICP4 would then have little to no effect on the most inaccessible chromatin of the transcriptional incompetent genomes. ICP4 colocalizes to the viral replication compartments, where both accessible and inaccessible genomes localize, too. It is not yet clear why the transcriptional incompetent genomes stay silent and do not replicate. One possibility is that the tegument proteins, including VP16 and ICP4, that enter the nuclei form a proteinaceous domain (later known as the herpes nuclear domain) that favors chromatin

remodelling and transcription. The silenced chromatin of any HSV-1 genomes that happen to be located to these domains would be remodeled and these genomes would become transcriptional competent. Other silenced HSV-1 genomes away from the herpes nuclear domains remain silenced. Under to this model, the transcriptional competent and most accessible HSV-1 genomes observed in my experiments would likely be associated with more viral transcription activators, VP16 and ICP4, in comparison to the transcriptional incompetent and inaccessible HSV-1 genomes.

According to standard models of regulation of cellular transcription, the chromatin on the IE, E or L genes would be expected to be differently accessible at different times after infection. However, some previous studies had already indicated that the regulation of transcription in HSV-1 chromatin might not follow same models proposed for the regulation of cellular transcription. Immunoprecipitation of histone H3 had showed a relatively high apparent histone H3 occupancy on ICP4 (an IE gene) and ICP8 (an E gene) at 3 h pi, occupancy which had decreased by more than threefold on both genes at 8 h pi (Cliffe and Knipe 2008). The decrease of apparent H3 occupancy was independent of HSV-1 DNA replication, in that PAA had no effects. It was also independent of active transcription, in that the same trend to decreased in apparent H3 occupancy was observed in infections with an ICP4 null virus (Cliffe and Knipe 2008). In another study, the apparent histone H3 occupancy was tested on the promoters of ICP0, TK, and VP16 (Oh and Fraser 2008). The apparent H3 occupancy was also high at or

before 3 h pi, and decreased by more than five-fold at 6 h pi (Oh and Fraser 2008). All these results indicate a simultaneous general decrease in stable histone H3 occupancy on HSV-1 genes from all three kinetic classes, suggesting that the epigenetic regulation of HSV-1 might not be at the level of individual gene level, but rather at the level of entire HSV-1 genomes. Consistently, HSV-1 DNA was not yet enriched as the most accessible chromatin at 2 h after infection but started to be enriched at 4 h and was most enriched at 7 h or 15 h (Fig 18, 20).

HSV-1 chromatin was proposed to be enriched in histones bearing silencing markers at early times of infection (Lee, Raja et al. 2016). The silencing markers were then proposed to start to decrease as early as 2 h pi, independently of DNA replication (Lee, Raja et al. 2016). The apparent level of histone H3 with HSV-1 DNA also started to decrease at 3 h pi, as already discussed (Oh and Fraser 2008), while the total histone H3 level of the infected nucleus remained constant. The euchromatin marker H3K9ac started to be enriched in the promoters of genes of all three kinetic classes (ICP0, TK, and VP16) as early as 3 h pi (Kent, Zeng et al. 2004). HSV-1 chromatin post-translation modifications thus do not correlate well with the transcription levels of a given gene or gene class.

In my own experiments, genes of all three kinetic classes were enriched in the least accessible chromatin at 2 h pi, and also at 7 h pi in infections treated with CHX or Rosco. The enrichment of all genes in the most accessible chromatin started at 4 h pi,

to become more marked at 7 h and 15 h pi (Fig 16, 17, 19, 20).

More recently, the histone landscape on HSV-1 genomes has been mapped by ChIP-seq. The apparent histone H3 occupancy changed throughout infections (Gao, Chen et al. 2020). However, these changes did not correlate with any particular gene, gene kinetic class, or genome region, at any time (Gao, Chen et al. 2020). Even though this study differs from my experiments, in that ChIP-seq measures apparent histone H3 occupancy whereas my experiment (MCN-fractionation-seq) measures chromatin accessibility, these results are both consistent with models in which the accessibility of HSV-1 chromatin relates to the overall transcription level of the entire genomes rather than that of any specific gene.

Early compaction of individual HSV-1 genomes could be visualized by infection with 5-ethynyl-2'-deoxycytidine (EdC) labelled HSV-1 (Sekine, Schmidt et al. 2017). HSV-1 genomes then became more relaxed at 4 h (Sekine, Schmidt et al. 2017). These results are also constant with models under which HSV-1 genomes are in least accessible chromatin at early times of infection, when transcription level is low, but become more accessible as infection progresses. Inhibition or restriction of HSV-1 transcription by act D, CHX, or PAA decreased the numbers of HSV-1 genomes undergo decompaction, as well as the sizes of the decompacted genomes (Sekine, Schmidt et al. 2017). In our results, the most accessible HSV-1 chromatin also started to be enriched at 4 h pi (Fig 20), and the fractions containing the most accessible HSV-1 chromatin also contained

all HSV-1 genes. When HSV-1 transcription was limited to only the IE genes or inhibited through the genome, less than 4% of the HSV-1 chromatin fractionated as the most accessible chromatin enriched in fully sampled genes. Yet, this 4% or less DNA still contained all HSV-1 genes (Fig 17B). Although my experiments lack the resolution to analyze individual HSV-1 genomes, these results are consistent with models under which there are two populations of HSV-1 genomes in infected cell nuclei. The silenced ones are in least accessible chromatin, and the transcriptionally active ones are in most accessible chromatin. When transcription levels are low, there are only few genomes in transcriptionally active state (transcriptionally competent). On these genomes, however, the entire genome may well be equally accessible regardless of whether particular gene is transcribed or not.

The possibility of the existence of two populations of herpes genomes in infected cells had been proposed before. Dr. Enquist's group created a pseudorabies virus (PRV) strain containing three fluorescent proteins, each flanked by different Cre-dependent recombination sites. Recombination happens randomly at one of the recombination sites and results in expression of only one of the three fluorescent proteins per viral genome (Kobiler, Lipman et al. 2010). Under the model that all intracellular viral genomes in a cell are equally transcribed or transcription competent, a single cell infected by many of this “brainbow” cassette PRV virions would be expected to express a mix of the three colors. Moreover, each of the three colored PRV virions would have

equal possibility to egress from this infected cell (plaque center) to infect neighbourhood cells, resulting a multi-colored plaque. The ratios of the three colors (color profile) of this colored plaque would change over time, as randomly colored PRV virions would egress from each previously infected cell to infect adjacent ones (Kobiler, Lipman et al. 2010). However, most of the infected cells expressed only one, or at most, two colors (Kobiler, Lipman et al. 2010). The color profile of any plaque remained constant as it was at the start of plaque formation, suggesting that the color of the plaque raised from the color of the originally infected single cell (Kobiler, Lipman et al. 2010). Cells infected with equal mix of PRV expressing dTomato, EYFP, or cyan at high moi resulted in most of the infected cells expressing only one, or at most two, of the three colors (Kobiler, Brodersen et al. 2011). The authors proposed a model in which only a small number of herpes genomes are expressed in an infected cell nuclei, and these expressed genomes were the ones that replicate and egress (Kobiler, Lipman et al. 2010).

To estimate the number of expressed genomes, cells were infected with equal mixture of 14 HSV-1 different recombinants (Cohen and Kobiler 2016). Each of these 14 recombinants contained one unique bar code that can be identified by PCR. Knowing that only the expressed genomes replicate and egress, the ratio of these 14 bar codes in one plaque would represent the genomes expressed in the originally infected single cell (Cohen and Kobiler 2016). Only 3.4 or 7.6 of the infecting genomes replicated in a given cell at moi of 10 or 100, respectively (Cohen and Kobiler 2016). Consistently, my

results showed that intracellular HSV-1 chromatin was enriched in the most accessible and most inaccessible chromatin (Fig 17). These findings support the models under which two populations of HSV-1 genomes co-exist in an infected cell. The transcription competent genomes would be in accessible chromatin, and be transcribed, then replicate, and egress. The transcription incompetent genomes would be in silenced, inaccessible, chromatin and would not be transcribed or replicated, or egress.

DNA replication could also increase the accessibility of the viral chromatin, as it does for cellular chromatin. However, neither the decrease in apparent histone occupancy on HSV-1 DNA, nor the increase in dynamics of all core histone, depended on HSV-1 DNA replication, in that PAA treatment did not alter either (Cliffe and Knipe 2008, Conn, Hendzel et al. 2008, Conn, Hendzel et al. 2011, Conn, Hendzel et al. 2013, Gibeault, Conn et al. 2016, Lee, Raja et al. 2016). Furthermore, PAA did not alter HSV-1 chromatin accessibility, as evaluated by MCN protection assay (Lacasse and Schang 2012), nor did it alter the decompaction of HSV-1 genome as evaluated by EdC signal (Sekine, Schmidt et al. 2017). Our results are most consistent with all those previous studies. Treatment with PAA did not reduce the enrichment of HSV-1 DNA in the most accessible chromatin containing fully sampled genes, neither did it affect the fractionation of any gene.

Several models have been proposed regarding the potential topologies of the HSV-1 chromatin during lytic infections. One proposes that only specific regions of HSV-1

genes are in nucleosomes. This model is based in that only some regions of HSV-1 genomes were protected to nucleosome-sized fragments after complete MCN digestion (Oh, Sanders et al. 2015). Under the conditions of these experiments, approximately 40% of cellular and only 15% of the viral DNA was protected against MCN digestion (Oh, Sanders et al. 2015), a stringent digestion. In my experiments, approximately 70% of the cellular and approximately 60% of the viral DNA was protected against MCN digestion, which is consistent with previous MCN protection assay from our lab, that had also recovered approximately 70% of the cellular and viral DNA (Lacasse and Schang 2012).

Under the stringent digestion conditions used by others, only 10 - 20% of the entire ICP0 gene was protected in nucleosomes, and most of these nucleosomes were towards the mid or 3' of the ICP0 gene body (Oh, Sanders et al. 2015). Approximately 50% of the entire ICP4 gene was also protected in nucleosomes, and the protected region was more evenly distributed across the gene body than that of ICP0 (Oh, Sanders et al. 2015). The protection of E and L genes was similar to that of the IE genes. Approximately 35% of the E genes and 30% of the L genes were protected in nucleosomes (Oh, Sanders et al. 2015). Less than 40% of the protected regions were in the promoters (Oh, Sanders et al. 2015). Nucleosome position was uneven. Short genes had relatively lower apparent nucleosome occupancy, and the apparent occupancy tended to cluster to the middle of longer genes (Oh, Sanders et al. 2015).

If only specific regions of HSV-1 genes were indeed protected by stable nucleosomes, then my experiments would have also yielded qualitatively results consistent with those of Oh, Sanders et al. 2015, even though my digestion conditions were less stringent (I recovered approximately 70% of intracellular HSV-1 DNA in comparison to only 15% in Dr. Oh's study). Nucleosome protected regions would had been cleaved less frequently and thus would have fractionated differently than those non-protected regions, which would had been cleaved more frequently. However, no genes fractionated differentially, regardless of their sizes (Fig 16A, 19A), and entire genes fractionated together indicating that they were approximately equally accessible (Fig 16B, 19B). The entire HSV-1 genome was also approximately equally protected against MCN under a given condition in my experiments (Fig 21-25). Had some specific regions been better protected by nucleosomes than others, then they would have fractionated differentially (Fig 21-25).

The protection pattern of HSV-1 chromatin under stringent digestions may reflect the dynamic nature of HSV-1 chromatin in lytic infections. HSV-1 gene sizes range from less than 200 bp to approximately 10,000 bp. The small genes are only capable of assembling one or just a few nucleosomes whereas the large ones are capable of assembling hundreds. Shorter genes would not be immunoprecipitated efficiently if cleaved by MCN only once, or twice, as that gene would lose its nucleosome (Fig 29 right). Large genes can still be immunoprecipitated even when cleaved multiple times,

as other regions of that gene are still nucleosomal (Fig 29 left). Consequently, short genes would more likely to appear to be nucleosome-free under stringent digestions. The authors (Oh, Sanders et al. 2015) indeed acknowledged that the apparently nucleosome-free regions could also be nucleosomes that are loosely bound or labile nucleosomes as described in earlier work from our lab (Lacasse and Schang 2012).

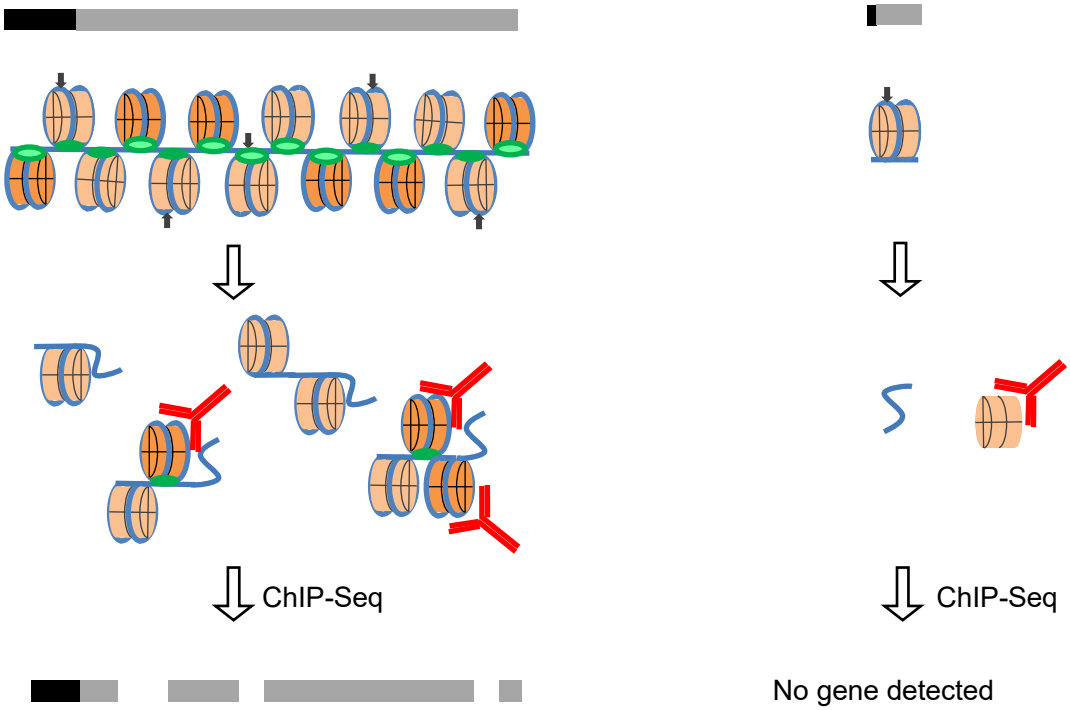

Figure 29: Cartoon presenting the possible digestion consequence of a long HSV-1 gene (left) or a shorter gene (right). Black rectangle, promoters; Gray rectangle, gene bodies; Red Y shape, histone antibodies; Dark brown, stable nucleosomes; Light brown, dynamic nucleosomes; Green oval, histone H1; Blue line, DNA.

HSV-1 DNA could of course be protected in capsids. However, the major capsid protein VP5 was barely detectable in the insoluble or soluble chromatin at 7 h, whereas HSV-1 DNA immunoprecipitated with histone H3 in all fractions (Hu, Depledge et al. 2019). HSV-1 also encodes several DNA-binding proteins. ICP8 is a single-strand DNA binding protein that binds to HSV-1 ssDNA during replication. ICP8 fractionated to the most inaccessible fractions at 7 h and could thus have protected some of the HSV-1 DNA in them. As there was little ICP8 in the most accessible ones. ICP8 could not have protected the DNA in them. ICP8 binds to the ssDNA and a single ICP8 molecule is 128 k Da, approximately the size of 8 to 10 histones. Crystal structures of short ICP8-DNA filaments have been resolved, and the linker DNA between two ICP8 molecules is only approximately 10 bp (Mapelli, Panjikar et al. 2005). Such tight ICP8-DNA structure is expected to be less accessible to MCN in comparison to poly-nucleosome complexes with longer linker region. ICP8-DNA complex would thus be expected to fractionate to more inaccessible fractions, as observed in my experiments.

ICP4 is another viral-DNA binding protein that may protect HSV-1 DNA in the nucleus of lytically infected cells. The crystal structure of the ICP4 DNA-binding domain bound to its DNA target has been resolved (Tunnicliffe, Lockhart-Cairns et al. 2017). The structure shows the ICP4 DNA binding domain interacting with approximately 13bp (Tunnicliffe, Lockhart-Cairns et al. 2017). As the crystal structure was resolved as a monomer, it is still not entirely clear how multiple ICP4 molecules may bind to a longer

piece of DNA. The ICP4 DNA-binding domain is about 1/6 of the protein. Binding of full ICP4 to a relatively short DNA sequence (approximately 13 bp of DNA in the binding pocket) would be expected to result in large linker DNA because of steric hindrance. If ICP4 protected HSV-1 DNA to some extent, the DNA in ICP4-DNA complexes would still be accessible to MCN and would likely be protected to only small DNA fragments (about 13 bp). In my experiments, 70% of ICP4 was in the insoluble fraction, whereas the 30% of ICP4 in the soluble fraction fractionated similarly to the HSV-1 DNA. ICP4 colocalizes with HSV-1 genomes during lytic infections (Dembowski and DeLuca 2015), and binds to naked double-stranded DNA. Considering that HSV-1 chromatin is highly dynamic during lytic infections, it is possible that ICP4 fractionated similarly as HSV-1 chromatin by interacting with the highly accessible HSV-1 DNA in the soluble fractions. However, most ICP4 was in the insoluble fractions. ICP4 might perhaps protect HSV-1 genomes in the inaccessible chromatin.

PML has also been proposed to "shield" HSV-1 genomes during quiescent infections (Boutell, Sadis et al. 2002), and thus could also protect the HSV-1 genomes in lytic infection. However, PML is expected to be disrupted by ICP0 at 7 h after infections with wild type HSV-1. Indeed, under my experimental conditions, PML was not detected in any fractions (Fig 30) whereas histone H3 is detectable in all (Fig 30). I did not analyze the fractionation of PML under conditions of inhibition of HSV-1 transcription or at earlier times after infection. PML might thus have protected the HSV-1

DNA to some extent in these conditions.

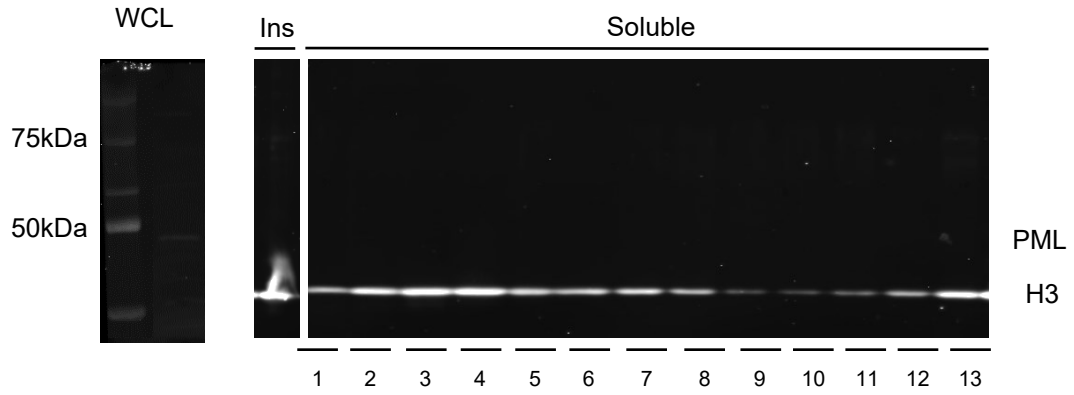

Figure 30: No detectable PML in any fraction at 7 h HSV-1 lytic infections. Western blot for PML (MW 42-78) and histone H3 in all fractions, each resolved by SDS PAGE and probed with corresponding antibodies. Ins, insoluble chromatin. WCL, whole cell lysate for the detection of PML.

Intracellular HSV-1 DNA pulled down using EdU-labelling and click chemistry was apparently associated mostly with ICP4, VP16 and ICP22 (Dembowski and DeLuca 2015). Infections with EdC-labelled HSV-1 showed ICP4 co-localized tightly to packed HSV-1 genomes (EdC signal as bright punctuate foci) at 1 h (Sekine, Schmidt et al. 2017). At 3 h, some of the punctuate foci were dispersed (as the genomes decondensed), and ICP4 also localized to the dispersed areas (Sekine, Schmidt et al. 2017). CHX- or Act D- treated infections resulted in condensed EdC labelled HSV-1 foci at 3 h pi, at the time when EdC signal would already be disperse in wild type infections (Sekine, Schmidt et al. 2017). My results are consistent with these results. Only 2, 4, or

7% HSV-1 DNA fractionated to the most accessible chromatin with all HSV-1 genes when transcription was inhibited by Rosco, or restricted by CHX, or at early times of infections (Fig 17, 20). At 4, 7 or 15 h pi, HSV-1 DNA was enriched as most accessible chromatin, and these fractions contained all HSV-1 genes.

Besides ICP4, ICP22 and VP16, immunoprecipitation of EdU-labelled HSV-1 chromatin also pulled down 41 chromatin remodelers and chromatin proteins, including INO80, NURD, and SWI/SNF, and histone H1 (Dembowski and DeLuca 2015). They concluded that no histones were detected associated with HSV-1 DNA. However, four-fold increase in reads over those in cells infected with non-labelled HSV-1 were considered as hits. Under such stringent enrichment criterion, it would be very difficult to detect specific interactions with the most abundant nuclear proteins, such as histones. The EdU-mediated immunoprecipitation may also enrich the most dynamic HSV-1 chromatin, as such chromatin is more accessible. This chromatin would be expected to be enriched in chromatin remodelers, and also to be dynamically associated with histones. The many chromatin remodelers and proteins identified contain bromo- or chromo-domain, which recognizes acetylated lysine or methylated lysine, correspondently, in histone tails for example, suggesting that the HSV-1 DNA was indeed associated with histones. Moreover, these remodelers may very well contribute to the dynamic state of HSV-1 chromatin.

The effects of chromatin remodelers on HSV-1 transcription and replication have

been studied extensively. The histone deacetylase inhibitors TSA (trichostatin) and sodium butyrate (NaBu) activated quiescent HSV-1 genomes in PC12 cells (Danaher, Jacob et al. 2005). The HAT inhibitors suberoylanilide hydroxamic and anacardic acid did not alter the levels of HSV-1 DNA replication at moi of 10, 50, or 100 (Shapira, Ralph et al. 2016). In contrast, TSA, suberohydroxamic acid (SBX), and valproic acid (VPA) reduced the number of viral genomes replicating in infections at high moi (50 or 100 pfu/cell). The antiviral activities of some HDAC inhibitors were concluded to result from the activation of intrinsic cell immunity, as TSA increased the levels of PML, ATRX, and hDaxx in HFF cells (Shapira, Ralph et al. 2016). Other epigenetic inhibitors have also been proposed to activate cellular innate antiviral responses by increasing levels of PML, IFN-α, and IL-8, the EZH2/1 inhibitors GSK126, GSK343, and UNC1999. Treatment with these inhibitors decreased the levels of mRNA of ICP4, ICP22 and ICP27 (Arbuckle, Gardina et al. 2017).

Lysine specific demethylase 1 (LSD1) demethylates mono-, or di-methylated lysines 4 and 9 in histone H3. LSD1 is a flavin-dependent MAO that catalyzes the oxidative deamination of amines using flavin as a cofactor, and thus is inhibited by MAO inhibitors. Inhibition of LSD1 would be expected to increase the di- and tri-methylation levels of H3K4 and H3K9. Treatment with MAO inhibitors or knockdown of LSD1 indeed increased the levels of tri-methylated H3K9 on the promoters of HSV-1 IE genes (Liang, Vogel et al. 2009). It also resulted in lower levels of HSV-1 IE gene transcripts and

decreased viral replication (Liang, Vogel et al. 2009). An MAO inhibitor (OG-L002) was selected for its high potency against LSD1 (IC_{50} 0.02μM) over MAO (IC_{50} 0.72 to 1.38 μM) (Liang, Quenelle et al. 2013). Treatment with OG-L002 and TCP (which discriminates less between LSD1 and MAO or OG-L002) decreased the transcript levels of ICP4 and ICP27 in a dose-dependent manner. EC_{50} were 10 μM in HeLa or 3 μM in HFF cells for OG-L002 and 1 mM in both cell lines for TCP (Liang, Quenelle et al. 2013). Treatment with 50 μM OG-L002 or 2 mM TCP increased by more than 20-fold the apparent levels of total histone H3 and H3K9Me2 on the promoters of ICP0 and ICP27 genes. Twenty mg/kg/day of OG-L002 also resulted in fewer viral genomes in mice trigeminal ganglia. The activity in vivo was similar to that of 100 mg/kg/day ACV (Liang, Quenelle et al. 2013).

Another MAO inhibitor, SP-2509, also inhibited LSD1 in vitro and HSV-1 replication in culture (Harancher, Packard et al. 2020). Surprisingly, whereas OG-L002 inhibited transcription of IE genes, SP-2509 had no effects on the levels of HSV-1 IE (ICP4 and ICP27) or E gene (ICP8) transcripts. Instead, SP-2509 inhibited HSV-1 DNA replication and, consequently, transcription of UL42 (leaky late genes) and gC (true late gene), to an even greater extent (Harancher, Packard et al. 2020). The authors proposed a model attempting to explain the differential effects of OG-l002 and SP-2509 on HSV-1 transcription and replication. However, the specificity of SP-2509 for LSD1 is questionable, as discussed in Sonnemann, Zimmermann et al. 2018. SP-2509 and

three other LSD1 inhibitors (ORY-1001, GSK2879522, or TCP) all induced acute myeloid leukaemia cell death. However, SP2509 is equally active in inducing cell death in LSD1 knockout cells, whereas the other three well characterized LSD1 inhibitors had no effects, as expected of any molecule acting on LSD1 itself (Sonnemann, Zimmermann et al. 2018). This evidence suggested that SP-2509 is not specific for LSD1. Therefore, the unique effects of SP-2509 on HSV-1 transcription and replication might be an issue of lacking specificity for LSD1.

In LNCaP (androgen-sensitive human prostate adenocarcinoma) cell line, LSD1 was upregulated to promote cell survival, and RNAi knockdown of LSD1 decreased cell viability (Sehrawat, Gao et al. 2018). Interestingly, inhibitors that block FAD binding to LSD1 (GSK2879552, GSK-LSD1 and RN1) did not alter LNCaP cell survival, whereas SP-2509 reduced cell viability similarly as the RNAi knockdown of LSD1 (Sehrawat, Gao et al. 2018). RNAi knockdown resulted in 1447 genes that were up-regulation and 225 genes that were down-regulated. The levels of H3K9me2 and H3K4me2 did not change in these 1672 genes whose expression levels were altered by LSD1 knockdown (Sehrawat, Gao et al. 2018). Together with the lack of specificity of SP-2509 against LSD1 as showed in Sonnemann, Zimmermann et al. 2018, these findings indicate that SP-2509 has some important biological activities on targets other than on LSD1. Therefore, the effects of SP-2509 on HSV-1 infection may not be a direct effect of inhibiting LSD1.

Removal of H3K9me3, which is not affected by LSD1, requires JMJD2 family demethylases. HCF-1 recruits JMJD2 to the infecting HSV-1 genomes (Liang, Vogel et al. 2013). The JMJD2 family includes JMJD2A, JMJD2B, JMJD2C, and JMJD2D. Knockout of one of these redundant proteins moderately decreased the mRNA levels of ICP0, ICP27 and ICP4 (Liang, Vogel et al. 2013), while also moderately increased the levels of H3K9me3 on these genes (Liang, Vogel et al. 2013). Knockout two or three of JMJD2A, B, C, or D or knockout of all JMJD2 resulted in reductions of five- to ten- fold of ICP4 and ICP27 mRNA levels, respectively, and increase in the H3K9me3 levels on these genes by two- to four- fold (Liang, Vogel et al. 2013). Treatment with the JMJD2 inhibitor DMOG decreased the ICP4, ICP22, and ICP27 mRNA levels, while increasing H3K9me3 levels on these genes (Liang, Vogel et al. 2013). ML324 is a more potent inhibitor of JMJD2 than DMOG with an IC_{50} about 75 fold lower (Liang, Vogel et al. 2013). Treatment with ML324 also decreased the mRNA levels of ICP22, ICP4 and ICP27, and inhibited HSV-1 replication (Liang, Vogel et al. 2013).

MTA (5'-deoxy-5'-methylthioadenosine) inhibits methylation of many proteins, including histones. Treatment of HSV-1 infected cells with 1mM MTA decreased by half the levels of H3K4me3 on IE (ICP0), E (TK), and L (VP16) genes, but not those of H3K4me2 (Huang, Kent et al. 2006). Treatment with 1mM MTA, starting at 1, 3, 6, or 10 h after infection, also reduced the mRNA levels of these genes by half to 5-fold. If H3K4 methylation was a critical step regulating HSV-1 transcription, depletion of the histone

H3 methylase Set1 would be expected to decrease HSV-1 transcription. However, siRNA knockout of Set1 only partially decreased mRNA levels of VP16 (by half) and ICP0 (about 30%), but not those of TK (Huang, Kent et al. 2006). It also only decreased H3K4me3 levels on VP16 and ICP0 genes by half at the most (Huang, Kent et al. 2006). As the authors discussed, the limited changes in H3K4me3 or transcripts were not too surprising, as HCF-1 also recruits MLL1 to the IE promoters (another histone methylase) (Narayanan, Ruyechan et al. 2007). SiRNA knockout of Set1 also decreases H3K4me3 levels on the cellular chromatin, and decreases its dynamics (Huang, Kent et al. 2006). Perhaps, knocking out Set1 before infection may also decrease the histones available to chromatinize and silence the infecting HSV-1 genomes.

Many epigenetic inhibitors had been found to have anti-HSV-1 activities, but the levels of the relevant histone modifications haven't been always evaluated. Other times, they were evaluated only on specific HSV-1 loci. There is still insufficient evidence to conclude that the anti-HSV-1 activities of these inhibitors are indeed a direct result of any changes in the corresponding epigenetic modifications on specific HSV-1 genes.

The epigenetic landscape of the entire HSV-1 genome was recently evaluated (Gao, Chen et al. 2020). Most consistently with our results, the levels of H3K9me3, H3K27me3, H3K4me3, and H3K27ac were all independent of the transcription level of any specific gene throughout the entire HSV-1 genome (Gao, Chen et al. 2020). The distribution of these histone modifications did not show any locus-specificity either.

However, they all changed as the infection progressed (Gao, Chen et al. 2020). There was no correlation between the different histone modifications that are associated with transcription or silencing onto the HSV-1 genome either. In contrast, and as expected, the levels of H3K9me3 of cellular genes correlated with those of H3K27me3, and those of H3K4me3 with those of H3K27ac (Gao, Chen et al. 2020), for example. In my experiments, all HSV-1 genes were similarly sampled in each fraction, and their fractionation was independent of their transcription level. Furthermore, the fractionation of the HSV-1 genes changed as infection progress, not according to individual transcription levels.

From the analyses of the body of literature on epigenetic modifications, ChIP-PCR, epigenetic inhibitors, and epigenetic landscapes evaluated by ChIP-seq, epigenetics plays a role in the regulation of HSV-1 transcription. However, the mechanism of action appears to differ from those involved in the typical regulation of cellular gene transcription.

In 2006, several chromatin insulator-like sequence elements were identified on the HSV-1 genome (Amelio, McAnany et al. 2006). The identified CTCF-binding sequences were named CTRL1 and CTRL2 in the repeat long (RL) region, CTa'm in the "a" sequence, CTRS1, CTRS2, and CTRS3 in the repeat short (RS) region, and CTUS1 in the unique short region (Amelio, McAnany et al. 2006). All these sites were enriched in CTCF binding during latency, as shown by ChIP (Amelio, McAnany et al. 2006). One of

the CTCF binding sites, CTRL2, was further studied because it is located between a region that is transcribed during latency (LAT) and one that is not transcribed (ICP0 gene). The chromatin of the LAT region is acetylated during latency whereas that of the ICP0 gene is hypoacetylated (Kubat, Tran et al. 2004).

The CTRL2 cluster were transfected into Drosophila S3 cells to test for potential insulation function. Briefly, drosophila embryo was injected with a vector containing two genes, w and lacZ. The LacZ gene was next to an enhancer IAB5 and the w gene next to an enhancer PE. PE enhanced genes are expressed at the ventral most region and its transcripts, visualized through RNA in-situ hybridization, as anterior-posterior stripes. IAB5 enhanced genes are expressed posterior and the transcripts shown as a vertical band in the embryo (Chen, Lin et al. 2007) (Fig 31).

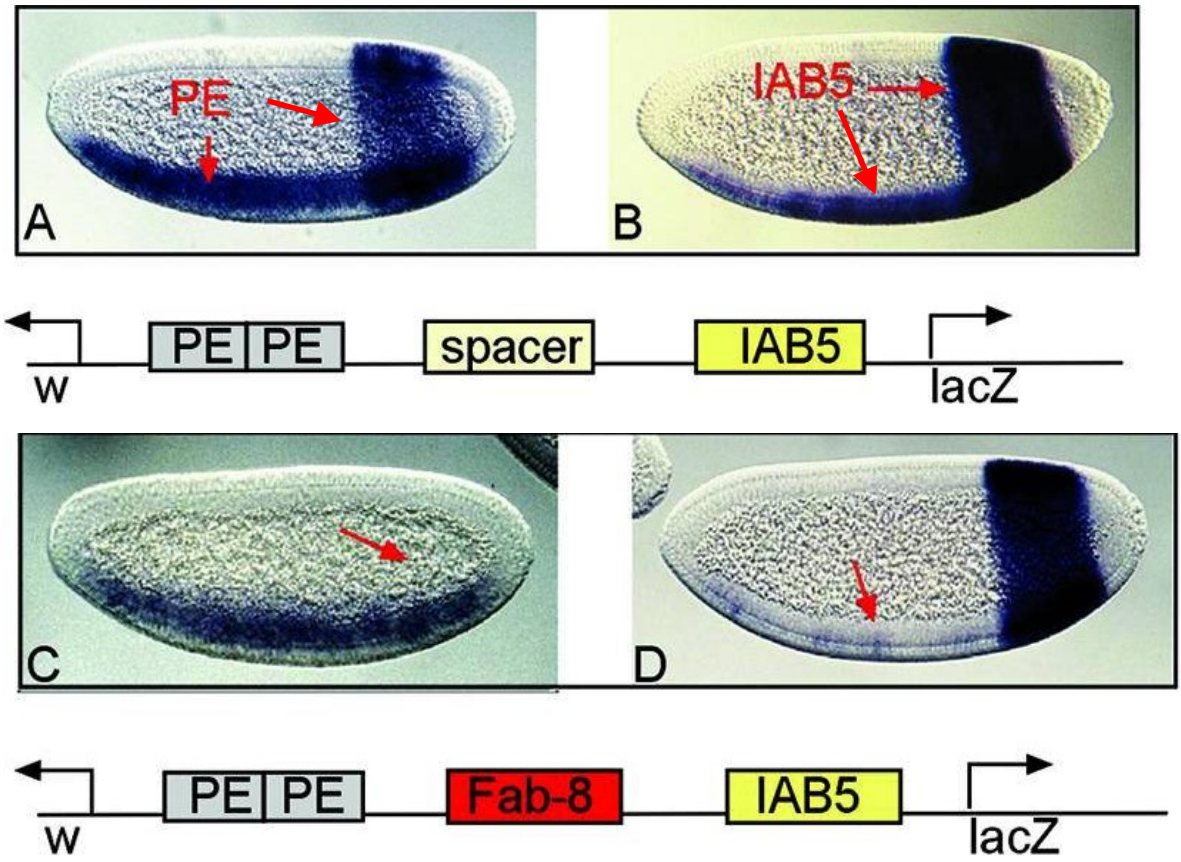

Figure 31: Drosophila gene activity analyses for CTRL2 insulator elements by (Chen, Lin et al. 2007). Figure used under CC-BY 4.0 license

When no insulator elements were placed in between the two enhancers, PE and IAB5 both activates the forward w gene (Fig 31A) or the backward LacZ gene (Fig 31B). The resulting w gene and LacZ gene transcripts were visualized as both an anterior stripe and a vertical band. When the spacer DNA was replaced by an insulator, Fab-8, PE only activated transcription of the w gene, resulting its transcripts being only visualized as an anterior stripe, whereas IAB5 only activated transcription of LacZ gene, resulting its transcripts being only visualized as a vertical band (Fig 31C and D).

Replacement of the spacer DNA with the 2 kb, 1.4 kb, or 0.8 kb LAT, but not the LAT intron lacking CTRL2, all resulted in expression of PE only as an anterior stripe and IAB5 only as a vertical band (Chen, Lin et al. 2007). These results indicated that CTRL 2 has enhancer-blocking activities (Chen, Lin et al. 2007). The 0.8kb LAT region, containing CTRL2, also interacted with human and drosophila CTCF by EMSA, and in latently infected mouse TG, by ChIP (Chen, Lin et al. 2007).

CTRL2 knockout mutant HSV-1 showed no differences in genome copy number or ICP0 and ICP27 expression levels during lytic infections, or in genome copy number or LAT transcript levels during latency (Lee, Raja et al. 2018). However, the levels of H3K27me3 increased on the LAT intron (Lee, Raja et al. 2018).

An independent study showed that a different CTRL2 knockout in a different strain resulted in decreased viral replication in lytic infections. It also resulted in decreased genome copy number and increased ICP0, ICP4, ICP27 and VP16 mRNA levels in latently infected mouse TG (Washington, Singh et al. 2019). Nonetheless, Dr. Knipe's study found that the level of H3K27me3 increased 1.5-fold at the LAT intron, but not at the adjacent ICP0 promoter during latency, whereas the level of H3K9me3 did not change in either of these two regions (Lee, Raja et al. 2018). The authors concluded that such differences might result from the different strains used in each experiment, HSV-1 KOS or strain 17 (Washington, Singh et al. 2019). Beyond the difference in viral strains, the two studies used different techniques to evaluate viral replication. Dr.

Knipe's group infected HeLa and HFF cells at a relatively higher moi (0.1 pfu/cell), and viral replication was measured by plaquing assay (Lee, Raja et al. 2018). Loss of CTCF binding to CTRL2 were confirmed by ChIP in latently infected mouse TG (Lee, Raja et al. 2018). In contrast, Dr. Neumann's group infected rabbit skin, U2OS, 3T3, and Neuro 2A cells with lower moi (0.01 pfu/cell), and viral replication was measured by qPCR (Washington, Singh et al. 2019). Furthermore, the loss of CTCF binding to HSV-1 genomes during latency was not evaluated in their study. These studies suggest that CTCF binding to CTRL2 during latency prevents heterochromatin spread into the transcribed LAT region.

Latent HSV-1 infections were established in mouse TG by ocular infections (Ertel, Cammarata et al. 2012). CTCF was co-immunoprecipitated and its enrichment on three CTCF binding sites, CTRL2, CTa'm and CTRS3, was measured (Ertel, Cammarata et al. 2012). All three sites were enriched in CTCF during latency, with a 7- to 20-fold increase compared to the gC gene (Ertel, Cammarata et al. 2012). The latent HSV-1 genomes in mouse TG were then reactivated by NaBu treatment, and CTCF was co-immunoprecipitated at different times after reactivation. CTCF enrichment decreased to approximately half at 1 h after reactivation on CTRL2 and Cta'm and decreased even more to about 5- to 20- fold less at 6 h after reactivation. CTCF enrichment at CTRS3 did not change 1 h after reactivation, but still decreased 10-fold at 6 h (Ertel, Cammarata et al. 2012). Even at 6 h after reactivation, CTCF was still relatively

enriched in CTRL2, with a 5-fold increase comparing to gC genes (Ertel, Cammarata et al. 2012). The level of CTCF remained the same until 4 h after NaBu induced reactivation (Ertel, Cammarata et al. 2012). Notably, CTCF was more enriched at CTRL1 (3-fold more enriched) than CTRL2, Cta'm, CTRS1/2 and CTRS3. CTCF was still relatively enriched at CTRL1 in comparison to gC genes at 6 h after NaBu induced reactivation (Washington, Musarrat et al. 2018). Findings are also consistent with my results. Firstly, chromatin insulator-like elements function as a barrier between transcribed and non-transcribed genes during lytic HSV-1 infection, and CTCF was enriched at the barriers (Fig 25, 26) like in the cellular chromatin. In the cellular chromatin, the modifications on transcribed and non-transcribed regions are different. During HSV-1 lytic infections, however, the levels of the heterochromatin marker H3K27me3 were not different at two sites separated by chromatin insulator-like elements. In my experiments, the accessibility of the two regions separated by CTCF binding sites was also similar. Both loci fractionated together even when one site was transcribed and the other one was not (Fig 25, 26). Therefore, CTCF still appears to function as a barrier between transcribed and non-transcribed region on HSV-1 genome but might not function as a chromatin barrier. To the resolution of my experiments, the accessibility on both sites was similar.

My experiments could not address either whether CTCF associate with HSV-1 genome first or HSV-1 genome is chromatinized first. If CTCF associated first and

chromatin remodelling occurred afterwards, then CTCF would likely stop the spread of the remodelling and result in different accessible chromatins (likely different histone modifications, too) at the two sites. However, both the ChIP-Seq results of H3K27me3 (Gao, Chen et al. 2020) or of my experiments showed no differences on chromatin modification or accessibility at both sites.

Twenty-five more potential CTCF binding sites were identified on the HSV-1 genome during lytic infections (Lang, Li et al. 2017). Infection of CTCF-knockdown cells resulted in viral replication to lower levels and inhibition of ICP0, ICP4, ICP8, UL30 and UL36 transcription. Levels of H3K27me3 and H3K9me3 increased on the promoters and gene bodies of ICP0, ICP4, ICP8 and TK (Lang, Li et al. 2017). CTCF was concluded to promote HSV-1 transcription by facilitating the active form of RNA Pol II (Ser2P) as CTCF knockdown resulted in reducing of levels of RNA Pol II on HSV-1 genome. However, these experiments could not differentiate whether CTCF or RNA Pol II was the first to associate with the HSV-1 genome. As discussed above, CTCF association appear to happen after HSV-1 chromatin becomes accessible. Otherwise, CTCF would be expected to function as a barrier between the accessible and inaccessible chromatin. Thus HSV-1 chromatin may first be remodelled during lytic infections into a very dynamic (transcriptional competent) state, and such dynamic chromatin would likely allow recruitment of RNA Pol II and its corresponding phosphorylase to the IE promoters by the VP16/Oct-1/HCF complexes, and of CTCF to

its binding sites. The bound CTCF then could function as a barrier to prevent transcription spreading to locus that are not yet supposed to be transcribed (i.e., early or late genes at early times of infection).

Interestingly, the overrepresented potential CTCF binding sites in my experiments were identified by their lower accessibility in the untreated, unfractionated samples in comparison to the digested, fractionated ones (Fig 27). CTCF binds with high binding affinity (K_D 5nM) to its consensus sequence through its eleven zinc fingers (Hashimoto, Wang et al. 2017). Its binding efficiency did not change even at 150mM NaCl (Hashimoto, Wang et al. 2017). Notably, only zinc fingers 3 to 7 form base-specific contacts, with about 15bp DNA (CCAGCAGGGGGCGCT). Cytosine methylation at the second cytosine base inhibit CTCF binding to the oligomer (23-fold reduction in CTCF K_D), whereas methylation of other cytosine bases does not affect binding (only 1.5-fold reduction) (Hashimoto, Wang et al. 2017). Binding of the other zinc fingers (ZF1, 2, 10 and 11) to their consensus sequences could not be resolved, suggesting that these bindings were more dynamic (Hashimoto, Wang et al. 2017). Nonetheless, CTCF-bound HSV-1 DNA may well be difficult to extract in the undigested, unfractionated samples, resulting in low DNA recovery of the CTCF binding sites. However, nuclease could cleave the DNA at the edge of the CTCF-DNA complexes, resulting a higher recovery of the sequences adjacent to the actual binding sites than the undigested samples. When analyzed in a 250bp sliding window of deep sequencing this recovery would mask any

lack of recovery of the actual binding sites (Fig 27).

At 2 h after infection, there were 47 overrepresented relatively inaccessible peaks (Fig 28). Some of them mapped to the previously identified CTCF binding sites. Others might also be recognized by CTCF or other nuclear proteins (such as lamin A/C) to form also fairly inaccessible protein-DNA structures. The number of inaccessible short DNA sequences was reduced to 25 at 4 h, and to 1 and zero at 7 h and 15 h, correspondingly (Fig 28). The HSV-1 genome is relatively dense on genes, more than 80 genes in a 152kb genome, in comparison to cellular chromosomes (approximately 2000 genes in 248,956kb human chromosome 1). Yet, these 80 HSV-1 genes follow different transcription kinetics. Although the exact mechanism of CTCF removal from HSV-1 genomes is not clear, one can speculate that the highly dynamic, highly accessible HSV-1 chromatin require many CTCF complexes to bind to stop transcription spreading to E and L genes at early times of infections. As infection progresses, more and more genes are transcribed, and no longer as many CTCF molecules bind to the HSV-1 chromatin.

The overrepresented peaks resulted from higher recovery of the DNA in the digested, fractionated samples over undigested, unfractionated ones. Overall, the entire HSV-1 genome was fairly equally accessible under each treatment or time, although the accessibility differed among treatments (Fig 21-24). These findings are most consistent with the evidence that histone modifications changed genome-wide, without any locus

specificity (Gao, Chen et al. 2020). Several pieces of evidence have been integrated as suggesting that epigenetic inhibitors alter histone modifications of specific genes. However, most of these studies tested the levels of histone modifications of only selected HSV-1 genes. Recent ChIP-Seq evidence showed that histone modifications change genome-wide as infection progress, (Gao, Chen et al. 2020), whereas my results suggest that HSV-1 chromatin regulates transcription competency of the entire HSV-1 genome rather than individual gene transcription. Together, these evidences suggest that HSV-1 chromatin is regulated on the level of entire HSV-1 genome, and that is coupled with HSV-1 transcription levels.

Previous evidence had indicated that there are two populations of HSV-1 genomes in the nucleus, transcribed and non-transcribed ones. Furthermore, histone modifications change genome-wide, rather than locus-by-locus or gene-by-gene. My findings suggest that the actual relationship between HSV-1 chromatin accessibility and transcription are also genome-wide rather than gene or locus specific. Thus, I propose a model whereby chromatin dynamics provides a first level of regulation of HSV-1 gene expression. Cells attempt to silence the infecting HSV-1 genomes by chromatinizing the protein-free infecting HSV-1 DNA to a silenced compacted chromatin. If not all HSV-1 genomes are successfully silenced, then a lytic infection is established.

The promoters of the E and L genes are unable to recruit multiple transcription factors to disrupt silencing, whereas those of the IE genes do so via the presence of

multiple transcription factors and epigenetic modifiers binding sites. The insulator-like elements anchor the genomes to nuclear structures and prevent transcription from extending to neighboring regions. The viral transcriptional activators, such as ICP0 and ICP4, either as virion proteins or expressed de novo in the infected cell, then increase the dynamics of the chromatin in entire HSV-1 genomes, resulting a more relaxed HSV-1 chromatin state and also upregulating E and L gene transcription (Fig 32). Only a few genomes need not be silenced early in infection and become biologically active, while most of the infecting genomes would remain constrained and compacted in silenced chromatin and remain biologically inactive.

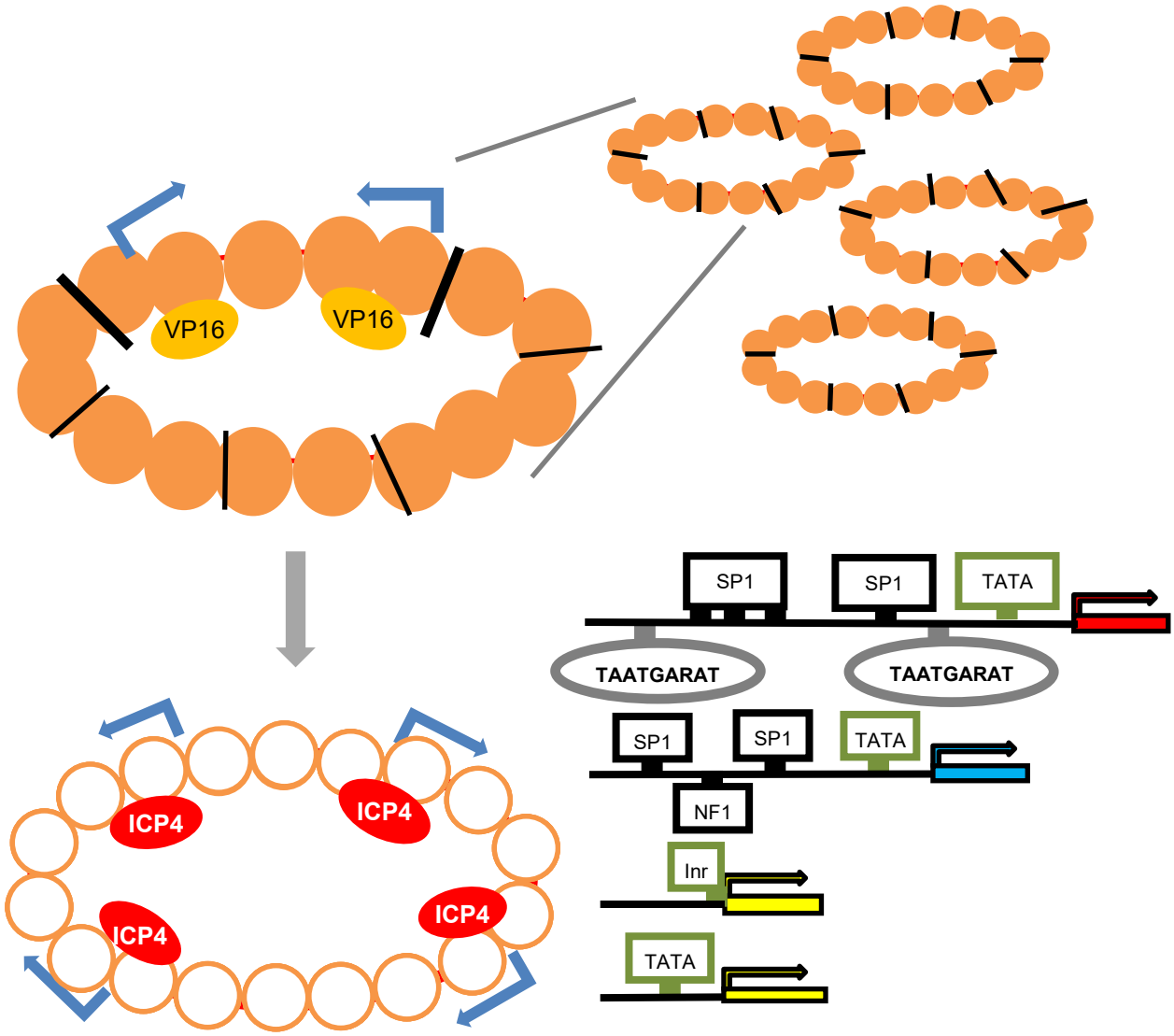

Figure 32: Cartoon presenting the model of intracellular HSV-1 chromatin. Dark brown, stable nucleosomes; Empty brown, dynamic nucleosomes; Yellow oval, VP16; Red oval, ICP4; Black bold line, CTCF; Black thin line, potential CTCF binding or other nuclear protein binding sites. Right bottom, Fig 3 represented for comparison of the promoters of IE, E and L genes.

4.1 Future directions

Summary of the model. the transcriptional competent HSV-1 genomes were in most dynamic chromatin, within which the transcriptional competent genes and the incompetent genes were separated by insulator elements such as CTCF. The transcriptional incompetent HSV-1 genomes were in least accessible chromatin. It is thus critical to identify whether the chromatin of these two populations of HSV-1 genome differ in their composition, as a first step to characterize the mechanisms resulting in the highly dynamic state of the lytic HSV-1 chromatin.

To separate HSV-1 chromatin and cellular chromatin, I propose to use iPOND as established by Dr. DeLuca's group (Dembowski and DeLuca 2015). To separate the dynamic and stable chromatin, I propose to first serially digest chromatin into different sized poly-nucleosome complexes followed by sucrose gradient centrifugation as performed in my Thesis (Fig 33). Briefly, cells will be infected with HSV-1 virions containing EdU-labeled genomes. Chromatin of infected cell nuclei will be extracted and serially digested as described in this thesis. Digested chromatin fragments will be separated in sucrose gradients, and the DNA-protein complexes in each fraction will be cross-linked with formaldehyde. HSV-1 DNA in each fraction will then be precipitated by "click chemistry" as described by Dr. DeLuca (Dembowski and DeLuca 2015), and the proteins associated with the parental HSV-1 DNA will be analyzed by mass spectrometry. Coupling nuclease digestion, sucrose fractionation, and iPOND together

has several advantages. Crosslinking and immunoprecipitation of each fraction would minimize the background detection of nuclear matrix proteins. The accessible chromatin would be physically separated into different fractions from the inaccessible one. Only HSV-1 DNA will be immunoprecipitated and analyzed. As any approach, it also has some limitations. Digestion of the HSV-1 genome might result in some chromatin fragments containing no EdU-labeled DNA, which consequently could not be purified by “click chemistry”. Generating EdU-labeled HSV-1 genomes require double knockout of UL2/UL50 genes. UL2 gene encodes viral uracil DNA glycosylase and UL50 gene encodes viral dUTPase. The viral uracil DNA glycosylase has been shown to interact with the HSV-1 DNA polymerase subunits and knockout of UL2 genes results in some genome instability (Bogani, Corredeira et al. 2010). Knockout of UL50 did not obviously affect lytic HSV-1 replication (Kato, Hirohata et al. 2014). As already discussed in the thesis, EdU mediated pull down would favor the isolation of the most dynamic chromatin, which is the most accessible.

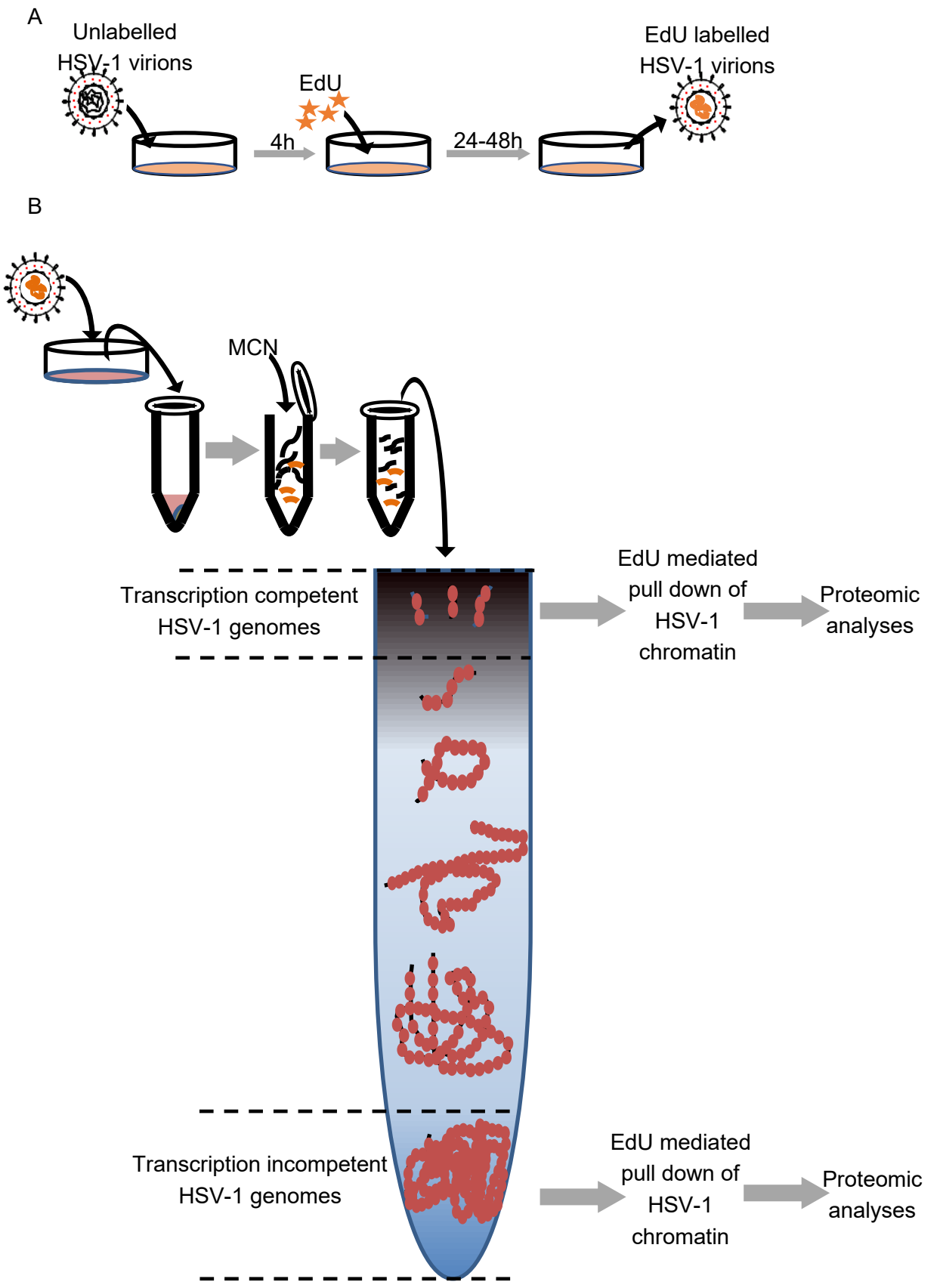
A
Unlabelled
HSV-1 virions
EdU
4h
24-48h
EdU labelled
HSV-1 virions
B
MCN
Transcription competent
HSV-1 genomes
EdU mediated
pull down of
HSV-1
chromatin
Proteomic
analyses
Transcription incompetent
HSV-1 genomes
EdU mediated
pull down of
HSV-1
chromatin
Proteomic
analyses

Figure 33: Cartoon depicting the methodology of MCN-fractionation-iPOND. (A) Cartoon representing the production of EdU-labelled HSV-1 virions, as proposed by Dembowski and DeLuca, 2015. (B) Cartoon depicting MCN-fractionation-iPOND

After mass spectrometry identification of the proteins in the two populations of HSV-1 genomes, the protein compositions (histones and their modifications) of the dynamic or stable HSV-1 chromatins could be consistent or not. Under the assumption that the protein composition is consistent (i.e., no significant differences in the levels of each histone variant or histone modifications), then the dynamic HSV-1 chromatin could well result from enrichment in chromatin remodelers. To follow up on this possibility, I propose to repeat the nuclease digestion coupled with sucrose fractionation and iPOND using a longer chain crosslinker. Formaldehyde has a cross-link span of approximately 2 Å (Zeng, Vakoc et al. 2006). Thus, it is difficult to capture other than direct protein-DNA interactions by formaldehyde cross-linking. The long crosslinkers (i.e., dimethyl adipimidate (Kurdistani and Grunstein 2003), or disuccinimidyl glutarate (Fujita, Jaye et al. 2003) can capture more chromatin remodelers and their subunits, which are more distant to the DNA. My expectation under this model is that the most dynamic chromatin of HSV-1 genomes would be more enriched in chromatin remodelers in comparison to the least dynamic one.

To further analyze the mechanism resulting in the highly dynamic HSV-1 chromatin

under the model in which chromatin remodelers were enriched, cells treated with CHX could be infected with EdU-labelled HSV-1. The chromatin would be extracted and the digestion-fractionation-iPOND protocol discussed above would be followed. If the chromatin remodelers are not enriched in the dynamic chromatin population under these conditions, then IE proteins, more likely, ICP4, may recruit these remodelers. If the chromatin remodelers are still enriched, then VP16 or other tegument proteins may well be responsible of recruiting them.

Alternatively, the protein composition of the dynamic and stable HSV-1 chromatin might differ (i.e., histone H3K4me may be enriched in the dynamic chromatin, and histone H3K9me in the stable chromatin). To further analyze the protein composition, using H3K4me and H3K9me as examples, the iPOND purified HSV-1 DNA could be immunoprecipitated in each fraction using H3K4me or H3K9me antibodies coupled with sequencing (ChIP-seq). My expectation is that neither H3K4me or H3K9me would show any region-specificity in either most or least dynamic HSV-1 chromatin. If they did, it would be most interesting to identify the genomic regions in which these histone modifications are enriched or depleted. CHX-treated cells infected with EdU-labeled HSV-1 could answer if ICP4 (or other IE proteins) or VP16 (or other proteins in the tegument) mediate the enrichment in particular histone modifications or variants in the most dynamic HSV-1 chromatin like in the previous discussion.

In summary, the proposed experiments infecting with EdU-labeled HSV-1 coupled

with nuclease digestion, sucrose fractionation, and iPOND would address any differences in the protein composition of the most and least dynamic HSV-1 chromatins, and identify whether ICP4 or VP16 participate in generating these differences.

References

Abrams, E., L. Neigeborn and M. Carlson (1986). "Molecular analysis of SNF2 and SNF5, genes required for expression of glucose-repressible genes in Saccharomyces cerevisiae." Mol Cell Biol **6**(11): 3643-3651.

Adhireksan, Z., D. Sharma, P. L. Lee and C. A. Davey (2020). "Near-atomic resolution structures of interdigitated nucleosome fibres." Nat Commun **11**(1): 4747.

Adkins, M. W. and J. K. Tyler (2006). "Transcriptional activators are dispensable for transcription in the absence of Spt6-mediated chromatin reassembly of promoter regions." Mol Cell **21**(3): 405-416.

Agez, M., J. Chen, R. Guerois, C. van Heijenoort, J. Y. Thuret, C. Mann and F. Ochsenbein (2007). "Structure of the histone chaperone ASF1 bound to the histone H3 C-terminal helix and functional insights." Structure **15**(2): 191-199.

Allahverdi, A., R. Yang, N. Korolev, Y. Fan, C. A. Davey, C. F. Liu and L. Nordenskiold (2011). "The effects of histone H4 tail acetylations on cation-induced chromatin folding and self-association." Nucleic Acids Res **39**(5): 1680-1691.

Amelio, A. L., N. V. Giordani, N. J. Kubat, E. O'Neil J and D. C. Bloom (2006). "Deacetylation of the herpes simplex virus type 1 latency-associated transcript (LAT) enhancer and a decrease in LAT abundance precede an increase in ICP0 transcriptional permissiveness at early times postexplant." J Virol **80**(4): 2063-2068.

Amelio, A. L., P. K. McAnany and D. C. Bloom (2006). "A chromatin insulator-like element in the herpes simplex virus type 1 latency-associated transcript region binds CCCTC-binding factor and displays enhancer-blocking and silencing activities." J Virol **80**(5): 2358-2368.

Angelov, D., A. Molla, P. Y. Perche, F. Hans, J. Cote, S. Khochbin, P. Bouvet and S. Dimitrov (2003). "The histone variant macroH2A interferes with transcription factor binding and SWI/SNF nucleosome remodeling." Mol Cell **11**(4): 1033-1041.

Arbuckle, J. H., P. J. Gardina, D. N. Gordon, H. D. Hickman, J. W. Yewdell, T. C. Pierson, T. G. Myers and T. M. Kristie (2017). "Inhibitors of the Histone Methyltransferases EZH2/1 Induce a Potent Antiviral State and Suppress Infection by Diverse Viral Pathogens." mBio **8**(4).

Arbuckle, J. H. and T. M. Kristie (2014). "Epigenetic repression of herpes simplex virus infection by the nucleosome remodeler CHD3." MBio **5**(1): e01027-01013.

Arthur, J. L., C. G. Scarpini, V. Connor, R. H. Lachmann, A. M. Tolkovsky and S. Efstathiou (2001). "Herpes simplex virus type 1 promoter activity during latency establishment, maintenance, and reactivation in primary dorsal root neurons in vitro." J Virol **75**(8): 3885-3895.

Arvey, A., I. Tempera and P. M. Lieberman (2013). "Interpreting the Epstein-Barr Virus (EBV) epigenome using high-throughput data." Viruses **5**(4): 1042-1054.

Atanasiu, D., W. T. Saw, G. H. Cohen and R. J. Eisenberg (2010). "Cascade of events governing cell-cell fusion induced by herpes simplex virus glycoproteins gD, gH/gL, and gB." J Virol **84**(23): 12292-12299.

Atanasiu, D., W. T. Saw, R. J. Eisenberg and G. H. Cohen (2016). "Regulation of Herpes Simplex Virus Glycoprotein-Induced Cascade of Events Governing Cell-Cell Fusion." J Virol **90**(23): 10535-10544.

Au, T. J., J. Rodriguez, J. A. Vincent and T. Tsukiyama (2011). "ATP-dependent chromatin remodeling factors tune S phase checkpoint activity." Mol Cell Biol **31**(22): 4454-4463.

Banaszynski, L. A., D. Wen, S. Dewell, S. J. Whitcomb, M. Lin, N. Diaz, S. J. Elsasser, A. Chapgier, A. D. Goldberg, E. Canaani, S. Rafii, D. Zheng and C. D. Allis (2013). "Hira-dependent histone H3.3 deposition facilitates PRC2 recruitment at developmental loci in ES cells." Cell **155**(1): 107-120.

Bano, D., A. Piazzesi, P. Salomoni and P. Nicotera (2017). "The histone variant H3.3 claims its place in the crowded scene of epigenetics." Aging (Albany NY) **9**(3): 602-614.

Bao, Y., K. Konesky, Y. J. Park, S. Rosu, P. N. Dyer, D. Rangasamy, D. J. Tremethick, P. J. Laybourn and K. Luger (2004). "Nucleosomes containing the histone variant H2A.Bbd organize only 118 base pairs of DNA." EMBO J **23**(16): 3314-3324.

Barbera, A. J., J. V. Chodaparambil, B. Kelley-Clarke, V. Joukov, J. C. Walter, K. Luger and K. M. Kaye (2006). "The nucleosomal surface as a docking station for Kaposi's sarcoma herpesvirus LANA." Science **311**(5762): 856-861.

Barski, A., S. Cuddapah, K. Cui, T. Y. Roh, D. E. Schones, Z. Wang, G. Wei, I. Chepelev and K. Zhao (2007). "High-resolution profiling of histone methylations in the human genome." Cell **129**(4): 823-837.

Bartholomew, B. (2014). "ISWI chromatin remodeling: one primary actor or a coordinated effort?" Curr Opin Struct Biol **24**: 150-155.

Bauer, D. W., D. Li, J. Huffman, F. L. Homa, K. Wilson, J. C. Leavitt, S. R. Casjens, J. Baines and A. Evilevitch (2015). "Exploring the Balance between DNA Pressure and Capsid Stability in Herpesviruses and Phages." J Virol **89**(18): 9288-9298.

Baum, L. and A. Ng (2004). "Curcumin interaction with copper and iron suggests one possible mechanism of action in Alzheimer's disease animal models." J Alzheimers Dis **6**(4): 367-377; discussion 443-369.

Becker, P. B. and J. L. Workman (2013). "Nucleosome remodeling and epigenetics." Cold Spring Harb Perspect Biol **5**(9).

Bednar, J., R. A. Horowitz, J. Dubochet and C. L. Woodcock (1995). "Chromatin conformation and salt-induced compaction: three-dimensional structural information from cryoelectron microscopy." J Cell Biol **131**(6 Pt 1): 1365-1376.

Benboudjema, L., M. Mulvey, Y. Gao, S. W. Pimplikar and I. Mohr (2003). "Association of the herpes simplex virus type 1 Us11 gene product with the cellular kinesin light-chain-related protein PAT1 results in the redistribution of both polypeptides." J Virol **77**(17): 9192-9203.

Bernstein, E., E. M. Duncan, O. Masui, J. Gil, E. Heard and C. D. Allis (2006). "Mouse polycomb proteins bind differentially to methylated histone H3 and RNA and are enriched in facultative heterochromatin." Mol Cell Biol **26**(7): 2560-2569.

Boeger, H., J. Griesenbeck, J. S. Strattan and R. D. Kornberg (2003). "Nucleosomes unfold completely at a transcriptionally active promoter." Mol Cell **11**(6): 1587-1598.

Boeger, H., J. Griesenbeck, J. S. Strattan and R. D. Kornberg (2004). "Removal of promoter nucleosomes by disassembly rather than sliding in vivo." Mol Cell **14**(5): 667-673.

Bogani, F., I. Corredeira, V. Fernandez, U. Sattler, W. Rutvisuttinunt, M. Defais and P. E. Boehmer (2010). "Association between the herpes simplex virus-1 DNA polymerase and uracil DNA glycosylase." J Biol Chem **285**(36): 27664-27672.

Bonaldi, T., G. Langst, R. Strohner, P. B. Becker and M. E. Bianchi (2002). "The DNA chaperone HMGB1 facilitates ACF/CHRAC-dependent nucleosome sliding." EMBO J **21**(24): 6865-6873.

Boutell, C., S. Sadis and R. D. Everett (2002). "Herpes simplex virus type 1 immediate-early protein ICP0 and is isolated RING finger domain act as ubiquitin E3 ligases in vitro." J Virol **76**(2): 841-850.

Bowman, S. K., A. M. Deaton, H. Domingues, P. I. Wang, R. I. Sadreyev, R. E. Kingston and W. Bender (2014). "H3K27 modifications define segmental regulatory domains in the Drosophila bithorax complex." Elife **3**: e02833.

Bracken, A. P., G. L. Brien and C. P. Verrijzer (2019). "Dangerous liaisons: interplay between SWI/SNF, NuRD, and

Polycomb in chromatin regulation and cancer." Genes Dev **33**(15-16): 936-959.
Brehm, A., G. Langst, J. Kehle, C. R. Clapier, A. Imhof, A. Eberharter, J. Muller and P. B. Becker (2000). "dMi-2 and ISWI chromatin remodelling factors have distinct nucleosome binding and mobilization properties." EMBO J **19**(16): 4332-4341.
Briggs, S. D., T. Xiao, Z. W. Sun, J. A. Caldwell, J. Shabanowitz, D. F. Hunt, C. D. Allis and B. D. Strahl (2002). "Gene silencing: trans-histone regulatory pathway in chromatin." Nature **418**(6897): 498.
Brosch, G., P. Loidl and S. Graessle (2008). "Histone modifications and chromatin dynamics: a focus on filamentous fungi." FEMS Microbiol Rev **32**(3): 409-439.
Brown, C. E., T. Lechner, L. Howe and J. L. Workman (2000). "The many HATs of transcription coactivators." Trends Biochem Sci **25**(1): 15-19.
Brown, S. W. (1966). "Heterochromatin." Science **151**(3709): 417-425.
Bryant, K. F., R. C. Colgrove and D. M. Knipe (2011). "Cellular SNF2H chromatin-remodeling factor promotes herpes simplex virus 1 immediate-early gene expression and replication." MBio **2**(1): e00330-00310.
Byrd, K. and V. G. Corces (2003). "Visualization of chromatin domains created by the gypsy insulator of Drosophila." J Cell Biol **162**(4): 565-574.
Campbell, M. E., J. W. Palfreyman and C. M. Preston (1984). "Identification of herpes simplex virus DNA sequences which encode a trans-acting polypeptide responsible for stimulation of immediate early transcription." J Mol Biol **180**(1): 1-19.
Cao, L., J. Ding, L. Dong, J. Zhao, J. Su, L. Wang, Y. Sui, T. Zhao, F. Wang, J. Jin and Y. Cai (2015). "Negative Regulation of p21Waf1/Cip1 by Human INO80 Chromatin Remodeling Complex Is Implicated in Cell Cycle Phase G2/M Arrest and Abnormal Chromosome Stability." PLoS One **10**(9): e0137411.
Cardone, G., W. W. Newcomb, N. Cheng, P. T. Wingfield, B. L. Trus, J. C. Brown and A. C. Steven (2012). "The UL36 tegument protein of herpes simplex virus 1 has a composite binding site at the capsid vertices." J Virol **86**(8): 4058-4064.
Cardone, G., D. C. Winkler, B. L. Trus, N. Cheng, J. E. Heuser, W. W. Newcomb, J. C. Brown and A. C. Steven (2007). "Visualization of the herpes simplex virus portal in situ by cryo-electron tomography." Virology **361**(2): 426-434.
Carmen, A. A., L. Milne and M. Grunstein (2002). "Acetylation of the yeast histone H4 N terminus regulates its binding to heterochromatin protein SIR3." J Biol Chem **277**(7): 4778-4781.
Carrington-Lawrence, S. D. and S. K. Weller (2003). "Recruitment of polymerase to herpes simplex virus type 1 replication foci in cells expressing mutant primase (UL52) proteins." J Virol **77**(7): 4237-4247.
Chadwick, B. P. and H. F. Willard (2001). "Histone H2A variants and the inactive X chromosome: identification of a second macroH2A variant." Hum Mol Genet **10**(10): 1101-1113.
Chai, B., J. Huang, B. R. Cairns and B. C. Laurent (2005). "Distinct roles for the RSC and Swi/Snf ATP-dependent chromatin remodelers in DNA double-strand break repair." Genes Dev **19**(14): 1656-1661.
Challberg, M. D. (1986). "A method for identifying the viral genes required for herpesvirus DNA replication." Proc Natl Acad Sci U S A **83**(23): 9094-9098.
Chee, A. V., P. Lopez, P. P. Pandolfi and B. Roizman (2003). "Promyelocytic leukemia protein mediates interferon-based anti-herpes simplex virus 1 effects." J Virol **77**(12): 7101-7105.
Chelbi-Alix, M. K. and H. de The (1999). "Herpes virus induced proteasome-dependent degradation of the nuclear bodies-associated PML and Sp100 proteins." Oncogene **18**(4): 935-941.
Chen, G., Y. Chen, N. Yang, X. Zhu, L. Sun and G. Li (2012). "Interaction between curcumin and mimetic

biomembrane." Sci China Life Sci **55**(6): 527-532.
Chen, Q., L. Lin, S. Smith, J. Huang, S. L. Berger and J. Zhou (2007). "CTCF-dependent chromatin boundary element between the latency-associated transcript and ICP0 promoters in the herpes simplex virus type 1 genome." J Virol **81**(10): 5192-5201.
Chen, S. H., M. F. Kramer, P. A. Schaffer and D. M. Coen (1997). "A viral function represses accumulation of transcripts from productive-cycle genes in mouse ganglia latently infected with herpes simplex virus." J Virol **71**(8): 5878-5884.
Chen, Z. A., A. Jawhari, L. Fischer, C. Buchen, S. Tahir, T. Kamenski, M. Rasmussen, L. Lariviere, J. C. Bukowski-Wills, M. Nilges, P. Cramer and J. Rappsilber (2010). "Architecture of the RNA polymerase II-TFIIF complex revealed by cross-linking and mass spectrometry." EMBO J **29**(4): 717-726.
Chung, J. H., M. Whiteley and G. Felsenfeld (1993). "A 5' element of the chicken beta-globin domain serves as an insulator in human erythroid cells and protects against position effect in Drosophila." Cell **74**(3): 505-514.
Cirillo, L. A., F. R. Lin, I. Cuesta, D. Friedman, M. Jarnik and K. S. Zaret (2002). "Opening of compacted chromatin by early developmental transcription factors HNF3 (FoxA) and GATA-4." Mol Cell **9**(2): 279-289.
Cirillo, L. A., C. E. McPherson, P. Bossard, K. Stevens, S. Cherian, E. Y. Shim, K. L. Clark, S. K. Burley and K. S. Zaret (1998). "Binding of the winged-helix transcription factor HNF3 to a linker histone site on the nucleosome." EMBO J **17**(1): 244-254.
Clapier, C. R. and B. R. Cairns (2012). "Regulation of ISWI involves inhibitory modules antagonized by nucleosomal epitopes." Nature **492**(7428): 280-284.
Clapier, C. R., J. Iwasa, B. R. Cairns and C. L. Peterson (2017). "Mechanisms of action and regulation of ATP-dependent chromatin-remodelling complexes." Nat Rev Mol Cell Biol **18**(7): 407-422.
Clapier, C. R., G. Langst, D. F. Corona, P. B. Becker and K. P. Nightingale (2001). "Critical role for the histone H4 N terminus in nucleosome remodeling by ISWI." Mol Cell Biol **21**(3): 875-883.
Cliffe, A. R. and D. M. Knipe (2008). "Herpes simplex virus ICP0 promotes both histone removal and acetylation on viral DNA during lytic infection." J Virol **82**(24): 12030-12038.
Cloos, P. A., J. Christensen, K. Agger, A. Maiolica, J. Rappsilber, T. Antal, K. H. Hansen and K. Helin (2006). "The putative oncogene GASC1 demethylates tri- and dimethylated lysine 9 on histone H3." Nature **442**(7100): 307-311.
Cohen, E. M. and O. Kobiler (2016). "Gene Expression Correlates with the Number of Herpes Viral Genomes Initiating Infection in Single Cells." PLoS Pathog **12**(12): e1006082.
Coleman, H. M., V. Connor, Z. S. Cheng, F. Grey, C. M. Preston and S. Efstathiou (2008). "Histone modifications associated with herpes simplex virus type 1 genomes during quiescence and following ICP0-mediated de-repression." J Gen Virol **89**(Pt 1): 68-77.
Conerly, M. L., S. S. Teves, D. Diolaiti, M. Ulrich, R. N. Eisenman and S. Henikoff (2010). "Changes in H2A.Z occupancy and DNA methylation during B-cell lymphomagenesis." Genome Res **20**(10): 1383-1390.
Conn, K. L., M. J. Hendzel and L. M. Schang (2008). "Linker histones are mobilized during infection with herpes simplex virus type 1." J Virol **82**(17): 8629-8646.
Conn, K. L., M. J. Hendzel and L. M. Schang (2011). "Core histones H2B and H4 are mobilized during infection with herpes simplex virus 1." J Virol **85**(24): 13234-13252.
Conn, K. L., M. J. Hendzel and L. M. Schang (2013). "The differential mobilization of histones H3.1 and H3.3 by herpes simplex virus 1 relates histone dynamics to the assembly of viral chromatin." PLoS Pathog **9**(10): e1003695.
Conn, K. L., M. J. Hendzel and L. M. Schang (2016). "Correction: The Differential Mobilization of Histones H3.1 and

H3.3 by Herpes Simplex Virus 1 Relates Histone Dynamics to the Assembly of Viral Chromatin." PLoS Pathog **12**(4): e1005575.

Conn, K. L. and L. M. Schang (2013). "Chromatin dynamics during lytic infection with herpes simplex virus 1." Viruses **5**(7): 1758-1786.

Cooper, R. S., E. R. Georgieva, P. P. Borbat, J. H. Freed and E. E. Heldwein (2018). "Structural basis for membrane anchoring and fusion regulation of the herpes simplex virus fusogen gB." Nat Struct Mol Biol **25**(5): 416-424.

Cote, J., J. Quinn, J. L. Workman and C. L. Peterson (1994). "Stimulation of GAL4 derivative binding to nucleosomal DNA by the yeast SWI/SNF complex." Science **265**(5168): 53-60.

Danaher, R. J., R. J. Jacob, M. R. Steiner, W. R. Allen, J. M. Hill and C. S. Miller (2005). "Histone deacetylase inhibitors induce reactivation of herpes simplex virus type 1 in a latency-associated transcript-independent manner in neuronal cells." J Neurovirol **11**(3): 306-317.

Day, L., C. M. Chau, M. Nebozhyn, A. J. Rennekamp, M. Showe and P. M. Lieberman (2007). "Chromatin profiling of Epstein-Barr virus latency control region." J Virol **81**(12): 6389-6401.

de Dieuleveult, M., K. Yen, I. Hmitou, A. Depaux, F. Boussouar, D. Bou Dargham, S. Jounier, H. Humbertclaude, F. Ribierre, C. Baulard, N. P. Farrell, B. Park, C. Keime, L. Carriere, S. Berlivet, M. Gut, I. Gut, M. Werner, J. F. Deleuze, R. Olaso, J. C. Aude, S. Chantalat, B. F. Pugh and M. Gerard (2016). "Genome-wide nucleosome specificity and function of chromatin remodellers in ES cells." Nature **530**(7588): 113-116.

de Wit, E., E. S. Vos, S. J. Holwerda, C. Valdes-Quezada, M. J. Verstegen, H. Teunissen, E. Splinter, P. J. Wijchers, P. H. Krijger and W. de Laat (2015). "CTCF Binding Polarity Determines Chromatin Looping." Mol Cell **60**(4): 676-684.

Deckert, J. and K. Struhl (2001). "Histone acetylation at promoters is differentially affected by specific activators and repressors." Mol Cell Biol **21**(8): 2726-2735.

Delmas, V., D. G. Stokes and R. P. Perry (1993). "A mammalian DNA-binding protein that contains a chromodomain and an SNF2/SWI2-like helicase domain." Proc Natl Acad Sci U S A **90**(6): 2414-2418.

Dembowski, J. A. and N. A. DeLuca (2015). "Selective recruitment of nuclear factors to productively replicating herpes simplex virus genomes." PLoS Pathog **11**(5): e1004939.

Deshmane, S. L. and N. W. Fraser (1989). "During latency, herpes simplex virus type 1 DNA is associated with nucleosomes in a chromatin structure." J Virol **63**(2): 943-947.

Diwan, P., J. J. Lacasse and L. M. Schang (2004). "Roscovitine inhibits activation of promoters in herpes simplex virus type 1 genomes independently of promoter-specific factors." J Virol **78**(17): 9352-9365.

Dorigo, B., T. Schalch, A. Kulangara, S. Duda, R. R. Schroeder and T. J. Richmond (2004). "Nucleosome arrays reveal the two-start organization of the chromatin fiber." Science **306**(5701): 1571-1573.

Dorman, E. R., A. M. Bushey and V. G. Corces (2007). "The role of insulator elements in large-scale chromatin structure in interphase." Semin Cell Dev Biol **18**(5): 682-690.

Dover, J., J. Schneider, M. A. Tawiah-Boateng, A. Wood, K. Dean, M. Johnston and A. Shilatifard (2002). "Methylation of histone H3 by COMPASS requires ubiquitination of histone H2B by Rad6." J Biol Chem **277**(32): 28368-28371.

Drolet, B. S., G. C. Perng, J. Cohen, S. M. Slanina, A. Yukht, A. B. Nesburn and S. L. Wechsler (1998). "The region of the herpes simplex virus type 1 LAT gene involved in spontaneous reactivation does not encode a functional protein." Virology **242**(1): 221-232.

Du, T., G. Zhou and B. Roizman (2013). "Modulation of reactivation of latent herpes simplex virus 1 in ganglionic organ cultures by p300/CBP and STAT3." Proc Natl Acad Sci U S A **110**(28): E2621-2628.

Ebbert, R., A. Birkmann and H. J. Schuller (1999). "The product of the SNF2/SWI2 paralogue INO80 of Saccharomyces cerevisiae required for efficient expression of various yeast structural genes is part of a high-molecular-weight protein complex." Mol Microbiol **32**(4): 741-751.

Eberharter, A. and P. B. Becker (2002). "Histone acetylation: a switch between repressive and permissive chromatin. Second in review series on chromatin dynamics." EMBO Rep **3**(3): 224-229.

Eberharter, A., S. Ferrari, G. Langst, T. Straub, A. Imhof, P. Varga-Weisz, M. Wilm and P. B. Becker (2001). "Acf1, the largest subunit of CHRAC, regulates ISWI-induced nucleosome remodelling." EMBO J **20**(14): 3781-3788.

Eberharter, A., I. Vetter, R. Ferreira and P. B. Becker (2004). "ACF1 improves the effectiveness of nucleosome mobilization by ISWI through PHD-histone contacts." EMBO J **23**(20): 4029-4039.

Eichner, J., H. T. Chen, L. Warfield and S. Hahn (2010). "Position of the general transcription factor TFIIF within the RNA polymerase II transcription preinitiation complex." EMBO J **29**(4): 706-716.

Ercan, S. and R. T. Simpson (2004). "Global chromatin structure of 45,000 base pairs of chromosome III in a- and alpha-cell yeast and during mating-type switching." Mol Cell Biol **24**(22): 10026-10035.

Ertel, M. K., A. L. Cammarata, R. J. Hron and D. M. Neumann (2012). "CTCF occupation of the herpes simplex virus 1 genome is disrupted at early times postreactivation in a transcription-dependent manner." J Virol **86**(23): 12741-12759.

Euskirchen, G. M., R. K. Auerbach, E. Davidov, T. A. Gianoulis, G. Zhong, J. Rozowsky, N. Bhardwaj, M. B. Gerstein and M. Snyder (2011). "Diverse roles and interactions of the SWI/SNF chromatin remodeling complex revealed using global approaches." PLoS Genet **7**(3): e1002008.

Everett, R. D. (2016). "Dynamic Response of IFI16 and Promyelocytic Leukemia Nuclear Body Components to Herpes Simplex Virus 1 Infection." J Virol **90**(1): 167-179.

Everett, R. D., S. Rechter, P. Papior, N. Tavalai, T. Stamminger and A. Orr (2006). "PML contributes to a cellular mechanism of repression of herpes simplex virus type 1 infection that is inactivated by ICP0." J Virol **80**(16): 7995-8005.

Fan, J. Y., D. Rangasamy, K. Luger and D. J. Tremethick (2004). "H2A.Z alters the nucleosome surface to promote HP1alpha-mediated chromatin fiber folding." Mol Cell **16**(4): 655-661.

Fan, W. H., A. P. Roberts, M. McElwee, D. Bhella, F. J. Rixon and R. Lauder (2015). "The large tegument protein pUL36 is essential for formation of the capsid vertex-specific component at the capsid-tegument interface of herpes simplex virus 1." J Virol **89**(3): 1502-1511.

Farooq, A. V. and D. Shukla (2012). "Herpes simplex epithelial and stromal keratitis: an epidemiologic update." Surv Ophthalmol **57**(5): 448-462.

Farrell, M. J., A. T. Dobson and L. T. Feldman (1991). "Herpes simplex virus latency-associated transcript is a stable intron." Proc Natl Acad Sci U S A **88**(3): 790-794.

Feng, Q. and Y. Zhang (2001). "The MeCP1 complex represses transcription through preferential binding, remodeling, and deacetylating methylated nucleosomes." Genes Dev **15**(7): 827-832.

Ferenczy, M. W. and N. A. DeLuca (2009). "Epigenetic modulation of gene expression from quiescent herpes simplex virus genomes." J Virol **83**(17): 8514-8524.

Finch, J. T. and A. Klug (1976). "Solenoidal model for superstructure in chromatin." Proc Natl Acad Sci U S A **73**(6): 1897-1901.

Flanagan, J. F. and C. L. Peterson (1999). "A role for the yeast SWI/SNF complex in DNA replication." Nucleic Acids Res **27**(9): 2022-2028.

Flower, K., D. Thomas, J. Heather, S. Ramasubramanyan, S. Jones and A. J. Sinclair (2011). "Epigenetic control of viral life-cycle by a DNA-methylation dependent transcription factor." PLoS One **6**(10): e25922.

Foster, C. T., O. M. Dovey, L. Lezina, J. L. Luo, T. W. Gant, N. Barlev, A. Bradley and S. M. Cowley (2010). "Lysine-specific demethylase 1 regulates the embryonic transcriptome and CoREST stability." Mol Cell Biol **30**(20): 4851-4863.

Frazier, D. P., D. Cox, E. M. Godshalk and P. A. Schaffer (1996). "The herpes simplex virus type 1 latency-associated transcript promoter is activated through Ras and Raf by nerve growth factor and sodium butyrate in PC12 cells." J Virol **70**(11): 7424-7432.

Fudenberg, G., M. Imakaev, C. Lu, A. Goloborodko, N. Abdennur and L. A. Mirny (2016). "Formation of Chromosomal Domains by Loop Extrusion." Cell Rep **15**(9): 2038-2049.

Fujita, N., D. L. Jaye, M. Kajita, C. Geigerman, C. S. Moreno and P. A. Wade (2003). "MTA3, a Mi-2/NuRD complex subunit, regulates an invasive growth pathway in breast cancer." Cell **113**(2): 207-219.

Fyodorov, D. V. and J. T. Kadonaga (2002). "Dynamics of ATP-dependent chromatin assembly by ACF." Nature **418**(6900): 897-900.

Gaillard, H., D. J. Fitzgerald, C. L. Smith, C. L. Peterson, T. J. Richmond and F. Thoma (2003). "Chromatin remodeling activities act on UV-damaged nucleosomes and modulate DNA damage accessibility to photolyase." J Biol Chem **278**(20): 17655-17663.

Gaillard, P. H., E. M. Martini, P. D. Kaufman, B. Stillman, E. Moustacchi and G. Almouzni (1996). "Chromatin assembly coupled to DNA repair: a new role for chromatin assembly factor I." Cell **86**(6): 887-896.

Gaillard, P. H., J. G. Moggs, D. M. Roche, J. P. Quivy, P. B. Becker, R. D. Wood and G. Almouzni (1997). "Initiation and bidirectional propagation of chromatin assembly from a target site for nucleotide excision repair." EMBO J **16**(20): 6281-6289.

Gao, C., L. Chen, S. B. Tang, Q. Y. Long, J. L. He, N. A. Zhang, H. B. Shu, Z. X. Chen, M. Wu and L. Y. Li (2020). "The epigenetic landscapes of histone modifications on HSV-1 genome in human THP-1 cells." Antiviral Res **176**: 104730.

Garber, D. A., S. M. Beverley and D. M. Coen (1993). "Demonstration of circularization of herpes simplex virus DNA following infection using pulsed field gel electrophoresis." Virology **197**(1): 459-462.

Garber, D. A., P. A. Schaffer and D. M. Knipe (1997). "A LAT-associated function reduces productive-cycle gene expression during acute infection of murine sensory neurons with herpes simplex virus type 1." J Virol **71**(8): 5885-5893.

Garcia-Ramirez, M., C. Rocchini and J. Ausio (1995). "Modulation of chromatin folding by histone acetylation." J Biol Chem **270**(30): 17923-17928.

Geoffroy, M. C., S. M. Cote, C. E. Giguere, G. Dionne, P. D. Zelazo, R. E. Tremblay, M. Boivin and J. R. Seguin (2010). "Closing the gap in academic readiness and achievement: the role of early childcare." J Child Psychol Psychiatry **51**(12): 1359-1367.

Gerhold, C. B. and S. M. Gasser (2014). "INO80 and SWR complexes: relating structure to function in chromatin remodeling." Trends Cell Biol **24**(11): 619-631.

Gibeault, R. L., K. L. Conn, M. D. Bildersheim and L. M. Schang (2016). "An Essential Viral Transcription Activator Modulates Chromatin Dynamics." PLoS Pathog **12**(8): e1005842.

Gibson, W. and B. Roizman (1971). "Compartmentalization of spermine and spermidine in the herpes simplex virion." Proc Natl Acad Sci U S A **68**(11): 2818-2821.

Gilbert, N., S. Boyle, H. Fiegler, K. Woodfine, N. P. Carter and W. A. Bickmore (2004). "Chromatin architecture of the

human genome: gene-rich domains are enriched in open chromatin fibers." Cell **118**(5): 555-566.
Giordani, N. V., D. M. Neumann, D. L. Kwiatkowski, P. S. Bhattacharjee, P. K. McAnany, J. M. Hill and D. C. Bloom (2008). "During herpes simplex virus type 1 infection of rabbits, the ability to express the latency-associated transcript increases latent-phase transcription of lytic genes." J Virol **82**(12): 6056-6060.
Goldman, J. A., J. D. Garlick and R. E. Kingston (2010). "Chromatin remodeling by imitation switch (ISWI) class ATP-dependent remodelers is stimulated by histone variant H2A.Z." J Biol Chem **285**(7): 4645-4651.
Grigoryev, S. A., G. Arya, S. Correll, C. L. Woodcock and T. Schlick (2009). "Evidence for heteromorphic chromatin fibers from analysis of nucleosome interactions." Proc Natl Acad Sci U S A **106**(32): 13317-13322.
Gu, B. and N. DeLuca (1994). "Requirements for activation of the herpes simplex virus glycoprotein C promoter in vitro by the viral regulatory protein ICP4." J Virol **68**(12): 7953-7965.
Gunther, T. and A. Grundhoff (2010). "The epigenetic landscape of latent Kaposi sarcoma-associated herpesvirus genomes." PLoS Pathog **6**(6): e1000935.
Gyory, I., S. Boller, R. Nechanitzky, E. Mandel, S. Pott, E. Liu and R. Grosschedl (2012). "Transcription factor Ebf1 regulates differentiation stage-specific signaling, proliferation, and survival of B cells." Genes Dev **26**(7): 668-682.
Hagmann, M., O. Georgiev, W. Schaffner and P. Douville (1995). "Transcription factors interacting with herpes simplex virus alpha gene promoters in sensory neurons." Nucleic Acids Res **23**(24): 4978-4985.
Hammerschmidt, W. (2015). "The Epigenetic Life Cycle of Epstein-Barr Virus." Curr Top Microbiol Immunol **390**(Pt 1): 103-117.
Han, M. and M. Grunstein (1988). "Nucleosome loss activates yeast downstream promoters in vivo." Cell **55**(6): 1137-1145.
Hanssen, L. L. P., M. T. Kassouf, A. M. Oudelaar, D. Biggs, C. Preece, D. J. Downes, M. Gosden, J. A. Sharpe, J. A. Sloane-Stanley, J. R. Hughes, B. Davies and D. R. Higgs (2017). "Tissue-specific CTCF-cohesin-mediated chromatin architecture delimits enhancer interactions and function in vivo." Nat Cell Biol **19**(8): 952-961.
Hara, R. and A. Sancar (2002). "The SWI/SNF chromatin-remodeling factor stimulates repair by human excision nuclease in the mononucleosome core particle." Mol Cell Biol **22**(19): 6779-6787.
Harancher, M. R., J. E. Packard, S. P. Cowan, N. A. DeLuca and J. A. Dembowski (2020). "Antiviral Properties of the LSD1 Inhibitor SP-2509." J Virol.
Harkness, J. M., M. Kader and N. A. DeLuca (2014). "Transcription of the herpes simplex virus 1 genome during productive and quiescent infection of neuronal and nonneuronal cells." J Virol **88**(12): 6847-6861.
Harris, R. A., R. D. Everett, X. X. Zhu, S. Silverstein and C. M. Preston (1989). "Herpes simplex virus type 1 immediate-early protein Vmw110 reactivates latent herpes simplex virus type 2 in an in vitro latency system." J Virol **63**(8): 3513-3515.
Hartlepp, K. F., C. Fernandez-Tornero, A. Eberharter, T. Grune, C. W. Muller and P. B. Becker (2005). "The histone fold subunits of Drosophila CHRAC facilitate nucleosome sliding through dynamic DNA interactions." Mol Cell Biol **25**(22): 9886-9896.
Hasan, N. and N. Ahuja (2019). "The Emerging Roles of ATP-Dependent Chromatin Remodeling Complexes in Pancreatic Cancer." Cancers (Basel) **11**(12).
Hashimoto, H., D. Wang, J. R. Horton, X. Zhang, V. G. Corces and X. Cheng (2017). "Structural Basis for the Versatile and Methylation-Dependent Binding of CTCF to DNA." Mol Cell **66**(5): 711-720 e713.
Hebbes, T. R., A. L. Clayton, A. W. Thorne and C. Crane-Robinson (1994). "Core histone hyperacetylation co-maps with generalized DNase I sensitivity in the chicken beta-globin chromosomal domain." EMBO J **13**(8): 1823-1830.

Heine, J. W., R. W. Honess, E. Cassai and B. Roizman (1974). "Proteins specified by herpes simplex virus. XII. The virion polypeptides of type 1 strains." J Virol **14**(3): 640-651.
Heinz, S., C. Benner, N. Spann, E. Bertolino, Y. C. Lin, P. Laslo, J. X. Cheng, C. Murre, H. Singh and C. K. Glass (2010). "Simple combinations of lineage-determining transcription factors prime cis-regulatory elements required for macrophage and B cell identities." Mol Cell **38**(4): 576-589.
Heming, J. D., J. F. Conway and F. L. Homa (2017). "Herpesvirus Capsid Assembly and DNA Packaging." Adv Anat Embryol Cell Biol **223**: 119-142.
Henikoff, S. (2009). "Labile H3.3+H2A.Z nucleosomes mark 'nucleosome-free regions'." Nat Genet **41**(8): 865-866.
Herrera, F. J. and S. J. Triezenberg (2004). "VP16-dependent association of chromatin-modifying coactivators and underrepresentation of histones at immediate-early gene promoters during herpes simplex virus infection." J Virol **78**(18): 9689-9696.
Hill, J. M., D. C. Quenelle, R. D. Cardin, J. L. Vogel, C. Clement, F. J. Bravo, T. P. Foster, M. Bosch-Marce, P. Raja, J. S. Lee, D. I. Bernstein, P. R. Krause, D. M. Knipe and T. M. Kristie (2014). "Inhibition of LSD1 reduces herpesvirus infection, shedding, and recurrence by promoting epigenetic suppression of viral genomes." Sci Transl Med **6**(265): 265ra169.
Hobbs, W. E., D. E. Brough, I. Kovesdi and N. A. DeLuca (2001). "Efficient activation of viral genomes by levels of herpes simplex virus ICP0 insufficient to affect cellular gene expression or cell survival." J Virol **75**(7): 3391-3403.
Hogan, C. J., S. Aligianni, M. Durand-Dubief, J. Persson, W. R. Will, J. Webster, L. Wheeler, C. K. Mathews, S. Elderkin, D. Oxley, K. Ekwall and P. D. Varga-Weisz (2010). "Fission yeast Iec1-ino80-mediated nucleosome eviction regulates nucleotide and phosphate metabolism." Mol Cell Biol **30**(3): 657-674.
Holstege, F. C., D. Tantin, M. Carey, P. C. van der Vliet and H. T. Timmers (1995). "The requirement for the basal transcription factor IIE is determined by the helical stability of promoter DNA." EMBO J **14**(4): 810-819.
Hon, G., W. Wang and B. Ren (2009). "Discovery and annotation of functional chromatin signatures in the human genome." PLoS Comput Biol **5**(11): e1000566.
Hon, G. C., R. D. Hawkins and B. Ren (2009). "Predictive chromatin signatures in the mammalian genome." Hum Mol Genet **18**(R2): R195-201.
Honess, R. W. (1984). "Herpes simplex and 'the herpes complex': diverse observations and a unifying hypothesis. The eighth Fleming lecture." J Gen Virol **65 (Pt 12)**: 2077-2107.
Horowitz-Scherer, R. A. and C. L. Woodcock (2006). "Organization of interphase chromatin." Chromosoma **115**(1): 1-14.
Hu, M., D. P. Depledge, E. Flores Cortes, J. Breuer and L. M. Schang (2019). "Chromatin dynamics and the transcriptional competence of HSV-1 genomes during lytic infections." PLoS Pathog **15**(11): e1008076.
Huang, H. and H. He (2011). "Super-resolution method for face recognition using nonlinear mappings on coherent features." IEEE Trans Neural Netw **22**(1): 121-130.
Huang, J., J. R. Kent, B. Placek, K. A. Whelan, C. M. Hollow, P. Y. Zeng, N. W. Fraser and S. L. Berger (2006). "Trimethylation of histone H3 lysine 4 by Set1 in the lytic infection of human herpes simplex virus 1." J Virol **80**(12): 5740-5746.
Imbalzano, A. N., D. M. Coen and N. A. DeLuca (1991). "Herpes simplex virus transactivator ICP4 operationally substitutes for the cellular transcription factor Sp1 for efficient expression of the viral thymidine kinase gene." J Virol **65**(2): 565-574.
Imbalzano, A. N., H. Kwon, M. R. Green and R. E. Kingston (1994). "Facilitated binding of TATA-binding protein to

nucleosomal DNA." Nature **370**(6489): 481-485.
Ishibashi, T., A. Li, J. M. Eirin-Lopez, M. Zhao, K. Missiaen, D. W. Abbott, M. Meistrich, M. J. Hendzel and J. Ausio (2010). "H2A.Bbd: an X-chromosome-encoded histone involved in mammalian spermiogenesis." Nucleic Acids Res **38**(6): 1780-1789.
Ishihara, M. and H. Sakagami (2005). "Re-evaluation of cytotoxicity and iron chelation activity of three beta-diketones by semiempirical molecular orbital method." In Vivo **19**(1): 119-123.
Ito, T., J. K. Tyler and J. T. Kadonaga (1997). "Chromatin assembly factors: a dual function in nucleosome formation and mobilization?" Genes Cells **2**(10): 593-600.
Jackson, V., A. Shires, N. Tanphaichitr and R. Chalkley (1976). "Modifications to histones immediately after synthesis." J Mol Biol **104**(2): 471-483.
Jacob, R. J. and B. Roizman (1977). "Anatomy of herpes simplex virus DNA VIII. Properties of the replicating DNA." J Virol **23**(2): 394-411.
Jakobovits, E. B., S. Bratosin and Y. Aloni (1980). "A nucleosome-free region in SV40 minichromosomes." Nature **285**(5762): 263-265.
Jasencakova, Z., A. N. Scharf, K. Ask, A. Corpet, A. Imhof, G. Almouzni and A. Groth (2010). "Replication stress interferes with histone recycling and predeposition marking of new histones." Mol Cell **37**(5): 736-743.
Jensen, K., C. Shiels and P. S. Freemont (2001). "PML protein isoforms and the RBCC/TRIM motif." Oncogene **20**(49): 7223-7233.
Jiao, R., C. Z. Bachrati, G. Pedrazzi, P. Kuster, M. Petkovic, J. L. Li, D. Egli, I. D. Hickson and I. Stagljar (2004). "Physical and functional interaction between the Bloom's syndrome gene product and the largest subunit of chromatin assembly factor 1." Mol Cell Biol **24**(11): 4710-4719.
Jin, T., A. Perry, J. Jiang, P. Smith, J. A. Curry, L. Unterholzner, Z. Jiang, G. Horvath, V. A. Rathinam, R. W. Johnstone, V. Hornung, E. Latz, A. G. Bowie, K. A. Fitzgerald and T. S. Xiao (2012). "Structures of the HIN domain:DNA complexes reveal ligand binding and activation mechanisms of the AIM2 inflammasome and IFI16 receptor." Immunity **36**(4): 561-571.
Johnson, K. E., V. Bottero, S. Flaherty, S. Dutta, V. V. Singh and B. Chandran (2014). "IFI16 restricts HSV-1 replication by accumulating on the hsv-1 genome, repressing HSV-1 gene expression, and directly or indirectly modulating histone modifications." PLoS Pathog **10**(11): e1004503.
Jones, D. O., I. G. Cowell and P. B. Singh (2000). "Mammalian chromodomain proteins: their role in genome organisation and expression." Bioessays **22**(2): 124-137.
Juillard, F., M. Tan, S. Li and K. M. Kaye (2016). "Kaposi's Sarcoma Herpesvirus Genome Persistence." Front Microbiol **7**: 1149.
Kahle, T., B. Volkmann, K. Eissmann, A. Herrmann, S. Schmitt, S. Wittmann, L. Merkel, N. Reuter, T. Stamminger and T. Gramberg (2015). "TRIM19/PML Restricts HIV Infection in a Cell Type-Dependent Manner." Viruses **8**(1).
Kalamvoki, M. and B. Roizman (2010). "Circadian CLOCK histone acetyl transferase localizes at ND10 nuclear bodies and enables herpes simplex virus gene expression." Proc Natl Acad Sci U S A **107**(41): 17721-17726.
Karpov, V. L., O. V. Preobrazhenskaya and A. D. Mirzabekov (1984). "Chromatin structure of hsp 70 genes, activated by heat shock: selective removal of histones from the coding region and their absence from the 5' region." Cell **36**(2): 423-431.
Kato, A., Y. Hirohata, J. Arii and Y. Kawaguchi (2014). "Phosphorylation of herpes simplex virus 1 dUTPase upregulated viral dUTPase activity to compensate for low cellular dUTPase activity for efficient viral replication." J

Virol **88**(14): 7776-7785.
Kawashima, S. and K. Imahori (1982). "Studies on histone oligomers. III. Effects of salt concentration and pH on the stability of histone octamer in chicken erythrocyte chromatin." J Biochem **91**(3): 959-966.
Kellum, R. and P. Schedl (1991). "A position-effect assay for boundaries of higher order chromosomal domains." Cell **64**(5): 941-950.
Kent, J. R., P. Y. Zeng, D. Atanasiu, J. Gardner, N. W. Fraser and S. L. Berger (2004). "During lytic infection herpes simplex virus type 1 is associated with histones bearing modifications that correlate with active transcription." J Virol **78**(18): 10178-10186.
Kieff, E. D., S. L. Bachenheimer and B. Roizman (1971). "Size, composition, and structure of the deoxyribonucleic acid of herpes simplex virus subtypes 1 and 2." J Virol **8**(2): 125-132.
Kim, J. L., D. B. Nikolov and S. K. Burley (1993). "Co-crystal structure of TBP recognizing the minor groove of a TATA element." Nature **365**(6446): 520-527.
Kimura, H. and P. R. Cook (2001). "Kinetics of core histones in living human cells: little exchange of H3 and H4 and some rapid exchange of H2B." J Cell Biol **153**(7): 1341-1353.
Kingston, R. E. and G. J. Narlikar (1999). "ATP-dependent remodeling and acetylation as regulators of chromatin fluidity." Genes Dev **13**(18): 2339-2352.
Kireeva, N., M. Lakonishok, I. Kireev, T. Hirano and A. S. Belmont (2004). "Visualization of early chromosome condensation: a hierarchical folding, axial glue model of chromosome structure." J Cell Biol **166**(6): 775-785.
Kleff, S., E. D. Andrulis, C. W. Anderson and R. Sternglanz (1995). "Identification of a gene encoding a yeast histone H4 acetyltransferase." J Biol Chem **270**(42): 24674-24677.
Klose, R. J., E. M. Kallin and Y. Zhang (2006). "JmjC-domain-containing proteins and histone demethylation." Nat Rev Genet **7**(9): 715-727.
Knezetic, J. A. and D. S. Luse (1986). "The presence of nucleosomes on a DNA template prevents initiation by RNA polymerase II in vitro." Cell **45**(1): 95-104.
Kobiler, O., P. Brodersen, M. P. Taylor, E. B. Ludmir and L. W. Enquist (2011). "Herpesvirus replication compartments originate with single incoming viral genomes." MBio **2**(6).
Kobiler, O., Y. Lipman, K. Therkelsen, I. Daubechies and L. W. Enquist (2010). "Herpesviruses carrying a Brainbow cassette reveal replication and expression of limited numbers of incoming genomes." Nat Commun **1**: 146.
Koche, R. P., Z. D. Smith, M. Adli, H. Gu, M. Ku, A. Gnirke, B. E. Bernstein and A. Meissner (2011). "Reprogramming factor expression initiates widespread targeted chromatin remodeling." Cell Stem Cell **8**(1): 96-105.
Kolb, G. and T. M. Kristie (2008). "Association of the cellular coactivator HCF-1 with the Golgi apparatus in sensory neurons." J Virol **82**(19): 9555-9563.
Konev, A. Y., M. Tribus, S. Y. Park, V. Podhraski, C. Y. Lim, A. V. Emelyanov, E. Vershilova, V. Pirrotta, J. T. Kadonaga, A. Lusser and D. V. Fyodorov (2007). "CHD1 motor protein is required for deposition of histone variant H3.3 into chromatin in vivo." Science **317**(5841): 1087-1090.
Kornberg, R. D. (1974). "Chromatin structure: a repeating unit of histones and DNA." Science **184**(4139): 868-871.
Kothandapani, A., K. Gopalakrishnan, B. Kahali, D. Reisman and S. M. Patrick (2012). "Downregulation of SWI/SNF chromatin remodeling factor subunits modulates cisplatin cytotoxicity." Exp Cell Res **318**(16): 1973-1986.
Krietenstein, N., M. Wal, S. Watanabe, B. Park, C. L. Peterson, B. F. Pugh and P. Korber (2016). "Genomic Nucleosome Organization Reconstituted with Pure Proteins." Cell **167**(3): 709-721 e712.
Kristie, T. M. and B. Roizman (1986). "DNA-binding site of major regulatory protein alpha 4 specifically associated

with promoter-regulatory domains of alpha genes of herpes simplex virus type 1." Proc Natl Acad Sci U S A **83**(13): 4700-4704.

Krogan, N. J., J. Dover, A. Wood, J. Schneider, J. Heidt, M. A. Boateng, K. Dean, O. W. Ryan, A. Golshani, M. Johnston, J. F. Greenblatt and A. Shilatifard (2003). "The Paf1 complex is required for histone H3 methylation by COMPASS and Dot1p: linking transcriptional elongation to histone methylation." Mol Cell **11**(3): 721-729.

Kruger, W., C. L. Peterson, A. Sil, C. Coburn, G. Arents, E. N. Moudrianakis and I. Herskowitz (1995). "Amino acid substitutions in the structured domains of histones H3 and H4 partially relieve the requirement of the yeast SWI/SNF complex for transcription." Genes Dev **9**(22): 2770-2779.

Kubat, N. J., A. L. Amelio, N. V. Giordani and D. C. Bloom (2004). "The herpes simplex virus type 1 latency-associated transcript (LAT) enhancer/rcr is hyperacetylated during latency independently of LAT transcription." J Virol **78**(22): 12508-12518.

Kubat, N. J., R. K. Tran, P. McAnany and D. C. Bloom (2004). "Specific histone tail modification and not DNA methylation is a determinant of herpes simplex virus type 1 latent gene expression." J Virol **78**(3): 1139-1149.

Kubicek, S., G. Schotta, M. Lachner, R. Sengupta, A. Kohlmaier, L. Perez-Burgos, Y. Linderson, J. H. Martens, R. J. O'Sullivan, B. D. Fodor, M. Yonezawa, A. H. Peters and T. Jenuwein (2006). "The role of histone modifications in epigenetic transitions during normal and perturbed development." Ernst Schering Res Found Workshop(57): 1-27.

Kuddus, R., B. Gu and N. A. DeLuca (1995). "Relationship between TATA-binding protein and herpes simplex virus type 1 ICP4 DNA-binding sites in complex formation and repression of transcription." J Virol **69**(9): 5568-5575.

Kurdistani, S. K. and M. Grunstein (2003). "In vivo protein-protein and protein-DNA crosslinking for genomewide binding microarray." Methods **31**(1): 90-95.

Kutluay, S. B., S. L. DeVos, J. E. Klomp and S. J. Triezenberg (2009). "Transcriptional coactivators are not required for herpes simplex virus type 1 immediate-early gene expression in vitro." J Virol **83**(8): 3436-3449.

Kutluay, S. B., J. Doroghazi, M. E. Roemer and S. J. Triezenberg (2008). "Curcumin inhibits herpes simplex virus immediate-early gene expression by a mechanism independent of p300/CBP histone acetyltransferase activity." Virology **373**(2): 239-247.

Kwon, H., A. N. Imbalzano, P. A. Khavari, R. E. Kingston and M. R. Green (1994). "Nucleosome disruption and enhancement of activator binding by a human SW1/SNF complex." Nature **370**(6489): 477-481.

Kyrchanova, O., S. Toshchakov, Y. Podstreshnaya, A. Parshikov and P. Georgiev (2008). "Functional interaction between the Fab-7 and Fab-8 boundaries and the upstream promoter region in the Drosophila Abd-B gene." Mol Cell Biol **28**(12): 4188-4195.

Lacasse, J. J. and L. M. Schang (2012). "Herpes simplex virus 1 DNA is in unstable nucleosomes throughout the lytic infection cycle, and the instability of the nucleosomes is independent of DNA replication." J Virol **86**(20): 11287-11300.

Lang, F., X. Li, O. Vladimirova, B. Hu, G. Chen, Y. Xiao, V. Singh, D. Lu, L. Li, H. Han, J. M. Wickramasinghe, S. T. Smith, C. Zheng, Q. Li, P. M. Lieberman, N. W. Fraser and J. Zhou (2017). "CTCF interacts with the lytic HSV-1 genome to promote viral transcription." Sci Rep **7**: 39861.

Langst, G., E. J. Bonte, D. F. Corona and P. B. Becker (1999). "Nucleosome movement by CHRAC and ISWI without disruption or trans-displacement of the histone octamer." Cell **97**(7): 843-852.

Lans, H., J. A. Marteijn, B. Schumacher, J. H. Hoeijmakers, G. Jansen and W. Vermeulen (2010). "Involvement of global genome repair, transcription coupled repair, and chromatin remodeling in UV DNA damage response changes during development." PLoS Genet **6**(5): e1000941.

Lazear, E., A. Carfi, J. C. Whitbeck, T. M. Cairns, C. Krummenacher, G. H. Cohen and R. J. Eisenberg (2008). "Engineered disulfide bonds in herpes simplex virus type 1 gD separate receptor binding from fusion initiation and viral entry." J Virol **82**(2): 700-709.

Lee, H. S., J. H. Park, S. J. Kim, S. J. Kwon and J. Kwon (2010). "A cooperative activation loop among SWI/SNF, gamma-H2AX and H3 acetylation for DNA double-strand break repair." EMBO J **29**(8): 1434-1445.

Lee, J. S., P. Raja and D. M. Knipe (2016). "Herpesviral ICP0 Protein Promotes Two Waves of Heterochromatin Removal on an Early Viral Promoter during Lytic Infection." mBio **7**(1): e02007-02015.

Lee, J. S., P. Raja, D. Pan, J. M. Pesola, D. M. Coen and D. M. Knipe (2018). "CCCTC-Binding Factor Acts as a Heterochromatin Barrier on Herpes Simplex Viral Latent Chromatin and Contributes to Poised Latent Infection." mBio **9**(1).

Leinbach, S. S. and W. C. Summers (1980). "The structure of herpes simplex virus type 1 DNA as probed by micrococcal nuclease digestion." J Gen Virol **51**(Pt 1): 45-59.

Lentine, A. F. and S. L. Bachenheimer (1990). "Intracellular organization of herpes simplex virus type 1 DNA assayed by staphylococcal nuclease sensitivity." Virus Res **16**(3): 275-292.

Li, B., M. Carey and J. L. Workman (2007). "The role of chromatin during transcription." Cell **128**(4): 707-719.

Li, H., S. Liu, J. Hu, X. Luo, N. Li, M. B. A and Y. Cao (2016). "Epstein-Barr virus lytic reactivation regulation and its pathogenic role in carcinogenesis." Int J Biol Sci **12**(11): 1309-1318.

Li, M., X. Xia, Y. Tian, Q. Jia, X. Liu, Y. Lu, M. Li, X. Li and Z. Chen (2019). "Mechanism of DNA translocation underlying chromatin remodelling by Snf2." Nature **567**(7748): 409-413.

Liang, Y., D. Quenelle, J. L. Vogel, C. Mascaro, A. Ortega and T. M. Kristie (2013). "A novel selective LSD1/KDM1A inhibitor epigenetically blocks herpes simplex virus lytic replication and reactivation from latency." MBio **4**(1): e00558-00512.

Liang, Y., J. L. Vogel, J. H. Arbuckle, G. Rai, A. Jadhav, A. Simeonov, D. J. Maloney and T. M. Kristie (2013). "Targeting the JMJD2 histone demethylases to epigenetically control herpesvirus infection and reactivation from latency." Sci Transl Med **5**(167): 167ra165.

Liang, Y., J. L. Vogel, A. Narayanan, H. Peng and T. M. Kristie (2009). "Inhibition of the histone demethylase LSD1 blocks alpha-herpesvirus lytic replication and reactivation from latency." Nat Med **15**(11): 1312-1317.

Liashkovich, I., W. Hafezi, J. M. Kuhn, H. Oberleithner and V. Shahin (2011). "Nuclear delivery mechanism of herpes simplex virus type 1 genome." J Mol Recognit **24**(3): 414-421.

Lieberman, P. M. (2015). "Chromatin Structure of Epstein-Barr Virus Latent Episomes." Curr Top Microbiol Immunol **390**(Pt 1): 71-102.

Lieu, P. T. and E. K. Wagner (2000). "Two leaky-late HSV-1 promoters differ significantly in structural architecture." Virology **272**(1): 191-203.

Linger, J. G. and J. K. Tyler (2007). "Chromatin disassembly and reassembly during DNA repair." Mutat Res **618**(1-2): 52-64.

Litt, M. D., M. Simpson, F. Recillas-Targa, M. N. Prioleau and G. Felsenfeld (2001). "Transitions in histone acetylation reveal boundaries of three separately regulated neighboring loci." EMBO J **20**(9): 2224-2235.

Liu, C. L., T. Kaplan, M. Kim, S. Buratowski, S. L. Schreiber, N. Friedman and O. J. Rando (2005). "Single-nucleosome mapping of histone modifications in S. cerevisiae." PLoS Biol **3**(10): e328.

Lorch, Y., J. W. LaPointe and R. D. Kornberg (1987). "Nucleosomes inhibit the initiation of transcription but allow chain elongation with the displacement of histones." Cell **49**(2): 203-210.

Luger, K., A. W. Mader, R. K. Richmond, D. F. Sargent and T. J. Richmond (1997). "Crystal structure of the nucleosome core particle at 2.8 A resolution." Nature **389**(6648): 251-260.

Luk, E., A. Ranjan, P. C. Fitzgerald, G. Mizuguchi, Y. Huang, D. Wei and C. Wu (2010). "Stepwise histone replacement by SWR1 requires dual activation with histone H2A.Z and canonical nucleosome." Cell **143**(5): 725-736.

Luk, E., N. D. Vu, K. Patteson, G. Mizuguchi, W. H. Wu, A. Ranjan, J. Backus, S. Sen, M. Lewis, Y. Bai and C. Wu (2007). "Chz1, a nuclear chaperone for histone H2AZ." Mol Cell **25**(3): 357-368.

Macao, B., M. Olsson and P. Elias (2004). "Functional properties of the herpes simplex virus type I origin-binding protein are controlled by precise interactions with the activated form of the origin of DNA replication." J Biol Chem **279**(28): 29211-29217.

Makhov, A. M., P. E. Boehmer, I. R. Lehman and J. D. Griffith (1996). "The herpes simplex virus type 1 origin-binding protein carries out origin specific DNA unwinding and forms stem-loop structures." EMBO J **15**(7): 1742-1750.

Maltby, V. E., B. J. Martin, J. M. Schulze, I. Johnson, T. Hentrich, A. Sharma, M. S. Kobor and L. Howe (2012). "Histone H3 lysine 36 methylation targets the Isw1b remodeling complex to chromatin." Mol Cell Biol **32**(17): 3479-3485.

Mapelli, M., S. Panjikar and P. A. Tucker (2005). "The crystal structure of the herpes simplex virus 1 ssDNA-binding protein suggests the structural basis for flexible, cooperative single-stranded DNA binding." J Biol Chem **280**(4): 2990-2997.

Marhold, J., K. Kramer, E. Kremmer and F. Lyko (2004). "The Drosophila MBD2/3 protein mediates interactions between the MI-2 chromatin complex and CpT/A-methylated DNA." Development **131**(24): 6033-6039.

Martinez, R., R. T. Sarisky, P. C. Weber and S. K. Weller (1996). "Herpes simplex virus type 1 alkaline nuclease is required for efficient processing of viral DNA replication intermediates." J Virol **70**(4): 2075-2085.

Mavrich, T. N., I. P. Ioshikhes, B. J. Venters, C. Jiang, L. P. Tomsho, J. Qi, S. C. Schuster, I. Albert and B. F. Pugh (2008). "A barrier nucleosome model for statistical positioning of nucleosomes throughout the yeast genome." Genome Res **18**(7): 1073-1083.

Mayran, A. and J. Drouin (2018). "Pioneer transcription factors shape the epigenetic landscape." J Biol Chem **293**(36): 13795-13804.

McGhee, J. D., W. I. Wood, M. Dolan, J. D. Engel and G. Felsenfeld (1981). "A 200 base pair region at the 5' end of the chicken adult beta-globin gene is accessible to nuclease digestion." Cell **27**(1 Pt 2): 45-55.

McKnight, J. N., K. R. Jenkins, I. M. Nodelman, T. Escobar and G. D. Bowman (2011). "Extranucleosomal DNA binding directs nucleosome sliding by Chd1." Mol Cell Biol **31**(23): 4746-4759.

Mellerick, D. M. and N. W. Fraser (1987). "Physical state of the latent herpes simplex virus genome in a mouse model system: evidence suggesting an episomal state." Virology **158**(2): 265-275.

Menon, T., J. A. Yates and D. A. Bochar (2010). "Regulation of androgen-responsive transcription by the chromatin remodeling factor CHD8." Mol Endocrinol **24**(6): 1165-1174.

Merkl, P. E. and D. M. Knipe (2019). "Role for a Filamentous Nuclear Assembly of IFI16, DNA, and Host Factors in Restriction of Herpesviral Infection." mBio **10**(1).

Messer, H. G., D. Jacobs, A. Dhummakupt and D. C. Bloom (2015). "Inhibition of H3K27me3-specific histone demethylases JMJD3 and UTX blocks reactivation of herpes simplex virus 1 in trigeminal ganglion neurons." J Virol **89**(6): 3417-3420.

Mizuguchi, G., X. Shen, J. Landry, W. H. Wu, S. Sen and C. Wu (2004). "ATP-driven exchange of histone H2AZ variant catalyzed by SWR1 chromatin remodeling complex." Science **303**(5656): 343-348.

Mocarski, E. S. and B. Roizman (1982). "Structure and role of the herpes simplex virus DNA termini in inversion, circularization and generation of virion DNA." Cell **31**(1): 89-97.
Monier, K., J. C. Armas, S. Etteldorf, P. Ghazal and K. F. Sullivan (2000). "Annexation of the interchromosomal space during viral infection." Nat Cell Biol **2**(9): 661-665.
Morettini, S., M. Tribus, A. Zeilner, J. Sebald, B. Campo-Fernandez, G. Scheran, H. Worle, V. Podhraski, D. V. Fyodorov and A. Lusser (2011). "The chromodomains of CHD1 are critical for enzymatic activity but less important for chromatin localization." Nucleic Acids Res **39**(8): 3103-3115.
Morillon, A., N. Karabetsou, J. O'Sullivan, N. Kent, N. Proudfoot and J. Mellor (2003). "Isw1 chromatin remodeling ATPase coordinates transcription elongation and termination by RNA polymerase II." Cell **115**(4): 425-435.
Morrison, A. J. and X. Shen (2009). "Chromatin remodelling beyond transcription: the INO80 and SWR1 complexes." Nat Rev Mol Cell Biol **10**(6): 373-384.
Murata, T. and T. Tsurumi (2013). "Epigenetic modification of the Epstein-Barr virus BZLF1 promoter regulates viral reactivation from latency." Front Genet **4**: 53.
Muravyova, E., A. Golovnin, E. Gracheva, A. Parshikov, T. Belenkaya, V. Pirrotta and P. Georgiev (2001). "Loss of insulator activity by paired Su(Hw) chromatin insulators." Science **291**(5503): 495-498.
Murawska, M. and A. Brehm (2011). "CHD chromatin remodelers and the transcription cycle." Transcription **2**(6): 244-253.
Muylaert, I. and P. Elias (2007). "Knockdown of DNA ligase IV/XRCC4 by RNA interference inhibits herpes simplex virus type I DNA replication." J Biol Chem **282**(15): 10865-10872.
Muylaert, I., K. W. Tang and P. Elias (2011). "Replication and recombination of herpes simplex virus DNA." J Biol Chem **286**(18): 15619-15624.
Nabatiyan, A., D. Szuts and T. Krude (2006). "Induction of CAF-1 expression in response to DNA strand breaks in quiescent human cells." Mol Cell Biol **26**(5): 1839-1849.
Narayanan, A., W. T. Ruyechan and T. M. Kristie (2007). "The coactivator host cell factor-1 mediates Set1 and MLL1 H3K4 trimethylation at herpesvirus immediate early promoters for initiation of infection." Proc Natl Acad Sci U S A **104**(26): 10835-10840.
Neigeborn, L. and M. Carlson (1984). "Genes affecting the regulation of SUC2 gene expression by glucose repression in Saccharomyces cerevisiae." Genetics **108**(4): 845-858.
Nekrasov, M., J. Amrichova, B. J. Parker, T. A. Soboleva, C. Jack, R. Williams, G. A. Huttley and D. J. Tremethick (2012). "Histone H2A.Z inheritance during the cell cycle and its impact on promoter organization and dynamics." Nat Struct Mol Biol **19**(11): 1076-1083.
Neumann, D. M., P. S. Bhattacharjee, N. V. Giordani, D. C. Bloom and J. M. Hill (2007). "In vivo changes in the patterns of chromatin structure associated with the latent herpes simplex virus type 1 genome in mouse trigeminal ganglia can be detected at early times after butyrate treatment." J Virol **81**(23): 13248-13253.
Ng, H. H., F. Robert, R. A. Young and K. Struhl (2003). "Targeted recruitment of Set1 histone methylase by elongating Pol II provides a localized mark and memory of recent transcriptional activity." Mol Cell **11**(3): 709-719.
Ng, H. H., R. M. Xu, Y. Zhang and K. Struhl (2002). "Ubiquitination of histone H2B by Rad6 is required for efficient Dot1-mediated methylation of histone H3 lysine 79." J Biol Chem **277**(38): 34655-34657.
Nicoll, M. P., J. T. Proenca and S. Efstathiou (2012). "The molecular basis of herpes simplex virus latency." FEMS Microbiol Rev **36**(3): 684-705.
Niller, H. H., K. Szenthe and J. Minarovits (2014). "Epstein-Barr virus-host cell interactions: an epigenetic dialog?"

Front Genet **5**: 367.
Nimonkar, A. V. and P. E. Boehmer (2003). "The herpes simplex virus type-1 single-strand DNA-binding protein (ICP8) promotes strand invasion." J Biol Chem **278**(11): 9678-9682.
Nimonkar, A. V. and P. E. Boehmer (2003). "On the mechanism of strand assimilation by the herpes simplex virus type-1 single-strand DNA-binding protein (ICP8)." Nucleic Acids Res **31**(18): 5275-5281.
Ogiwara, H., A. Ui, A. Otsuka, H. Satoh, I. Yokomi, S. Nakajima, A. Yasui, J. Yokota and T. Kohno (2011). "Histone acetylation by CBP and p300 at double-strand break sites facilitates SWI/SNF chromatin remodeling and the recruitment of non-homologous end joining factors." Oncogene **30**(18): 2135-2146.
Oh, H. S., K. F. Bryant, T. J. Nieland, A. Mazumder, M. Bagul, M. Bathe, D. E. Root and D. M. Knipe (2014). "A targeted RNA interference screen reveals novel epigenetic factors that regulate herpesviral gene expression." MBio **5**(1): e01086-01013.
Oh, J. and N. W. Fraser (2008). "Temporal association of the herpes simplex virus genome with histone proteins during a lytic infection." J Virol **82**(7): 3530-3537.
Oh, J., N. Ruskoski and N. W. Fraser (2012). "Chromatin assembly on herpes simplex virus 1 DNA early during a lytic infection is Asf1a dependent." J Virol **86**(22): 12313-12321.
Oh, J., I. F. Sanders, E. Z. Chen, H. Li, J. W. Tobias, R. B. Isett, S. Penubarthi, H. Sun, D. A. Baldwin and N. W. Fraser (2015). "Genome wide nucleosome mapping for HSV-1 shows nucleosomes are deposited at preferred positions during lytic infection." PLoS One **10**(2): e0117471.
Ozdemir, I. and M. C. Gambetta (2019). "The Role of Insulation in Patterning Gene Expression." Genes (Basel) **10**(10).
Park, J. H., E. J. Park, H. S. Lee, S. J. Kim, S. K. Hur, A. N. Imbalzano and J. Kwon (2006). "Mammalian SWI/SNF complexes facilitate DNA double-strand break repair by promoting gamma-H2AX induction." EMBO J **25**(17): 3986-3997.
Pchelintsev, N. A., T. McBryan, T. S. Rai, J. van Tuyn, D. Ray-Gallet, G. Almouzni and P. D. Adams (2013). "Placing the HIRA histone chaperone complex in the chromatin landscape." Cell Rep **3**(4): 1012-1019.
Peng, H., M. L. Nogueira, J. L. Vogel and T. M. Kristie (2010). "Transcriptional coactivator HCF-1 couples the histone chaperone Asf1b to HSV-1 DNA replication components." Proc Natl Acad Sci U S A **107**(6): 2461-2466.
Perng, G. C., S. M. Slanina, A. Yukht, H. Ghiasi, A. B. Nesburn and S. L. Wechsler (2000). "The latency-associated transcript gene enhances establishment of herpes simplex virus type 1 latency in rabbits." J Virol **74**(4): 1885-1891.
Perpelescu, M., N. Nozaki, C. Obuse, H. Yang and K. Yoda (2009). "Active establishment of centromeric CENP-A chromatin by RSF complex." J Cell Biol **185**(3): 397-407.
Peters, A. H., S. Kubicek, K. Mechtler, R. J. O'Sullivan, A. A. Derijck, L. Perez-Burgos, A. Kohlmaier, S. Opravil, M. Tachibana, Y. Shinkai, J. H. Martens and T. Jenuwein (2003). "Partitioning and plasticity of repressive histone methylation states in mammalian chromatin." Mol Cell **12**(6): 1577-1589.
Peters, A. H., J. E. Mermoud, D. O'Carroll, M. Pagani, D. Schweizer, N. Brockdorff and T. Jenuwein (2002). "Histone H3 lysine 9 methylation is an epigenetic imprint of facultative heterochromatin." Nat Genet **30**(1): 77-80.
Phelan, M. L., S. Sif, G. J. Narlikar and R. E. Kingston (1999). "Reconstitution of a core chromatin remodeling complex from SWI/SNF subunits." Mol Cell **3**(2): 247-253.
Pignatti, P. F. and E. Cassai (1980). "Analysis of herpes simplex virus nucleoprotein complexes extracted from infected cells." J Virol **36**(3): 816-828.
Pinnoji, R. C., G. R. Bedadala, B. George, T. C. Holland, J. M. Hill and S. C. Hsia (2007). "Repressor element-1

silencing transcription factor/neuronal restrictive silencer factor (REST/NRSF) can regulate HSV-1 immediate-early transcription via histone modification." Virol J **4**: 56.

Placek, B. J., J. Huang, J. R. Kent, J. Dorsey, L. Rice, N. W. Fraser and S. L. Berger (2009). "The histone variant H3.3 regulates gene expression during lytic infection with herpes simplex virus type 1." J Virol **83**(3): 1416-1421.

Ponjavic, J., B. Lenhard, C. Kai, J. Kawai, P. Carninci, Y. Hayashizaki and A. Sandelin (2006). "Transcriptional and structural impact of TATA-initiation site spacing in mammalian core promoters." Genome Biol **7**(8): R78.

Poon, A. P., H. Gu and B. Roizman (2006). "ICP0 and the US3 protein kinase of herpes simplex virus 1 independently block histone deacetylation to enable gene expression." Proc Natl Acad Sci U S A **103**(26): 9993-9998.

Poon, A. P., Y. Liang and B. Roizman (2003). "Herpes simplex virus 1 gene expression is accelerated by inhibitors of histone deacetylases in rabbit skin cells infected with a mutant carrying a cDNA copy of the infected-cell protein no. 0." J Virol **77**(23): 12671-12678.

Poon, A. P., S. J. Silverstein and B. Roizman (2002). "An early regulatory function required in a cell type-dependent manner is expressed by the genomic but not the cDNA copy of the herpes simplex virus 1 gene encoding infected cell protein 0." J Virol **76**(19): 9744-9755.

Preston, C. M. (2007). "Reactivation of expression from quiescent herpes simplex virus type 1 genomes in the absence of immediate-early protein ICP0." J Virol **81**(21): 11781-11789.

Preston, C. M., A. Rinaldi and M. J. Nicholl (1998). "Herpes simplex virus type 1 immediate early gene expression is stimulated by inhibition of protein synthesis." J Gen Virol **79 (Pt 1)**: 117-124.

Raisner, R. M., P. D. Hartley, M. D. Meneghini, M. Z. Bao, C. L. Liu, S. L. Schreiber, O. J. Rando and H. D. Madhani (2005). "Histone variant H2A.Z marks the 5' ends of both active and inactive genes in euchromatin." Cell **123**(2): 233-248.

Ramasubramanyan, S., K. Osborn, K. Flower and A. J. Sinclair (2012). "Dynamic chromatin environment of key lytic cycle regulatory regions of the Epstein-Barr virus genome." J Virol **86**(3): 1809-1819.

Rao, S. S., M. H. Huntley, N. C. Durand, E. K. Stamenova, I. D. Bochkov, J. T. Robinson, A. L. Sanborn, I. Machol, A. D. Omer, E. S. Lander and E. L. Aiden (2014). "A 3D map of the human genome at kilobase resolution reveals principles of chromatin looping." Cell **159**(7): 1665-1680.

Razin, S. V. and A. A. Gavrilov (2014). "Chromatin without the 30-nm fiber: constrained disorder instead of hierarchical folding." Epigenetics **9**(5): 653-657.

Robert, F., D. K. Pokholok, N. M. Hannett, N. J. Rinaldi, M. Chandy, A. Rolfe, J. L. Workman, D. K. Gifford and R. A. Young (2004). "Global position and recruitment of HATs and HDACs in the yeast genome." Mol Cell **16**(2): 199-209.

Rochat, R. H., C. W. Hecksel and W. Chiu (2014). "Cryo-EM techniques to resolve the structure of HSV-1 capsid-associated components." Methods Mol Biol **1144**: 265-281.

Sainsbury, S., J. Niesser and P. Cramer (2013). "Structure and function of the initially transcribing RNA polymerase II-TFIIB complex." Nature **493**(7432): 437-440.

Sampath, P. and N. A. Deluca (2008). "Binding of ICP4, TATA-binding protein, and RNA polymerase II to herpes simplex virus type 1 immediate-early, early, and late promoters in virus-infected cells." J Virol **82**(5): 2339-2349.

Sanborn, A. L., S. S. Rao, S. C. Huang, N. C. Durand, M. H. Huntley, A. I. Jewett, I. D. Bochkov, D. Chinnappan, A. Cutkosky, J. Li, K. P. Geeting, A. Gnirke, A. Melnikov, D. McKenna, E. K. Stamenova, E. S. Lander and E. L. Aiden (2015). "Chromatin extrusion explains key features of loop and domain formation in wild-type and engineered genomes." Proc Natl Acad Sci U S A **112**(47): E6456-6465.

Sanders, I., M. Boyer and N. W. Fraser (2015). "Early nucleosome deposition on, and replication of, HSV DNA

requires cell factor PCNA." J Neurovirol **21**(4): 358-369.
Santos-Rosa, H., R. Schneider, B. E. Bernstein, N. Karabetsou, A. Morillon, C. Weise, S. L. Schreiber, J. Mellor and T. Kouzarides (2003). "Methylation of histone H3 K4 mediates association of the Isw1p ATPase with chromatin." Mol Cell **12**(5): 1325-1332.
Schalch, T., S. Duda, D. F. Sargent and T. J. Richmond (2005). "X-ray structure of a tetranucleosome and its implications for the chromatin fibre." Nature **436**(7047): 138-141.
Schang, L. M., E. Coccaro and J. J. Lacasse (2005). "Cdk inhibitory nucleoside analogs prevent transcription from viral genomes." Nucleosides Nucleotides Nucleic Acids **24**(5-7): 829-837.
Schang, L. M., M. Hu, E. F. Cortes and K. Sun (2021). "Chromatin-mediated epigenetic regulation of HSV-1 transcription as a potential target in antiviral therapy." Antiviral Res **192**: 105103.
Schilling, E. M., M. Scherer, N. Reuter, J. Schweininger, Y. A. Muller and T. Stamminger (2017). "The Human Cytomegalovirus IE1 Protein Antagonizes PML Nuclear Body-Mediated Intrinsic Immunity via the Inhibition of PML De Novo SUMOylation." J Virol **91**(4).
Schnetz, M. P., C. F. Bartels, K. Shastri, D. Balasubramanian, G. E. Zentner, R. Balaji, X. Zhang, L. Song, Z. Wang, T. Laframboise, G. E. Crawford and P. C. Scacheri (2009). "Genomic distribution of CHD7 on chromatin tracks H3K4 methylation patterns." Genome Res **19**(4): 590-601.
Schultz, D. C., J. R. Friedman and F. J. Rauscher, 3rd (2001). "Targeting histone deacetylase complexes via KRAB-zinc finger proteins: the PHD and bromodomains of KAP-1 form a cooperative unit that recruits a novel isoform of the Mi-2alpha subunit of NuRD." Genes Dev **15**(4): 428-443.
Sears, A. E., V. Hukkanen, M. A. Labow, A. J. Levine and B. Roizman (1991). "Expression of the herpes simplex virus 1 alpha transinducing factor (VP16) does not induce reactivation of latent virus or prevent the establishment of latency in mice." J Virol **65**(6): 2929-2935.
Sehrawat, A., L. Gao, Y. Wang, A. Bankhead, 3rd, S. K. McWeeney, C. J. King, J. Schwartzman, J. Urrutia, W. H. Bisson, D. J. Coleman, S. K. Joshi, D. H. Kim, D. A. Sampson, S. Weinmann, B. V. S. Kallakury, D. L. Berry, R. Haque, S. K. Van Den Eeden, S. Sharma, J. Bearss, T. M. Beer, G. V. Thomas, L. M. Heiser and J. J. Alumkal (2018). "LSD1 activates a lethal prostate cancer gene network independently of its demethylase function." Proc Natl Acad Sci U S A **115**(18): E4179-E4188.
Sekine, E., N. Schmidt, D. Gaboriau and P. O'Hare (2017). "Spatiotemporal dynamics of HSV genome nuclear entry and compaction state transitions using bioorthogonal chemistry and super-resolution microscopy." PLoS Pathog **13**(11): e1006721.
Shapira, L., M. Ralph, E. Tomer, S. Cohen and O. Kobiler (2016). "Histone Deacetylase Inhibitors Reduce the Number of Herpes Simplex Virus-1 Genomes Initiating Expression in Individual Cells." Front Microbiol **7**: 1970.
Sheldrick, P., M. Laithier, D. Lando and M. L. Ryhiner (1973). "Infectious DNA from herpes simplex virus: infectivity of double-stranded and single-stranded molecules." Proc Natl Acad Sci U S A **70**(12): 3621-3625.
Shi, Y., F. Lan, C. Matson, P. Mulligan, J. R. Whetstine, P. A. Cole, R. A. Casero and Y. Shi (2004). "Histone demethylation mediated by the nuclear amine oxidase homolog LSD1." Cell **119**(7): 941-953.
Shibahara, K. and B. Stillman (1999). "Replication-dependent marking of DNA by PCNA facilitates CAF-1-coupled inheritance of chromatin." Cell **96**(4): 575-585.
Shogren-Knaak, M., H. Ishii, J. M. Sun, M. J. Pazin, J. R. Davie and C. L. Peterson (2006). "Histone H4-K16 acetylation controls chromatin structure and protein interactions." Science **311**(5762): 844-847.
Sims, R. J., 3rd, C. F. Chen, H. Santos-Rosa, T. Kouzarides, S. S. Patel and D. Reinberg (2005). "Human but not yeast

CHD1 binds directly and selectively to histone H3 methylated at lysine 4 via its tandem chromodomains." J Biol Chem **280**(51): 41789-41792.

Smith, A. E., C. Chronis, M. Christodoulakis, S. J. Orr, N. C. Lea, N. A. Twine, A. Bhinge, G. J. Mufti and N. S. Thomas (2009). "Epigenetics of human T cells during the G0-->G1 transition." Genome Res **19**(8): 1325-1337.

Smith, B. C. and J. M. Denu (2009). "Chemical mechanisms of histone lysine and arginine modifications." Biochim Biophys Acta **1789**(1): 45-57.

Smith, S., N. Reuven, K. N. Mohni, A. J. Schumacher and S. K. Weller (2014). "Structure of the herpes simplex virus 1 genome: manipulation of nicks and gaps can abrogate infectivity and alter the cellular DNA damage response." J Virol **88**(17): 10146-10156.

Smolle, M., S. Venkatesh, M. M. Gogol, H. Li, Y. Zhang, L. Florens, M. P. Washburn and J. L. Workman (2012). "Chromatin remodelers Isw1 and Chd1 maintain chromatin structure during transcription by preventing histone exchange." Nat Struct Mol Biol **19**(9): 884-892.

Sonnemann, J., M. Zimmermann, C. Marx, F. Ebert, S. Becker, M. L. Lauterjung and J. F. Beck (2018). "LSD1 (KDM1A)-independent effects of the LSD1 inhibitor SP2509 in cancer cells." Br J Haematol **183**(3): 494-497.

Sopta, M., R. W. Carthew and J. Greenblatt (1985). "Isolation of three proteins that bind to mammalian RNA polymerase II." J Biol Chem **260**(18): 10353-10360.

Sorenson, C. M., P. A. Hart and J. Ross (1991). "Analysis of herpes simplex virus-induced mRNA destabilizing activity using an in vitro mRNA decay system." Nucleic Acids Res **19**(16): 4459-4465.

Soufi, A., G. Donahue and K. S. Zaret (2012). "Facilitators and impediments of the pluripotency reprogramming factors' initial engagement with the genome." Cell **151**(5): 994-1004.

Spear, P. G. and B. Roizman (1972). "Proteins specified by herpes simplex virus. V. Purification and structural proteins of the herpesvirion." J Virol **9**(1): 143-159.

Steger, D. J. and J. L. Workman (1997). "Stable co-occupancy of transcription factors and histones at the HIV-1 enhancer." EMBO J **16**(9): 2463-2472.

Stern, M., R. Jensen and I. Herskowitz (1984). "Five SWI genes are required for expression of the HO gene in yeast." J Mol Biol **178**(4): 853-868.

Stevens, J. G., E. K. Wagner, G. B. Devi-Rao, M. L. Cook and L. T. Feldman (1987). "RNA complementary to a herpesvirus alpha gene mRNA is prominent in latently infected neurons." Science **235**(4792): 1056-1059.

Stingley, S. W., J. J. Ramirez, S. A. Aguilar, K. Simmen, R. M. Sandri-Goldin, P. Ghazal and E. K. Wagner (2000). "Global analysis of herpes simplex virus type 1 transcription using an oligonucleotide-based DNA microarray." J Virol **74**(21): 9916-9927.

Stokes, D. G. and R. P. Perry (1995). "DNA-binding and chromatin localization properties of CHD1." Mol Cell Biol **15**(5): 2745-2753.

Strang, B. L. and N. D. Stow (2005). "Circularization of the herpes simplex virus type 1 genome upon lytic infection." J Virol **79**(19): 12487-12494.

Stratmann, S. A., S. R. Morrone, A. M. van Oijen and J. Sohn (2015). "The innate immune sensor IFI16 recognizes foreign DNA in the nucleus by scanning along the duplex." Elife **4**: e11721.

Sun, Z. W. and C. D. Allis (2002). "Ubiquitination of histone H2B regulates H3 methylation and gene silencing in yeast." Nature **418**(6893): 104-108.

Suto, R. K., M. J. Clarkson, D. J. Tremethick and K. Luger (2000). "Crystal structure of a nucleosome core particle containing the variant histone H2A.Z." Nat Struct Biol **7**(12): 1121-1124.

Tachibana, M., K. Sugimoto, M. Nozaki, J. Ueda, T. Ohta, M. Ohki, M. Fukuda, N. Takeda, H. Niida, H. Kato and Y. Shinkai (2002). "G9a histone methyltransferase plays a dominant role in euchromatic histone H3 lysine 9 methylation and is essential for early embryogenesis." Genes Dev **16**(14): 1779-1791.

Tachiwana, H., W. Kagawa, T. Shiga, A. Osakabe, Y. Miya, K. Saito, Y. Hayashi-Takanaka, T. Oda, M. Sato, S. Y. Park, H. Kimura and H. Kurumizaka (2011). "Crystal structure of the human centromeric nucleosome containing CENP-A." Nature **476**(7359): 232-235.

Tagami, H., D. Ray-Gallet, G. Almouzni and Y. Nakatani (2004). "Histone H3.1 and H3.3 complexes mediate nucleosome assembly pathways dependent or independent of DNA synthesis." Cell **116**(1): 51-61.

Taylor, I. C., J. L. Workman, T. J. Schuetz and R. E. Kingston (1991). "Facilitated binding of GAL4 and heat shock factor to nucleosomal templates: differential function of DNA-binding domains." Genes Dev **5**(7): 1285-1298.

Thompson, R. L. and N. M. Sawtell (1997). "The herpes simplex virus type 1 latency-associated transcript gene regulates the establishment of latency." J Virol **71**(7): 5432-5440.

Thompson, R. L. and N. M. Sawtell (2001). "Herpes simplex virus type 1 latency-associated transcript gene promotes neuronal survival." J Virol **75**(14): 6660-6675.

Timmers, H. T. (1994). "Transcription initiation by RNA polymerase II does not require hydrolysis of the beta-gamma phosphoanhydride bond of ATP." EMBO J **13**(2): 391-399.

Tirosh, I., N. Sigal and N. Barkai (2010). "Widespread remodeling of mid-coding sequence nucleosomes by Isw1." Genome Biol **11**(5): R49.

Tolstorukov, M. Y., J. A. Goldman, C. Gilbert, V. Ogryzko, R. E. Kingston and P. J. Park (2012). "Histone variant H2A.Bbd is associated with active transcription and mRNA processing in human cells." Mol Cell **47**(4): 596-607.

Tong, J. K., C. A. Hassig, G. R. Schnitzler, R. E. Kingston and S. L. Schreiber (1998). "Chromatin deacetylation by an ATP-dependent nucleosome remodelling complex." Nature **395**(6705): 917-921.

Topp, C. N., C. X. Zhong and R. K. Dawe (2004). "Centromere-encoded RNAs are integral components of the maize kinetochore." Proc Natl Acad Sci U S A **101**(45): 15986-15991.

Torigoe, S. E., D. L. Urwin, H. Ishii, D. E. Smith and J. T. Kadonaga (2011). "Identification of a rapidly formed nonnucleosomal histone-DNA intermediate that is converted into chromatin by ACF." Mol Cell **43**(4): 638-648.

Toth, Z., K. Brulois and J. U. Jung (2013). "The chromatin landscape of Kaposi's sarcoma-associated herpesvirus." Viruses **5**(5): 1346-1373.

Toth, Z., D. T. Maglinte, S. H. Lee, H. R. Lee, L. Y. Wong, K. F. Brulois, S. Lee, J. D. Buckley, P. W. Laird, V. E. Marquez and J. U. Jung (2010). "Epigenetic analysis of KSHV latent and lytic genomes." PLoS Pathog **6**(7): e1001013.

Tremethick, D. J. (2007). "Higher-order structures of chromatin: the elusive 30 nm fiber." Cell **128**(4): 651-654.

Tsukada, Y., J. Fang, H. Erdjument-Bromage, M. E. Warren, C. H. Borchers, P. Tempst and Y. Zhang (2006). "Histone demethylation by a family of JmjC domain-containing proteins." Nature **439**(7078): 811-816.

Tunnicliffe, R. B., M. P. Lockhart-Cairns, C. Levy, A. P. Mould, T. A. Jowitt, H. Sito, C. Baldock, R. M. Sandri-Goldin and A. P. Golovanov (2017). "The herpes viral transcription factor ICP4 forms a novel DNA recognition complex." Nucleic Acids Res **45**(13): 8064-8078.

Ui, A., H. Ogiwara, S. Nakajima, S. Kanno, R. Watanabe, M. Harata, H. Okayama, C. C. Harris, J. Yokota, A. Yasui and T. Kohno (2014). "Possible involvement of LKB1-AMPK signaling in non-homologous end joining." Oncogene **33**(13): 1640-1648.

Umene, K. and T. Nishimoto (1996). "Inhibition of generation of authentic genomic termini of herpes simplex virus type 1 DNA in temperature-sensitive mutant BHK-21 cells with a mutated CCG1/TAF(II)250 gene." J Virol **70**(12):

9008-9012.
Uppal, T., H. C. Jha, S. C. Verma and E. S. Robertson (2015). "Chromatinization of the KSHV Genome During the KSHV Life Cycle." Cancers (Basel) **7**(1): 112-142.
Van Damme, E., K. Laukens, T. H. Dang and X. Van Ostade (2010). "A manually curated network of the PML nuclear body interactome reveals an important role for PML-NBs in SUMOylation dynamics." Int J Biol Sci **6**(1): 51-67.
Vermeulen, M., K. W. Mulder, S. Denissov, W. W. Pijnappel, F. M. van Schaik, R. A. Varier, M. P. Baltissen, H. G. Stunnenberg, M. Mann and H. T. Timmers (2007). "Selective anchoring of TFIID to nucleosomes by trimethylation of histone H3 lysine 4." Cell **131**(1): 58-69.
Verreault, A., P. D. Kaufman, R. Kobayashi and B. Stillman (1998). "Nucleosomal DNA regulates the core-histone-binding subunit of the human Hat1 acetyltransferase." Curr Biol **8**(2): 96-108.
Vignali, M., A. H. Hassan, K. E. Neely and J. L. Workman (2000). "ATP-dependent chromatin-remodeling complexes." Mol Cell Biol **20**(6): 1899-1910.
Vogelauer, M., J. Wu, N. Suka and M. Grunstein (2000). "Global histone acetylation and deacetylation in yeast." Nature **408**(6811): 495-498.
Wagner, E. K. and D. C. Bloom (1997). "Experimental investigation of herpes simplex virus latency." Clin Microbiol Rev **10**(3): 419-443.
Wagner, E. K., G. Devi-Rao, L. T. Feldman, A. T. Dobson, Y. F. Zhang, W. M. Flanagan and J. G. Stevens (1988). "Physical characterization of the herpes simplex virus latency-associated transcript in neurons." J Virol **62**(4): 1194-1202.
Walfridsson, J., O. Khorosjutina, P. Matikainen, C. M. Gustafsson and K. Ekwall (2007). "A genome-wide role for CHD remodelling factors and Nap1 in nucleosome disassembly." EMBO J **26**(12): 2868-2879.
Wallace, H. M., H. N. Baybutt, C. K. Pearson and H. M. Keir (1980). "The effect of polyamines on herpes simplex virus type 1 DNA polymerase purified from infected baby hamster kidney cells (BHK-21/C13)." J Gen Virol **49**(2): 397-400.
Wang, Q. Y., C. Zhou, K. E. Johnson, R. C. Colgrove, D. M. Coen and D. M. Knipe (2005). "Herpesviral latency-associated transcript gene promotes assembly of heterochromatin on viral lytic-gene promoters in latent infection." Proc Natl Acad Sci U S A **102**(44): 16055-16059.
Wapinski, O. L., T. Vierbuchen, K. Qu, Q. Y. Lee, S. Chanda, D. R. Fuentes, P. G. Giresi, Y. H. Ng, S. Marro, N. F. Neff, D. Drechsel, B. Martynoga, D. S. Castro, A. E. Webb, T. C. Sudhof, A. Brunet, F. Guillemot, H. Y. Chang and M. Wernig (2013). "Hierarchical mechanisms for direct reprogramming of fibroblasts to neurons." Cell **155**(3): 621-635.
Washington, S. D., S. I. Edenfield, C. Lieux, Z. L. Watson, S. M. Taasan, A. Dhummakupt, D. C. Bloom and D. M. Neumann (2018). "Depletion of the Insulator Protein CTCF Results in Herpes Simplex Virus 1 Reactivation In Vivo." J Virol **92**(11).
Washington, S. D., F. Musarrat, M. K. Ertel, G. L. Backes and D. M. Neumann (2018). "CTCF Binding Sites in the Herpes Simplex Virus 1 Genome Display Site-Specific CTCF Occupation, Protein Recruitment, and Insulator Function." J Virol **92**(8).
Washington, S. D., P. Singh, R. N. Johns, T. G. Edwards, M. Mariani, S. Frietze, D. C. Bloom and D. M. Neumann (2019). "The CCCTC Binding Factor, CTRL2, Modulates Heterochromatin Deposition and the Establishment of Herpes Simplex Virus 1 Latency In Vivo." J Virol **93**(13).
Watanabe, R., A. Ui, S. Kanno, H. Ogiwara, T. Nagase, T. Kohno and A. Yasui (2014). "SWI/SNF factors required for cellular resistance to DNA damage include ARID1A and ARID1B and show interdependent protein stability." Cancer

Res **74**(9): 2465-2475.
Weber, C. M. and S. Henikoff (2014). "Histone variants: dynamic punctuation in transcription." Genes Dev **28**(7): 672-682.
Weller, S. K. and D. M. Coen (2012). "Herpes simplex viruses: mechanisms of DNA replication." Cold Spring Harb Perspect Biol **4**(9): a013011.
Whitehouse, I., O. J. Rando, J. Delrow and T. Tsukiyama (2007). "Chromatin remodelling at promoters suppresses antisense transcription." Nature **450**(7172): 1031-1035.
Whitley, R., D. W. Kimberlin and C. G. Prober (2007). Pathogenesis and disease. Human Herpesviruses: Biology, Therapy, and Immunoprophylaxis. A. Arvin, G. Campadelli-Fiume, E. Mocarski et al. Cambridge.
Wong, H., J. M. Victor and J. Mozziconacci (2007). "An all-atom model of the chromatin fiber containing linker histones reveals a versatile structure tuned by the nucleosomal repeat length." PLoS One **2**(9): e877.
Workman, J. L. (2006). "Nucleosome displacement in transcription." Genes Dev **20**(15): 2009-2017.
Wright, D. E., C. Y. Wang and C. F. Kao (2012). "Histone ubiquitylation and chromatin dynamics." Front Biosci (Landmark Ed) **17**: 1051-1078.
Wysocka, J., T. Swigut, H. Xiao, T. A. Milne, S. Y. Kwon, J. Landry, M. Kauer, A. J. Tackett, B. T. Chait, P. Badenhorst, C. Wu and C. D. Allis (2006). "A PHD finger of NURF couples histone H3 lysine 4 trimethylation with chromatin remodelling." Nature **442**(7098): 86-90.
Xia, L., L. Jaafar, A. Cashikar and H. Flores-Rozas (2007). "Identification of genes required for protection from doxorubicin by a genome-wide screen in Saccharomyces cerevisiae." Cancer Res **67**(23): 11411-11418.
Xin, L., D. P. Liu and C. C. Ling (2003). "A hypothesis for chromatin domain opening." Bioessays **25**(5): 507-514.
Xu, P., S. Mallon and B. Roizman (2016). "PML plays both inimical and beneficial roles in HSV-1 replication." Proc Natl Acad Sci U S A **113**(21): E3022-3028.
Xu, X., Y. Che and Q. Li (2016). "HSV-1 tegument protein and the development of its genome editing technology." Virol J **13**: 108.
Xue, Y., C. Van, S. K. Pradhan, T. Su, J. Gehrke, B. G. Kuryan, T. Kitada, A. Vashisht, N. Tran, J. Wohlschlegel, C. L. Peterson, S. K. Kurdistani and M. F. Carey (2015). "The Ino80 complex prevents invasion of euchromatin into silent chromatin." Genes Dev **29**(4): 350-355.
Yang, D. and G. Arya (2011). "Structure and binding of the H4 histone tail and the effects of lysine 16 acetylation." Phys Chem Chem Phys **13**(7): 2911-2921.
Yao, W., D. A. King, S. L. Beckwith, G. J. Gowans, K. Yen, C. Zhou and A. J. Morrison (2016). "The INO80 Complex Requires the Arp5-Ies6 Subcomplex for Chromatin Remodeling and Metabolic Regulation." Mol Cell Biol **36**(6): 979-991.
Yao, X. D., M. Matecic and P. Elias (1997). "Direct repeats of the herpes simplex virus a sequence promote nonconservative homologous recombination that is not dependent on XPF/ERCC4." J Virol **71**(9): 6842-6849.
Yen, K., V. Vinayachandran, K. Batta, R. T. Koerber and B. F. Pugh (2012). "Genome-wide nucleosome specificity and directionality of chromatin remodelers." Cell **149**(7): 1461-1473.
Yen, K., V. Vinayachandran and B. F. Pugh (2013). "SWR-C and INO80 chromatin remodelers recognize nucleosome-free regions near +1 nucleosomes." Cell **154**(6): 1246-1256.
Yu, L. and R. H. Morse (1999). "Chromatin opening and transactivator potentiation by RAP1 in Saccharomyces cerevisiae." Mol Cell Biol **19**(8): 5279-5288.
Yuan, G. C., Y. J. Liu, M. F. Dion, M. D. Slack, L. F. Wu, S. J. Altschuler and O. J. Rando (2005). "Genome-scale

identification of nucleosome positions in S. cerevisiae." Science **309**(5734): 626-630.
Zabolotny, J. M., C. Krummenacher and N. W. Fraser (1997). "The herpes simplex virus type 1 2.0-kilobase latency-associated transcript is a stable intron which branches at a guanosine." J Virol **71**(6): 4199-4208.
Zanton, S. J. and B. F. Pugh (2006). "Full and partial genome-wide assembly and disassembly of the yeast transcription machinery in response to heat shock." Genes Dev **20**(16): 2250-2265.
Zeev-Ben-Mordehai, T., D. Vasishtan, A. Hernandez Duran, B. Vollmer, P. White, A. Prasad Pandurangan, C. A. Siebert, M. Topf and K. Grunewald (2016). "Two distinct trimeric conformations of natively membrane-anchored full-length herpes simplex virus 1 glycoprotein B." Proc Natl Acad Sci U S A **113**(15): 4176-4181.
Zegerman, P., B. Canas, D. Pappin and T. Kouzarides (2002). "Histone H3 lysine 4 methylation disrupts binding of nucleosome remodeling and deacetylase (NuRD) repressor complex." J Biol Chem **277**(14): 11621-11624.
Zeng, P. Y., C. R. Vakoc, Z. C. Chen, G. A. Blobel and S. L. Berger (2006). "In vivo dual cross-linking for identification of indirect DNA-associated proteins by chromatin immunoprecipitation." Biotechniques **41**(6): 694, 696, 698.
Zentner, G. E., T. Tsukiyama and S. Henikoff (2013). "ISWI and CHD chromatin remodelers bind promoters but act in gene bodies." PLoS Genet **9**(2): e1003317.
Zerboni, L., X. Che, M. Reichelt, Y. Qiao, H. Gu and A. Arvin (2013). "Herpes simplex virus 1 tropism for human sensory ganglion neurons in the severe combined immunodeficiency mouse model of neuropathogenesis." J Virol **87**(5): 2791-2802.
Zhang, Y., H. H. Ng, H. Erdjument-Bromage, P. Tempst, A. Bird and D. Reinberg (1999). "Analysis of the NuRD subunits reveals a histone deacetylase core complex and a connection with DNA methylation." Genes Dev **13**(15): 1924-1935.
Zhou, G., D. Te and B. Roizman (2010). "The CoREST/REST repressor is both necessary and inimical for expression of herpes simplex virus genes." MBio **2**(1): e00313-00310.
Zhou, H., C. S. Beevers and S. Huang (2011). "The targets of curcumin." Curr Drug Targets **12**(3): 332-347.
Zhou, J., J. Y. Fan, D. Rangasamy and D. J. Tremethick (2007). "The nucleosome surface regulates chromatin compaction and couples it with transcriptional repression." Nat Struct Mol Biol **14**(11): 1070-1076.
Zhu, P., W. Zhou, J. Wang, J. Puc, K. A. Ohgi, H. Erdjument-Bromage, P. Tempst, C. K. Glass and M. G. Rosenfeld (2007). "A histone H2A deubiquitinase complex coordinating histone acetylation and H1 dissociation in transcriptional regulation." Mol Cell **27**(4): 609-621.
Zlatanova, J. and A. Thakar (2008). "H2A.Z: view from the top." Structure **16**(2): 166-179.